

**The effects of interleukin-6 in a rat
model of hepatocellular carcinoma**

Diarmuid M Moran

**Supervised for the award of Doctor of Philosophy by
Professor Paul A. Cahill and Dr. Iain H. Mc Killop**

School of Biotechnology

Dublin City University

July 2005

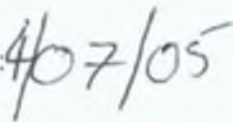
I hereby certify that this material, which I now submit for assessment on the programme of study leading to the award of Ph.D. is entirely my own work and has not been taken from the work of others save and to the extent that such work has been cited and acknowledged within the text of my own work.

Signed:

A handwritten signature in cursive script, appearing to read "David M.", written in black ink.

ID No.: 96071672

Date:

A handwritten date "4/07/05" written in black ink, with the month and day separated by a slash.

Acknowledgements

I am indebted to all who have helped me throughout the course of my study. First and foremost I would like to thank my research mentor in the University of Rochester and University of North Carolina at Charlotte, Dr. Iain H. McKillop. His continued support and devotion to my work has been invaluable to the development of my career as a research scientist. Furthermore, his friendship and his ability to resolve all sorts of major and minor crises outside of work have made my stay in the USA a great one.

I would also like to thank my supervisor Professor Paul A. Cahill in Dublin City University for making all this possible. He has acted as a constant source of advice and guidance throughout my study for which I am sincerely grateful.

I also would like to thank all my lab colleagues. I am indebted to Dr. Eugene Sokolov and Dr. Didier Dreau for their instruction and guidance on new techniques. I owe a special thanks to Liz who has kept me sane and stopped me from taking myself too seriously along the way. Further thanks are owed to Carolyn and Dijana who both have assisted me greatly with all sorts of experiments through the years. I also want to give a special thanks to Dr. Craig Halberstadt for teaching me all about cell encapsulation.

I also want to thank all the great friends that I have made during my time in the USA. They have all made me very welcome, supported me through the tough times and been a great source of good humour. I would like to especially thank Eileen and John in Rochester who made my move to the USA an easy one. I also need to give a special thanks to my close friends outside of work in Charlotte; Andrea, Cameron, the Daves, Eric, Hollis, James, Jeff, all the Matts, Will and everyone else I have met along the way. My friends in Ireland have also been a great support. I want to thank Gavin, Gemma, David and Nick for being there when I needed to hear an Irish accent.

Above all I wish to thank my parents and family They have invested time, love and money in my future and made sure that I have never wanted for anything I could not have achieved this without them

The effects of interleukin-6 in a rat model of hepatocellular carcinoma

Diarmuid M Moran

Abstract

Interleukin-6 (IL-6) is integrally linked to normal hepatic growth and liver regeneration. The aim of the present study was to determine the expression and function of IL-6 signalling pathways in a rat model of hepatocellular carcinoma (HCC).

In these studies HCC was characterised by dysregulated expression of IL-6 signalling components *in vivo* and *in vitro*, including downregulated expression of the IL-6 receptor and increased IL-6 production and secretion. Recombinant human IL-6 (rhIL-6) treatment of isolated rat HCC cells and hepatocytes *in vitro* led to the activation of janus kinase-signal transducer and activator of transcription (Jak-STAT) and Ras-mitogen activated protein kinase intracellular signalling pathways. Cyclin dependent kinase (cdk) inhibitor expression was increased in HCC cells after treatment with IL-6, an effect that was not observed in isolated hepatocytes. Decreases in cdk activity after rhIL-6 treatment result in a G0/G1 growth arrest in HCC cells.

As a result of these *in vitro* studies, an alginate based cell microencapsulation system was developed to provide continual *in vivo* rhIL-6 delivery in a rat model of HCC. CHO cells transfected to supra-express rhIL-6 were encapsulated in alginate and implanted in HCC tumour burdened rats resulting in high serum levels of biologically active rhIL-6. Recombinant human IL-6 was detected in both normal and tumour liver tissues resulting in activation of the Jak-STAT pathway. Due to tumour volume variability, no conclusions on the effects of rhIL-6 on tumour progression *in vivo* could be determined. However, rhIL-6 treatment did result in increased total hepatic weight.

Collectively this study demonstrates a role for IL-6 in HCC progression and identifies alginate encapsulated CHO cells as an effective method for rhIL-6 delivery *in vivo* which has potential in the study of normal and abnormal liver growth.

Table of Contents

Chapter 1 Introduction	1
1 1 Hepatocellular Carcinoma	1
1 1 1 Epidemiology	1
1 1 2 Aetiology	1
1 1 2 1 Hepatitis C virus	2
1 1 2 2 Hepatitis B virus	3
1 1 2 3 Aflatoxins	4
1 1 2 4 Ethanol	5
1 1 3 Natural History of HCC	5
1 1 3 1 Pathology	6
1 1 3 2 Molecular Mechanisms of HCC	7
1 1 4 Diagnosis and Treatment	8
1 1 4 1 Diagnosis	8
1 1 4 2 Treatment and Prevention	9
1 1 5 Summary	11
1 2 Interleukin-6	13
1 2 1 Introduction	13
1 2 2 Structure of Interleukin-6	13
1 2 3 Expression of Interleukin-6	14
1 2 4 The Interleukin-6 Receptor	15
1 2 4 1 Class I Cytokine Receptors	15
1 2 4 2 IL-6R α	16
1 2 4 3 Gp130	17

1 2 5 Interleukin-6 Signalling	17
1 2 5 1 The Jak-STAT Pathway	18
1 2 5 2 The Ras-MAPK Pathway	21
1 2 5 3 Integration of IL-6 Signalling Pathways	21
1 2 5 4 Negative Regulation of IL-6 Signalling	24
1 2 6 Physiological and Pathophysiological Functions of IL-6	25
1 2 6 1 Physiological Functions of IL-6	25
1 2 6 2 IL-6 and the Liver	27
1 2 6 3 IL-6 and Disease	29
1 2 6 4 IL-6 and Cancer	30
1 2 7 Summary	33
1 3 Aims of the Present Study	35
Chapter 2 General Methods	36
2 1 Animals	36
2 2 Cell Culture and Cell lines	36
2 2 1 Materials	35
2 2 2 Cell Lines	37
2 2 3 Cell Culture Media	37
2 2 4 Cell Propagation	38
2 2 5 Cell Passaging and Splitting	38
2 2 6 Cell Storage	38
2 2 7 H4IIE cell Isolation	39
2 2 8 Hepatocyte Isolation	39
2 3 HCC Tumour Model	40
2 3 1 H4IIE Tumour Model	40

2 4 Preparation of Cell Lysates	42
2 4 1 Materials	42
2 4 2 Preparation of Cultured Cell Lysates for Protein Analysis	42
2 4 3 Preparation of Tissue Cell Lysates for Protein Analysis	42
2 5 Immunoblotting	43
2 5 1 Materials	43
2 5 2 BCA Protein Assay	44
2 5 3 Western Blotting	44
2 6 IL-6 ELISA (Enzyme Linked Immunosorbent Assay)	45
2 6 1 Materials	45
2 6 2 Rat IL-6 ELISA	46
2 6 3 Human IL-6 ELISA	47
2 7 Statistics	47
Chapter 3 Altered Expression of IL-6 Signalling Components in HCC	48
3 1 Introduction	48
3 2 Methods	51
3 2 1 Tumour Model	51
3 2 2 Preparation of Tissue Cell Lysates for Protein Analysis	51
3 2 3 Immunoblotting	51
3 2 4 RNA Isolation	52
3 2 4 1 Materials	52
3 2 4 2 Total RNA Isolation from Tissue	52
3 2 4 3 Total RNA Isolation from Cultured Cells	53

3 2 4 4	Determination of Total RNA Concentration and Integrity	53
3 2 5	Reverse Transcriptase-Polymerase Chain Reaction	55
3 2 5 1	Materials	55
3 2 5 2	Method	55
3 2 6	Histochemistry	57
3 2 6 1	Materials	57
3 2 6 2	Tissue Processing	58
3 2 6 3	Haematoxylin and Eosin (H&E) Staining	58
3 2 6 4	Immunofluorescence	59
3 2 7	IL-6 ELISA	59
3 2 7 1	Materials	59
3 2 7 2	Sample Preparation for ELISA	59
3 2 7 3	Rat IL-6 ELISA	60
3 3	Results	61
3 3 1	Tumour Model	61
3 3 2	IL-6 Receptor Expression in HCC <i>In Vivo</i>	61
3 3 3	Expression and Activity of IL-6 Dependent Signalling Pathway Components in HCC <i>In Vivo</i>	66
3 3 4	IL-6 Expression in HCC	70
3 4	Discussion	79
Chapter 4	Interleukin-6 Signalling in HCC	84
4 1	Introduction	84
4 2	Methods	87
4 2 1	Tumour Model and H4IIE Cell Isolation	87

4 2 2 Primary Hepatocyte Isolation	87
4 2 3 Recombinant Human IL-6 Treatment	87
4 2 4 Immunoblotting	87
4 2 4 1 Materials	87
4 2 4 2 Western Blotting	88
4 2 5 Pharmacological Inhibition of Jak-STAT and Ras-MAPK pathways	88
4 2 5 1 Materials	88
4 2 5 2 Pharmacological Inhibition of the Ras-MAPK pathway	89
4 2 5 3 Pharmacological Inhibition of the Jak-STAT pathway	89
4 2 6 Transient Transfection of H4IIE Cells with Dominant Negative STAT3	89
4 2 6 1 Materials	89
4 2 6 2 Transformation of E coli	91
4 2 6 3 Plasmid DNA Miniprep	92
4 2 6 4 Restriction Digests	92
4 2 6 5 Plasmid DNA Miniprep	96
4 2 6 6 DNA Quantification	97
4 2 6 7 Transient Transfection of H4IIE Cells	97
4 2 7 Cyclin Dependent Kinase Activity Assays	98
4 2 7 1 Materials	98
4 2 7 2 Method	98
4 2 8 Confocal Microscopy	99

4 3 Results	101
4 3 1 Characteristics of H4IIE Cells and Hepatocytes	101
<i>In Vitro</i>	
4 3 2 Effect of IL-6 on STAT3 activity in H4IIE Cells and	104
Hepatocytes <i>In Vitro</i>	
4 3 3 Effect of IL-6 on MEK activity in H4IIE Cells and	111
Hepatocytes <i>In Vitro</i>	
4 3 4 Downstream Effects of IL-6 Signalling in H4IIE Cells	111
and Hepatocytes	
4 3 5 Pharmacological Inhibition of IL-6 Stimulated ERK	123
Activation in H4IIE Cells <i>In Vitro</i>	
4 3 6 Inhibition of IL-6 Stimulated STAT3 Activation in H4IIE	127
Cells <i>In Vitro</i>	
4 4 Discussion	140
Chapter 5 Growth Regulatory Effects of IL-6 in HCC	148
5 1 Introduction	148
5 2 Methods	150
5 2 1 Nuclear Thymidine Incorporation	150
5 2 1 1 Materials	150
5 2 1 2 Method	150
5 2 2 Alamar Blue Proliferation Assay	151
5 2 2 1 Materials	151
5 2 2 2 Method	151

5 2 3 Cell Counting	152
5 2 3 1 Materials	152
5 2 3 2 Method	152
5 2 4 FACS Cell Cycle Analysis	153
5 2 4 1 Materials	153
5 2 4 2 Method	153
5 3 Results	154
5 3 1 Effect of rhIL-6 on HCC Cell Proliferation <i>In Vitro</i>	154
5 3 2 Effect of rhIL-6 on HCC Cell Cycle Progression <i>In Vitro</i>	157
5 4 Discussion	164
Chapter 6 Microencapsulation of Engineered CHO Cells for IL-6	168
Delivery <i>In Vivo</i>	
6 1 Introduction	168
6 2 Methods	172
6 2 1 Tumour model	172
6 2 2 CHO Cell Culture	172
6 2 3 Alginate Microencapsulation of CHO Cells	172
6 2 3 1 Materials	172
6 2 3 2 Cell Encapsulation	173
6 2 3 3 Poly-L-lysine Coating of Alginate Beads	176
6 2 4 IL-6 ELISA	176
6 2 4 1 Plasma Preparation for IL-6 ELISA	176
6 2 4 2 Culture Media Preparation for IL-6 ELISA	177
6 2 4 3 IL-6 ELISA	177

6 2 5 Live/Dead Cell Viability Assay	177
6 2 5 1 Materials	177
6 2 5 2 Method	177
6 2 6 Alginate Bead Implantation	178
6 2 7 Preparation of Tissue Lysates	178
6 2 8 Immunoblotting	178
6 3 Results	180
6 3 1 Encapsulation of CHO-IL6 and CHO-CTRL Cells	180
6 3 2 Rat Implantation of Microencapsulated CHO-IL6 and CHO-CTRL Cells	192
6 3 3 Effects of IL-6 on Liver and HCC Tumour Growth <i>In Vivo</i>	200
6 4 Discussion	211
Chapter 7 Discussion	219
7 1 The Role of Interleukin-6 in Hepatocellular Carcinoma Progression	219
7 2 Cell Microencapsulation for IL-6 Delivery <i>In Vivo</i>	230
References	238

List of Tables

Table 3 1 Primers used for the PCR amplification of the cDNA for IL-6, S9, gp130 and IL-6R α	56
Table 4 1 Reaction mixtures for the restriction digest of pEFHASTAT3F and pEFHASTAT3	93
Table 5 1 Effect of serum deprivation on cell cycle progression in H4IIE (HCC) cells	160
Table 6 1 Human IL-6 production by CHO-IL6 and CHO-CTRL cells <i>in vitro</i>	182
Table 6 2 Effects of physical parameters on alginate bead size and sphericity	183
Table 6 3 IL-6 production by alginate encapsulated CHO-IL6 and CHO-CTRL cells <i>in vitro</i>	190
Table 6 4 Plasma IL-6 levels in CHO-IL6, CHO-CTRL and empty bead implanted rats	198
Table 6 5 IL-6 production by CHO-IL6, CHO-CTRL and empty beads retrieved from rats <i>in vitro</i>	199
Table 6 6 Effects of CHO-CTRL, CHO-IL6 and empty alginate bead implantation on HCC tumour volume and rat liver weight	201
Table 6 7 Effects of CHO-CTRL, CHO-IL6 and empty alginate bead implantation on HCC tumour volume and rat liver weight	202

List of Figures

Figure 1 1	The Jak-STAT Pathway	19
Figure 1 2	The Ras-MAPK Pathway	22
Figure 2 1	Hepatocyte isolation perfusion system	41
Figure 3 1	Sample RNA integrity gel	54
Figure 3 2	Photographs of HCC tumours	62
Figure 3 3	Histological sections of HCC and normal hepatic tissues stained with haematoxylin and eosin	63
Figure 3 4	HCC is characterised by decreased expression of IL-6R α <i>versus</i> normal liver tissue <i>in vivo</i>	64
Figure 3 5	HCC is characterised by decreased expression of gp130 <i>versus</i> normal liver tissue <i>in vivo</i>	65
Figure 3 6	Immunofluorescent staining of IL-6 receptor components at the normal liver/HCC interface	67
Figure 3 7	Decreased IL-6 receptor mRNA expression in HCC <i>versus</i> normal liver tissue <i>in vivo</i>	68
Figure 3 8	HCC is characterised by increased STAT3 activity <i>versus</i> normal liver tissue <i>in vivo</i>	69
Figure 3 9	HCC is characterised by increased expression of p21 ^{waf1/cip1} <i>versus</i> normal liver tissue <i>in vivo</i>	71
Figure 3 10	HCC is characterised by increased expression of p27 ^{Kip1} <i>versus</i> normal liver tissue <i>in vivo</i>	72
Figure 3 11	HCC is characterised by increased expression of SOCS-1 <i>versus</i> normal liver tissue <i>in vivo</i>	73

Figure 3 12	HCC is characterised by decreased expression of SOCS-3 <i>versus</i> normal liver tissue <i>in vivo</i>	74
Figure 3 13	Increased IL-6 mRNA expression in HCC <i>versus</i> normal liver tissue <i>in vivo</i>	75
Figure 3 14	IL-6 mRNA expression in HCC <i>in vitro</i>	77
Figure 3 15	IL-6 protein expression in HCC <i>in vivo</i> and <i>in vitro</i>	78
Figure 4 1	Schematic representation of expression vectors pEFHASTAT3F and pEFHASTAT3	90
Figure 4 2	Restriction digestion of pEFHASTAT3F expression vector using BAMH1/Sal1	94
Figure 4 3	Restriction digestion of pEFHASTAT3 expression vector using EcoRV/Sal1	95
Figure 4 4	Confocal images of isolated H4IIE (HCC) cells and rat hepatocytes cultured <i>in vitro</i>	102
Figure 4 5	H4IIE (HCC) cells are characterised by decreased IL-6 receptor expression versus primary rat hepatocytes <i>in vitro</i>	103
Figure 4 6	H4IIE (HCC) cells retain a decreased IL-6 receptor expression phenotype during serial passaging <i>in vitro</i>	105
Figure 4 7	RhIL-6 stimulates Jak1 activity in H4IIE (HCC) cells and isolated cultured rat hepatocytes in a time dependent manner in the absence of changes in total Jak1 expression <i>in vitro</i>	106
Figure 4 8	RhIL-6 stimulates Jak2 activity in H4IIE (HCC) cells and isolated cultured rat hepatocytes in a time dependent manner in the absence of changes in total Jak2 expression <i>in vitro</i>	107

Figure 4 9	RhIL-6 stimulates Tyk2 activity in H4IIE (HCC) cells and isolated cultured rat hepatocytes in a time dependent manner in the absence of changes in total Tyk2 expression <i>in vitro</i>	109
Figure 4 10	RhIL-6 stimulates STAT3 activity in H4IIE (HCC) cells and isolated cultured rat hepatocytes in a time dependent manner in the absence of changes in total STAT3 expression <i>in vitro</i>	110
Figure 4 11	RhIL-6 stimulates STAT3 activity in H4IIE (HCC) cells and isolated cultured rat hepatocytes in a dose dependent manner in the absence of changes in total STAT3 expression <i>in vitro</i>	112
Figure 4 12	RhIL-6 stimulates MEK activity in H4IIE (HCC) cells and isolated cultured rat hepatocytes in a time-dependent manner in the absence of changes in total ERK expression <i>in vitro</i>	113
Figure 4 13	RhIL-6 treatment does not alter the expression of cyclins A, D1 and D3 in H4IIE (HCC) cells <i>in vitro</i>	115
Figure 4 14	RhIL-6 treatment does not alter the expression of cyclins A and D3 but does suppress cyclin D1 expression in isolated cultured rat hepatocytes <i>in vitro</i>	116
Figure 4 15	RhIL-6 treatment does not alter the expression of cyclin dependent kinases cdc2 p34, cdk2 and cdk4 in H4IIE (HCC) cells <i>in vitro</i>	118
Figure 4 16	RhIL-6 treatment does not alter the expression of cyclin dependent kinases cdc2 p34, cdk2 and cdk4 in isolated cultured rat hepatocytes <i>in vitro</i>	119
Figure 4 17	RhIL-6 treatment does not alter the expression of PCNA in H4IIE (HCC) cells or isolated cultured rat hepatocytes <i>in vitro</i>	120

Figure 4 18 RhIL-6 stimulates expression of the cyclin dependent kinase inhibitor p21 ^{waf1/cip1} in H4IIE (HCC) but does not alter its expression in isolated cultured rat hepatocytes <i>in vitro</i>	121
Figure 4 19 RhIL-6 stimulates expression of the cyclin dependent kinase inhibitor p27 ^{Kip1} in H4IIE (HCC) but does not alter its expression in isolated cultured rat hepatocytes <i>in vitro</i>	122
Figure 4 20 RhIL-6 treatment in H4IIE (HCC) cells is associated with a decreased level of phosphorylation of the retinoblastoma protein <i>in vitro</i>	124
Figure 4 21 rhIL-6 treatment of H4IIE (HCC) cells is associated with a decreased level of cdk2 activity <i>in vitro</i>	125
Figure 4 22 RhIL-6 treatment of H4IIE (HCC) cells is associated with a decreased level of cdk4 activity <i>in vitro</i>	126
Figure 4 23 PD98059 (MEK inhibitor) treatment of H4IIE (HCC) cells abolishes rhIL-6 stimulation of MEK activity <i>in vitro</i>	128
Figure 4 24 RhIL-6 stimulation of STAT3 activity is not altered by PD98059 (MEK inhibitor) treatment of H4IIE (HCC) cells <i>in vitro</i>	129
Figure 4 25 PD98059 (MEK inhibitor) treatment of H4IIE (HCC) cells does not inhibit the rhIL-6 stimulated expression of p21 ^{waf1/cip1} and p27 ^{Kip1} <i>in vitro</i>	130
Figure 4 26 HA-Tag was not detectable in cell lysates of H4IIE (HCC) cells transfected with HA-tagged wild type expressing or HA-tagged dominant negative expressing STAT3 plasmids <i>in vitro</i>	132

Figure 4 27	Transfection of H4IIE (HCC) cells with a plasmid expressing dominant negative STAT3 failed to inhibit rhIL-6 stimulation of STAT3 activity	134
Figure 4 28	AG490 inhibits rhIL-6 stimulation of STAT3 activity in a dose dependent manner <i>in vitro</i>	135
Figure 4 29	RhIL-6 stimulation of STAT3 activity is ablated by AG490 (Jak inhibitor) treatment of H4IIE (HCC) cells <i>in vitro</i>	136
Figure 4 30	RhIL-6 ability to stimulate MEK activity is not altered by AG490 (Jak inhibitor) treatment of H4IIE (HCC) cells <i>in vitro</i>	137
Figure 4 31	AG490 (Jak inhibitor) treatment of H4IIE (HCC) cells inhibits the rhIL-6 stimulated expression of p21 ^{waf1/cip1} but does not affect the expression of p27 ^{Kip1} <i>in vitro</i>	139
Figure 5 1	RhIL-6 inhibits DNA synthesis in H4IIE (HCC) cells <i>in vitro</i>	156
Figure 5 2	RhIL-6 inhibits H4IIE (HCC) cell proliferation as evidenced by Alamar Blue reduction <i>in vitro</i>	158
Figure 5 3	RhIL-6 inhibits H4IIE (HCC) cell proliferation as evidenced by cell counting <i>in vitro</i>	159
Figure 5 4	RhIL-6 induces a G0/G1 growth arrest in H4IIE cells <i>in vitro</i>	162
Figure 5 5	RhIL-6 inhibits exit from G0/G1 phase of the H4IIE cell cycle <i>in vitro</i>	163
Figure 6 1	Illustrated representation of the apparatus used for alginate cell encapsulation	174
Figure 6 2	Photograph of the apparatus used for alginate cell encapsulation	175
Figure 6 3	Photomicrographs of cultured CHO-IL6 and CHO-CTRL cells	181
Figure 6 4	Two step filtration of beads results in a uniform sized bead population	185

Figure 6 5	Encapsulated CHO-IL6 and CHO-CTRL cell viability and colony morphology <i>in vitro</i>	186
Figure 6 6	CHO cells escape from alginate beads after 7 days culture <i>in vitro</i>	188
Figure 6 7	Poly-L-lysine (PLL) coating of encapsulated CHO cell beads diminishes bead integrity	189
Figure 6 8	IL-6 production by alginate encapsulated CHO-IL6 and CHO-CTRL cells <i>in vitro</i>	191
Figure 6 9	Fibrotic overgrowth present on CHO-CTRL and CHO-IL6 beads retrieved from rats 4 days after implantation	193
Figure 6 10	Appearance of CHO-IL6 and CHO-CTRL beads retrieved from rats 4 days after implantation	194
Figure 6 11	Appearance of CHO-IL6 and CHO-CTRL beads retrieved from rats 7 days after implantation	195
Figure 6 12	Empty alginate beads do not induce fibrotic overgrowth <i>in vivo</i>	197
Figure 6 13	Effects of CHO-CTRL, CHO-IL6 and empty alginate bead implantation on rat liver weight	203
Figure 6 14	IL-6 was detectable in HCC and normal liver tissues resected from CHO-IL6 implanted rats	204
Figure 6 15	Gp130 expression in HCC and normal liver tissues resected from CHO-IL6, CHO-CTRL and empty bead implanted rats	206
Figure 6 16	IL-6R α expression in HCC and normal liver tissues resected from CHO-IL6, CHO-CTRL and empty bead implanted rats	207
Figure 6 17	PSTAT3 expression was increased in HCC and normal liver tissues resected from CHO-IL6 implanted rats	208
Figure 6 18	PERK 1/2 expression in HCC and normal liver tissues resected from CHO-IL6, CHO-CTRL and empty bead implanted rats	209

Figure 6 19 PCNA expression in HCC and normal liver tissues resected from CHO-IL6, CHO-CTRL and empty bead implanted rats	210
Figure 7 1 Proposed mechanism for IL-6 induced growth arrest in H4IIE cells	223

List of Abbreviations

Cdk	Cyclin Dependent Kinase
CHO	Chinese Hamster Ovary
EGF	Epidermal Growth Factor
ERK	Extracellular Signal Regulated Kinase
Gp130	Glycoprotein 130
HCC	Hepatocellular Carcinoma
HGF	Hepatocyte Growth Factor
IL-6	Interleukin-6
IL-6Ra	Interleukin-6 Receptor- α
Jak	Janus Kinase
MAPK	Mitogen Activated Protein Kinase
PCNA	Proliferating Cell Nuclear Antigen
pERK	Phospho-Extracellular Signal Regulated Kinase
PLL	Poly-L-Lysine
pSTAT	Phospho-Signal Transducer and Activator of Transcription
Rb	Retinoblastoma Protein
RhIL-6	Recombinant Human Interleukin-6
SOCS	Suppressor of Cytokine Signalling
STAT	Signal Transducer and Activator of Transcription
TGF	Transforming Growth Factor
TNF	Tumour Necrosis Factor

List of Publications & Presentations

Moran, DM, Mayes N, Koniaris, LG, Cahill, PA & McKillop, IH (2005) Interleukin-6 (IL-6) inhibits cell proliferation in a rat model of hepatocellular carcinoma *Liver International* 25(2), 445-457

Moran, DM, Koniaris, LG, Cahill PA & McKillop, IH (2005) Interleukin-6 causes a G0/G1 growth arrest in hepatocellular carcinoma *FASEB Experimental Biology 2005, San Diego, CA USA*

Moran, DM, Koniaris, LG, Cahill PA & McKillop, IH (2005) Interleukin-6 inhibits cell growth at the G1/S interphase in hepatocellular carcinoma *Nature Biotechnology Winter Symposium 2005, Miami, FL, USA*

Moran, DM, Zimmers, TA, Koniaris, LG, Cahill PA & McKillop, IH (2004) Interleukin-6 inhibits hepatocellular carcinoma progression *Keystone Symposia (Jaks and STATs Development to Disease), Whistler, BC, Canada*

Moran, DM, Zimmers, TA, Koniaris, LG, Cahill PA & McKillop, IH (2003) Inhibition of hepatocellular carcinoma (HCC) cell growth by interleukin-6 54th Annual Meeting of the American Association for the Study of Liver Diseases, *Boston, MA, USA Hepatology*, 38, 570A-571A

Moran, DM, Zimmers, TA, Koniaris, LG, Cahill PA & McKillop, IH (2003) Interleukin-6 (IL-6) inhibits mitogenesis in a rat model of hepatocellular carcinoma (HCC) *Proceedings of the 94th Meeting of the American Association of Cancer Research*, 44 950

Chapter 1: Introduction

1.1 Hepatocellular Carcinoma

1.1.1 Epidemiology

Hepatocellular carcinoma (HCC) accounts for approximately 85% of the primary malignant tumours of the liver (Kew, 2002). Hepatocellular Carcinoma is the fifth most common malignancy in the world and is the third most common cause of cancer related death worldwide (Okuda, 2000, Parkin et al, 2001). The age adjusted worldwide incidence is between 5.5-14.9 per 100,000 population. The occurrence of this malignancy is more prevalent in men than women with an incidence ratio of approximately 3:1 respectively (Kew, 2002). Furthermore, incidence increases with age, presentation usually being rare before the age of forty in developed countries (Kew, 2002, Bosch et al, 1999). HCC is most prevalent in regions of eastern and south-eastern Asia and sub-Saharan Africa (>15 per 100,000 population) (Kew, 2002, Bosch et al, 1999). Recent analysis reports the incidence of HCC has nearly doubled in the USA over the past two decades (Bergsland and Venook, 2000) while in Japan the levels of HCC have increased by 15-20% over the past three decades (Kew, 2002). These increases are related to higher incidence of Hepatitis C virus (HCV) infection and chronic alcohol abuse, two of the main causal factors of HCC (Kew, 2002).

1.1.2 Aetiology

Cirrhosis of the liver represents the major underlying factor predisposing the development of HCC. The underlying cause of this cirrhosis affects the level of

associated risk of HCC development. For example, viral hepatitis related macronodular cirrhosis poses a greater cancer risk than alcohol induced micronodular cirrhosis (el-Serag, 2001). Furthermore, HCV related cirrhosis carries a greater cancer risk than cirrhosis with underlying Hepatitis B virus (HBV) infection (el-Serag, 2001). Approximately 75-80% of worldwide HCC cases are related to chronic infection with the hepatitis viruses, HCV and HBV (Bosch et al., 1999). In addition to hepatitis infection and chronic alcohol abuse, aflatoxin exposure (from infected food) represents a common cause of hepatic cirrhosis (Kew, 2002, Bosch et al., 1999).

1 1.2.1 Hepatitis C virus

Approximately 170 million people worldwide are seropositive for anti-HCV and, of these, an estimated 127 million are chronically infected (Ray Kim, 2002). Markers of HCV infection are found in 28% to 76% of HCC cases in Europe, with an increasing gradient from north to south, and in 80 to 90% of HCC cases in Japan (el-Serag, 2001). In other parts of Asia and Africa, HCV infection is related to only 20% of HCC cases due largely to the prevalence of HBV infection in these areas (Bosch et al., 1999).

Hepatitis C virus is a RNA virus of the flaviviridae family. This virus has no reverse transcriptase activity and does not integrate itself into the host genome. As such, HCV should, in theory, have no direct oncogenic potential (Romeo and Colombo, 2002). However, chronic HCV infection leads to the development of liver fibrosis, and ultimately cirrhosis, which predisposes the liver to develop HCC (el-Serag, 2001). More recently, direct oncogenic effects of HCV infection have been elucidated. It has been suggested, based on both clinical and epidemiological studies, that HCV may be more hepatocarcinogenic than HBV (Okuda, 2000, Ikeda et al., 1993). The HCV genome is translated into a 3000 amino acid polyprotein that is cleaved into a number

of proteins with different functions. The HCV core protein has transcriptional regulating functions on different cellular genes including the proto-oncogene *c-myc* suggesting involvement in the deregulation of normal cell growth (Ray et al, 1995). Furthermore, transgenic mice expressing the HCV core protein develop hepatic tumours that first appear as adenomas containing fat droplets in the cytoplasm. A more poorly differentiated neoplasia then evolves within the adenomas presenting the 'nodule in nodule' histopathological feature typical of early HCC patients with chronic HCV infection (Moriya et al, 1998). Other possible mechanisms for the carcinogenic effects of HCV core protein include its ability to inhibit both Fas and Tumour Necrosis Factor- α (TNF- α) mediated apoptosis (Marusawa et al, 1999) and its ability to constitutively activate a mitogen activated protein kinase/extracellular signal regulated kinase (MAPK/ERK) signalling cascade (Hayashi et al, 2000). In addition, the HCV non structural proteins NS3 and NS5A have been shown to have direct oncogenic potential as indicated by their ability to promote anchorage independent growth when expressed in fibroblasts and tumour formation in nude mice (Sakamuro et al, 1995, Ghosh et al, 1999).

1 1 2 2 Hepatitis B Virus

Hepatitis B virus is among the most common diseases in the world with an estimated 350 million chronically infected carriers worldwide (Maddrey, 2001). Hepatitis B virus infection is the main causal factor for HCC globally and the geographical distribution of HBV infection closely reflects that of HCC (Bosch et al, 1999). Hepatitis B virus infection levels at their highest are greater than 8% in regions such as Asia, Africa and the Western Pacific while in Western Europe, North America and Australia the levels are lower than 2% of the population (Maddrey, 2001). A landmark cohort study in Taiwan of over 22,000 HBV surface antigen (HBsAg)

seropositive males showed that chronic HBV infection precedes HCC development and that the relative risk of development of HCC is approximately 100 fold greater for these carriers (Beasley et al , 1981)

Cirrhosis as a consequence of chronic HBV infection is the principal factor predisposing to HCC development in these patients (el-Serag, 2001) Unlike HCV, HBV is a single stranded DNA virus of the hepadnavirus family that is integrated into the host genome Integration of HBV DNA may activate cellular proto-oncogenes or suppress growth regulating genes in *cis* however, no consistent integration sites have been observed (Lok, 2000) The HBV X gene encodes a viral protein that plays a central role in HBV infection and in hepatocarcinogenesis Transgenic mice expressing the entire HBV X gene under its own regulatory elements developed HCC beginning with multifocal areas of altered hepatocytes, followed by appearance of benign adenomas and then malignant carcinoma (Kim et al , 1991) The HBV X protein is a transcriptional factor that can alter the expression of many cellular genes including a subset of oncogenes such as *c-myc* and *c-myb* as well as tumour suppressor genes such as *APC*, *p53*, *p21^{waf1/cip1}* and *WT1* in primary human hepatocytes (Wu et al , 2001) Furthermore, the X protein has the ability to sequester the tumour suppressor p53 *in vitro* and can block p53 mediated apoptosis *in vivo* which contributes to the development of preneoplastic and neoplastic hepatocytes (Huo et al , 2001)

Overall, HBV infection causes 80% of HCC throughout the world however only a minority of chronic HBV carriers develop HCC in their lifetime This indicates the possible involvement of other cofactors for the development of HCC

1 1 2 3 Aflatoxins

Aflatoxins are mycotoxins from *Aspergillus flavus* and *Aspergillus parasiticus* and are the most potent naturally occurring carcinogens known They are common,

particularly in Asia and sub-Saharan Africa, where nuts and meals are often stored under hot and humid conditions allowing for growth of these moulds (Romeo and Colombo, 2002) The contamination of foodstuffs with Aflatoxin B1 correlates with HCC incidence in areas where there is high levels of HBV infection (el-Serag, 2001) A specific mutation at codon 249 of the tumour suppressor gene *p53* is common in HCC tissue of patients who have ingested high levels of aflatoxins (Ozturk, 1991) While this may account in part for the oncogenic effect of aflatoxins it appears that the synergistic cancer causing effect of this toxin in association with HBV infection presents a greater HCC risk (Sun et al , 1999)

1 1 2 4 Ethanol

Ethanol has no mutagenic properties however it is associated with an increased risk of cancer in several organs (Romeo and Colombo, 2002) The hepatocarcinogenic effects of chronic alcohol intake are most likely a result of the alcohol mediated liver cirrhosis (el-Serag, 2001) Ethanol metabolism results in the development of reactive oxygen species and carbon centred free radicals which can cause peroxidation of the polyunsaturated side chains of membrane phospholipids Cell membrane peroxidation ultimately results in liver cell damage, inflammation and often immunologically mediated liver injury (Day, 1996) Alcohol has also been identified as a strong synergistic cofactor in HBV and HCV mediated liver carcinogenesis (Stickel et al , 2002)

1.1.3 Natural History of HCC

The molecular mechanisms of hepatocarcinogenesis remain poorly understood Hepatocytes have a high level of metabolic function which is affected by many expressed genes As a result these genes are expected to undergo much more complex

alterations during carcinogenesis than in other cancers (Okuda, 2000) There are currently no consistent genetic sequences of events that lead to HCC formation with much of the past research indicating that there are multiple pathways to its development (Feitelson et al , 2002) There are however a number of molecular changes that occur in high frequency within cirrhotic tissue and small tumours which may constitute the early stages of hepatocarcinogenesis (Feitelson et al , 2002) Overall it is apparent that hepatocarcinogenesis is a multistep process which leads to progressive loss of differentiation, loss of normal cell adhesion, degradation of the extracellular matrix and constitutive activation of selected survival and growth promoting pathways

1 1 3 1 Pathology

Hepatocarcinogenesis initiated by HBV, HCV or environmental carcinogens usually follow the same sequence of necroinflammatory changes, hepatitis, fibrosis, cirrhosis, hepatocellular adenoma and finally HCC (Lim, 2002) It was first reported in 1986 that early HCC evolved in adenomatous hyperplastic nodules within the context of chronic hepatitis and/or cirrhosis (Arakawa et al , 1986) Since then it has been established that these dysplastic nodules will become malignant in approximately half of these patients and should be considered an absolute precursor of transformation (Takayama et al , 1990) Early histological changes which precede malignant transformation in these nodules include an increase in cellularity (nuclear crowding), an irregular, thin trabecular pattern with frequent acinus and pseudogland formation This early HCC is well differentiated, from which less well differentiated HCC develops (Okuda, 2000) As this small HCC becomes dedifferentiated the number of portal tracts decrease and the number of intratumoural arterioles increase (Nakashima et al , 1999) As the tumour grows the cells invade the neighbouring portal tracts and the fibrous stroma of the cirrhotic liver (Okazaki et al , 1997) Elevated levels of MMP1 are seen at

this point of development allowing the tumour to break down the extracellular matrix of the portal tract tissue and permitting further tumour growth (Okazaki et al , 1997) The result of this process is a large, poorly differentiated tumour capable of vascular invasion

1 1 3 2 Molecular Mechanisms of HCC

An extensive study of HCC resulting from three of the main aetiological factors HCV infection, HBV infection and chronic alcohol intake indicates common molecular/genetic changes (Edamoto et al , 2003), Rb1, p53 and Wnt being the main pathways affected Typically tumours associated with alcoholism have more frequent alterations of Rb1 and p53 pathways than those caused by HCV infection The most common alterations were *p16^{INK4A}* methylation, loss of Rb1 expression through promoter methylation and Cyclin D1 amplification (Edamoto et al , 2003) Microarray analysis of differential gene expression in HCC shows upregulation of the MAPK pathway as well as genes associated with an activated cell cycle (Okabe et al , 2001) The downregulated genes mainly encode hepatocyte specific gene products and detoxification enzymes producing a less differentiated phenotype (Okabe et al , 2001) Later in hepatocarcinogenesis tumour cells undergo increasing levels of chromosomal aberrations including loss of gene heterozygosity (Kimura et al , 1996)

P16^{INK4A} normally inhibits cyclin dependent kinases (cdk) 4 and 6 which block G1 phase progression *via* dephosphorylation of Rb, the latter of which binds to and inactivates E2F1 (Feitelson et al , 2002) Germ line mutations of this tumour suppressor protein have been identified in adult cases of HCC in Switzerland suggesting familial HCC however, this concept of inheritable HCC is relatively new and requires confirmation (Chaubert et al , 1997) Diethylmtrosamme-thioacetamide treatment of Fischer rats, which induces HCC, also causes hypermethylation of the *p16^{INK4A}* exon 1

in the later stages of carcinogenesis, further highlighting its importance in this process (Lim, 2002)

Mutations of β -Catenin are commonly observed in the early development of HCC and disruption of this Wnt signalling protein affects the expression of its target genes including *c-myc*, *c-jun*, *cyclin D1* and *fibronectin* (Calvisi et al , 2001) β -Catenin is an important submembranous protein that functions in cell-cell adhesion. Its mutation disrupts normal cell-cell interactions and strongly stimulates hepatocellular growth (Feitelson et al , 2002, Cadoret et al , 2001)

P53 is the most common molecular target in human carcinogenesis. However, a study of primary HCCs from many different origins shows that frequency of mutation of this tumour suppressor was low (Buetow et al , 1992). Usually mutations of p53 are recognised only in advanced stages of HCC and it is not a prerequisite for hepatocarcinogenesis (Teramoto et al , 1994). The most common mutations of p53 in HCC are the G to T transversions in codon 249 caused by aflatoxin exposure (Ozturk, 1991)

1.1.4 Diagnosis and Treatment

Generally, small HCC tumours cause few symptoms and the large functional reserve of the liver tends to delay symptomatic presentation (Johnson, 2000). As a result tumours usually present late and the cancer is generally large once discovered. The insidious nature of HCC in addition to tumour size and location represent the major limiting factors in the treatments available for the HCC patient.

1.1.4.1 Diagnosis

Continuous surveillance of cirrhotic patients is recommended in order to decrease tumour related deaths. This surveillance involves ultrasonography and the measurement

of serum alpha-fetoprotein (AFP) levels every six months (Bruix et al , 2001) Screening is usually only carried out in patients that can potentially be treated (Bruix et al , 2001) Ultrasonography can detect lesions as small as 0.5cm making it good for screening in cirrhotic patients (Okuda, 2000) However its level of detection of small nodules is low and other imaging techniques such as helical computerised tomography (CT) and magnetic resonance imaging (MRI) with contrast enhancement tend to provide greater accuracy of diagnosis (Johnson, 2000)

Serum AFP is elevated above the normal reference range of 0-10ng/mL in 50-80% of patients at the time of presentation making it a useful HCC marker (Johnson, 2000) Hepatocellular Carcinoma specific isoforms of AFP have also been discovered which are proving useful in differentiating between benign liver disease and HCC (Brebrowicz et al , 1981) However, many HCC tumours do not produce AFP or do so minimally (Okuda, 2000) Protein induced by vitamin K absence or antagonist II (PIVKA II) is also proving to be a viable marker of HCC in the absence of AFP levels (Kuromatsu et al , 1997)

1.1.4.2 Treatment and Prevention

Surgical resection, including complete hepatic transplant, remains as the most common treatment for HCC however, the majority of tumours are unresectable at the time of presentation This is primarily due to the size and location of the tumour, the presence of extrahepatic metastases and complications due to associated cirrhosis (Johnson, 2000) Tumour recurrence tends to complicate greater than 70% of cases at 5 years post resection representing both *de novo* tumours and true recurrence, usually due to secondary metastasis (Bruix and Llovet, 2002) The use of post operative adjuvant therapy using a synthetic retinoid polyphenolic acid has resulted in decreased tumour recurrence and increased survival in tumour resected HCC patients (Muto et al , 1996)

Liver transplantation can theoretically cure HCC and underlying cirrhosis in the absence of vascular tumour invasion (Suehiro et al , 2002) In patients with early HCC, cadaveric liver transplantation can achieve a 70% 5 year survival rate with a recurrence rate below 15% (Bruix and Llovet, 2002) However, there is a shortage of liver donors and the wait time involved tends to worsen the results of the liver transplantation (Bruix and Llovet, 2002) Moreover, immunosuppression after liver transplantation is also associated with increased recurrence (Bruix and Llovet, 2002) Living donor transplantation is the most feasible alternative however this procedure is associated with a high level of surgical morbidity for recipients (Suehiro et al , 2002)

Percutaneous treatments, which involve the destruction of neoplastic cells by chemical substances or by modifying the temperature of the tumour, are the best option for unresectable HCC Percutaneous ethanol injection has been reported to give long term survival rates as high as 70% in cirrhotic patients with small (<3cm diameter) tumours (Rust and Gores, 2001) These are similar survival rates as those seen for surgical resection however tumours recur in more than half of the patients two years post treatment (Rust and Gores, 2001) Other percutaneous treatments such as microwave coagulation or cryoablation are associated with many complications and do not tend to show significant survival advantage (Aguayo and Patt, 2001)

Palliative treatments such as arterial embolisation and systemic chemotherapy have been applied in more advanced tumours Chemoembolisation with agents such as gelatin causes tumour devascularisation which in turn cuts off the tumours nutrient and oxygen supply inducing extensive tumour necrosis Randomised studies demonstrate this therapy can induce HCC shrinkage however, it does not show any overall survival advantage (Aguayo and Patt, 2001) Systemic chemotherapy using single agents or combination therapies have not shown any clear advantage in terms of overall survival (Bergsland and Venook, 2000) The innate resistance of these tumours to

chemotherapeutic agents may be due, at least in part, to the drug metabolising functions of hepatocytes and the overexpression of multidrug resistance protein in these tumours (Di Maio et al , 2002)

Due to the poor success rates of most therapies the prevention of HCC development offers the greatest hope This includes the avoidance of exposure to carcinogens, avoidance of hepatitis infection and/or prevention of cirrhosis development in viral hepatitis Vaccination against HBV infection will greatly reduce HCC incidence worldwide A mass vaccination program against HBV was introduced in Taiwan, firstly for all children of mothers that were HBV carriers in 1984, and then universally in 1986 HBV carriage in these children has decreased approximately 10 fold and there has been a 50% reduction in the occurrence and mortality rate of HCC in those immunised (Chang et al , 1997) In the case of HCV infection there is currently no vaccine available and hence the prevention of the progression of chronic HCV infection to cirrhosis is more important (Forns et al , 2002) Interferon α (IFN- α) or its L-nucleoside analogue lamivudine (ribavirin) therapy has eradicated HCV infection in patients with persistent infection who are sustained responders to these drugs (Bergsland and Venook, 2000) A large retrospective study demonstrates that patients with chronic HCV infection show a significantly reduced incidence of HCC when treated with IFN- α (Ikeda et al , 2001)

1.1.5 Summary

HCC is one of the most common life threatening malignancies in the world This cancer generally arises from well defined causal factors which are viral hepatitis infection, aflatoxin exposure and chronic alcohol abuse Despite the identification of these aetiological agents, hepatocarcinogenesis remains poorly understood The molecular mechanisms leading to the development of HCC have only been partially

established and a great deal of further research remains to be performed. Currently surgical resection, including liver transplantation, offers the best cure for HCC, however, these therapies are hindered by tumour recurrence and/or donor shortages. A lack of suitable therapeutic strategies has led to a greater focus on prevention of HCC using antiviral agents and vaccination. Overall the outlook for HCC patients is bleak, however, a better understanding of the molecular and genetic basis of this cancer should lead to the development of more efficacious therapies.

1.2 Interleukin-6

1.2.1 Introduction

Cytokines are a group of low molecular mass proteins that are critical for cell-cell communication in multicellular organisms. Unlike hormones they are not stored in glands but are rapidly synthesised and secreted by different cell types, usually in response to specific stimuli. Cytokines are generally pleiotropic and carry out their actions in an auto-, para- or endocrine manner *via* specific cell surface receptors. They usually act in the picomolar/nanomolar range and their target cells are often adjacent to the producer cells making it difficult to detect cytokines in serum. Cytokines regulate growth, survival, differentiation and effector functions in target cells (Vilcek, 2003).

Interleukins are a group of cytokines that are produced by lymphocytes, monocytes and many other cell types in response to both antigenic and antigen non specific stimuli. Interleukins modulate inflammation and immunity by regulating growth, mobility and differentiation of lymphoid and other cell types (Vilcek, 2003).

Interleukin-6 (IL-6) was first cloned in 1980 during an effort to isolate the virally induced protein Interferon- β (IFN- β) and was subsequently named IFN- β 2 (Weissenbach et al., 1980). An antigen-non specific B cell differentiation factor that induced B cells to produce immunoglobulins was later discovered and named B-cell stimulatory factor 2 (BSF-2). This protein was identical to IFN- β 2 and was identical to other independently cloned proteins such as hepatocyte-stimulating factor, hybridoma/plasmacytoma growth factor and 26KDa protein (Naka et al., 2002). All of these names were resolved to the protein's current name, interleukin-6.

1.2.2 Structure of Interleukin-6

Human IL-6 has a molecular weight of between 21-28 KDa depending on the extent of post-translational modification including glycosylation and phosphorylation.

(May et al , 1988b, May et al , 1988a) The IL-6 peptide contains 212 amino acids (aa) of which a 28 aa hydrophobic signal peptide is cleaved resulting in the mature, 184 aa IL-6 protein (Keller et al , 1996) The protein contains four cysteines and two potential N-linked glycosylation sites (Hirano et al , 1986) X-ray crystallography and nuclear magnetic resonance (NMR) spectroscopy indicates the presence of a four- α -helix bundle arranged in an “up-up-down-down” topology (Heinrich et al , 1998) Mouse and rat IL-6 share approximately 42% and 58% homology respectively, to human IL-6 at the amino acid level however, they do not possess N-glycosylation sites and may only be O-glycosylated (Northemann et al , 1989, Van Snick et al , 1988) Human IL-6 can stimulate responsive cells from both rats and mice, probably due to the highly conserved central region of the protein common to each species (Keller et al , 1996) A virally encoded form of the IL-6 protein is produced by the human Kaposi’s sarcoma associated herpesvirus (KSHV) This protein is 204 aa long and shares 25% sequence homology with human IL-6 at the amino acid level The protein is considered to be a response to the host defence systems by the virus and is possibly involved in virus-induced neoplasia (Burger et al , 1998, Moore et al , 1996)

1.2.3 Expression of Interleukin-6

The human *IL-6* gene is located on chromosome 7p21-p14, contains four introns and five exons and is approximately 5 Kb long (Yasukawa et al , 1987) The gene contains three transcription initiation sites or TATA-like sequences (Yasukawa et al , 1987) The promoter of the *IL-6* gene contains several *cis*-acting response elements including those for AP-1, nuclear factor IL-6 (NF-IL6), NF- κ B and the multiple response element (MRE) (Keller et al , 1996) The expression of IL-6 can be induced by various factors including tissue plasminogen activator (TPA), tumour necrosis factor (TNF), interleukin-1 α (IL-1 α) and serum, all of which augment expression through the

MRE (Ray et al , 1989) The IL-6 promoter can be repressed by various combinations of *cis*-acting and *trans*-acting elements including retinoblastoma protein binding to the retinoblastoma control element (RCE) and the effects of various steroids such as glucocorticoids, oestrogens and androgens (Keller et al , 1996)

Interleukin-6 can be produced by both lymphoid and non-lymphoid cells such as monocytes, T cells, B cells, fibroblasts, mesangial cells, endothelial cells and several tumour cells (Naka et al , 2002) In normal individuals the circulating level of IL-6 in the blood is typically in the pg/mL range (Yamamura et al , 1998) These levels are moderately elevated in some cancers such as adult T cell leukaemia/lymphoma (median IL-6 concentration is 8pg/mL) and melanoma where the levels correlate closely with tumour burden (Mouawad et al , 1996, Yamamura et al , 1998) Large increases in circulating IL-6 levels are seen after surgery where blood concentrations often range between 30-430pg/mL (Sakamoto et al , 1994)

1.2.4 The Interleukin-6 Receptor

1.2.4.1 Class I Cytokine Receptors

The functional IL-6 receptor is a complex of two transmembrane glycoproteins that are members of the class I cytokine receptor superfamily The main characteristic of the receptors in this family is the presence of at least two fibronectin type III domains in the extracellular region (Keller et al , 1996) One of these domains contains four conserved cysteines while a second type III domain shows a Trp-Ser-x-Trp-Ser (WSxWS) motif (Heinrich et al , 1998) Cytokine receptors in this group include leukaemia inhibitory factor receptor, ciliary neurotrophic factor-receptor α , oncostatin M receptor β , interleukin-11 receptor α and the IL-6 receptor components, interleukin-6 receptor α (IL-6R α) and glycoprotein 130 (gp130)

1 2 4 2 IL-6R α

The human IL-6R α was first cloned from a human natural killer cell line, YT (Yamasaki et al , 1988) and then was later cloned from the hepatoma cell line, HepG2 (Schooltink et al , 1991) Human IL-6R α is an 80 KDa transmembrane glycoprotein consisting of 468aa The mature protein, which is 449 aa, has a 339 aa extracellular region, a 28 aa transmembrane domain and an 82 aa intracellular region (Yamasaki et al , 1988) The extracellular domain has two tandem fibronectin type III motifs which contain the four conserved cysteine residue and the WSxWS motif that are characteristic of this receptor family (Yamasaki et al , 1988) The intracellular domain does not possess intrinsic kinase activity (Yamasaki et al , 1988) and requires association with gp130 for active signalling The IL-6R α receptor component is expressed by many cell types including CD4+ and CD8+ T cells, hepatocytes, neurons, neutrophils and osteoblasts (Keller et al , 1996)

Human IL-6R α also exists in a soluble form that was first identified in urine (Novick et al , 1989) Soluble IL-6R α (sIL-6R α) is a 55 KDa protein that arises *via* proteolytic shedding of the membrane bound receptors or through alternative mRNA splicing (Heinrich et al , 1998) This alternative form of IL-6R α can form active signalling complexes with IL-6 and membrane bound gp130, thereby acting as an agonist in IL-6 signalling (Taga et al , 1989, Cichy et al , 1996) In healthy patients, the circulating levels of sIL-6R α typically ranges from 75-80ng/mL (Honda et al , 1992, Gaillard et al , 1993) The blood concentration of sIL-R α is elevated in many diseases including myeloma (130-190ng/mL) (Gaillard et al , 1993) and human immunodeficiency virus (170ng/mL) (Honda et al , 1992) The cell types expressing membrane bound IL-6R α do not fully represent the cell types that can respond to IL-6 since sIL-6R α in the presence of IL-6 can theoretically induce signalling in all cell types expressing gp130 alone (Peters et al , 1996)

1 2 4 3 Gp130

Glycoprotein 130 is the signal transducing component of the IL-6 receptor. The molecular weight of the membrane bound form of gp130 ranges from 130-145 KDa depending on the extent of glycosylation (Hibi et al, 1990). Human gp130 is an 896 aa long glycoprotein comprised of a 597 aa extracellular region, a 22 aa transmembrane domain and a 277 aa cytoplasmic segment (Hibi et al, 1990). There are six type III fibronectin domains in the extracellular region in addition to the expected WSxWS motif and the four conserved cysteine residues (Hibi et al, 1990). The cytoplasmic segment does not possess intrinsic tyrosine kinase activity but does contain at least three boxes to which cytoplasmic tyrosine kinases can bind (Murakami et al, 1993). The intracellular tail of gp130 also contains six tyrosine residues which act as docking sites for various signalling proteins during IL-6 type cytokine signalling (Yamanaka et al, 1996, Stahl et al, 1995). Glycoprotein 130 is ubiquitously expressed (Imada and Leonard, 2000).

Glycoprotein 130 can also exist in a soluble form referred to as sgp130. This form of the protein is the product of alternate mRNA splicing and occurs at a concentration of approximately 400ng/mL in the blood of healthy individuals (Narazaki et al, 1993). This protein acts antagonistically in IL-6 signalling and may function as a physiological buffer of circulating sIL-6R α activity (Heinrich et al, 1998). The soluble form of gp130 can only bind sIL-6R α when IL-6 is present (Heinrich et al, 1998).

1.2.5 Interleukin-6 Signalling

Interleukin-6 is a member of a family of related cytokines collectively termed IL-6 type cytokines. This family includes IL-6, leukaemia inhibitory factor, oncostatin M, ciliary neurotrophic factor, cardiotrophin-1, interleukin-11 and cardiotrophin-like

cytokine The common characteristic between these cytokines is that they all activate gp130 to induce signalling (Heinrich et al , 1998)

1 2 5 1 The Jak-STAT Pathway

Interleukin-6 signalling is initiated by the binding of IL-6 to IL-6R α at the cell surface (Figure 1 1) Interleukin-6 binds to IL-6R α with a very low affinity, however, this interaction triggers the formation of a high affinity complex comprising two molecules each of IL-6, IL-6R α and gp130 (Ward et al , 1994, Hibi et al , 1990) Signalling occurs when two trimeric complexes associate to form a hexamer where disulphide-linked homodimerisation of gp130 can occur (Ward et al , 1994, Ward et al , 1996, Murakami et al , 1993) Glycoprotein 130 associated tyrosine kinases, Janus kinases (Jaks), become activated upon stimulation Janus kinases are intracellular tyrosine kinases with molecular masses of 120-140 KDa The members of this protein family are Jak1, Jak2 and Tyk2 which are widely expressed and Jak3 which is predominantly found in haematopoietic cells (Imada and Leonard, 2000) The Jaks associate with the membrane proximal box1/box2 region of the cytoplasmic tail of gp130 (Heinrich et al , 1998) The dimerisation induced by ligand binding brings associated Jaks within proximity leading to their activation *via* inter- or intra- molecular tyrosine phosphorylation within the activation loop of their kinase domains (Feng et al , 1997) Interleukin-6 signalling leads to the activation of Jak1, Jak2 and/or Tyk2 (Lutticken et al , 1994, Narazaki et al , 1994, Stahl et al , 1994) The extent to which each Jak is activated varies among cells and may reflect levels of expression of each Jak (Stahl et al , 1994, Matsuda et al , 1994)

Activated Jaks phosphorylate tyrosine residues in the cytoplasmic tail of gp130 which in turn become docking sites for Signal Transducers and Activators of Transcription (STATs), primarily STAT3 and STAT1 (Stahl et al , 1995) Seven

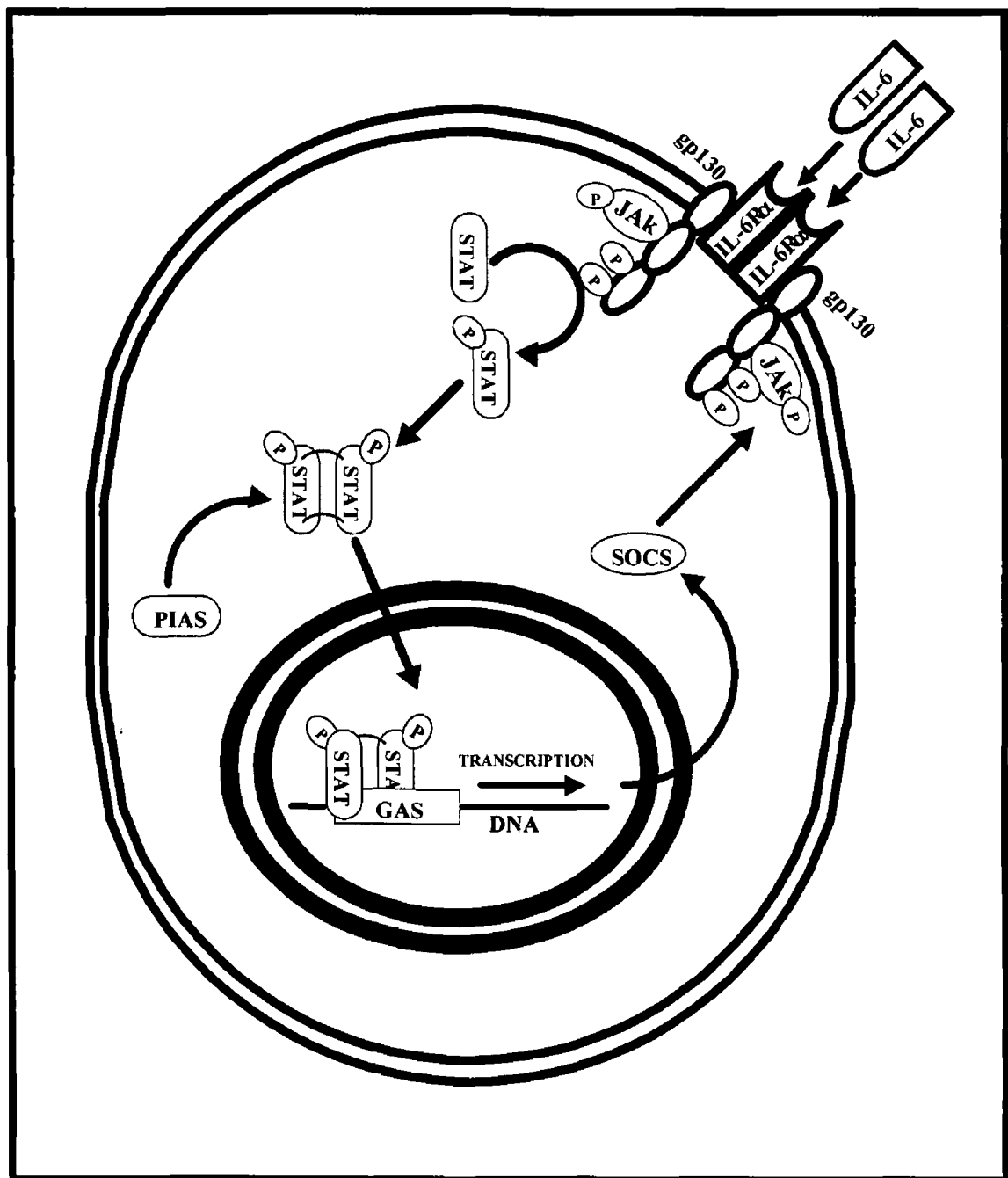


Figure 1 1 The Jak-STAT Pathway. IL-6 signalling is initiated by the binding of IL-6 to IL-6R α which can then recruit gp130 to form the IL-6 signalling complex. Gp130 associated Jaks are activated by phosphorylation which then proceed to phosphorylate tyrosine residues in the gp130 tail. STATs are recruited to the tail of gp130 and are phosphorylated. Phosphorylated STATs form dimers and translocate to the nucleus where they modulate gene expression. SOCS proteins can bind Jaks and activated tyrosine residues in the gp130 structure inhibiting IL-6 signalling while PIAS inhibit IL-6 signalling through interference with STAT dimers.

mammalian STAT genes have been identified, STAT 1, 2, 3, 4, 5a, 5b, and 6 (Bromberg and Chen, 2001) With the exception of STAT4 which is expressed only in myeloid cells and the testis, STATs are ubiquitously expressed (Bromberg and Chen, 2001) They have various domains in their structure including an oligomerisation domain and a leucine-zipper-like domain at the N terminus, a DNA binding domain in the middle, an Src homology 3 (SH3)-like domain, a SH2 domain and a transactivation domain at the C-terminus (Heinrich et al , 1998, Bromberg and Chen, 2001) STATs bind to the phosphorylated tyrosine residues in gp130 *via* their SH2 domains and do so only when these residues occur as part of specific amino acid sequences (Stahl et al , 1995, Gerhartz et al , 1996) STAT3 binds to phosphorylated tyrosine residues in a pYXXQ motif (Stahl et al , 1995, Gerhartz et al , 1996) while STAT1 only binds tyrosine in the more restricted pYXPQ sequence in gp130 (Gerhartz et al , 1996) Upon binding, STAT1 and STAT3 are tyrosine phosphorylated by the Jaks at activating residues within their kinase domains (Bromberg and Chen, 2001, Imada and Leonard, 2000) Activated STAT1 and STAT3 can form homo- and/or hetero- dimers Dimerisation is a prerequisite for DNA binding (Shuai et al , 1994) Active STAT dimers translocate to the nucleus where they modulate gene transcription (Zhang et al , 1995, Heinrich et al , 1998) Activated STATs bind to DNA gamma interferon activation site (GAS) elements/motifs (TTN₅AA) in the promoter regions of target genes leading to the stimulation or repression of their expression (Seidel et al , 1995) Serine phosphorylation of STAT1 and STAT3 partially regulates this transactivation domain activity (Zhang et al , 1995) The kinase responsible for serine phosphorylation appears to depend on both the signalling pathway and cellular context Many serine kinases have been implicated in this modification of STATs including ERKs (extracellular signal regulated kinases), p38 and JNK (Zhang et al , 1995, Imada and Leonard, 2000)

1 2 5 2 The Ras-MAPK Pathway

In addition to the Jak-STAT pathway, the Ras-MAPK pathway can also be activated following IL-6 binding (Figure 1 2) SH2 containing protein tyrosine phosphatase 2 (SHP2) is an ubiquitously expressed tyrosine phosphatase which contains two SH2 domains at its N terminus (Heinrich et al , 1998) This phosphatase binds to activated gp130 receptors through its SH2 domains and forms a link to the MAPK pathway (Stahl et al , 1995) SHP2 is rapidly recruited to the second phosphotyrosine from the membrane in the tail of gp130 and becomes phosphorylated in a Jak1/Jak2 dependent manner (Fukada et al , 1996, Schaper et al , 1998, Yin et al , 1997) Subsequently, activated SHP2 interacts with a Grb2-SOS Growth factor receptor bound protein/Son of Sevenless (Grb2-SOS) complex and/or the scaffold protein Grb2-associated binder-1 (Gab1) (Schiemann et al , 1997, Holgado-Madruga et al , 1996, (Schiemann et al , 1997, Holgado-Madruga et al , 1996, Fukada et al , 1996, Takahashi-Tezuka et al , 1998) Recruitment of the guanine nucleotide exchange factor, SOS, to the receptor converts inactive Ras-GDP to active Ras-GTP (Seger and Krebs, 1995) Ras phosphorylates the serine threonine kinase, Raf-1, which once activated can serine phosphorylate MEK (mitogen activated ERK kinase) In turn MEK phosphorylates both tyrosine and threonine residues in ERKs leading to their activation (Seger and Krebs, 1995) The active ERKs then phosphorylate various targets, including transcription factors and other kinases which proceed to regulate gene expression (Seger and Krebs, 1995)

1 2 5 3 Integration of IL-6 Signalling Pathways

Overall, the balance and interplay of the Jak-STAT and Ras-MAPK pathways ultimately determines the outcome of IL-6 signalling in each cellular context For example, IL-6 induces growth arrest and macrophage differentiation of the myeloid

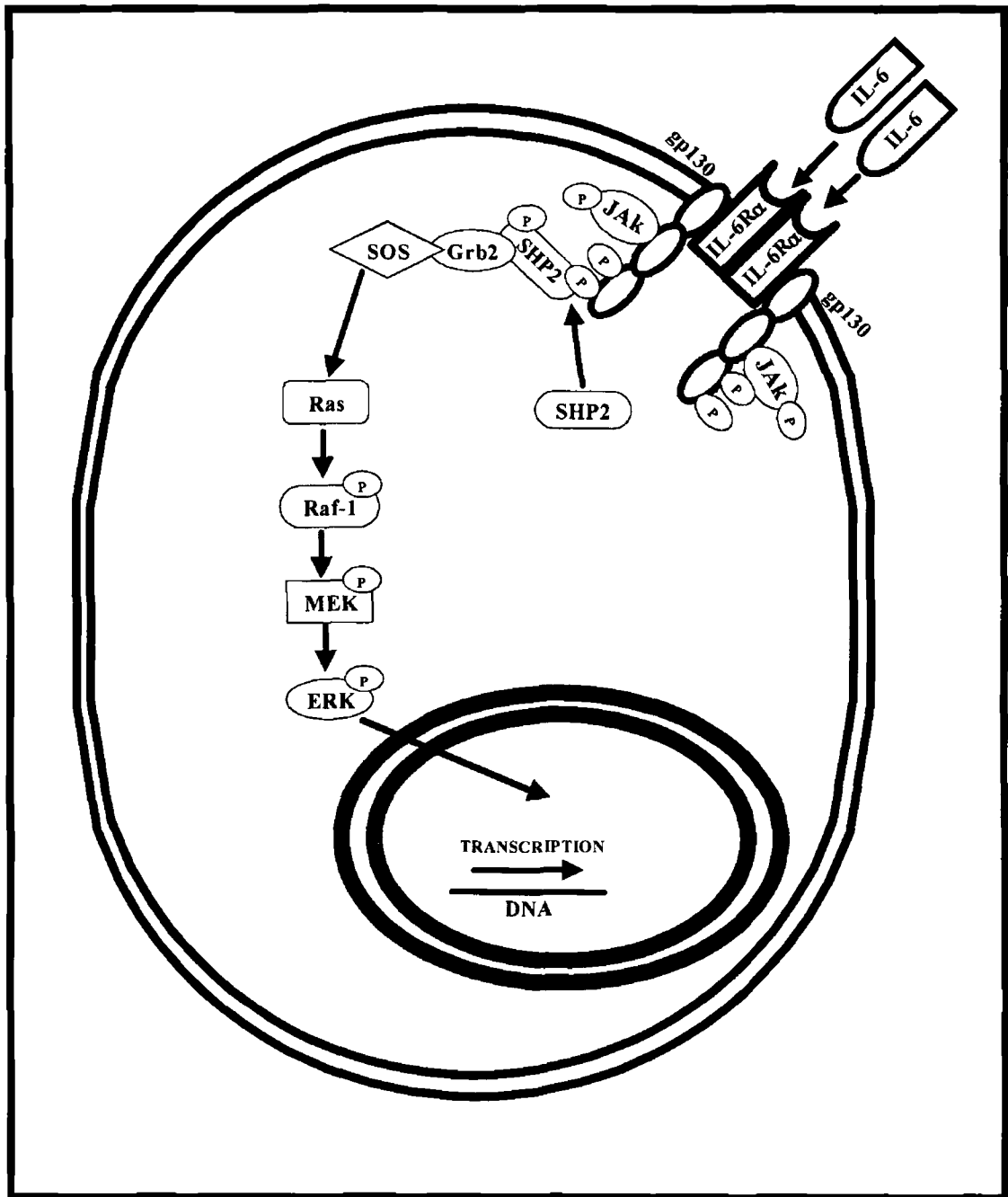


Figure 1.2 The Ras-MAPK Pathway IL-6 signalling is initiated by the binding of IL-6 to IL-6R α which can then recruit gp130 to form the IL-6 signalling complex. Gp130 associated Jaks are activated by phosphorylation which then phosphorylate tyrosine residues in the gp130 tail. SHP2 is recruited to the tail of gp130, becomes phosphorylated and recruits the guanine nucleotide exchange factor SOS via the adaptor protein, Grb2. SOS activates the small GTP binding protein, Ras. Ras proceeds to phosphorylate Raf-1 which once activated phosphorylates MEK. MEK phosphorylates ERK which then phosphorylates various transcription factors and kinases that regulate gene expression.

leukaemic cell line M1 (Minami et al , 1996, Nakajima et al , 1996) The expression of a dominant negative form of STAT3 in these cells inhibits IL-6 induced STAT3 activation and prevents growth inhibition and differentiation that is typically induced Furthermore, IL-6 stimulation of the dominant negative STAT3 expressing M1 cells leads to growth enhancement Therefore IL-6 is simultaneously inducing growth enhancing signals as well as growth arrest and differentiation signals, but the former are only apparent when STAT3 activation is suppressed (Minami et al , 1996, Nakajima et al , 1996) Similarly, in IL-6 induced differentiation of the PC12 pheochromocytoma cell line, the balance of Ras-MAPK and Jak-STAT signalling determines the outcome (Ihara et al , 1997) Interleukin-6 induces neurite outgrowth in PC12 cells that have been pre-treated with nerve growth factor (NGF) The activation of the Ras-MAPK pathway promotes this cellular differentiation while STAT3 activity blocks differentiation Nerve growth factor acts as a negative regulator of STAT3 activity in the differentiation process (Ihara et al , 1997)

Studies on gp130 mediated growth signals indicates that two distinct signals are required (Fukada et al , 1996) It was shown that in gp130 stimulated growth enhancement of pro-B cell lines both MAPK and STAT3 activation are necessary MAPK signalling stimulates cell cycle progression while STAT3 signalling prevents apoptosis *via* induction of anti-apoptotic proteins (Fukada et al , 1996, Naka et al , 2002)

More recently the PI3K/Akt pathway has been implicated in IL-6 signalling The mechanisms through which IL-6 activates this pathway are poorly understood but most likely involves the adaptor protein Gab-1 (Takahashi-Tezuka et al , 1998) PI3K is an enzyme that modifies specific phosphatidylinositides so that the serine threonine kinase B/Akt is recruited to the plasma membrane where it becomes activated by Phosphoinositide Kinase-1 Some of Akt's substrates include the forkhead transcription

factor FKHR and the pro-apoptotic factor Bad (Katso et al , 2001) The activation of PI3K has been observed to be important in the IL-6 mediated prevention of apoptosis in both basal cell carcinoma and hepatoma cells (Chen et al , 1999, Jee et al , 2002)

1 2 5 4 Negative Regulation of IL-6 Signalling

In most cases the activation of each IL-6 signalling pathway is transient indicating the presence of inherent negative regulatory mechanisms Many of these processes have now been established including receptor degradation and the expression of negative regulators

The removal of cytokine receptors from the cell surface is an efficient mechanism to terminate signalling After binding IL-6, the IL-6R α /IL-6 complex is internalised resulting in depletion of IL-6 surface binding sites within 30 to 60 minutes Reappearance of these receptors can take up to 8 hours and is sensitive to cycloheximide treatment This indicates receptor degradation and *de novo* protein synthesis is required for replenishment (Zohlhofer et al , 1992) A di-leucine internalisation motif in the cytoplasmic domain of gp130 has been established to be necessary for internalisation (Dittrich et al , 1994) however, it is unclear whether gp130 is degraded or recycled during this event (Heinrich et al , 1998)

The negative regulation of Jak-STAT signalling is also affected by a family of negative regulators called Protein Inhibitors of Activated STATs (PIAS) This family of constitutively expressed proteins comprises five mammalian members PIAS1, PIAS3, PIAS α , PIAS β and PIAS γ (Naka et al , 2002) The exact mechanisms through which these inhibitors negatively regulate STATs is not completely clear (Naka et al , 2002) PIAS1 and PIAS3 are the best understood members of this family PIAS1 specifically inhibits STAT1 signalling by preventing DNA binding (Liu et al , 1998) while PIAS3 blocks STAT3-DNA binding (Chung et al , 1997) The interaction between PIAS and

STATs requires tyrosine phosphorylation of STATs suggesting that PIAS may act *via* inhibition of dimerisation (Naka et al , 2002, Imada and Leonard, 2000)

A family of cytokine inducible inhibitors of the Jak-STAT pathway has also been discovered (Starr et al , 1997) Suppressors Of Cytokine Signalling (SOCS) are a family of 8 proteins (CIS, SOCS1-7) which negatively feedback on cytokine signalling induced through gp130 (Naka et al , 2002) They all contain a central SH2 domain and directly interact with the kinase domain of Jaks leading to reduced kinase activity (Endo et al , 1997) Interleukin-6 signalling causes rapid upregulation of CIS, SOCS1, SOCS2 and SOCS3 expression (Starr et al , 1997) The mechanism of inhibition by SOCS varies between members SOCS-1 binds to Jaks thereby inhibiting phosphorylation of gp130, STATs and the Jaks themselves (Starr et al , 1997, Naka et al , 1997) SOCS3, in addition to binding Jaks, also associates with specific phosphotyrosine residues within activated gp130 preventing signalling molecules, in particular SHP2, binding their target sites (Naka et al , 2002)

1.2.6 Physiological and Pathophysiological Functions of IL-6

Interleukin-6 plays a role in many diverse physiological responses IL-6 is a key signalling cytokine in the immune system, the development of inflammatory responses, the processes of liver regeneration and bone metabolism and the development of various cancers Aberrant IL-6 signalling has also been associated with the progression of numerous diseases

1.2.6.1 Physiological Functions of IL-6

Interleukin-6 is an important cytokine in the development of immune responses IL-6 induces the differentiation of activated but not resting B cells to produce

immunoglobulins (Muraguchi et al , 1988, Takatsuki et al , 1988) Normal resting B cells do not express the IL-6 receptor, expression only occurring on the surface of the activated cell type (Taga et al , 1987) Furthermore, IL-6 stimulates macrophage differentiation Treatment of the myeloid cell line, M1, with IL-6 results in the induction of phagocytic activity and morphologic changes characteristic of mature macrophages (Chiu and Lee, 1989) Interleukin-6 also plays a role in the development of T cells IL-6 stimulates the proliferation of thymic and peripheral T cells (Lotz et al , 1988, Uyttenhove et al , 1988) and, in co-operation with interleukin-1, can induce T cell differentiation to cytolytic T cells (Renauld et al , 1989) A role for IL-6 in the activation of natural killer cells has also been reported (Luger et al , 1989)

Interleukin-6 has been identified as an important regulator of bone metabolism Interleukin-6 induces osteoclastogenesis and osteoclast activity (Kurihara et al , 1990, Tamura et al , 1993) Osteoclasts are the large multinucleate cells derived from differentiated macrophages which are responsible for breakdown and resorption of bone tissue Through these effects IL-6 can contribute to bone remodelling

Interleukin-6 also plays a role in the reproductive system Interleukin-6 levels increase in the endometrium during the menstrual cycle suggesting a role for IL-6 in the preparation for implantation and the process of menstrual shedding (Tabibzadeh et al , 1995) Furthermore, IL-6 appears to be a paracrine regulator of the seminiferous epithelium, IL-6 exerting an inhibitory effect on meiotic DNA synthesis during spermatogenesis (Hakovirta et al , 1995)

In addition to these processes IL-6 has effects in the skin, blood and neural systems Interleukin-6 induces the proliferation of cultured human keratinocytes giving it a role in skin renewal (Grossman et al , 1989) Interleukin-6 also stimulates the proliferation of megakaryocytes, the large bone marrow cells that give rise to blood platelets (Hill et al , 1991, Navarro et al , 1991) In the neural system it has been

demonstrated that IL-6 is capable of inducing neural cell differentiation and proliferation (Ihara et al , 1997)

1 2 6 2 IL-6 and the Liver

In order to maintain homeostasis, inflammatory cytokines such as IL-6 are rapidly removed from the circulation. The liver is the main site of IL-6 degradation in the body. ^{125}I -IL6 injected into rats is cleared with a plasma half life of approximately two minutes (Castell et al , 1988, Castell et al , 1990a). After 20 minutes, approximately 80% of the IL-6 is removed from the circulation and is located in the liver. The IL-6 primarily accumulates around the hepatocytes and in particular around the bile canaliculi. Degradation products of this radiolabelled IL-6 eventually accumulate in the bile.

In addition to the degradation process, IL-6 has other important functions in the liver. The acute phase response is an inflammatory reaction which comprises fever, corticosteroid release and hepatic production of acute phase proteins (Streetz et al , 2000). Interleukin-6 stimulates hepatocytes to produce acute phase proteins such as serum amyloid A, fibrinogen, C-reactive protein, α_1 -antitrypsin while simultaneously suppressing the production of albumin (Ramadori and Christ, 1999, Gauldie et al , 1987, Castell et al , 1990b, Andus et al , 1987). Interleukin-6 deficient mice are unable to mount an inflammatory response to localised tissue damage and the induction of acute phase proteins is dramatically reduced in these animals (Fattori et al , 1994).

It was long considered that the induction of acute phase proteins was the main function of IL-6 in the liver, however, it later became apparent that IL-6 has a fundamental role in the process of liver regeneration. Partial hepatectomy (PHx) involves the removal of specific liver lobes accounting for approximately two thirds of the organs mass. The residual undamaged liver lobe increases in size in order to

compensate for the deficiency in liver mass (Fausto, 2000) During this regeneration process hepatocytes divide in a process which takes 24-48 hours and the rest of the cell lineages follow during the next five days before returning to quiescence (Fausto, 2000) It has been observed that tumour necrosis factor- α (TNF- α) and then IL-6 serum levels become elevated during the first hours after PHx in rats (Cressman et al, 1995) Furthermore, strong activation of STAT3 has been described during this period (Cressman et al, 1995) The proliferative response during liver regeneration in IL-6-/- mice is severely impaired (Cressman et al, 1996) The G1 phase is abnormal in these mice resulting in a reduced rate of DNA synthesis This further correlates with a lack of STAT3 activation and decreased expression of AP-1, Myc and cyclin D1 mRNA Injection of IL-6 prior to hepatectomy rescues this phenotype and prevents hepatic damage (Cressman et al, 1996) In TNF Receptor-1 knockout mice there is no increase in IL-6 serum levels following PHx (Yamada et al, 1997) In this instance mice show similar defects in liver regeneration to those observed in IL-6-/- mice and IL-6 injection again rescues this phenotype Collectively this has led to a model of cytokine signalling in liver regeneration that involves activation of IL-6 expression by TNF- α followed by hepatocyte priming by IL-6 (Streetz et al, 2000) Hepatocytes must be primed in this manner before they can respond to growth factors such as hepatocyte growth factor (HGF), transforming growth factor- α (TGF α) and epidermal growth factor (EGF) (Fausto, 2000)

IL-6 also has protective effects on the liver which are mediated in part by its ability to stimulate regeneration Following liver injury the levels of gut derived endotoxins increase and stimulate Kupffer and endothelial cells to produce acute reactant cytokines such as IL-6 and TNF- α (Clavien et al, 1996) These cytokines stimulate the repair process including hepatocyte proliferation IL-6 also protects the liver from liver ischaemia and promotes post-reperfusion hepatocyte proliferation

(Camargo et al , 1997) Administration of recombinant IL-6 almost completely blocks Con-A dependent or T cell associated liver failure through multiple mechanisms (Mizuhara et al , 1994) Protective effects of IL-6 have also been observed in liver injury induced by bile duct ligation, caecal ligation and puncture, sepsis and tetrachloride administration (Streetz et al , 2000)

1 2 6 3 IL-6 and Disease

Aberrant IL-6 signalling is linked to many human diseases including autoimmune diseases, chronic proliferative diseases, viral infections and malignancies. Increased levels of IL-6 signalling are observed in many autoimmune diseases. For example, rheumatoid arthritis (RA) is associated with elevated expression of IL-6 and sIL-6R in the synovial fluids (Kotake et al , 1996). Rheumatoid Arthritis is a systemic inflammatory disease characterised by the destruction of cartilage and bones in the affected joints (Naka et al , 2002). The observation that IL-6 and its soluble receptor are upregulated in this disorder gives a possible explanation for the increased osteoclastic activity observed and a mechanism for joint destruction (Kotake et al , 1996). Humanised anti-IL-6R antibody treatment has been proposed as a possible therapy for RA and has entered clinical trials (Naka et al , 2002).

Osteoporosis is another bone wasting disease which is closely linked to IL-6 signalling. As previously described, IL-6 stimulates osteoclast activity and increases bone resorption. The inhibition of IL-6 gene expression partially explains oestrogens ability to prevent osteoclast activation (Jilka et al , 1992, Girasole et al , 1992). In post-menopausal osteoporosis, the absence of oestrogens results in increased IL-6 levels demonstrating a possible mechanism for the increased bone breakdown associated with this disorder (Jilka et al , 1992, Girasole et al , 1992). Interleukin-6^{-/-} mice are

protected from bone loss associated with ovariectomy providing further evidence for IL-6 involvement in this disease (Poli et al , 1994)

Many proliferative disorders are intrinsically linked to IL-6 signalling. Overexpression of IL-6 in mice produces a syndrome resembling the systemic lymphoproliferative disorder Castleman's disease (Brandt et al , 1990). Furthermore, the epidermal hyperplasia seen in the psoriatic epithelium has been linked to IL-6 signalling and its ability to stimulate keratinocyte proliferation (Grossman et al , 1989).

The Human Immunodeficiency Virus-1 TAT protein induces the expression of IL-6 (Scala et al , 1994). This infection is associated with severe psoriasis, B cell lymphoma and Kaposi's sarcoma. The over expression of IL-6 may, in part, account for these associated diseases (Scala et al , 1994). In other infections, such as meningococcal septic shock, the median serum concentration of IL-6 can reach levels as high as 189ng/mL demonstrating a potential role for IL-6 in sepsis (Waage et al , 1989).

1 2 6 4 IL-6 and Cancer

Interleukin-6 contributes to the progression of numerous malignancies, being recognised as both a growth promoter and inhibitor. The immunomodulatory functions of IL-6 can also affect the advancement of a multitude of tumours. Dysregulated activation of IL-6 signalling pathways and signalling components has also been identified in the progression of several malignancies.

The immunogenic effects of IL-6 have an impact on the progression of many cancers *in vivo*. For example, recombinant human IL-6 (rhIL-6) administration in mice results in the regression of pulmonary micrometastases from weakly immunogenic tumours but not from non immunogenic tumours (Mule et al , 1992). *In vivo* generation of tumour specific cytotoxic T lymphocytes (CTLs) was observed in the responder

animals This indicates a potential role for IL-6 in the treatment of solid tumours that have the capacity to elicit T cell responses (Mulè et al , 1992) *In vitro* studies using a combination of B7-1 (CD80), IL-6 and interleukin-12 (IL-12) demonstrated an ability to stimulate the development of tumour specific CTLs (Gajewski et al , 1995) In this case B7-1 induced interleukin-2 production by CD8+ T cells, IL-6 stimulated their proliferation and IL-12 enhanced lytic ability (Gajewski et al , 1995) Interleukin-6 may also affect cancer progression through tumour specific antigen expression It has been demonstrated that IL-6 can act directly on human colon carcinoma cells and selectively increase Carinoembryonic antigen and Histocompatibility Leukocyte Antigen class I antigen expression providing a possible mechanism by which IL-6 suppresses tumour growth *in vivo* (Ullmann et al , 1992) The role of IL-6 in the recruitment and/or proliferation of tumour-associated macrophages has also been proposed as a possible anti-tumour effect of IL-6 *in vivo* (Bonta and Ben-Efraim, 1993)

Interleukin-6 can also influence proliferation of many cancer cells directly Interleukin-6 has been identified as an autocrine growth factor for various malignancies including renal cell carcinoma (Miki et al , 1989), plasmacytoma (Nordan et al , 1987), human multiple myeloma (Kawano et al , 1988, Jernberg et al , 1991, Levy et al , 1991, Okuno et al , 1992) and Kaposi's sarcoma (Miles et al , 1990) Interleukin-6 is also an autocrine growth factor for several lymphomas (Yee et al , 1989) including Hairy Cell Leukaemia in which it does not directly affect growth but rather mediates TNF-induced DNA synthesis *via* intracytoplasmic mechanisms (Barut et al , 1993) Interleukin-6 has additionally been reported to inhibit the growth of numerous other cancers Interleukin-6 inhibits the growth of human breast carcinoma cells, an effect that is further enhanced by the addition of sIL-6R (Novick et al , 1992, Chen et al , 1988) At concentrations that stimulate growth in B cell hybridomas and plasmacytomas, IL-6 was also shown to strongly inhibit growth in a number of leukaemia/lymphoma cell lines (Chen et al ,

1988) Interestingly, IL-6 behaves as a paracrine growth inhibitor in early stage melanoma cells however it switches to an autocrine growth stimulator within the same cell lineage during melanoma progression (Lu et al , 1992, Lu and Kerbel, 1993) It appears the advanced stages of melanoma become resistant to the inhibitory effects of IL-6 and, in some cases, can use it to support its own proliferation The IL-6 mediated inhibition of melanoma cells is sensitive to STAT3 and is associated with the upregulation of the cell cycle dependent kinase inhibitors p21^{waf1/cip1} (Florenes et al , 1999) and p27^{kip1} (Kortylewski et al , 1999) A STAT3 dependent growth inhibition in the prostate carcinoma cell line, LNCAP, has also been observed (Spiotto and Chung, 2000)

The dysregulated activation of STATs appears to be involved in both viral and oncogene-mediated cellular transformations STAT3 is constitutively activated in cells transformed by Src tyrosine kinase (Yu et al , 1995) Disruption of STAT3 signalling blocks the transformation of mouse fibroblasts by this oncoprotein (Bromberg et al , 1998) Constitutively activated STATs have also been described in cells transformed by viruses including Epstein Barr Virus and the Human T-cell lymphotropic virus-1 (Imada and Leonard, 2000) Furthermore, unremittingly active STATs are present in a variety of primary tumour cells including active STAT1 and/or STAT3 in multiple myeloma, leukaemia, lymphomas, melanoma, lung cancer and prostate cancer (Bowman et al , 2000) Bromberg et al have demonstrated that STAT3 can act as an oncogene (Bromberg et al , 1999) The expression of a constitutively activated form of STAT3, STAT3C, in immortalised fibroblasts leads to transformation as scored by colony formation in soft agar and tumour formation in nude mice (Bromberg et al , 1999) Dysregulated signalling is a possible reason for these constitutively activated forms of STAT3 An IL-6 autocrine or paracrine loop is responsible in the case of certain myeloma and prostate cancer cell lines (Lou et al , 2000, Catlett-Falcone et al ,

1999) In human HCC the expression of SOCS-1 is silenced by methylation resulting in uncontrolled STAT3 activation (Yoshikawa *et al* , 2001a)

The role of IL-6 in the advancement of HCC remains unclear Stimulation of the IL-6R α in the human HepG2 hepatoma cell line results in p27^{kpl} accumulation and growth arrest in the G1 phase (Klausen *et al* , 2000) Similarly, Kim *et al* have identified a growth inhibitory effect of IL-6 in the H-35 rat hepatoma cell line however the underlying mechanisms of this effect were not determined (Kim and Baumann, 1999) In contrast, IL-6 has been indicated as an autocrine growth factor in other hepatoma cells In the IL-6 producing HCC-M hepatoma cell line, proliferation is inhibited following IL-6 antisense treatment (Kumagai *et al* , 2002) Interleukin-6 has also been implicated in the survival of hepatoma cells as suggested by its ability to inhibit TGF- β -induced apoptosis in human Hep3B cells (Chen *et al* , 1999) The overexpression of IL-6 in a rat hepatocellular carcinoma cell line is linked to increased metastatic potential *in vivo* (Reichner *et al* , 1998) while the transfection of an IL-6 expression vector in a murine tumour cell line was inhibitory to *in vivo* tumour growth (Dougherty *et al* , 1994) These reports, coupled with the observation that serum levels of IL-6 are often increased in human HCC patients (Goydos *et al* , 1998, Giannitrapani *et al* , 2002), suggests a potentially significant role for IL-6 in this malignancy

1.2.7 Summary

Interleukin-6 is a pleiotropic cytokine with diverse functions in many biological systems throughout the human body Interleukin-6 signalling, which is transduced through the gp130 receptor, activates both the Jak-STAT and the Ras-MAPK pathways The interplay and balance between these stimulated pathways determines the ultimate outcome of IL-6 signalling in each cellular context Interleukin-6 has multiple effects in many physiological processes and is associated with the pathogenesis of numerous

autoimmune, hyperproliferative and infectious diseases. This cytokine has important regulatory functions in liver protein production, liver regeneration and has a protective role in liver failure. Interleukin-6 is also an important factor in the progression of many malignancies. Interleukin-6 has been identified as both a growth factor and in other cases a growth inhibitor of several cancer types. The effects of IL-6 in HCC remain poorly defined. Various reports have indicated possible functions for IL-6 in this cancer however no unified theory of its effects has yet been established.

1.3 Aims of the Present Study

Interleukin-6 is inextricably linked to normal hepatocyte proliferation and liver function. Several reports demonstrate growth regulatory effects of IL-6 in cancer progression. While previous studies have established an inhibitory effect of IL-6 on HCC progression, others have identified growth promoting and survival effects after IL-6 treatment. Past research on the effects of IL-6 in HCC has primarily been performed *in vitro* with only limited *in vivo* data currently available.

The current studies proposed to establish the effects of IL-6 in HCC using complementary *in vitro* and *in vivo* HCC models. The initial aim of these studies was to determine if HCC is associated with alterations in the tissue expression of IL-6 signalling components compared to normal liver. The next aim was to establish the effects of IL-6 signalling in cultured HCC cells and isolated hepatocytes primarily focusing on the activation of the Jak-STAT and Ras-MAPK pathways in addition to the expression and function of cell cycle regulatory proteins. These studies also aimed to establish the effect of IL-6 on HCC proliferation *in vitro*. The aim of the final section of these studies was to establish an alginate based cell microencapsulation system for sustained IL-6 delivery *in vivo*.

Chapter 2: General Methods

2.1 Animals

Male ACI rats (Harlan Inc , Indianapolis, IN, USA, 175-225g) were used in these studies. All experiments were approved by the University of North Carolina at Charlotte Institutional Animal Care and Use Committee (IACUC) and conform to the Care and Use of Laboratory Animal Guidelines.

2.2 Cell Culture and Cell Lines

2.2.1 Materials

Alpha's Modification of Minimum Essential Media (AMEM), Eagle's Minimum Essential Media (EMEM) with glutamine, foetal bovine serum (FBS, prime and dialysed), Fungizone (amphotericin B), 7.5% (w/v) sodium bicarbonate solution and phosphate buffered saline (PBS) were all purchased from Biosource (Camarillo, Ca, USA). Glutamax, 0.25% (v/v) trypsin-EDTA and Trypan Blue stain were purchased from Gibco/Invitrogen Life Sciences (Carlsbad, CA, USA). Methotrexate (amethopterin) was purchased from Calbiochem/EMD Biosciences (San Diego, CA, USA). Molecular grade dimethyl sulphoxide (DMSO) and isoflurane were purchased from Fisher Scientific (Pittsburgh, PA, USA). Gentamycin was purchased from Mediatech (Hendon, VA, USA). Tissue culture treated sterile flasks and plates were purchased from BD Biosciences (San Diego, Ca, USA). A bright line counting chamber/haemocytometer was purchased from Hausser Scientific (Horsham, PA, USA). Potassium chloride, sodium chloride, magnesium sulphate, sodium bicarbonate,

ethylenediaminetetraacetic acid (EDTA), lactic acid, pyruvic acid, glucose, potassium phosphate and collagenase were all purchased from Sigma-Aldrich (St Louis, MO, USA) Biocoat collagen coated plates were purchased from Becton Dickinson Laboratories (Bedford, MA, USA)

2 2 2 Cell Lines

The rat hepatoma cell line, H4IIE, was originally derived from the Reuber-35 hepatoma (Pitot et al, 1964) and was purchased from the American Type Culture Collection (ATCC, Manassas, VA, USA) A CHO (Chinese hamster ovary) cell line stably expressing IL-6 (CHO-IL6) and a mock transfected CHO cell line (CHO-CTRL) were a kind gift from Dr Leonard G Komaris and Dr Teresa Zimmers (University of Miami School of Medicine, Miami, FL, USA) These lines were generated by introduction of a plasmid vector containing human IL-6 complimentary DNA (CHO-IL6) or empty vector (CHO-CTRL) into DHFR-deficient CHO-DUXX cells by protoplast fusion followed by methotrexate selection Primary rat hepatocytes were isolated as described in section 2 2 8

2 2 3 Cell Culture Media

H4IIE cells and primary isolated hepatocytes were cultured in high serum media composed of EMEM with glutamine (2mM) supplemented with Fungizone (2.5µg/mL), gentamycin (50µg/mL), sodium bicarbonate (1.5mg/mL) and 10% (v/v) prime FBS For preparing stocks of H4IIE cells, a freezing media comprising EMEM, DMSO and prime FBS at a ratio of 3:1:5 was used

CHO cells were cultured in high serum media composed of AMEM supplemented with Fungizone (2.5µg/mL), gentamycin (50µg/mL), sodium bicarbonate (1.5mg/mL), Glutamax (2mM), methotrexate (0.2µM) and 10% (v/v) dialysed FBS

CHO cells were frozen in a freezing media containing dialysed FBS supplemented with 7% (v/v) DMSO

2 2 4 Cell Propagation

Both H4IIE and CHO cells were stored in cryo-vials submerged in liquid nitrogen. These vials were thawed by immersion in a 37°C water bath. Thawed cells were immediately placed in high serum media (HSM) and centrifuged at 300 x g for 3 mins. Media was aspirated and the cell pellet was resuspended in HSM. Cells were placed in a tissue culture flask (150cm²) and were grown to 90% confluency at 37°C in a 5% CO₂, humidified incubator.

2 2 5 Cell Passaging and Splitting

H4IIE or CHO cells were washed twice in PBS (37°C) and then trypsinised using 0.25% (v/v) trypsin-EDTA. Cells were incubated at 37°C for 3-5 mins until cells had detached prior to the addition of HSM to stop trypsin digestion. Cells were pelleted at 300 x g for 3 mins and resuspended in HSM. Viable cells were counted on a haemocytometer using trypan blue exclusion. Cells were then diluted appropriately for seeding in tissue culture flasks or plates and cultured at 37°C in a 5% CO₂, humidified incubator. A split ratio of 1:4 was used for further passaging of cells in tissue culture flasks (150 cm²) while seeding density in tissue culture plates was dependent on the experimental conditions required.

2 2 6 Cell Storage

H4IIE or CHO cells (150cm² flask) were washed twice in PBS and then trypsinised using 0.25% (v/v) trypsin-EDTA. Cells were incubated at 37°C for 3-5 mins until cells had detached prior to the addition of HSM to stop trypsin digestion. Cells

were pelleted at 300 x g for 3 mins and resuspended in cell freezing media. Cells were aliquoted into cryo-vials and placed in a Nalgene Cryo 1°C freezing container which allows a cooling rate of 1°C/min. This was placed at -80°C overnight and then vials were transferred to liquid nitrogen for long term storage.

2.2.7 H4IIE Cell Isolation

H4IIE cells were passaged alternatively between culture and animal. This prevents the complete adaptation of these cells to either the *in vitro* or *in vivo* environment and selects for optimal clonogenic characteristics as previously described (Evans and Kovacs, 1977). H4IIE cells were grown for three serial passages *in vitro* prior to their inoculation into the parenchyma of the left hepatic lobe of male ACI rats as described in section 2.3.1. The resulting tumour mass which developed after 14-16 days was resected and minced with sterile scissors in HSM. The suspension was placed in tissue culture dishes and incubated for 4h at 37°C. Cells were washed twice with PBS (37°C) and then grown to confluency in HSM at 37°C in a 5% CO₂ humidified, incubator.

2.2.8 Hepatocyte Isolation

Fresh hepatocytes were isolated from male adult ACI rats using a modification of the two step perfusion technique as initially described by Seglen et al (Seglen, 1976). Male ACI rats were anaesthetised using an isoflurane/oxygen mixture to a depth that abolished the hind leg withdrawal reflex. A mid ventral laparotomy was then performed and the hepatic portal vein was cannulated with tubing (polyethylene, 0.28mm i.d.) at a region proximal to bifurcation and attached by 3-0 (USP) nylon suture. Prewarmed (37°C) oxygenated Krebs's buffer (119mM NaCl, 1.2mM MgSO₄, 1.2mM KH₂PO₄, 4.65mM KCl, 25mM NAHCO₃, 0.1mM EDTA, 5mM C₃H₆O₃, 1mM C₃H₃O₃Na and

5mM $C_6H_{12}O_6$; oxygenated with 95% O_2 / 5% CO_2) was pumped at trickle rate into liver. The descending aorta was severed and the speed of pump delivering oxygenated Kreb's buffer was briefly increased (allowing the liver to swell slightly) forcing red blood cells from the liver and then returned to initial rate. The liver was removed from the rat and suspended in a liver perfusion system (Figure 2.1). Using this system the liver was initially perfused with oxygenated Kreb's buffer ($37^\circ C$) for 5 mins and then with a recirculating collagenase solution (1mg/mL in oxygenated Kreb's buffer; $37^\circ C$) for 10-12 mins. The uppermost layer of the liver was disrupted and cells released through gentle agitation in Kreb's buffer under sterile conditions. Cells were washed three times in Kreb's buffer and resuspended in high serum culture media. Cells were seeded in collagen coated six well plates at 2×10^6 cells/well and were allowed to attach for 4h at $37^\circ C$ in a 5% CO_2 , humidified incubator. Cells were washed in PBS and were quiesced using serum free cell culture media for 12h at $37^\circ C$ in a 5% CO_2 , humidified incubator.

2.3 HCC Tumour Model

2.3.1 H4IIE Tumour Model

In vivo studies were performed using a rat model of HCC that was initially described by Evans and Kovacs (Evans and Kovacs, 1977; Kovacs et al., 1977). H4IIE cells were cultured as described in section 2.2. Cultured H4IIE cells were washed twice in sterile PBS, trypsinised and then resuspended in sterile PBS at a concentration of 1×10^7 cells/mL. Male ACI rats were anaesthetised using isoflurane/oxygen mixture and a mid ventral laparotomy was performed. 0.1mL of resuspended H4IIE cells were injected directly into the parenchyma of the left hepatic lobe using a 30 gauge needle. Rats were sutured, allowed to recover and then maintained for 14-16 days on a 12h/12h light dark schedule with water and chow pellet *ad libitum*. This technique

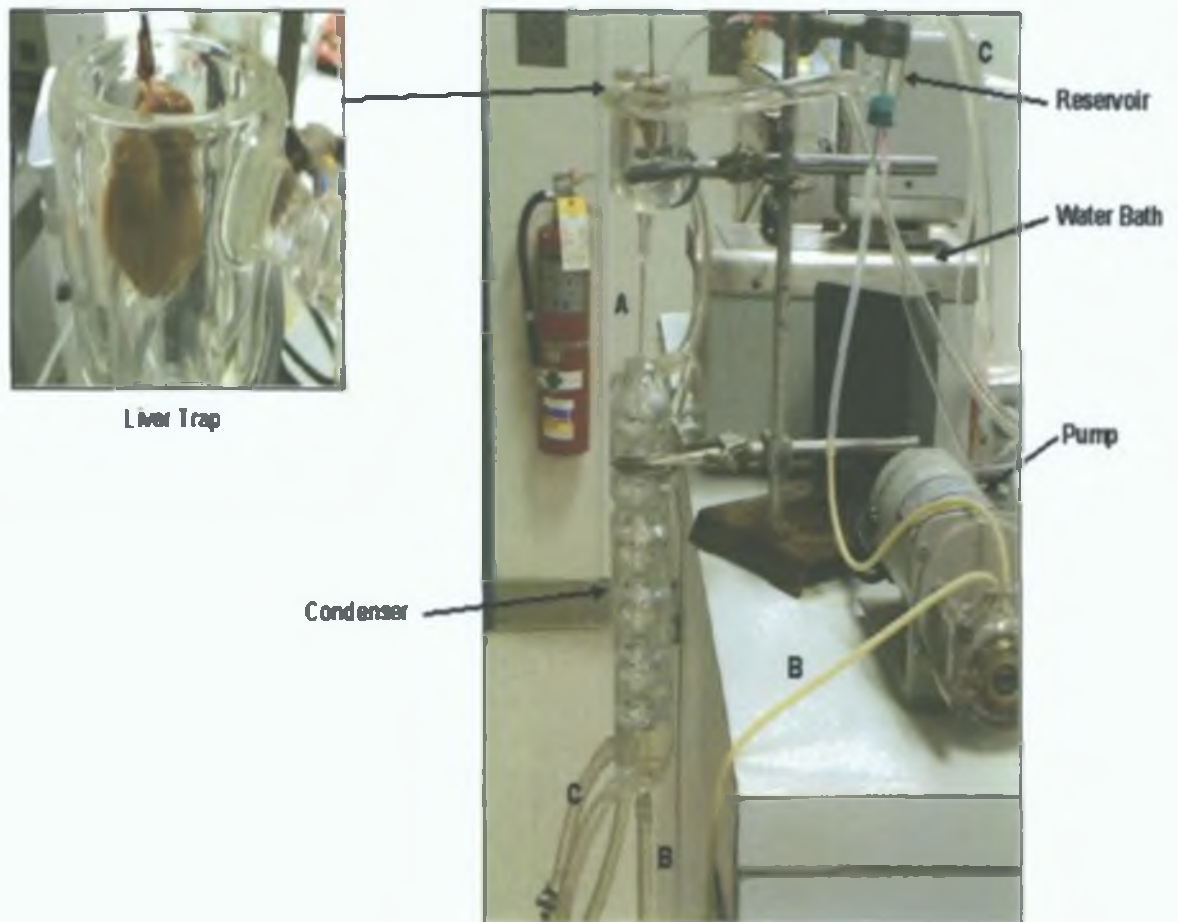


Figure 2.1 Hepatocyte isolation perfusion system. Kreb's buffer/collagenase mix was loaded into a condenser and oxygenated with 95% O₂/5% CO₂ which was delivered *via* tube A. Kreb's buffer/collagenase was pumped from the condenser *via* tube B to the reservoir. From the reservoir the solution was delivered to the liver which was suspended in the liver trap or recirculated back to condenser. Line C recirculated the Kreb's buffer/collagenase solution through the water bath to the reservoir in order to maintain the solution at 37°C.

resulted in reproducible HCC tumour formation Sham operated specimens were treated identically with the exception that the inoculation of the left hepatic lobe was performed using 0.1 mL PBS only

2.4 Preparation of Cell Lysates

2.4.1 Materials

HEPES, sodium chloride (NaCl), magnesium chloride (MgCl₂), Triton X-100, β-glycerophosphate, sodium dodecyl sulphate (SDS), sodium deoxycholate, dithiothreitol (DTT), Tris-HCl, sodium vanadate were all purchased from Sigma Aldrich (St Louis, MO, USA) Cell scrapers were purchased from Corning (Corning, NY, USA) Sonic Dismembrator model 100 ultrasonicator and Ultra Turrax T8 homogeniser were both purchased from Fisher Scientific (Pittsburgh, PA, USA) Complete protease inhibitor tablets (containing PMSF, aprotinin and leupeptin) were purchased from Roche Applied Science (Indianapolis, IN, USA)

2.4.2 Preparation of Cultured Cell Lysates for Protein Analysis

Primary hepatocytes and cell lines were cultured as described in section 2.2 Cells were rinsed with PBS (4°C) and lysed using ice cold mitogen activated protein kinase (MAPK) lysis buffer (25mM HEPES, 300mM NaCl, 1.5mM MgCl₂, 200μM EDTA, 1% (v/v) Triton X-100, 20mM β-glycerophosphate, 0.1% (w/v) SDS, 0.5% (w/v) sodium deoxycholate, 0.5mM DTT, 100mM sodium vanadate, 100μg/mL PMSF, 2μg/mL leupeptin, 2μg/mL aprotinin, pH 7.5) Plates were scraped and collected lysates were then sonicated and stored at -80°C prior to analysis

2.4.3 Preparation of Tissue Cell Lysates for Protein Analysis

HCC tumours were generated as described in section 2.3 Tumour, normal and

sham liver tissues were resected and immediately snap frozen in liquid nitrogen. To create whole cell tissue lysates, approximately 200-300mg of tissue was placed in MAPK lysis buffer (Section 2.4.2) and homogenised on ice. The preparation was then sonicated (4°C) and centrifuged at 500 x g for 5 mins (4°C). The resulting supernatant was collected, re-sonicated, and stored at -80°C prior to analysis.

To create cell membrane preparations approximately 200-300mg of tissue was placed in 50mM Tris-HCl containing 100µg/mL PMSF, 2µg/mL leupeptin and 2µg/mL aprotinin. The tissue was homogenised (4°C) until dispersed prior to centrifugation at 10,000 x g for 75 mins (4°C). The supernatant was discarded and the resulting pellet resuspended in 50mM Tris-HCl containing 100µg/mL PMSF, 2µg/mL leupeptin and 2µg/mL aprotinin. Samples were sonicated prior to storage at -80°C.

2.5 Immunoblotting

2.5.1 Materials

BCA Protein Assay Reagent Kit and CL-XPosure x-ray film were purchased from Pierce Biotechnology (Rockford, IL, USA). Disposable 96 well ELISA plates were purchased from Corning (Corning, NY, USA). Tris, acrylamide, N,N'-methylene-bisacrylamide, glycine, ammonium persulphate (APS), TEMED, Ponceau S solution, Tween-20, sodium chloride (NaCl), concentrated hydrochloric acid (HCL) and β-mercaptoethanol were all purchased from Sigma-Aldrich (St Louis, MO, USA). Laemmli buffer, Mini-Protean 3 electrophoresis system, Mini Trans-Blot module and blotting grade non fat dry milk (NFDM) were purchased from Biorad Laboratories (Hercules, CA, USA). Nitrocellulose membranes and ECL detection reagents were purchased from Amersham Biosciences (Piscataway, NJ, USA). See Blue Plus II prestained protein size marker was purchased from Invitrogen Life Sciences (Carlsbad,

CA, USA) X-ray film was developed using a SRX-101 Medical Film Developer (Konica, Mahwah, NJ, USA) and densitometry performed using the Kodak EDAS290 imaging software (Kodak, Rochester, NY, USA)

2 5 2 BCA Protein Assay

Protein concentrations were determined using a BCA protein assay kit Protein standards ranging between 0-2000 μ g/mL were prepared using bovine serum albumin (BCA kit) diluted in MAPK lysis buffer (Section 2 4 2) Standards and lysates were loaded in duplicate in a 96 well ELISA plate Working BCA reagent was prepared by mixing 50 parts of BCA reagent A with 1 part BCA reagent B and this was added to each well The plate was sealed and incubated at 37°C for 30 mins Absorbance at 562nm was measured on a μ Quant microplate reader (Biotek instruments, Winooski, VT, USA) The mean absorbance for each standard was corrected for mean zero standard absorbance and plotted against protein concentration The resulting standard curve was used to determine protein concentration of the unknowns

2 5 3 Western Blotting

SDS-PAGE gels were prepared using the Mini-Protean 3 electrophoresis system The lower gel (resolving gel) contained 10-15% (v/v) acrylamide/N,N'-methylene-bisacrylamide solution (30% (w/v) acrylamide, 0 8% (w/v) N,N'-methylene-bisacrylamide), 25% (v/v) SDS PAGE lower buffer (1 5M Tris, 0 014M SDS, pH 8 8), ultrapure water, APS (0 75mM) and TEMED (7mM) The upper gel (stacking gel) contained 13 5% (v/v) acrylamide/N,N'-methylene-bisacrylamide solution (30% (w/v) acrylamide, 0 8% (w/v) N,N'-methylene-bisacrylamide), 30% (v/v) SDS PAGE lower buffer (0 5M Tris, 0 014M SDS, pH 6 8), ultrapure water, APS (0 75mM) and TEMED (7mM) Wells for protein loading were created in the upper gel

Sample protein concentrations were equalised using MAPK lysis buffer (Section 2.4.2) and boiled with Laemmli working buffer (Laemmli buffer with 0.05% (v/v) β -mercaptoethanol) for 5 mins prior to loading on SDS-PAGE gels. Prestained protein size marker was loaded on gel. Proteins were electrophoresed using the Mini-Protean 3 electrophoresis system and electrophoresis running buffer containing 25mM Tris, 0.2M glycine and 3.5mM SDS. Proteins were transferred to nitrocellulose membranes in the Mini Trans-Blot module using electrophoresis transfer buffer (25mM Tris, 0.2M glycine, 20% (v/v) methanol). Membranes were stained with Ponceau S solution to confirm equal loading. Membranes were then blocked with blocking solution containing 5% (w/v) non fat dry milk (NFDM) in Tris buffered saline (TBS, 50mM Tris, 4mM MgCl₂, 140mM NaCl, 0.34% (v/v) conc HCl) with 0.1% (v/v) Tween-20 for 1h at room temperature (RT). Membranes were washed three times in TTBS (0.1% (v/v) Tween-20 in TBS). Membranes were incubated overnight with primary antibody at the appropriate dilution in blocking solution at 4°C. Membranes were washed 3 times in TTBS. Membranes were then incubated for 2h with appropriate peroxidase conjugated secondary antibodies diluted 1:5000 in blocking solution at RT. Membranes were washed 3 times in TTBS followed by 2 rinses in TBS. Membranes were incubated with ECL detection reagents and exposed to x-ray film. Film was processed using a Konica Medical Film Developer. Densitometric analysis of optical integrated volume was performed using Kodak EDAS290 imaging software.

2.6 IL-6 ELISA (Enzyme-Linked Immunosorbent Assay)

2.6.1 Materials

The BD Pharmingen TMB substrate reagent set was purchased from BD Biosciences (San Diego, CA, USA). Disposable 96 well ELISA plates were purchased

from Corning (Corning, NY, USA) Sodium carbonate (Na_2CO_3) and phosphoric acid (H_3PO_4) were purchased from Sigma-Aldrich (St Louis, MO, USA)

2.6.2 Rat IL-6 ELISA

ELISA for rat IL-6 was performed using a BD Opteia Rat IL-6 ELISA kit (BD Biosciences, San Diego, CA, USA) ELISA plates were coated with capture antibody (anti-rat IL-6) diluted 1:125 in Coating Buffer (0.1M NaHCO_3 , 34mM Na_2CO_3 , pH 9.5) overnight at 4°C All the following steps were performed at room temperature Wells were washed with wash buffer (WB, PBS with 0.05% (v/v) Tween-20) Plates were blocked with assay diluent (10% (v/v) FBS in PBS) for 1h Wells were washed again with WB prior to the addition of standards or samples to the plate in duplicate Standards were created using recombinant rat IL-6 Plates were incubated for 2h After washing with WB, the detection antibody (biotinylated anti-rat IL-6) was added to each well (1:250 in assay diluent) for 30 mins Plates were then washed with WB and incubated for 30 mins with enzyme reagent (avidin-horseradish peroxidase conjugate, 1:250 in assay diluent) Plates were washed again in WB Equal parts of TMB substrate components (tetramethylbenzidine and hydrogen peroxide) were combined and added to each well Plates were incubated for 30 mins in the dark prior to the addition of the stopping solution (1M H_3PO_4) Absorbance was measured at 450/570nm on a μ Quant microplate reader (Biotek Instruments, Winooski, VT, USA) The mean absorbance (450-570nm) for each standard was corrected for mean zero standard absorbance and plotted against rat IL-6 concentration The IL-6 concentrations of unknown samples were determined from this standard curve

2 6 3 Human IL-6 ELISA

ELISA for human IL-6 was performed using the BD Opteia Human IL-6 ELISA kit (BD Biosciences, San Diego, CA, USA) ELISA plates were coated with capture antibody (anti-human IL-6) diluted 1 250 in coating buffer (0 1M NaHCO₃, 34mM Na₂CO₃ , pH 9 5) overnight at 4°C All the following steps were performed at room temperature Wells were washed with wash buffer (WB, PBS with 0 05% (v/v) Tween-20) Plates were blocked with assay diluent (10% (v/v) FBS in PBS) for 1h Wells were washed again with WB prior to the addition of standards or samples to the plate in duplicate Standards were created using recombinant human IL-6 Plates were incubated for 2h After washing with WB the working detector was added to each well for 1h The working detector was biotinylated anti-human IL-6 and avidin horseradish peroxidase both diluted 1 250 in assay diluent Plates were washed again in WB Equal parts of TMB substrate components (tetramethylbenzidine and hydrogen peroxide) were combined and added to each well Plates were incubated for 30 mins in the dark prior to the addition of the stopping solution (1M H₃PO₄) Absorbance was measured at 450/570nm on a μ Quant microplate reader (Biotek Instruments, Winooski, VT, USA) The mean absorbance (450-570nm) for each standard was corrected for mean zero standard absorbance and plotted against human IL-6 concentration The IL-6 concentrations of unknown samples were determined from this standard curve

2.7 Statistics

Experimental values were expressed as mean values \pm the standard error of the mean (SEM) Statistical significance was calculated using the student's t-test for comparison of two groups and analysis of variance (ANOVA) followed by the Bonferroni post-hoc test for multiple comparisons Probability values of $p < 0 05$ were considered significant

Chapter 3: Altered Expression of IL-6 Signalling

Components in HCC

3.1 Introduction

Interleukin-6 is a pleiotropic cytokine with diverse biological functions (Naka et al, 2002) Liver specific functions of IL-6 include the stimulation of acute phase protein production (Ramadori and Christ, 1999, Gauldie et al, 1987, Castell et al, 1990b, Andus et al, 1987), protection against many forms of liver injury (Clavien et al, 1996, Camargo et al, 1997, Mizuhara et al, 1994) and stimulation of liver regeneration (Fausto, 2000, Streetz et al, 2000) During liver regeneration IL-6 plays a pivotal role in priming hepatocytes for proliferation Increased IL-6 serum levels and STAT3 activation in the liver are observed immediately following partial hepatectomy (PHx) (Cressman et al, 1995) Interleukin-6^{-/-} mice are characterised by a severely impaired proliferative response due to abnormal G1 phase progression after PHx (Cressman et al, 1996) This defect can be corrected by pre-operative IL-6 administration Interleukin-6 sensitises hepatocytes to growth factors such as hepatocyte growth factor (HGF), transforming growth factor- α (TGF α) and epidermal growth factor (EGF) (Yamada et al, 1997, Fausto, 2000) Further corroborating evidence of the importance of IL-6 signalling in hepatocellular proliferation is demonstrated in studies involving double transgenic mice expressing human IL-6 and soluble IL-6R (sIL-6R) In these studies co-expression of IL-6 and sIL-6R causes

nodular regenerative hyperplasia and adenoma development in the liver (Maione et al , 1998, Schirmacher et al , 1998)

Interleukin-6 is also involved with the progression of many malignancies. Interleukin-6 acts as an autocrine growth factor for many cancer types including renal cell carcinoma (Miki et al , 1989), plasmacytoma (Nordan et al , 1987), human multiple myeloma (Kawano et al , 1988, Levy et al , 1991, Okuno et al , 1992) and various lymphomas (Yee et al , 1989). Interleukin-6 also inhibits proliferation in other malignant cell types including human breast carcinoma cells (Novick et al , 1992, Chen et al , 1988), a number of leukaemia/lymphoma cell lines (Chen et al , 1988) and human melanoma cells (Florenes et al , 1999, Kortylewski et al , 1999). Furthermore, many cancer cell types are characterised by dysregulated expression of IL-6 signalling pathway components. Most notably, constitutively activated STATs are observed in a variety of primary tumour cells (Bowman et al , 2000). Active STAT3 can act as an oncogene (Bromberg et al , 1999) and is implicated in both viral and oncogene mediated cellular transformations (Bromberg et al , 1998, Yu et al , 1995). In the case of certain myeloma and prostate cancer cell lines, an IL-6 autocrine or paracrine loop is responsible for the constitutive activation of STAT3 (Catlett-Falcone et al , 1999, Lou et al , 2000) and, in some other cases, dysregulated SOCS expression is involved (Yoshikawa *et al* , 2001a).

Hepatocellular carcinoma, like other cancers, is characterised by aberrant cellular proliferation. The intrinsic link between IL-6 signalling and normal hepatocellular proliferation suggests a possible role for IL-6 in HCC progression. The function of IL-6 in HCC is unclear. IL-6 has been shown to inhibit human HepG2 (Klausen et al , 2000) and rat H-35 (Kim and Baumann, 1999) hepatoma cell growth *in vitro*. On the other hand, IL-6 acts as an autocrine growth factor for HCC-M hepatoma cells (Kumagai et al , 2002) and a survival factor for human Hep3B hepatoma cells.

(Chen et al , 1999) *in vitro* The relationship between IL-6 signalling and HCC progression *in vivo* remains poorly defined HCC cells transfected to overexpress IL-6 have increased metastatic potential *in vivo* (Reichner et al , 1998), while IL-6 expression in transfected HCC cells inhibited proliferation *in vivo* (Dougherty et al , 1994) In the clinical setting, serum levels of IL-6 are often elevated in human HCC patients (Giannitrapani et al , 2002, Goydos et al , 1998) although whether this is part of an autoimmune response in the cirrhotic liver or directly attributable to the tumour is unclear

The aim of the current study was to examine the expression of IL-6 signalling components in tumour and normal liver tissues from a rat model of HCC

3.2 Methods

3.2.1 Tumour Model

A rat HCC tumour model was established by direct injection of H4IIE cells into the left liver lobe of male ACI rats as described in section 2.3. Tumours were photographed using a Fuji Finepix S602 zoom camera (Fujifilm USA, Valhalla, NY, USA).

3.2.2 Preparation of Tissue Cell Lysates for Protein Analysis

Tissue cell membrane preparations and whole cell lysates were prepared from resected HCC, normal liver tissue (NL) from tumour burdened and NL from sham operated male ACI rats as described in section 2.4.3.

3.2.3 Immunoblotting

Western blots were performed as described in section 2.5. Antisera specific against gp130 (M-20), IL-6R α (M-20), p21^{waf1/cip1} (F-5), SOCS-1 (C-20), SOCS-3 (H-103) and STAT3 (H-190) were purchased from Santa Cruz Biotechnology (Santa Cruz, CA, USA). Antisera specific against p27^{Kip1} and Phospho-STAT3 (Tyr705) were purchased from Cell Signaling Technology (Beverly, MA, USA). All primary antibodies were diluted 1:1000 in 5% (w/v) non fat dry milk (NFDM)/0.1% (v/v) Tween/tris buffered saline (TBS) except for Phospho-STAT3 which was diluted 1:2000. Horseradish peroxidase conjugated goat anti-rabbit Ig and goat anti-mouse Ig were purchased from Jackson ImmunoResearch Laboratories (West Grove, PA, USA) and used at a dilution of 1:5000 in 5% (w/v) NFDM/0.1% (v/v) Tween/TBS.

3.2.4 RNA Isolation

3.2.4.1 Materials

TRIzol reagent was purchased from Invitrogen Life Technologies (Carlsbad, CA, USA) Chloroform, isopropanol, ethanol, sodium chloride, Tris, boric acid, ethylenediaminetetraacetic acid (EDTA), ethidium bromide and disodium citrate were purchased from Sigma-Aldrich (St Louis, MO, USA) DEPC treated water was purchased from Ambion (Austin, TX, USA) RNase free pestles and agarose were purchased from Fisher Scientific (Pittsburgh, PA, USA) Mini Sub Cell GT electrophoresis unit was purchased from Biorad Laboratories (Hercules, CA, USA) Kodak EDAS290 gel visualisation unit was purchased from Kodak (Rochester, NY, USA) Genesys 2 UV/Visible Spectrophotometer was purchased from Thermo Spectronic (Rochester, NY, USA) DNA loading buffer was purchased from Eppendorf (Hamburg, Germany)

3.2.4.2 Total RNA Isolation From Tissue

Approximately 100mg of resected tissue from HCC tumour burdened or sham operated male ACI rats (section 2.3) were snap frozen in liquid nitrogen and stored at -80°C prior to analysis To isolate RNA, liver tissue was placed in TRIzol and homogenised using an RNase free pestle 20% (v/v) chloroform was added and the sample agitated Samples were then centrifuged at 10,000 x g for 15 mins (4°C) The aqueous phase was removed to a fresh tube and 0.25 vol of isopropanol added followed by 0.25 vol of RNA precipitation solution (1.2M NaCl, 0.8M disodium citrate) The sample was then incubated at room temperature for 10 mins and centrifuged at 10,000 x g for 10 mins (4°C) The pellet was next washed twice in 75% ethanol, air dried and re-solubilised in DEPC water

3 2 4 3 Total RNA Isolation from Cultured Cells

Cultured H4IIE cells (section 2 2) were washed twice with PBS and collected in TRIzol. Samples were mixed and incubated at room temperature for 5 mins. 20% (v/v) chloroform was added and the sample agitated. The sample was centrifuged at 10,000 x g for 15 mins (4°C). The aqueous phase was removed to a fresh tube and 0.25 vol of isopropanol added followed by 0.25 vol of RNA precipitation solution (1.2M NaCl, 0.8M disodium citrate). The sample was then incubated at room temperature for 10 mins and centrifuged at 10,000 x g for 10 mins (4°C). The pellet was next washed twice in 75% ethanol, air dried and re-solubilised in DEPC water.

3 2 4 4 Determination of Total RNA Concentration and Integrity

RNA concentration was calculated using the spectrophotometric determination of sample absorbance at 260nm and the following equation

$$RNA\ CONCENTRATION\ (\mu g/mL) = 40(ABSORBANCE_{260nm}) \times DILUTION\ FACTOR$$

Where

RNA CONCENTRATION = Concentration of RNA (μ g/mL)

ABSORBANCE_{260nm} = Absorbance of sample at 260nm

In order to establish RNA integrity, RNA samples were combined with DNA loading buffer and run on a 2% (w/v) agarose gel made up in DEPC treated TBE buffer (45mM Tris-Borate, 1mM EDTA) containing ethidium bromide (2 μ L in 50mL agarose). Gels were placed in a gel electrophoresis unit containing DEPC treated TBE and run at 60V. Gels were visualised using a Kodak EDAS290 visualisation unit, intact RNA appearing as sharp, clear 18s and 28s RNA bands in denaturing gels (Figure 3 1)

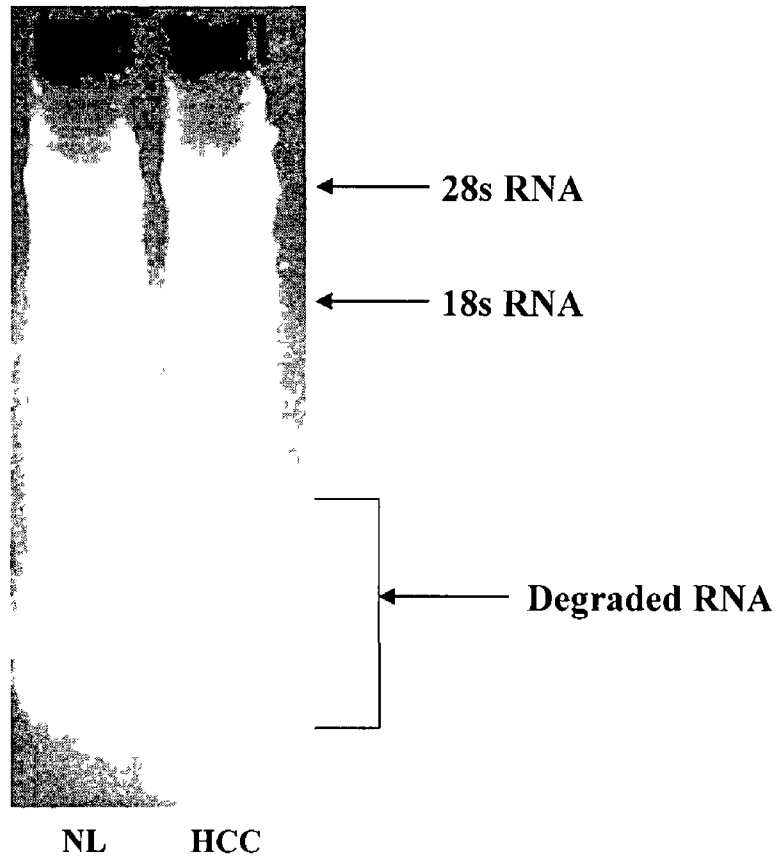


Figure 3 1 Sample RNA integrity gel Total RNA was isolated from normal liver resected from HCC burdened animals (NL) and HCC tissue RNA was electrophoresed on a 2% (w/v) agarose gel containing ethidium bromide and visualised under UV

3.2.5 Reverse Transcriptase – Polymerase Chain Reaction

3.2.5.1 Materials

Superscript™ first strand cDNA synthesis kit and RNaseOUT RNase inhibitor were purchased from Invitrogen Life Technologies (Carlsbad, CA, USA). ThermoPol 10x concentrate buffer, Taq polymerase and dNTPs were purchased from New England Biolabs (Beverly, MA, USA). PCR primers were synthesised by IDT (Coralville, IA, USA). Eppendorf Mastercycler Gradient Thermal Cycler was supplied by Eppendorf (Hamburg, Germany).

3.2.5.2 Method

First strand cDNA synthesis was performed on 5µg of total RNA using a Superscript™ first strand synthesis kit and Oligo(dT) as primers. RNA was initially incubated at 65°C for 5 mins in the presence of 0.5µg Oligo(dT)₁₂₋₁₈ and 10nmol of dNTP mix and then placed on ice for 3 mins. 9µL of reaction mixture (2µL 10X RT buffer, 4µL 25mM MgCl₂, 2µL 0.1M DTT, 1µL RNaseOUT) was added to each RNA sample/primer mix and samples incubated at 42°C for 2 mins. 1µL of Superscript II RT was added to each tube. Reverse transcription (RT) was carried out at 42°C for 50 mins. The RT reaction was terminated at 70°C for 15 mins. 1µL of RNase H was then added to each tube and samples were incubated for 20 mins at 37°C. 1µL of this RT product was then used in a polymerase chain reaction (PCR). PCR was carried out in 20µL (total volume) of reaction buffer (containing 2µL ThermoPol 10X buffer, 0.5µM of each primer, 5 units of Taq polymerase and 250µM dNTP's). The oligonucleotides used for amplification of the cDNA for IL-6, S9, gp130 and IL-6Rα were as described in Table 3.1.

After an initial 5 mins denaturation at 95°C, PCR was performed for 32 cycles in the case of IL-6, 25 cycles in the case of S9 and 22 cycles for the amplification of

Gene	Sense Primer	Antisense Primer
IL-6	5'ACAGTGCATCATCGCTGTT3'	5'CCGGAGAGGAGACTTCACAG3'
S9	5'GCTGAGACGACTTGTTCTGAATTG3'	5'TGGCATTCTTCCTCTTCACTCG3'
Gp130	5'TCAACTGTGGAACCATGTGG3'	5'TCCAAGTACACAGCATGTT3'
IL-6Rα	5'TCACAGAGCAGAGAATGGACT3'	5'GTATGGCTGATACCACAAGGT3'

Table 3 1 Primers used for the PCR amplification of the cDNA for IL-6, S9, gp130 and IL-6R α

both gp130 and IL-6R α using an Eppendorf Mastercycler Gradient Thermal Cycler. Each cycle for IL-6 amplification consisted of 30 secs denaturation at 95°C, 30 secs annealing at 55°C followed by 45 secs polymerization at 72°C. For S9 amplification a cycle consisted of 30 secs at 95°C followed by 30 secs at 60°C and then 45 sec at 72°C. For the amplification of both gp130 and IL-6R α a cycle consisted of 30 secs at 95°C followed by 30 secs at 56°C and then 45 secs at 72°C.

PCR products were combined with 2 μ L of DNA loading buffer and run on a 2% (w/v) agarose gels made up in TBE (45mM Tris-Borate, 1mM EDTA) containing ethidium bromide (2 μ L in 50mL agarose gel). Gels were placed in a gel electrophoresis unit filled with TBE and run at 60V. Gel images were captured using a Kodak EDAS 290 image capture system.

3.2.6 Histochemistry

3.2.6.1 Materials

Citrisolv clearing agent, Permount mounting media, haematoxylin, TissuePrep paraffin based embedding media, HistoPrep tissue capsules, xylene, microscope slides, glass coverslips and eosin were purchased from Fisher Scientific (Pittsburgh, PA, USA). Paraformaldehyde was purchased from Sigma-Aldrich (St Louis, MO, USA). GVA mounting solution and goat serum were purchased from Zymed Laboratories (San Francisco, CA, USA). HM 315 rotary microtome was purchased from Richard-Allan Scientific (Kalamazoo, MI, USA). ATP1 automatic tissue processor was purchased from Triangle Biomedical Sciences Inc (Durham, NC, USA). IX51 fluorescence microscope, IP LAB version 3.55 scientific image processing software, Fluoview FV500 IX70 confocal laser scanning biological microscope and Fluoview FV500 version 4.3 image processing software were all purchased from Olympus America (Melville, NY, USA). Phosphate buffered saline (PBS) was purchased from Biosource

(Camarillo, Ca, USA) Donkey serum and Texas Red conjugated donkey anti rabbit IgG were purchased from Jackson ImmunoResearch Laboratories (West Grove, PA, USA) Antisera specific against gp130 (M-20) and IL-6R α (M-20) were purchased from Santa Cruz Biotechnology (Santa Cruz, CA, USA)

3 2 6 2 Tissue Processing

Liver tissues resected from HCC tumour burdened and sham operated ACI rats (section 2 3) were fixed for 24h in 4% (w/v) paraformaldehyde at 4°C Tissue was placed in 50% (v/v) ethanol for 1h at 4°C followed by 1h incubation in 70% (v/v) ethanol (4°C) Tissue was placed in tissue capsules, dehydrated and paraffinised using an automatic tissue processor Tissue was embedded in paraffin blocks Tissue sections (5 μ m thickness) were cut using a rotary microtome and attached to positively charged microscope slides Slides were dried overnight at 37°C

3 2 6 3 Haematoxylin and Eosin (H & E) Staining

Liver tissues were processed as described in section 3 2 6 2 Tissues were deparaffinised by dipping slides in xylene for 5 mins and rehydrated by dipping slides in descending grades of ethanol (100%, 95%, 80%, 70%, 50% v/v) for 5 mins each Following incubation in PBS for 10 mins slides were dipped in haematoxylin for 15 mins Slides were washed in 80% (v/v) ethanol and then stained with eosin for 1 min Tissues were then dipped consecutively in 80% (v/v), 95% (v/v) and 100% (v/v) ethanol followed by xylene Coverslips were then mounted using Permount based mounting media and viewed on an Olympus IX51 microscope, images being captured using IP LAB software

3 2 6 4 Immunofluorescence

Liver tissues were processed as described in section 3 2 6 2 Tissues were deparaffinised by dipping slides in Citrisolv for 5 mins and rehydrated by dipping slides in descending grades of ethanol (100%, 95%, 80%, 70%, 50% v/v) for 5 mins each Tissues were then incubated in PBS for 20 mins Tissues were blocked with 5% (v/v) donkey serum (in PBS) Slides were washed in PBS and then incubated with appropriate primary antibody (1 100 in PBS) overnight in a humidified chamber (4°C) Slides were then washed in PBS and incubated with appropriate fluorophore conjugated secondary antibody (1 500 in PBS) for 2h at room temperature in a darkened, humidified chamber Slides were washed in PBS and coverslips mounted using GVA mounting media Slides were allowed to dry at 4°C before viewing on an Olympus Fluoview FV500 IX70 confocal laser scanning microscope Images were captured using Fluoview FV500 software

3.2.7 IL-6 ELISA

3 2 7 1 Materials

Heparin was purchased from Fisher Scientific (Pittsburgh, PA, USA) Amicon Ultra-15 centrifugal filters were purchased from Millipore (Billerica, MA, USA) *Escherichia coli* derived lipopolysaccharide (LPS) was purchased from Sigma-Aldrich (St Louis, MO, USA)

3 2 7 2 Sample Preparation for ELISA

Blood (5-7mL) was collected from HCC tumour burdened and sham operated male ACI rats (section 2 3) two weeks after H4IIE cell injection by cardiac puncture using a 27g needle and collected in a syringe containing 50 units heparin Blood was centrifuged at 1000 x g for 10 mins The plasma was then removed and concentrated

using an Amicon Ultra-15 centrifugal filter device (10 KDa cutoff) centrifuged at 3000 x g for 75 mins (4°C)

H4IIE cells were grown in culture (section 2.2) in the absence or presence of LPS (100ng/mL). Media samples were removed 24h later and concentrated using Amicon Ultra-15 centrifugal filter devices (10KDa cutoff) centrifuged at 3000 x g for 45 mins (4°C)

3.2.7.3 Rat IL-6 ELISA

Samples were collected and concentrated as described in section 3.2.7.2. An ELISA specific for rat IL-6 was performed on concentrated samples as described in section 2.6.2.

3.3 Results

3.3.1 Tumour Model

H4IIE cells inoculated directly into the left hepatic lobe of male ACI rats resulted in an encapsulated reproducible tumour mass forming after 14-16 days (Figure 3.2). H&E histological analysis performed on adjacent non-tumour bearing liver lobes and HCC specimens (Figure 3.3) showed a typical hepatocyte trabecular arrangement running radially from central veins and separated by sinusoids (Figure 3.3a). This trabecular structure was diminished in HCC due to reduced connective tissue (Figure 3.3b). HCC was further characterised by increased cellularity or nuclear crowding and neo-vascularisation (Figure 3.3b and 3.3c).

3.3.2 IL-6 Receptor Expression in HCC *In Vivo*

The expression of IL-6R α and gp130 components of the IL-6 receptor complex were measured in HCC, normal liver resected from tumour burdened animals (NL) and normal liver from sham operated animals (SH) by Western blot using antibodies specific against either IL-6R α or gp130. Using these antibodies single protein bands were detected at either 80kDa (IL-6R α) or 130kDa (gp130, Figures 3.4 and 3.5 respectively). Following protein transfer, data were analyzed for optical integrated volume. These data demonstrated no significant difference in IL-6R α expression in NL versus SH (Figure 3.4). In contrast, IL-6R α expression was significantly decreased in HCC *versus* normal liver from sham operated and HCC burdened animals (61.4 \pm 8.3% decrease in expression *versus* NL, n=4 per group, p<0.05, Figure 3.4). Analysis of gp130 data demonstrated no significant differences between NL and SH while gp130 expression was significantly decreased in HCC as compared to both NL and SH (60.4 \pm 9.3% decrease in expression *versus* NL, n=4 per group, p<0.05, Figure 3.5). Decreased IL-6 receptor expression in HCC *versus* normal tissue was

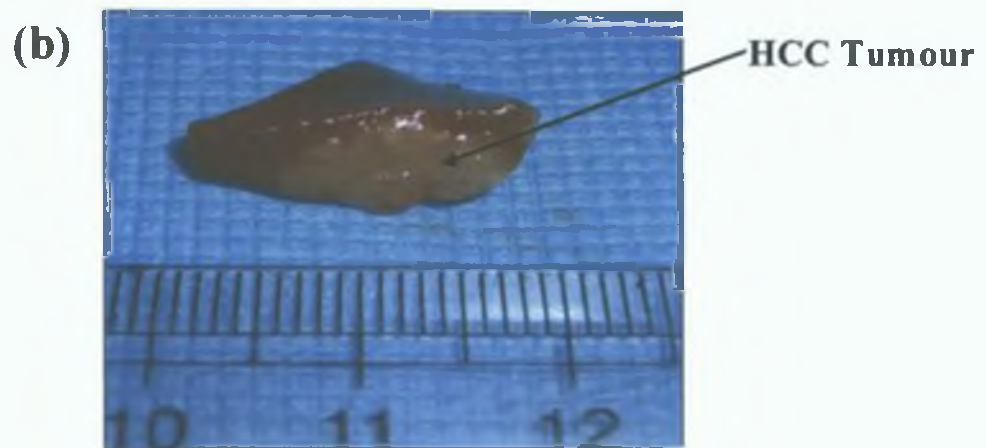
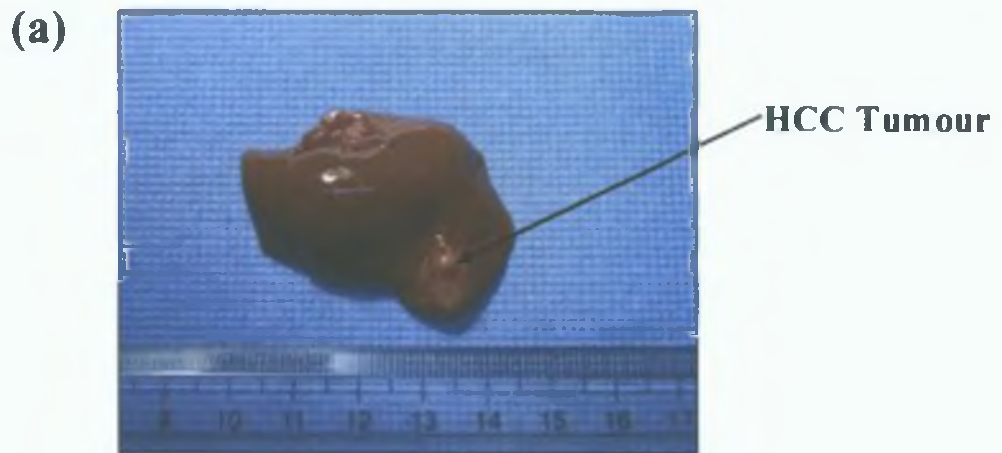
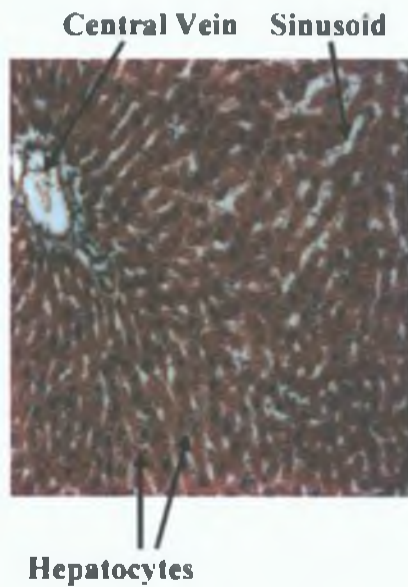
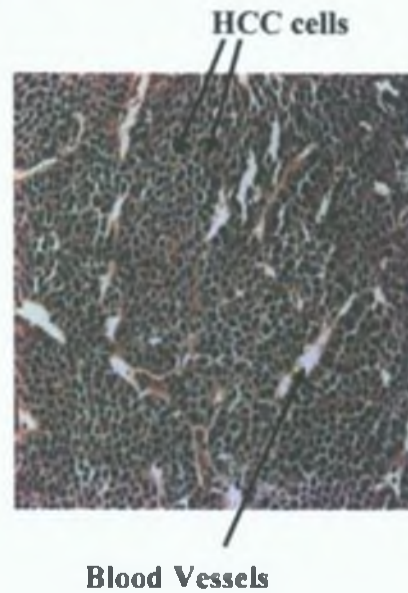


Figure 3.2 Photographs of HCC tumours. H4IIE cells were injected directly into the parenchyma of the left hepatic lobe of male ACI rats. After 14 days the liver was removed and photographed. a) External view of liver demonstrating large HCC tumour mass in the left hepatic lobe b) Cross section view of HCC tumour mass.

(a) NORMAL



(b) HCC



(c) TUMOUR BORDER

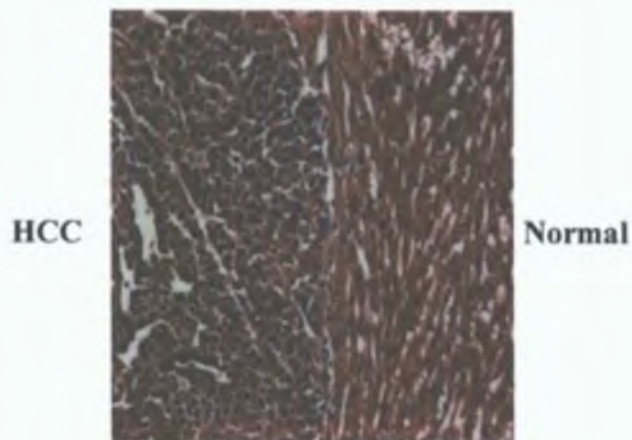


Figure 3.3 Histological sections of HCC and normal hepatic tissues stained with haematoxylin and eosin. H4IIE cells were injected directly into the parenchyma of the left hepatic lobe of male ACI rats. Sham operated animals were injected with PBS alone. After two weeks, HCC tumour tissue and normal liver tissue was resected, processed and stained with haematoxylin and eosin. Photomicrographs (20x) represent **a)** normal liver tissue from a sham operated rat, **b)** HCC tumour tissue and **c)** the HCC tumour/normal border.

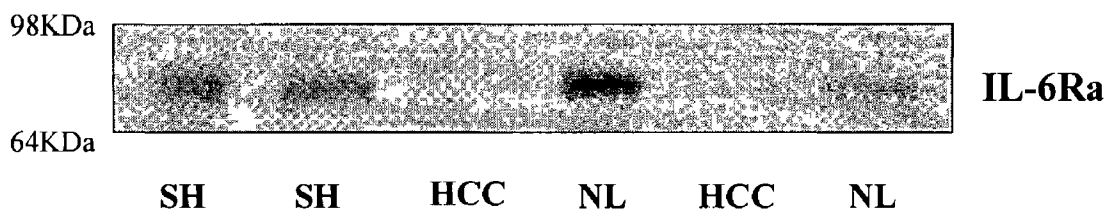


Figure 3 4 HCC is characterised by decreased expression of IL-6R α versus normal liver tissue *in vivo* Representative Western blot analysis performed on membrane lysates prepared from normal liver resected from sham operated animals (SH), normal liver resected from HCC burdened animals (NL) and HCC tissue using an antibody specific against IL-6R α . HCC tumours were established by direct injection of H4IIE cells into the left hepatic lobe of male ACI rats. Sham operated animals were injected with PBS alone.

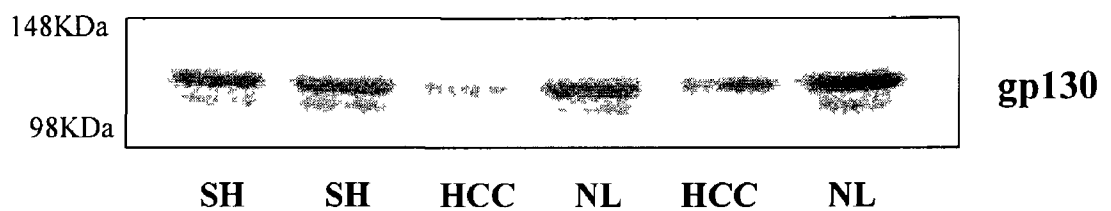


Figure 3 5 HCC is characterised by decreased expression of gp130 versus normal liver tissue *in vivo* Representative Western blot analysis performed on membrane lysates prepared from normal liver resected from sham operated animals (SH), normal liver resected from HCC burdened animals (NL) and HCC tissue using an antibody specific against gp130. HCC tumours were established by direct injection of H4IIE cells into the left hepatic lobe of male ACI rats. Sham operated animals were injected with PBS alone.

confirmed by immunofluorescent staining of liver tissue resected from tumour burdened rats. Tissue from the tumour/normal border was stained with antibodies specific for gp130 and IL-6R α (Figure 3.6, n=4). Specific staining for both gp130 (Figure 3.6a) and IL-6R α (Figure 3.6b) was abundant in normal tissue while tumour tissue stained only minimally for both of these receptor components. Further analysis indicated that both gp130 and IL-6R α were also downregulated at the RNA level in HCC. Semi quantitative RT-PCR analysis for gp130 (Figure 3.7a) and IL-6R α (Figure 3.7b) RNA expression in NL and HCC tissue detected single bands at ~375 bp and ~480 bp respectively. Densitometric analysis showed that IL-6R α RNA expression in HCC tissue was $55.85 \pm 16.4\%$ of that seen in NL (n=6 per group, $p < 0.05$, Figure 3.7b) while gp130 RNA expression was decreased to $58.88 \pm 10.38\%$ versus NL (n=6 per group, $p < 0.05$, Figure 3.7a). To ensure equal loading of samples, S9 ribosomal RNA was detected as an internal control (Figure 3.7c).

3.3.3 Expression and Activity of IL-6 Dependent Signalling Pathway Components in HCC *In Vivo*

To assess IL-6 dependent signalling in HCC and NL specimens, the expression and activity of STAT3 and downstream effectors (p21^{waf1/cip1} and p27^{Kip1}) in HCC, NL and SH specimens were assessed by Western blot analysis. Using an antibody specific against STAT3, a single protein band was detected at ~82kDa. Densitometric analysis of these data demonstrated no significant differences in total STAT3 expression between any of the samples analysed (Figure 3.8b, n=4 per group). In contrast, HCC was associated with increased STAT3 activity as assessed using an antibody specific against the tyrosine phosphorylated (Tyr705) isoform of STAT3 (pSTAT3) (n=4 per group, Figure 3.8a). Phospho-STAT3 expression was not detected in normal liver tissue

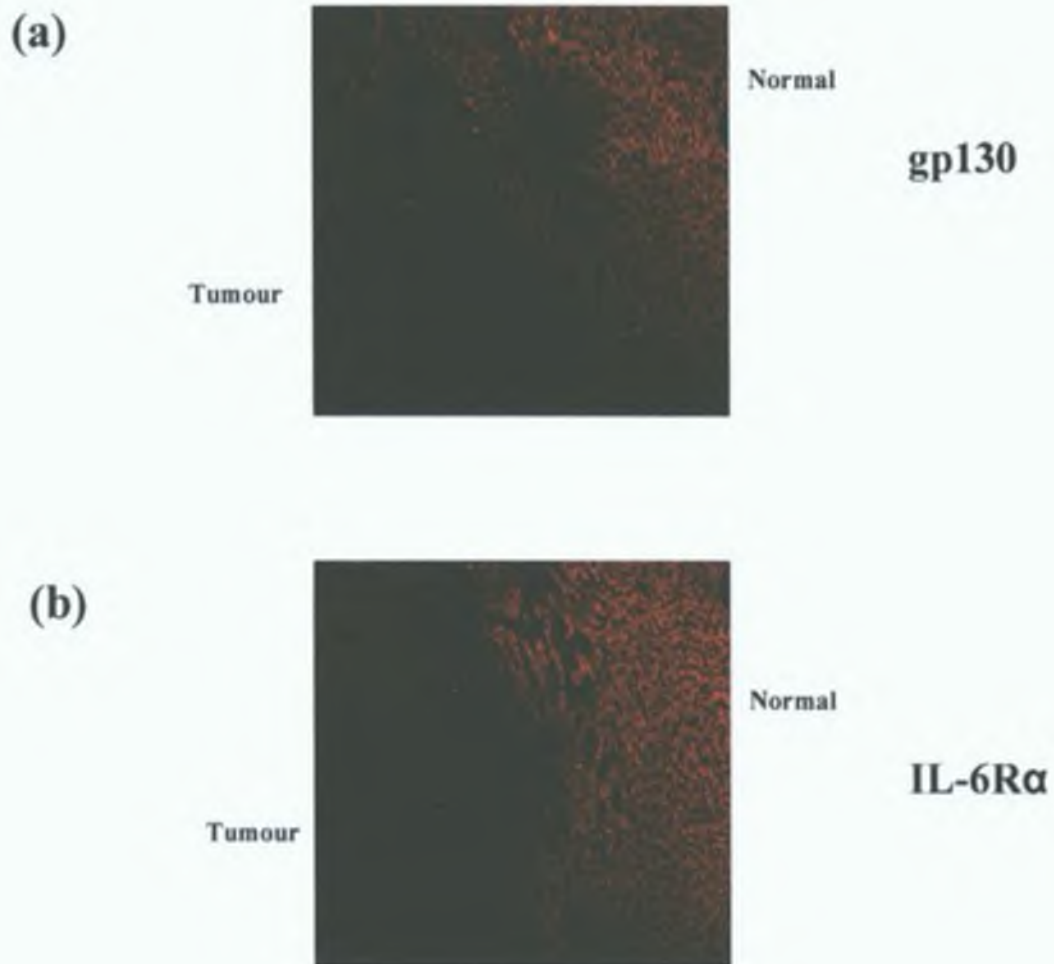


Figure 3.6 Immunofluorescent staining of IL-6 receptor components at the normal liver/HCC interface. Representative immunofluorescent staining for a) gp130 and b) IL-6R α in normal and HCC tissue at the tumour/normal border. HCC tumours were established by direct injection of H4IIE cells into the left hepatic lobe of male ACI rats. Resected tissue was processed and stained with antibodies specific against gp130 and IL-6R α . Texas Red conjugated secondary antibodies were used for detection.

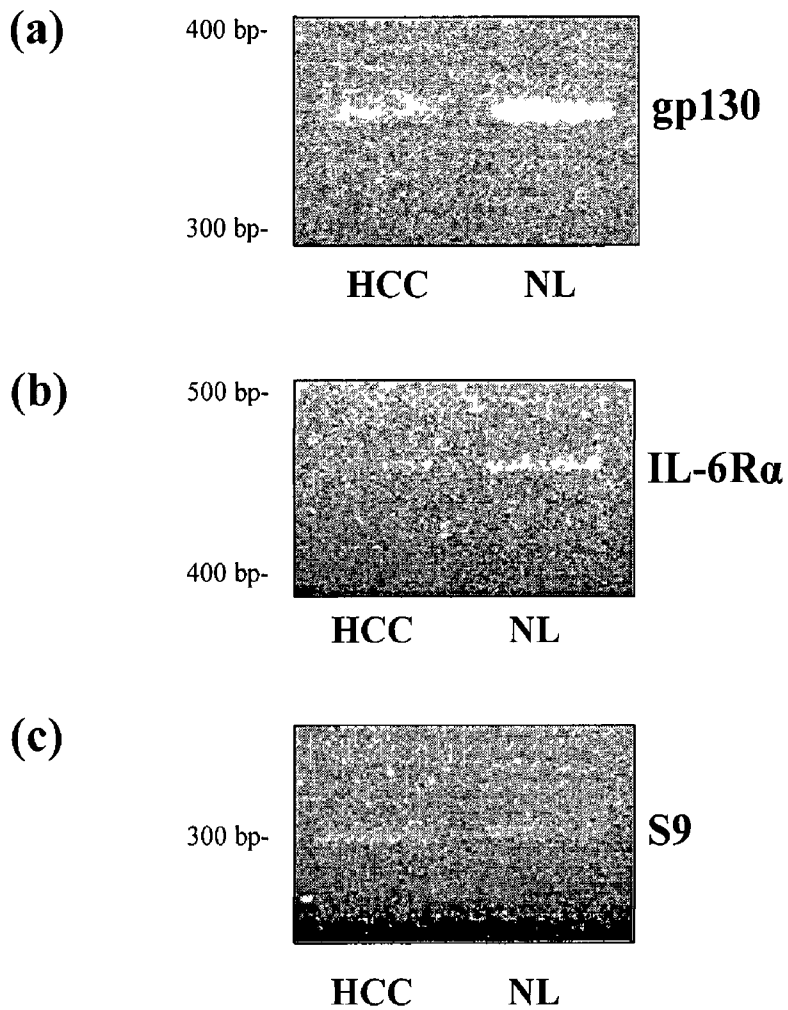


Figure 3 7 Decreased IL-6 receptor mRNA expression in HCC versus normal liver tissue *in vivo* RT-PCR analysis of RNA isolated from normal liver resected from HCC burdened animals (NL) and HCC tissue using primers specific for a) gp130, b) IL-6R α and c) S9 ribosomal RNA (control for equal loading) HCC tumours were established by direct injection of H4IIE cells into the left hepatic lobe of male ACI rats

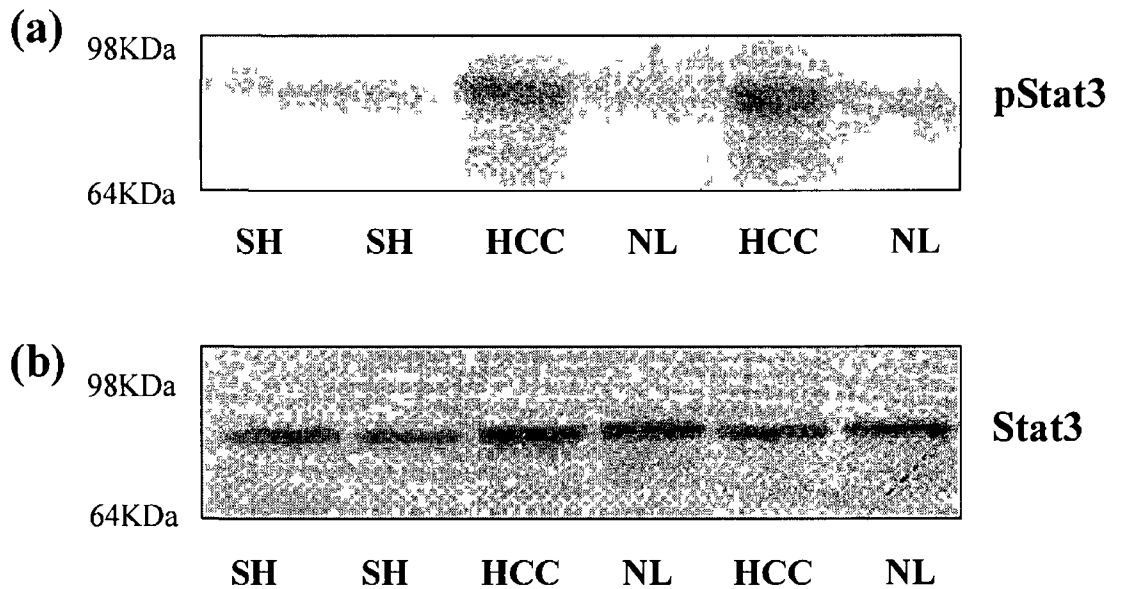


Figure 3 8 HCC is characterised by increased STAT3 activity *versus* normal liver tissue *in vivo* a) Representative Western blot analysis performed on whole cell lysates prepared from normal liver resected from sham operated animals (SH), normal liver resected from HCC burdened animals (NL) and HCC tissue using an antibody specific against active (phospho-) STAT3 b) Representative Western blot analysis performed on whole cell lysates prepared from normal liver resected from sham operated animals (SH), normal liver resected from HCC burdened animals (NL) and HCC tissue using an antibody specific against STAT3 HCC tumours were established by direct injection of H4IIE cells into the left hepatic lobe of male ACI rats Sham operated animals were injected with PBS alone

resected from tumour burdened animals or sham operated (Figure 3 8a) Analysis of downstream signalling pathways associated with STAT3 activation demonstrated similar expression patterns as those for STAT3 activity whereby increased amounts of p21^{waf1/cip1} and p27^{Kip1} were detected in HCC samples as compared to either NL or SH samples (Figure 3 9 and 3 10) Expression of p21^{waf1/cip1} was not detectable in normal or sham tissues while p27^{Kip1} expression in normal tissues was 41.5±8.1% that seen in HCC (n=4 per group, p<0.05) No differences in p21^{waf1/cip1} or p27^{Kip1} expression were detected between NL and SH samples (Figure 3 9 and 3 10)

Analysis of Jak inhibitor expression demonstrated upregulated expression of SOCS-1 and downregulated expression of SOCS-3 in HCC (Fig 3 11 and 3 12 respectively, n=4 per group) Western blot analysis using antibodies specific for SOCS-1 demonstrated increased SOCS-1 protein expression in HCC samples as compared to NL or SH samples SOCS-1 expression was not detected in NL or SH samples Immunoblotting with antibodies specific for SOCS-3 demonstrated significantly decreased SOCS-3 expression in HCC compared to NL or SH tissues (11.38±4.18% versus NL, p<0.05, n=4), no differences being detected between NL and SH

3.3.4 IL-6 Expression in HCC

To assess IL-6 production by HCC, IL-6 mRNA levels were determined by semi-quantitative RT-PCR. These experiments detected a single RT-PCR product at ~130bp's (Figure 3 13a) In these experiments, HCC was associated with increased IL-6 mRNA expression as compared to NL and SH samples IL-6 mRNA expression was not detected in NL or SH (Figure 3 13a) To ensure equal loading of samples, S9 ribosomal RNA was detected as an internal control (Figure 3 13b) Previous histological analysis of HCC tumours from these models demonstrated the presence of other cell types in HCC samples, most notably endothelial cells derived from tumour

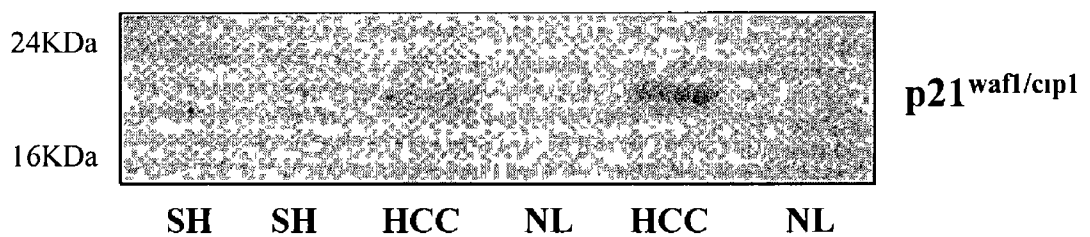


Figure 3 9 HCC is characterised by increased expression of p21waf1/cip1 versus normal liver tissue *in vivo* Representative Western blot analysis performed on whole cell lysates prepared from normal liver resected from sham operated animals (SH), normal liver resected from HCC burdened animals (NL) and HCC tissue using an antibody specific against p21^{waf1/cip1}. HCC tumours were established by direct injection of H4IIE cells into the left hepatic lobe of male ACI rats. Sham operated animals were injected with PBS alone.

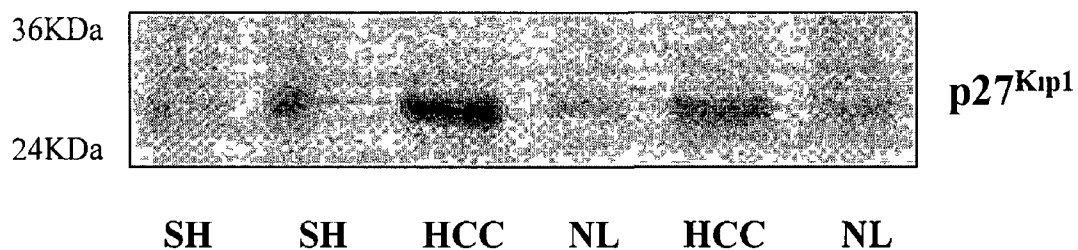


Figure 3 10 HCC is characterised by increased expression of p27^{Kip1} versus normal liver tissue *in vivo* Representative Western blot analysis performed on whole cell lysates prepared from normal liver resected from sham operated animals (SH), normal liver resected from HCC burdened animals (NL) and HCC tissue using an antibody specific against p27^{Kip1}. HCC tumours were established by direct injection of H4IIE cells into the left hepatic lobe of male ACI rats. Sham operated animals were injected with PBS alone.

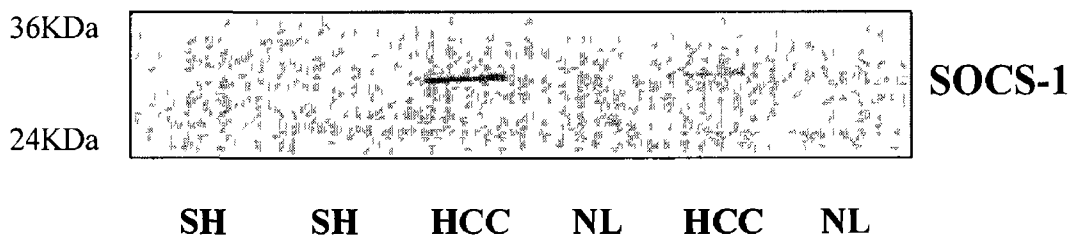


Figure 3 11 HCC is characterised by increased expression of SOCS-1 versus normal liver tissue *in vivo* Representative Western blot analysis performed on whole cell lysates prepared from normal liver resected from sham operated animals (SH), normal liver resected from HCC burdened animals (NL) and HCC tissue using an antibody specific against SOCS-1. HCC tumours were established by direct injection of H4IIE cells into the left hepatic lobe of male ACI rats. Sham operated animals were injected with PBS alone.

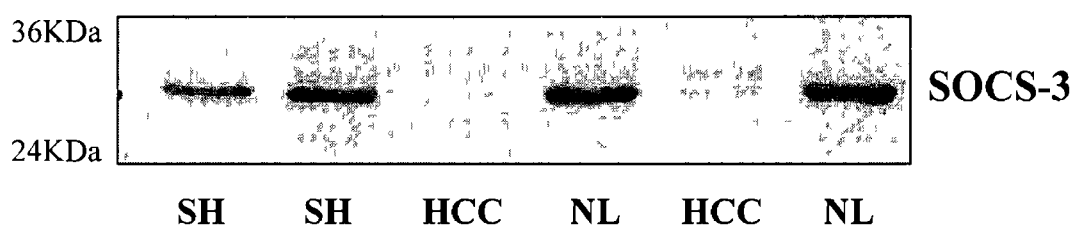


Figure 3 12 HCC is characterised by decreased expression of SOCS-3 versus normal liver tissue *in vivo* Representative Western blot analysis performed on whole cell lysates prepared from normal liver resected from sham operated animals (SH), normal liver resected from HCC burdened animals (NL) and HCC tissue using an antibody specific against SOCS-3 HCC tumours were established by direct injection of H4IIE cells into the left hepatic lobe of male ACI rats Sham operated animals were injected with PBS alone

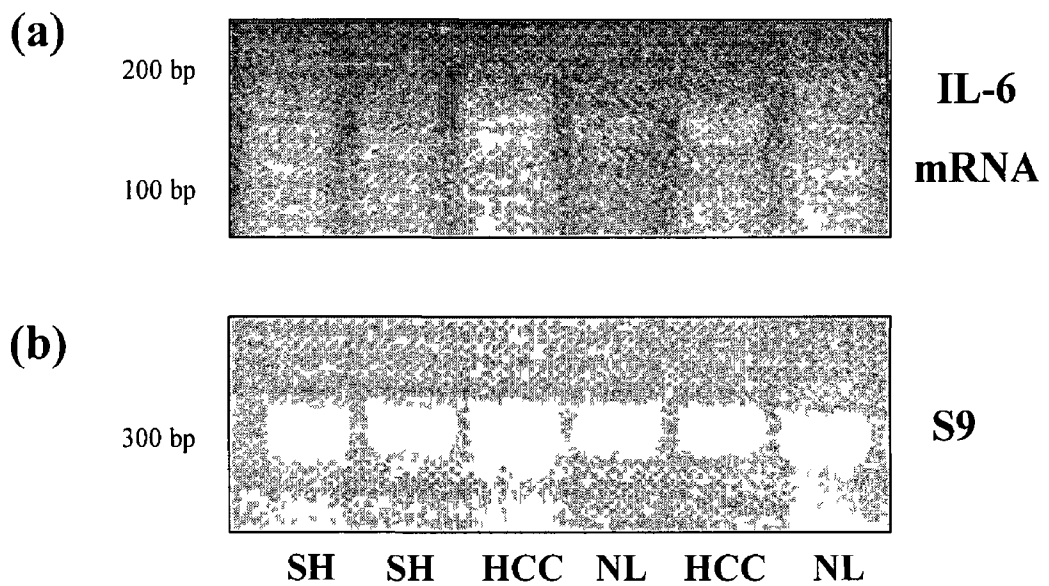


Figure 3 13 Increased IL-6 mRNA expression in HCC versus normal liver tissue *in vivo* RT-PCR analysis of RNA isolated from normal liver resected from sham operated animals (SH), normal liver resected from HCC burdened animals (NL) and HCC tissue using primers specific for **a)** IL-6 and **b)** S9 ribosomal RNA (control for equal loading) HCC tumours were established by direct injection of H4IIE cells into the left hepatic lobe of male ACI rats Sham operated animals were injected with PBS alone

neo-vascularisation and the possibility of increased blood derived cells in the tumours. To determine if the increased IL-6 mRNA detected in HCC samples is from HCC cells, and not other cell populations, pure populations of isolated H4IIE cells were analysed in culture in the absence or presence of lipopolysaccharide (LPS). These data demonstrated detectable basal IL-6 mRNA expression in H4IIE cells which were significantly elevated following LPS stimulation (2.5 fold increase, $p < 0.05$, $n=4$, Figure 3.14a). S9 ribosomal RNA acted as an internal loading control (Figure 3.14b).

IL-6 protein expression from plasma of sham operated and HCC tumour burdened animals were next assessed using a rat IL-6 specific ELISA. These failed to provide detectable levels of IL-6 in either sham operated or HCC burdened animals even following plasma concentration using Amicon Ultra-15 centrifugal filter devices (Figure 3.15). Plasma concentration was initially carried out in filters with 10,000Da cutoff membranes. Due to high albumin levels present in plasma, the retentate proved too viscous for use in ELISA and limited the achievable concentrating factor. In an effort to alleviate this problem a pre-filtration step using a filter with a 50,000Da cutoff was added to this procedure. This step precleared the albumin from the plasma and allowed a higher achievable concentration factor. However, plasma IL-6 still remained undetectable (Figure 3.15). To determine whether HCC cells were capable of producing IL-6, H4IIE cells were cultured in the presence or absence of LPS (100ng/ml). These data demonstrated no detectable levels of IL-6 in the media without cells. Following 24h of culture IL-6 was detected at a level of 2.2 ± 1.5 pg/ml in media removed from untreated cells (Figure 3.15, $n=6$ separate experiments per group assayed in duplicate). Treatment with LPS for 24h led to significantly increased IL-6 levels in media 22.5 ± 5.0 pg/ml as compared to media from untreated cells ($n=6$ separate experiments per group assayed in duplicate, $p < 0.05$).

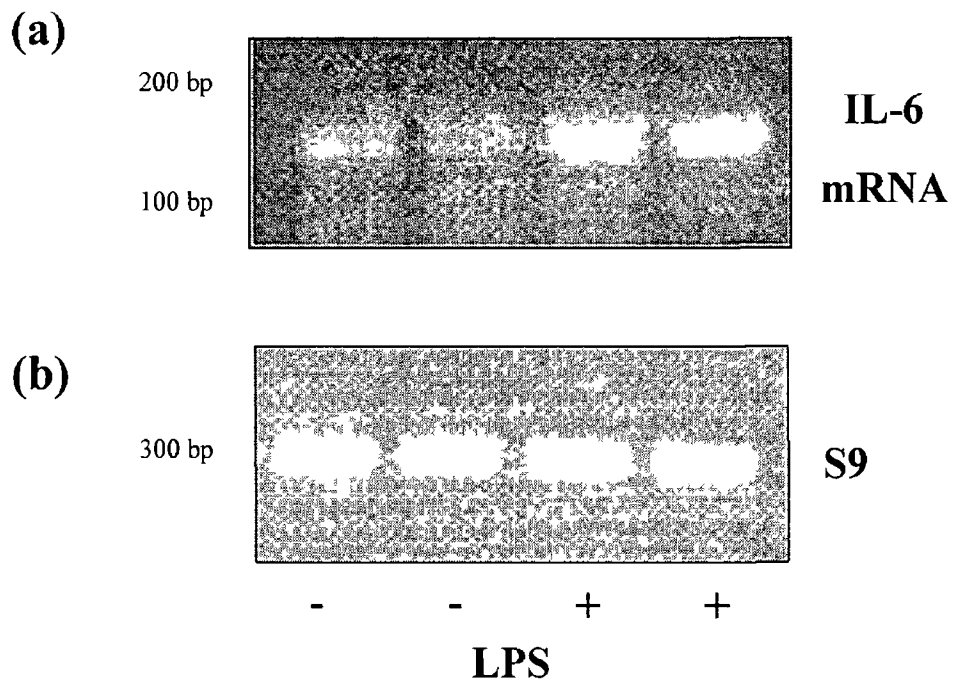


Figure 3 14 IL-6 mRNA expression in HCC *in vitro* RT-PCR analysis of RNA isolated from cultured H4IIE cells grown in the presence (+) or absence (-) of LPS (100ng/mL) over a 24h period using primers specific for **a) IL-6** and **b) S9** ribosomal RNA (control for equal loading)

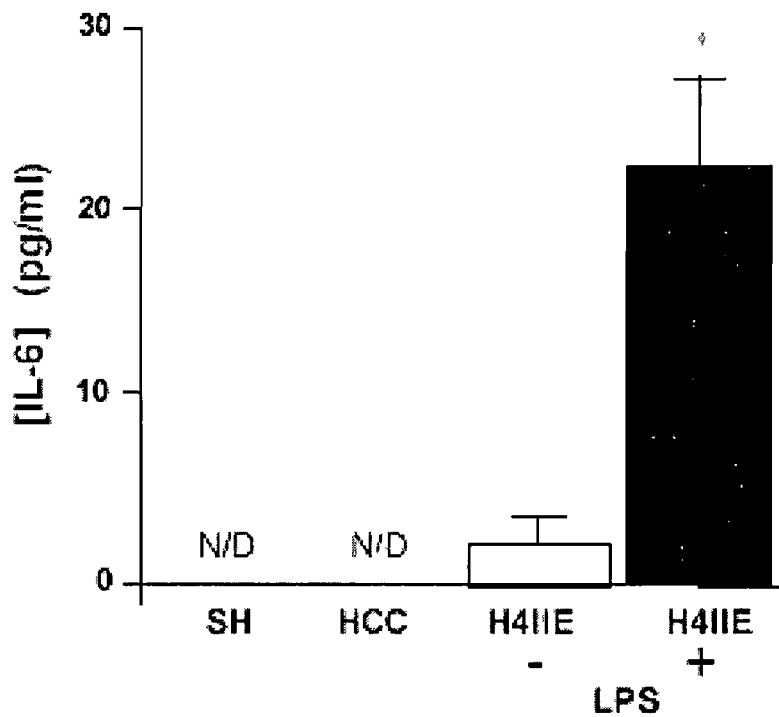


Figure 3 15 IL-6 protein expression in HCC *in vivo* and *in vitro* ELISA specific for rat IL-6 performed on plasma collected from sham operated (SH) and tumour burdened (HCC) male ACI rats. HCC tumours were established by direct injection of H4IIE cells into the left hepatic lobe of male ACI rats. Sham operated animals were injected with PBS alone. Plasma was collected two weeks after surgery. Concentration of circulating IL-6 was not detectable (N/D). ELISA specific for rat IL-6 was also performed on media collected from cultured H4IIE cells grown in the presence (+) or absence (-) of LPS (100ng/mL) over a 24h period. LPS treatment significantly increased IL-6 expression in H4IIE cells (* $p < 0.05$, $n = 6$ separate experiments per group assayed in duplicate).

3.4 Discussion

Previous reports demonstrate that IL-6 is critical in the process of normal hepatic growth and regeneration (Streetz et al , 2000, Fausto, 2000) To date relatively little is known about the role of IL-6 in HCC The results presented in this study demonstrate altered expression and activity of components of IL-6 dependent signalling pathways in tumourigenic hepatic tissue as compared to histologically normal liver specimens Specifically, these data demonstrate decreased expression of IL-6R α and gp130 subunits of the IL-6 receptor in HCC tissue as compared to normal liver Despite these observations, HCC tissue is characterised by increased IL-6 production and STAT3 activity as compared to pair-matched and sham operated NL Analysis of proteins involved in cell cycle progression clearly demonstrate increased expression of both p21^{waf1/cip1} and p27^{Kip1} in HCC, both common downstream effectors of IL-6 signalling Finally, the inducible inhibitors of cytokine signalling SOCS-1 was upregulated while SOCS-3 was downregulated in HCC tissue compared to pair matched NL tissue

Previous reports have identified IL-6 as a critical cytokine in the initiation phase of liver regeneration (Streetz et al , 2000, Fausto, 2000) Reduced liver mass causes increased serum TNF- α levels followed by increased IL-6 and downstream STAT3 activation STAT3 activation in collaboration with additional transcription factors, such as C/EBP β , enhance the expression of additional factors including NF-IL-6, c-myc, c-fos, IRF-1 enabling resting hepatocytes to progress into cell proliferation (Streetz et al , 2000, Fausto, 2000) More recently, Zimmers et al report the potential of IL-6 to act as a complete mitogen in the liver In this model circulating IL-6 levels were elevated in nude mice using a transfected CHO cell line, leading to dramatic hepatomegaly and hepatocyte hyperplasia in the absence of liver injury (Zimmers et al , 2003) In support of this observation, previous research using double transgenic mice expressing human

IL-6 and human soluble IL-6R under liver specific promoters also report hepatomegaly, hepatic hyperplasia and the presence of hepatic adenomas (Maione et al , 1998, Schirmacher et al , 1998)

The current studies demonstrate significantly decreased IL-6R α expression in HCC specimens as compared to normal liver. Normally the IL-6R α is present on a comparatively small number of cell types including hepatocytes, neutrophils, monocytes and some T- and B- cells (Kallen, 2002). In other tumour cells, a growth inhibitory effect of IL-6 is enhanced through the addition of sIL-6R α suggesting that IL-6R α expression may be the rate-limiting factor in cellular response to IL-6 (Oh et al , 1997, Ganapathi et al , 1996, Bellido et al , 1998). Evidence from these studies demonstrates that HCC tissue expresses higher IL-6 mRNA than normal liver. IL-6, however, was not detectable in rat plasma of tumour burdened or sham operated animals. One potential explanation of these observations may be the highly vascular nature of HCC and the increased blood flow/infiltration of blood borne cells into the tumour. However, following isolation and culture of pure HCC cell population, basal IL-6 mRNA and protein expression was clearly detectable and was further enhanced by treatment with LPS. IL-6 expression is upregulated in many haematological malignancies and solid tumours (Miki et al , 1989, Nordan et al , 1987, Kawano et al , 1988, Jernberg et al , 1991, Levy et al , 1991, Okuno et al , 1992, Miles et al , 1990, Yee et al , 1989). The tumour suppressors p53 and retinoblastoma protein have both demonstrated an ability to repress IL-6 expression while many mutated forms of these proteins lack this functionality (Santhanam et al , 1991). The mutation status of both of these proteins is unknown in H4IIE cells however, these tumour suppressors have been reported to be frequently mutated in human HCC (Edamoto et al , 2003) and may provide a possible mechanism for IL-6 upregulation. In other cases, such as that of glioblastomas, the amplification of the IL-6 gene at its locus appears to be responsible

for IL-6 overexpression (Tchirkov et al , 2001) Given that the tumour itself can express IL-6, down regulation of the IL-6R α in HCC may act to “mask” the tumour from the effects of autocrine IL-6 stimulation Indeed, studies using human cervical carcinoma cells, in which the IL-6R α subunit is down regulated at a transcriptional level, demonstrate decreased IL-6 responsiveness despite high IL-6 expression in these cells (Hess et al , 2000) Similarly, in melanoma cells, transduction of an IL-6 cDNA leads to decreased IL-6R α expression and confers IL-6 resistance to these cells (Silvani et al , 1995) IL-6 has also been shown to downregulate IL-6R α mRNA expression in rat hepatocytes (Nesbitt and Fuller, 1992) In these studies, we also show significantly lower gp130 expression in HCC as compared to normal liver Unlike IL-6R α , gp130 is ubiquitously expressed and is not normally subject to the same regulatory mechanisms as the IL-6R α subunit However, hyper-stimulation with IL-6 has been shown to down regulate gp130 expression in splenic T cells (Wang et al , 1998) and receptor internalisation and degradation in hepatic cells (Zohlhofer et al , 1992)

As is the case with other tumours, HCC is characterised by dysregulated expression and abnormal activation of many cell signalling proteins In this study increased STAT3 activity was identified in HCC tissue compared to normal hepatic tissue Furthermore, increased p21^{waf1/cip1} and p27^{Kip1} expression was observed in these tumours *in vivo* STAT3 is constitutively activated in cells transformed by SRC tyrosine kinase (Yu et al , 1995) and has been shown to have the ability to act as an oncogene (Bromberg et al , 1999) Constitutively activated STAT3 has also been discovered in many primary tumours including multiple myeloma and squamous cell carcinomas (Bromberg, 2001) Explanations for the persistent activation of STAT3 are varied For example, aberrant EGF/EGFR signalling accounts for constitutive activation of STAT3 in squamous cell carcinomas while in multiple myelomas overexpression and dysregulation of the IL-6R α and production of IL-6 stimulates

STAT3 activity (Bromberg, 2001) In a HCC cell line, Yoshikawa et al, have identified methylation induced silencing of SOCS-1, a Jak inhibitor, leads to constitutive STAT3 activation (Yoshikawa et al , 2001b) Interestingly, constitutive activation of STAT3 in murine plasmacytomas and hybridomas is associated with the acquisition of an IL-6 independent phenotype (Rawat et al , 2000) This raises the question of whether constitutive STAT3 activation in HCC tumours is directly related to increased tumour IL-6 production Alternatively, other cytokines and/or growth factors that have been demonstrated to utilise a STAT3 pathway (e.g EGF) may be produced, either by the tumour or in response to the tumour, that regulate STAT3 activity However, data from these studies also identified increased expression of SOCS-1 and decreased expression of SOCS-3 in HCC compared to NL SOCS-1 and SOCS-3 inhibit phosphorylation of Jak1, Jak2 and Jak3 and are induced by STAT signalling (Starr et al , 1997) While SOCS-1 and SOCS-3 genes are silenced in many malignancies, including certain human HCC (Watanabe *et al* , 2004, Yoshikawa *et al* , 2001a, He *et al* , 2003), overexpression has been identified in other tumours and has been linked to cytokine resistance (Raccurt et al , 2003, Sakai et al , 2002, Tannapfel et al , 2003) Indeed downregulated expression of SOCS-3 may be responsible for constitutively activated STAT3 in these HCC tumours due to the absence of adequate negative regulation of IL-6 signalling The absence of SOCS-3 expression has been demonstrated to prolong the activation of STAT3 during IL-6 signalling in the liver while IL-6 signalling remains normal in the absence of SOCS-1 expression (Croker *et al* , 2003)

The functional significance of constitutively activated STAT3 in this tumour model remains to be determined Many STAT3 target genes have been identified in other malignant cells including those involved in cell survival, angiogenesis, immune evasion and proliferation The dysregulated expression of both p21^{wal1/cip1} and p27^{Kip1} observed in these studies may be in response to an unremittingly active form of

STAT3 Both of these genes contain STAT responsive elements and can be modulated by IL-6 type cytokines (Bellido et al , 1998, Kortylewski et al , 1999, de Koning et al , 2000) p21^{waf1/cip1} and p27^{Kip1} are cyclin dependent kinase (cdk) inhibitors that can inhibit G1 associated cyclin complexes including CDK4/cyclin D and CDK2/Cyclin E and, in doing so, inhibit cell cycle progression At low stoichiometric concentrations, p21^{waf1/cip1} and p27^{Kip1} may serve as assembly factors for active cyclin/CDK complexes (LaBaer et al , 1997) and have been implicated as regulators of hepatocyte proliferation in the liver after partial hepatectomy where they determine the rate of progression through the G1 phase of the cell cycle (Albrecht et al , 1998) Overexpression of both p21^{waf1/cip1} and p27^{Kip1} has been previously observed in human HCC specimens and it is worth noting that genetic mutations in either of these genes are rare in human malignancies (Qin and Ng, 2001)

In conclusion, HCC is characterised by many aberrations in IL-6 signalling At present it is uncertain why HCC tumours produce significantly more IL-6 as compared to pair-matched normal liver although it is tempting to speculate that increased intra-tumour IL-6 is responsible for decreased IL-6 receptor expression in HCC If this is indeed the case, decreased IL-6 receptor levels in HCC tumours may act as a potentially evasive technique utilised by these cells to mask themselves from IL-6 Furthermore, overexpression of SOCS and constitutive activation of STAT3 have each been linked to cytokine resistance and IL-6 independence in other tumours (Raccurt et al , 2003, Sakai et al , 2002, Tannapfel et al , 2003, Rawat et al , 2000) Overall, it is clear that determining the effects of IL-6 in isolated HCC cells should provide a greater understanding of the differences in IL-6 signalling *in vivo*

Chapter 4: Interleukin-6 Signalling in HCC

4.1 Introduction

In chapter 3 HCC was demonstrated to be characterised by altered expression of IL-6 signalling components as compared to normal liver. Specifically, HCC displays decreased expression of both components of the IL-6 receptor, increased IL-6 production and constitutively activated STAT3. While the underlying reasons behind IL-6 upregulation in HCC tumours are unclear, it is possible that decreased IL-6 receptor expression may render the cells less responsive to IL-6.

Classically IL-6 binds to membrane-bound IL-6R α leading to the recruitment of trans-membrane gp130 receptor subunits into an active, hexameric IL-6 receptor complex. Homodimerisation of the gp130 proteins leads to phosphorylation of STATs *via* Jaks that are constitutively associated with gp130. Phosphorylation of STATs leads to STAT-dimer formation and translocation to the nucleus where target gene modulation occurs (Heinrich et al, 1998). In addition to this classical model of receptor activation and downstream signalling, IL-6 can also signal *via* a soluble IL-6 receptor (sIL-6R). In this instance, IL-6 binds a soluble form of the α -receptor and this complex activates signalling in cells expressing the gp130 receptor that may not inherently express IL-6R α , as well as potentiating IL-6 signalling in cells that do express IL-6R α . Importantly, many of the effects of the sIL-6R α /IL6 complex can be inhibited by the presence of soluble gp130 in the serum (Kallen, 2002).

Previous reports demonstrate that the majority of the intracellular effects of IL-6 are mediated *via* STAT3 activation although, involvement of STAT1 and/or STAT5

have also been reported in specific target cells (Heinrich et al , 1998) In addition to the Jak-STAT pathway the Ras-mitogen activated protein kinase (MAPK) pathway can also be activated following IL-6 receptor activation (Fukada et al , 1996) Following ligand binding, Src homology protein 2 tyrosine phosphatase-2 (SHP-2) interacts with gp130 and activates a downstream Ras-MAPK cascade Interleukin-6 signalling through this pathway ultimately leads to the phosphorylation/activation of extracellular regulated kinases (ERKs) which in turn serve as important regulators of nuclear transcription activity and cytoplasmic function (Chang and Karin, 2001) Collectively, the balance between the Jak-STAT and Ras-MAPK pathways determines the outcome of IL-6 signalling within each cellular context

Interleukin-6 is integrally linked to hepatic regeneration Following partial hepatectomy, IL-6 serum levels are elevated and this is accompanied by pronounced STAT3 activation in the liver (Streetz et al , 2000) IL-6^{-/-} mice show impaired liver regeneration, including abnormal G1 to S-phase progression and hepatocellular apoptosis The significance of IL-6 in this process is further confirmed as pre-operative IL-6 administration rescues the deficiency in hepatocyte proliferation (Cressman et al , 1996) Conversely hyperstimulation with IL-6 in human soluble IL-6R α transgenic mice prior to partial hepatectomy results in delayed cell cycle progression and over expression of the cyclin dependent kinase inhibitors p21^{waf1/cip1} and p27^{Kip1} (Wustefeld et al , 2000) While apparently contradictory, these data may be explained by the 40 fold induction of suppressors of cytokine signalling (SOCS) that occurs within two hours of IL-6 administration where the timing of gp130 stimulation is the rate limiting factor (Galun and Axelrod, 2002) *In vitro*, the role of IL-6 remains controversial, treatment of hepatocytes having been demonstrated to both stimulate and inhibit DNA synthesis (Kordula et al , 1991, Kuma et al , 1990, Satoh and Yamazaki, 1992)

In tumour biology, IL-6 has been identified as a growth factor for several cancer cell types including renal cell carcinoma (Miki et al , 1989), multiple myeloma (Kawano et al , 1988) and plasmacytoma (Nordan et al , 1987) In contrast, IL-6 has been reported to significantly inhibit the growth of other cancer cells Growth arrest and terminal differentiation is induced in M1 myeloid leukaemia cells, an effect that is blocked by the expression of dominant negative forms of STAT3 (Minami et al , 1996, Fukada et al , 1996) Interleukin-6 also induces an anti-proliferative effect in early stage human melanoma cells associated with STAT-mediated transcriptional up-regulation of p27^{Kip1} (Kortylewski et al , 1999) and p21^{waf1/cip1} (Florenes et al , 1999) Similarly IL-6-induced growth inhibition has been reported in prostate cancer (LNCaP) (Spiotto and Chung, 2000) and osteosarcoma cells (MG63) (Bellido et al , 1998) In hepatoma cells the effects of IL-6 on downstream effector pathways and cell proliferation remains uncertain Stimulation of the IL-6Ra in human HepG2 cells leads to the accumulation of p27^{Kip1} and growth arrest in the G1 phase (Klausen et al , 2000) an inhibitory effect similar to that observed by Kim et al in the H-35 rat hepatoma cell line however, the underlying mechanism of this inhibition was not determined (Kim and Baumann, 1999) In contrast, IL-6 has been indicated as an autocrine growth factor in other hepatoma cells IL-6 producing HCC-M hepatoma cell proliferation is inhibited following IL-6 antisense treatment (Kumagai et al , 2002) IL-6 is also implicated in cell survival during hepatic injury and inhibits TGF- β -induced apoptosis in the human hepatoma derived Hep3B cell line (Chen et al , 1999)

The aim of the current study was to examine IL-6 signalling and downstream cell cycle regulatory pathways in isolated HCC cells and hepatocytes *in vitro*

4.2 Methods

4.2.1 Tumour Model and H4IIE Cell Isolation

Rat HCC tumour model was established by direct injection of H4IIE cells into the left liver lobe of male ACI rats as described in section 2.3. H4IIE cells were isolated and cultured from the HCC tumour and passaged up to three times as described in section 2.2 prior to use in experiments.

4.2.2 Primary Hepatocyte Isolation

Fresh hepatocytes were isolated from male adult ACI rats using a modification of the two step perfusion technique as described in section 2.2.8.

4.2.3 Recombinant Human IL-6 Treatment

H4IIE cells and hepatocytes were quiesced for 16h (hepatocytes) or 24-48h (H4IIE) using serum free media prior to the addition of recombinant human IL-6 (rhIL-6, Biosource International, Camarillo, CA, USA) at varying concentrations (0-50ng/mL). Cell lysates for immunoblotting were prepared at varying time points (0-24h) after treatment as described in section 2.4.2.

4.2.4 Immunoblotting

4.2.4.1 Materials

Antisera specific against gp130 (M-20), IL-6R α (M-20), p21^{waf1/cip1} (F-5), STAT3 (H-190), ERK2 (K-23), cdk4 (H-22), cdk2 (M-2), cdc2 p34 (C-19), cyclin A (C-19), Jak1 (Q-19), Jak2 (C-20), Tyk2 (C-8), PCNA (PC-10) and KNRK nuclear extract were purchased from Santa Cruz Biotechnology (Santa Cruz, CA, USA). Antisera specific against Retinoblastoma protein (Rb) was purchased from BD Biosciences (San Diego, CA, USA). Antisera specific against p27^{Kip1}, Phospho-STAT3

(Tyr705), Phospho-p44/42 MAPK (Thr202/Tyr204), Phospho-Jak1 (Tyr1022/1023), Phospho-Jak2 (Tyr1007/1008), Phospho-Tyk2 (Tyr1054/1055), HA-Tag (262K), cyclin D3 (DCS22) and cyclin D1 (DCS6) were purchased from Cell Signaling Technology (Beverly, MA, USA) Horseradish peroxidase conjugated goat anti-rabbit Ig and goat anti mouse Ig were purchased from Jackson ImmunoResearch Laboratories (West Grove, PA, USA) Horseradish peroxidase conjugated rabbit anti goat Ig was purchased from Sigma Immunochemicals (St Louis, MO, USA)

4 2 4 2 Western Blotting

Western blots were performed as described in section 2 5 10 μ L of KNRK nuclear extract was loaded as a positive control for both p21^{waf1/cip1} and p27^{Kip1} expression Cell lysates from H4IIE cells stimulated with rhIL-6 (50ng/mL, 1h) or FBS (10% v/v, 10 mins) were used as positive controls for pSTAT3 and pERK 1/2 expression respectively All primary antibodies were diluted 1 1000 with the exception of Phospho-STAT3 (1 2000) in 5% (w/v) non fat dry milk (NFDM)/0 1% (v/v) tween/tris buffered saline (TBS) Phospho-Jak1 which was diluted 1 500 in 5% (w/v) BSA/0 1% (v/v) Tween/TBS All secondary antibodies were diluted 1 5000 in 5% (w/v) NFDM/0 1% (v/v) Tween/TBS

4 2 5 Pharmacological Inhibition of Jak-STAT and Ras-MAPK pathways

4 2 5 1 Materials

AG490 (a-Cyano-(3,4-dihydroxy)-N-benzylcinnamide Tyrphostin B42) was purchased from Calbiochem (San Diego, CA, USA) PD98059 (2-(2-amino-3-methoxyphenyl)-4H-1-Benzopyran-4-one) was purchased from Cell Signaling Technology (Beverly, MA, USA) DMSO was purchased from Fisher Scientific (Pittsburgh, PA, USA)

4.2.5.2 Pharmacological Inhibition of the RAS-MAPK pathway

Cultured H4IIE cells were quiesced for 48h in serum free media. PD98059 (MEK-1 inhibitor, 20 μ M) in serum free media was added to each well of quiesced H4IIE cells 1h prior to treatment with 50ng/mL rhIL-6. Control H4IIE cells were treated with DMSO (1 μ L/mL) in serum free media 1h prior to treatment with 50ng/mL rhIL-6. Cell protein lysates for immunoblotting were prepared at varying time points (0-24h) after treatment as described in section 2.4.2.

4.2.5.3 Pharmacological Inhibition of the Jak-STAT pathway

Cultured H4IIE cells were quiesced for 48h in serum free media. AG490 (Jak inhibitor) at varying concentrations (0-150 μ M) in serum free media was added to each well of quiesced H4IIE cells 1h prior to treatment with 50ng/mL rhIL-6. Control H4IIE cells were treated with DMSO (0-0.6 μ L/mL) in serum free media 1h prior to treatment with 50ng/mL rhIL-6. Cell lysates for immunoblotting were prepared at varying time points (0-24h) after treatment as described in section 2.4.2.

4.2.6 Transient Transfection of H4IIE Cells with Dominant Negative STAT3

4.2.6.1 Materials

pEFHASTAT3F (STAT3 dominant negative) and pEFHASTAT3 (STAT3 wild type) overexpression vectors (Figure 4.1a and 4.1b) were a kind gift from K. Nakajima (Department of Molecular Oncology, Osaka University Medical School, Japan) and have been previously described (Nakajima et al., 1996). Both vectors were originally constructed by cloning cDNA coding for either HASTAT3 or HASTAT3F mutant (Tyr705Phe) into a pEFBOS mammalian expression vector. TE buffer, One Shot TOP 10 chemically competent *E. coli*, SOC media, carbenicillin and ampicillin were

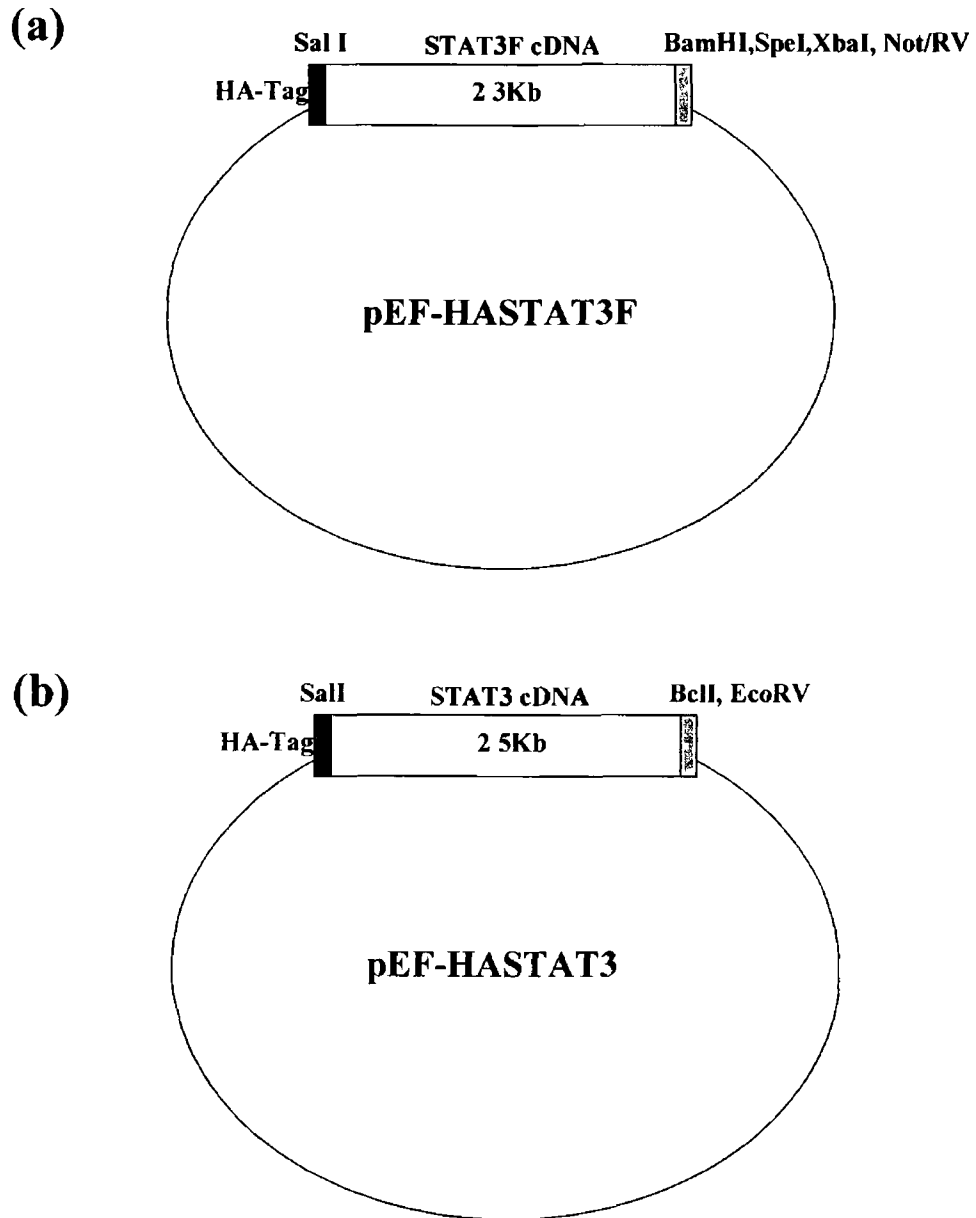


Figure 4.1 Schematic representation of expression vectors pEFHASTAT3F and pEFHASTAT3 Vectors expressing a) dominant negative STAT3 (pEFHASTAT3F) and b) wild type STAT3 (pEFHASTAT3) are shown. Both expression vectors were originally designed elsewhere through the cloning of cDNA for murine HA tagged STAT3 and STAT3F into the pEF-BOS plasmids. Both plasmids contain ampicillin resistance genes as prokaryotic selection markers. Restriction sites are labelled.

purchased from Invitrogen Life Technologies (Carlsbad, CA, USA) Glycerol, isopropanol, ethanol and agarose were purchased from Fisher Scientific (Pittsburgh, PA, USA) QIAprep spin miniprep kit and QIAfilter plasmid maxiprep kit were purchased from Qiagen (Valencia, CA, USA) BAMH1, Sal1, EcoRV, BAMH1 reaction buffer, Sal1 reaction buffer and 1Kb DNA ladder were purchased from New England Biolabs (Beverly, MA, USA) Tris, boric acid, ethylenediaminetetraacetic acid (EDTA) and ethidium bromide were purchased from Sigma-Aldrich (St Louis, MO, USA) Difco LB agar (Miller), Difco LB broth (Miller) and Difco Terrific Broth (TB) were purchased from BD Biosciences (San Diego, CA, USA) Mini Sub Cell GT electrophoresis unit was purchased from Biorad Laboratories (Hercules, CA, USA) Kodak EDAS290 gel visualisation unit was purchased from Kodak (Rochester, NY, USA) Genesys 2 UV/Visible Spectrophotometer was purchased from Thermo Spectronic (Rochester, NY, USA) DNA loading buffer was purchased from Eppendorf (Hamburg, Germany)

4 2 6 2 Transformation of *E coli*

50ng of plasmid DNA (pEFHASTAT3F/pEFHASTAT3) was added to 50 μ L TOP 10 *E coli* Cells were placed on ice for 30 mins and then heated to 42°C for 30 secs Cells were replaced on ice for 2 mins 250 μ L of S O C media (2% (w/v) tryptone, 0.5% (w/v) yeast extract, 10mM sodium chloride, 2.5mM potassium chloride, 10mM magnesium chloride, 10mM magnesium sulphate, 20mM glucose) was added and 50 μ L of this suspension was spread on LB agar plates (10g/L tryptone, 5g/L yeast extract, 10g/L sodium chloride, 15g/L agar) containing ampicillin (70 μ g/mL) and incubated overnight at 37°C One colony from the plate was used to inoculate 3mL of TB media (12g/L pancreatic digest of casein, 24g/L yeast extract, 9.4g/L dipotassium phosphate,

2.2g/L monopotassium phosphate) containing carbenicillin (70µg/mL). This culture was incubated from 6h to overnight at 37°C with high agitation. Transformed bacteria from these cultures were stored at -80°C in 40% (v/v) glycerol.

4.2.6.3 Plasmid DNA Miniprep

Plasmid DNA minipreps were prepared using a QIAprep spin miniprep kit. All centrifugations were carried out at 17,500 x g and all buffers described were supplied as part of the QIAprep kit. Overnight culture (3mL) of transformed *E. coli* was prepared as described in section 4.2.6.2. Cells were pelleted, resuspended in 250µL Buffer P1 and transferred to a microcentrifuge tube. 250µL of Buffer P2 was added and mixed gently. 350µL of Buffer N3 was then added and the sample centrifuged for 10 mins. Supernatant was added to a QIAprep spin column and centrifuged for 60 secs. The column was then washed using 0.75mL Buffer PE and centrifuged for 60 secs. Finally the column was centrifuged for an extra 60 secs to remove residual buffer prior to elution of DNA by centrifuging with 50µL of EB buffer for 60 secs.

4.2.6.4 Restriction Digests

Restriction digests were performed to confirm the identity of each plasmid. pEFHASTAT3F plasmid was cut with the restriction enzymes BAMHI and Sall releasing the ~2.3Kb cDNA coding for HASTAT3F (Figure 4.2). pEFHASTAT3 was cut with Sall and EcoRV releasing the ~2.5Kb cDNA coding for HASTAT3 (Figure 4.3). Reaction mixtures were prepared as described in Table 4.1 and were incubated at 37°C for 1h. Products were combined with 2µL of DNA loading buffer.

	pEFHASTAT3F	pEFHASTAT3
BAMH1 BUFFER	1.5 μ L	-
SalI BUFFER	-	1.5 μ L
BAMH1	0.5 μ L	-
SalI	0.5 μ L	0.5 μ L
EcoRV	-	0.5 μ L
PLASMID DNA	4 μ L	4 μ L
Double Distilled Water	8.5 μ L	8.5 μ L

Table 4.1 Reaction mixtures for the restriction digest of pEFHASTAT3F and pEFHASTAT3. Restriction digests were prepared using 4 μ L of miniprep pEFHASTAT3F or pEFHASTAT3 plasmid DNA. Reaction mixture comprising each component was incubated at 37°C for 1h. Reaction products were electrophoresed on a 0.8% (w/v) agarose gel containing ethidium bromide.

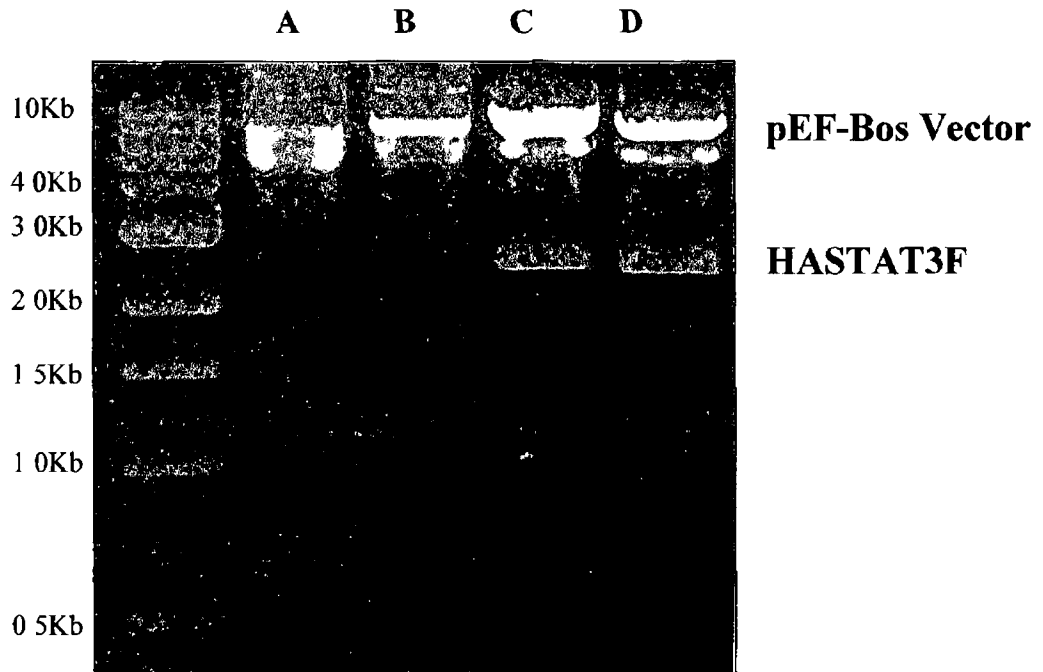


Figure 4.2 Restriction digestion of pEFHASTAT3F expression vector using **BAMHI/SalI** Restriction digests were prepared using 4 μ L of miniprep pEFHASTAT3F plasmid DNA. Reaction mixture containing **BAMHI** and **SalI** restriction enzymes was incubated at 37°C for 1h and products were electrophoresed on a 0.8% (w/v) agarose gel containing ethidium bromide. Reaction was performed in the absence of restriction enzymes as control (A,B). HASTAT3F cDNA coding region (~2.3Kb) was released from restriction digested pEFHASTAT3F (C,D).

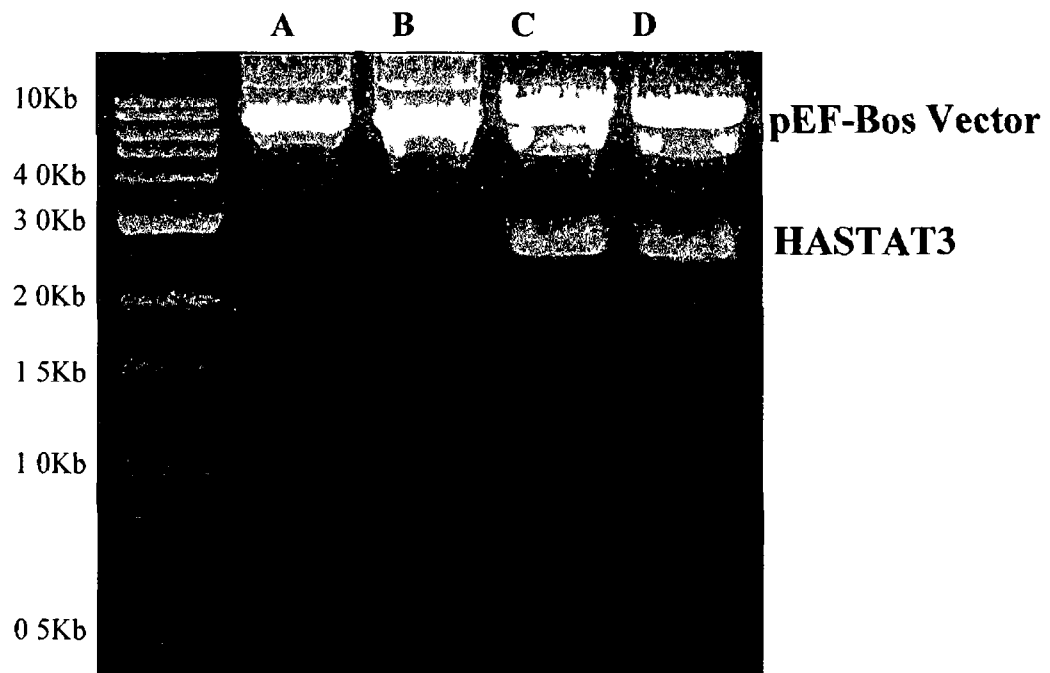


Figure 4.3 Restriction digestion of pEFHASTAT3 expression vector using EcoRV/SalI Restriction digests were prepared using 4 μ L of miniprepmed pEFHASTAT3 plasmid DNA. Reaction mixture containing EcoRV and SalI restriction enzymes was incubated at 37 $^{\circ}$ C for 1h and products were electrophoresed on a 0.8% (w/v) agarose gel containing ethidium bromide. Reaction was performed in the absence of restriction enzymes as control (A,B). HASTAT3 cDNA coding region (~2.5Kb) was released from restriction digested pEFHASTAT3 (C,D).

and then electrophoresed on a 0.8% (w/v) agarose gel made with TBE buffer (45mM Tris-Borate, 1mM EDTA) containing ethidium bromide (2µL in 50mL). Gels were placed in a gel electrophoresis unit containing TBE and were run at 60V. Gel images were captured using a Kodak EDAS 290 image capture system.

4.2.6.5 Plasmid DNA Maxiprep

Plasmid DNA was prepared using the QIAfilter plasmid Maxiprep kit. All buffers described were obtained as part of this kit. 10µL of the transformed *E. coli* culture described in section 4.2.6.2 was used to inoculate 150mL of LB media (10g/L pancreatic digest of casein, 5g/L yeast extract and 10g/L NaCl) containing 70µg/mL of carbenicillin and was grown overnight at 37°C. Cells were harvested by centrifugation at 6000 x g for 15 mins at 4°C. The pellet was resuspended in 10mL P1 buffer, 10mL of P2 buffer was added and the solution was incubated at room temperature for 5 mins. 10mL of chilled P3 buffer was then added to the lysate and the sample was then rested for 10 mins on ice prior to centrifugation at 6,000 x g for 20 mins (4°C). The lysate was then added to the barrel of a QIAfilter cartridge. A QIAfilter tip 500 was equilibrated by passing 10mL of buffer QBT through it. The cell lysate was then filtered through the equilibrated tip. After the lysate had passed through the resin, the QIAGEN tip was washed twice with 30mL of QC buffer. DNA was then eluted in 15mL of buffer QF and precipitated by the addition of 10.5mL of isopropanol at room temperature. The solution was then mixed and centrifuged at 3,000 x g for 10 mins. The DNA pellet was washed in 5mL of 70% (v/v) ethanol (room temperature) and then centrifuged at 6,000 x g for 10 mins. Finally the pellet was air dried and redissolved in 300µL of TE buffer. DNA yield was determined as described in section 4.2.6.6.

4 2 6 6 DNA Quantification

DNA was diluted 1 200 in nuclease free water Absorbance at 260nm was measured on a UV spectrophotometer DNA concentration was calculated using the following equation

$$\text{DNA CONCENTRATION (mg/mL)} = \text{ABSORBANCE}_{260\text{nm}} (\text{diluted } 1\ 200) \times 10$$

Where

DNA CONCENTRATION = Concentration of DNA (mg/mL)

ABSORBANCE_{260nm} = Absorbance of sample at 260nm

4.2.6.7 Transient Transfection of H4IIE Cells

H4IIE cells were grown to approximately 80% confluency in 6 well tissue culture plates Transfection was carried out in serum free EMEM media in the absence of antibiotics or buffering agents 36µg of maxiprepmed pEFHASTAT3F or pEFHASTAT3 plasmid DNA (section 4 2 6 5) was added to 600µL of serum free EMEM media 60µL of Lipofectamine was also added to 600µL of serum free EMEM media Both tubes were combined and were incubated at room temperature for 35-40 mins H4IIE cells were washed once with PBS followed by a second wash in serum free EMEM media 0.8mL of serum free EMEM media was added to each well 200µL of Lipofectamine/plasmid DNA mix was gently added to each well Cells were incubated for 5-20h at 37°C in a 5% CO₂ humidified incubator After incubation, 1mL of 20% (v/v) FBS H4IIE cell media (section 2 2 3) was added to each well After 16h of further incubation cells were quiesced in serum free media for a period of 24h prior to treatment with rhIL-6 as described in section 4 2 3

4 2 7 Cyclin Dependent Kinase Activity Assays

4 2 7.1 Materials

HEPES, sodium chloride, magnesium chloride, β -glycerophosphate, sodium dodecyl sulphate (SDS), dithiothreitol (DTT), adenosine triphosphate (ATP) solution (100mM), Tris-HCl, sodium vanadate, sodium fluoride, EDTA, EGTA and NP-40 were all purchased from Sigma Aldrich (St Louis, MO, USA) Cell scrapers were purchased from Corning (Corning, NY, USA) Complete protease inhibitor tablets (containing PMSF, aprotinin and leupeptin) were purchased from Roche Applied Science (Indianapolis, IN, USA) Protein A-agarose was purchased from Santa Cruz Biotechnology (Santa Cruz, CA, USA) Histone H1 (calf thymus) was purchased from Calbiochem (San Diego, CA, USA) Rb-C fusion protein was purchased from Cell Signaling Technology (Beverly, MA, USA) Redivue γ -P³² labelled ATP and nitrocellulose membrane was purchased from Amersham Biosciences (Piscataway, NJ, USA) Laemmli buffer was purchased from Biorad (Hercules, CA, USA) A large SE600 electrophoresis unit and TE transfer unit were purchased from Hoefer (San Francisco, CA, USA) X-ray film was developed using a SRX-101 Medical Film Developer (Konica, Mahwah, NJ, USA) and densitometry was performed using the Kodak EDAS290 imaging software (Kodak, Rochester, NY, USA)

4 2 7 2 Method

H4IIE cells were grown to approximately 80% confluency and quiesced for 48h in serum free media Cells were then treated with rhIL-6 at a concentration of 50ng/mL Cells were washed twice in PBS (4°C) and collected at varying time points (0-24h) in ice cold kinase extraction buffer (50mM Tris-HCl, 1% (v/v) NP-40, 150mM NaCl, 1mM EDTA, 1mM Na₃VO₄, 1mM NaF, 100g/mL PMSF, 2 μ g/mL leupeptin, 2 μ g/mL aprotinin) Cells were lysed in this buffer for 15 mins with agitation (4°C) Debris was

cleared from lysates by centrifugation at 14,000 x g for 15 mins (4°C) Supernatants were then precleared with 20µL of Protein A agarose beads for 10 mins with gentle agitation Beads were removed by centrifugation at (14,000 x g, 10 mins, 4°C) Protein concentration in each lysate was measured using the BCA protein assay as described in section 2 5 2 Protein concentration of each lysate was next adjusted to 1mg/mL using ice cold PBS 500µL of each cell lysate was then incubated with antibodies specific against either cdk2 or cdk4 at a dilution of 1 50 for 4h with gentle agitation 20µL of Protein A agarose beads were then added to each sample and incubated overnight with gentle agitation (4°C) The beads were then collected by pulse centrifugation (10 secs, 14,000 x g, 4°C) The supernatant was discarded The beads were washed once in ice cold kinase extraction buffer followed by two washes in ice cold PBS A final wash was carried out in ice cold 50mM Hepes/1mM DTT solution The beads were next resuspended in 10µL of 50mM Hepes/1mM DTT 20µL of 3x Kinase Reaction buffer (150mM Hepes, 3mM DTT, 30mM MgCl₂, 7 5mM EGTA, 0 3mM Na₃VO₄, 30mM β-glycerophosphate, 3mM NaF, 60µM ATP, 10µCi γ-P³² labelled ATP per reaction) containing either 2mg/mL of Histone H1 (cdk2) or Rb-C fusion protein (cdk4) as substrates was then added to the beads This reaction was carried out at 30°C for 30 mins and terminated by the addition of 15µL Laemmli buffer (100°C) Samples were loaded on a 12 5% SDS-PAGE gel, resolved by electrophoresis and transferred to a nitrocellulose membrane as described in section 2 5 3 Once transferred, the membranes were exposed to x-ray film and developed using a Konica SRX-101 Medical Film Developer

4 2 8 Confocal Microscopy

H4IIE cells and freshly isolated hepatocytes were cultured for 24h *in vitro* in HSM prior to fixation in methanol and visualisation using a Fluoview FV500 IX70

confocal laser scanning biological microscope and Fluoview FV500 version 4.3 image
processing software (Olympus America, Melville, NY, USA)

4.3 Results

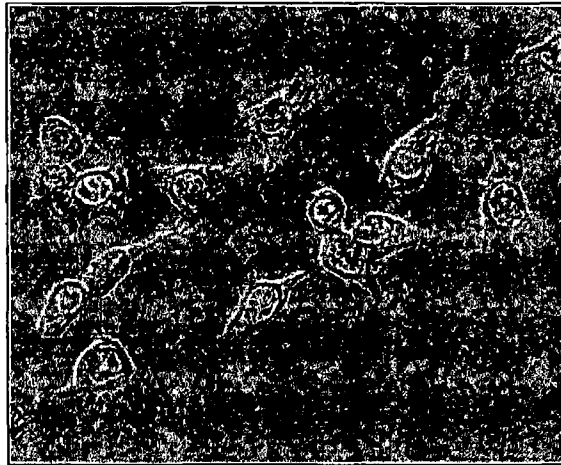
4.3.1 Characteristics of H4IIE Cells and Hepatocytes *In Vitro*

H4IIE cells were inoculated directly into the left hepatic lobe of male ACI rats. An encapsulated, reproducible tumour mass formed 14-16 days post inoculation. H4IIE cells were isolated from this tumour and grown in culture. Confocal microscopy demonstrated that H4IIE cells have a distinctive structural phenotype compared to isolated cultured rat hepatocytes. H4IIE cells were characterised by large nuclei, a low cytoplasm to nucleus ratio and an irregular shape with multiple cytoplasmic extensions (Figure 4.4a). Isolated cultured rat hepatocytes were larger, exhibited a regular polyhedral structure and were often binucleated (Figure 4.4b).

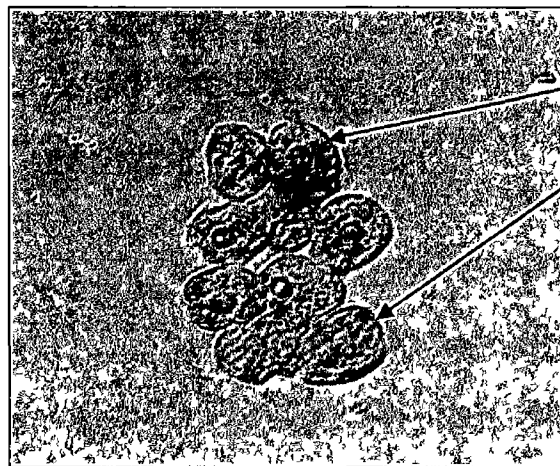
Immunoblotting using antibodies specific against IL-6R α and gp130 was performed on cell lysates from cultured H4IIE cells and isolated cultured hepatocytes in order to compare levels of IL-6 receptor complex expression. To normalise conditions, both cell types were cultured on collagen coated plates. Using these antibodies single protein bands were detected at ~80kDa (IL-6R α) or ~130kDa (gp130, Figures 4.5a and 4.5b respectively). Following protein transfer, data were analyzed for optical integrated volume. IL-6R α expression was significantly decreased in cultured H4IIE cells (48.6%) *versus* cultured rat hepatocytes (Figure 4.5a, $p < 0.05$, $n=4$ per group). Gp130 expression was dramatically lower in H4IIE cells compared to cultured rat hepatocytes (Figure 4.5b, upper panel, $n=4$ per group). During experimentation, differences in gp130 expression between hepatocytes and H4IIE cells in culture were so large that overexposure of the film was required in order for comparison of gp130 expression in H4IIE lysates and hepatocytes to be performed (Figure 4.5b, lower panel).

Having determined H4IIE cells retain the downregulated IL-6 receptor expression phenotype observed *in vivo* (section 3.3.2), the expression of the IL-6 receptor complex with serial passaging in culture was next analysed. Isolated H4IIE

(a)



(b)



Binucleated
Hepatocytes

Figure 4.4 Confocal images of isolated H4IIE (HCC) cells and rat hepatocytes cultured *in vitro* Isolated H4IIE cells and primary rat hepatocytes were cultured *in vitro* for 24 hours in high serum media. Confocal images (40x) represent a) H4IIE cells and b) rat hepatocytes fixed in methanol

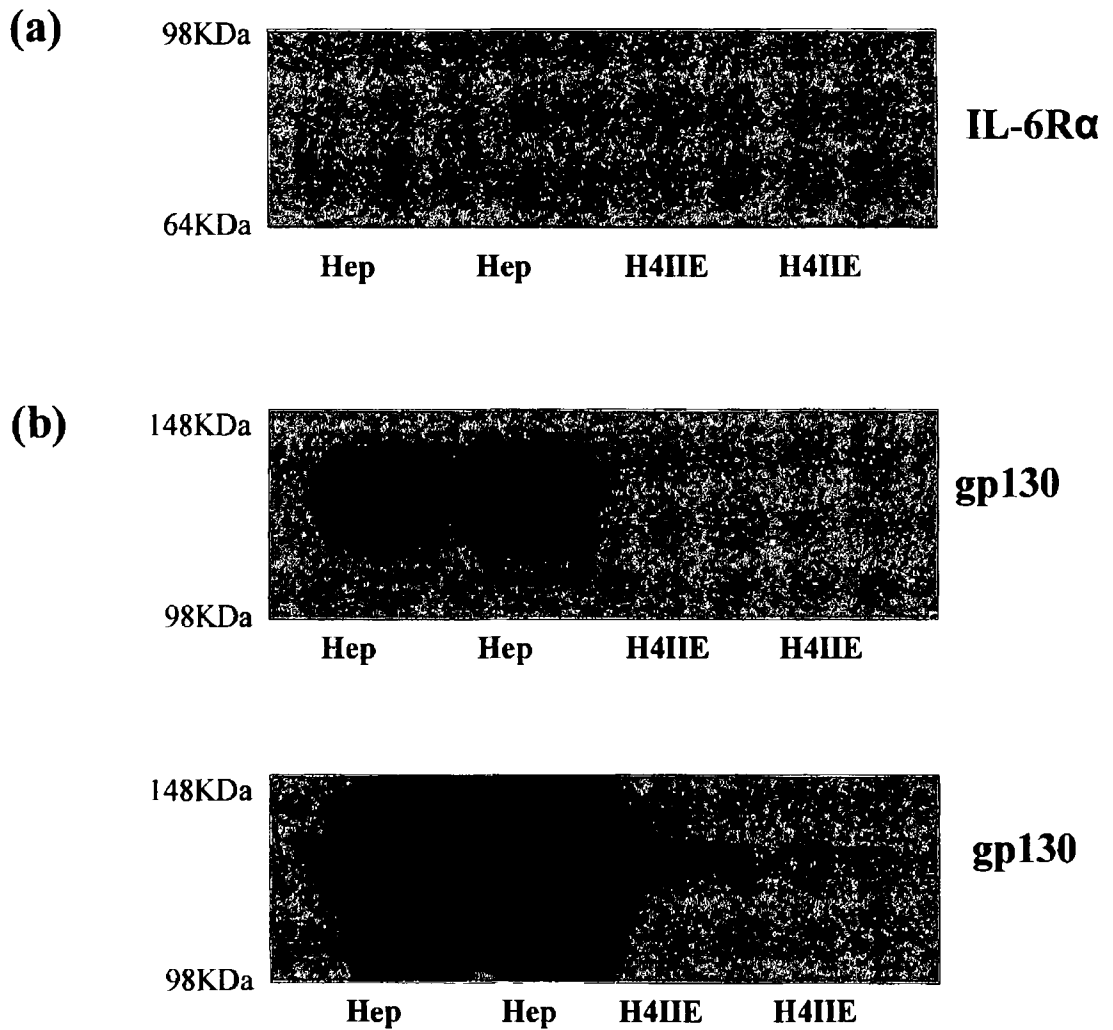


Figure 4 5 H4IIE (HCC) cells are characterised by decreased IL-6 receptor expression versus primary rat hepatocytes *in vitro* Representative Western blot analysis of whole cell lysates from isolated primary cultured rat hepatocytes (Hep) and isolated H4IIE cells cultured on collagen plates using an antibody specific against a) IL-6R α and b) gp130 In figure (b), the lower panel represents a higher exposure time of the blot in the upper panel

cells were cultured *in vitro* and passaged serially three times Immunoblotting using antibodies specific against IL-6R α and gp130 was performed on cell lysates from each passage Analysis of optical integrated volume on Western blots probed with these antibodies demonstrated there was no significant difference in expression of IL-6R α (Figure 4 6a, n=4 per group) or gp130 (Figure 4 6b, n=4 per group) with passaging *in vitro*

4 3 2 Effect of IL-6 on STAT3 Activity in H4IIE Cells and Hepatocytes

In Vitro

Previous studies demonstrated that STAT and ERK dependent pathways are activated following ligand binding to the IL-6R α Dose and time course studies were next performed to determine appropriate dose and temporal parameters for H4IIE cells and isolated cultured rat hepatocytes *in vitro* Initially, cell lysates were prepared and total Jak (Jak1, Jak2 and Tyk2) and active Jak (pJak1, pJak2 and pTyk2) were detected by Western blot In H4IIE cells a dose of 50ng/mL rhIL-6 caused a time dependent increase in pJak1 expression, an increase being detected 2 mins after addition and a maximal response occurring at 60 mins (Figure 4 7a, upper panel, n=4 per group) Analysis of total Jak1 expression demonstrated no change in expression throughout the time course of the experiments (Figure 4 7a, lower panel, n=4 per group) In cultured hepatocytes, rhIL-6 again led to increases in Jak1 activation in the absence of changes in total Jak1 expression (Figure 4 7b, n=4 per group), activation again occurring within 2 mins of addition and maximal activity was detected between 60-120 mins after addition (Figure 4 7b, upper panel, n=4 per group) Phospho-Jak2 expression was also increased in H4IIE cells after rhIL-6 treatment (50ng/mL) in a time dependent manner, an increase detected 10 mins after addition of rhIL-6 and a maximal response occurring between 40 and 60 mins (Figure 4 8a, upper panel, n=4 per group) No change in total

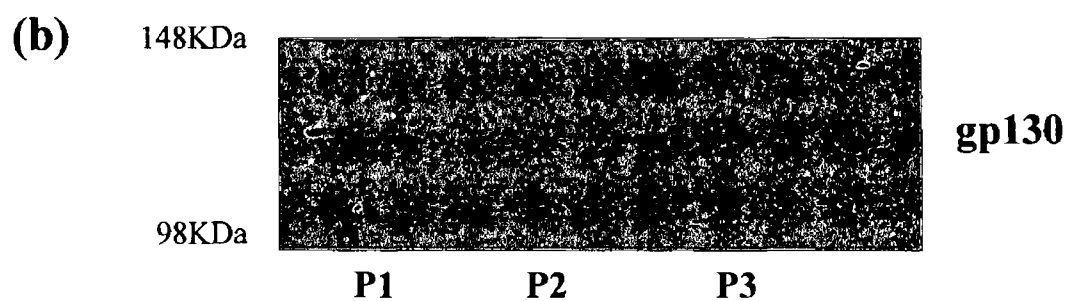
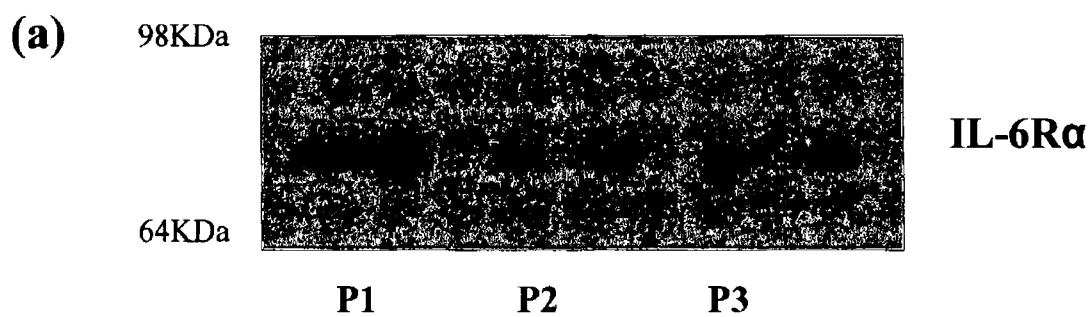
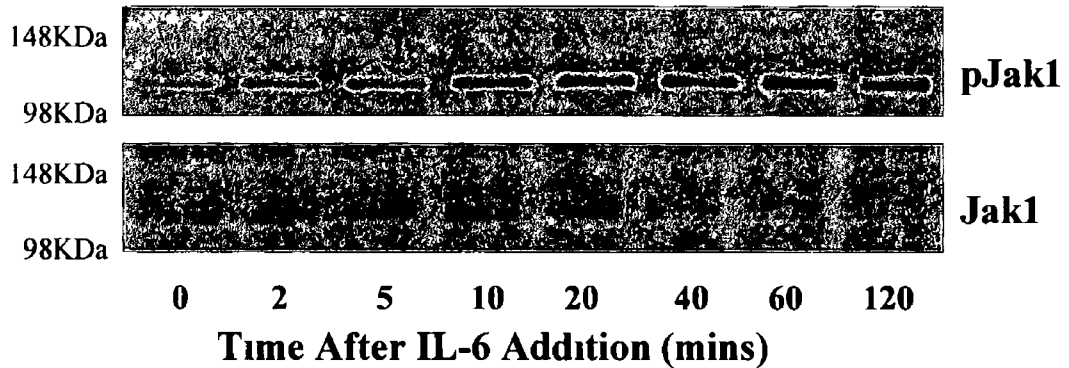


Figure 4 6 H4IIE (HCC) cells retain a decreased IL-6 receptor expression phenotype during serial passaging *in vitro* Representative Western blot analysis of whole cell lysates from H4IIE cells serially passaged in culture (P1-P3) using an antibody specific against a) IL-6R α and b) gp130

(a) H4IIE



(b) Hepatocytes

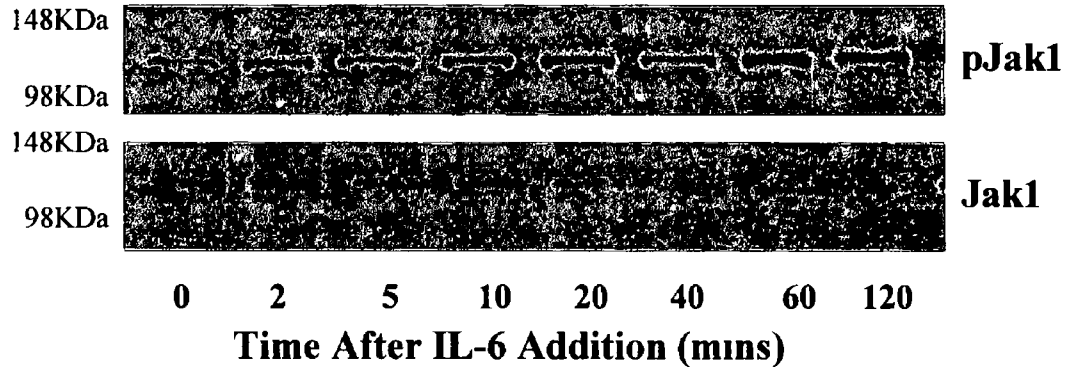
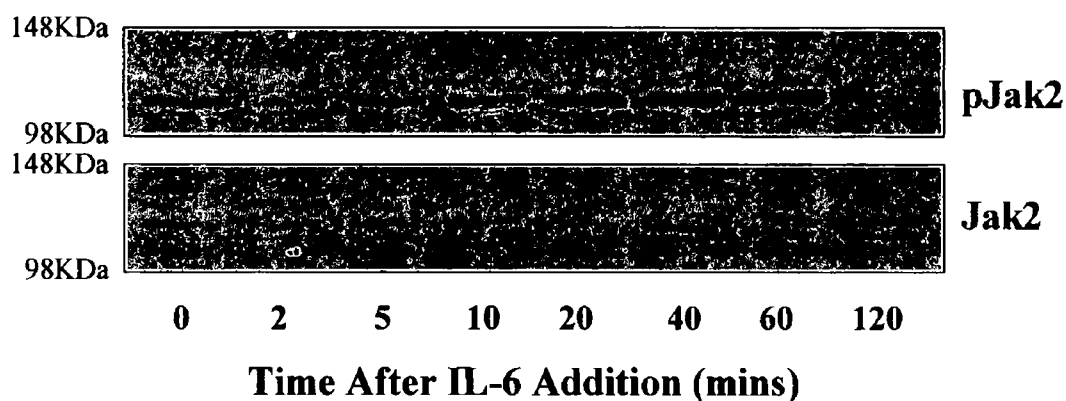


Figure 4 7 RhIL-6 stimulates Jak1 activity in H4IIE (HCC) cells and isolated cultured rat hepatocytes in a time dependent manner in the absence of changes in total Jak1 expression *in vitro* a) Representative Western blot analysis performed on cell lysate samples prepared from cultured H4IIE cells using an antibody specific against active (phospho-) Jak1 (pJak1, upper panel) or total Jak1 (lower panel) H4IIE cells were isolated and purified from *in vivo* HCC tissue and cultured prior to treatment with rhIL-6 (50ng/ml) in serum free media for varying time periods (0-120 mins) b) Representative Western blot analysis performed on cell lysate samples prepared from isolated cultured rat hepatocytes using an antibody specific against active (phospho-) Jak1 (pJak1, upper panel) or total Jak1 (lower panel) Hepatocyte cell populations were isolated from normal rat livers by perfusion Following attachment, hepatocytes were placed in serum free media prior to treatment with rhIL-6 (50ng/ml) for varying time periods (0-120 mins)

(a) H4IIE



(b) Hepatocytes

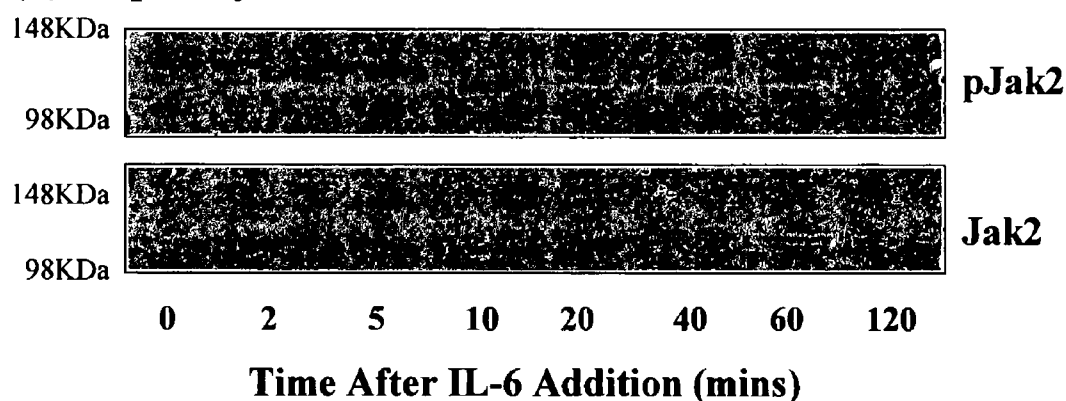
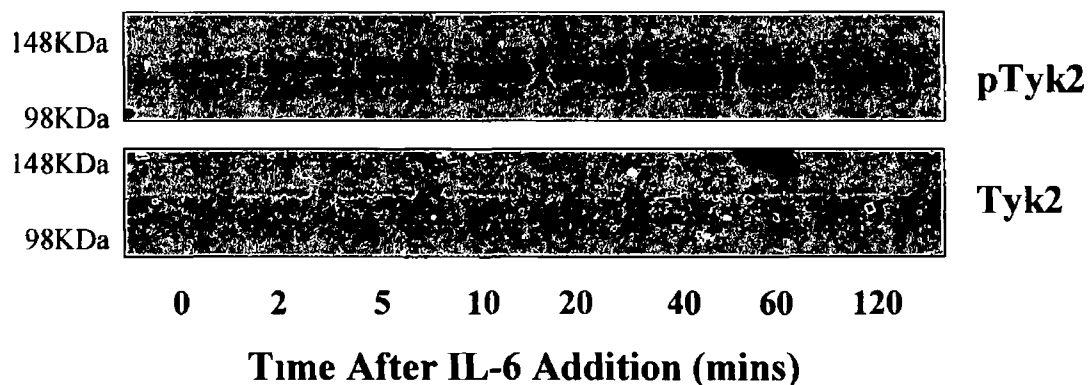


Figure 4 8 RhIL-6 stimulates Jak2 activity in H4IIE (HCC) cells and isolated cultured rat hepatocytes in a time dependent manner in the absence of changes in total Jak2 expression *in vitro* a) Representative Western blot analysis performed on cell lysate samples prepared from cultured H4IIE cells using an antibody specific against active (phospho-) Jak2 (pJak2, upper panel) or total Jak2 (lower panel) H4IIE cells were isolated and purified from *in vivo* HCC tissue and cultured prior to treatment with rhIL-6 (50ng/ml) in serum free media for varying time periods (0-120 mins) b) Representative Western blot analysis performed on cell lysate samples prepared from isolated cultured rat hepatocytes using an antibody specific against active (phospho-) Jak2 (pJak2, upper panel) or total Jak2 (lower panel) Hepatocyte cell populations were isolated from normal rat livers by perfusion Following attachment, hepatocytes were placed in serum free media prior to treatment with rhIL-6 (50ng/ml) for varying time periods (0-120 mins)

Jak2 expression was detected throughout the course of the experiments (Figure 4 8a, lower panel, n=4 per group) In cultured hepatocytes, rhIL-6 (50ng/mL) also stimulated Jak2 activation in the absence of changes in total Jak2 expression (Figure 4 8b, n=4 per group), increased pJak2 being detected at 2 mins and a maximal response observed at 40-60 mins (Figure 4 8b, upper panel, n=4 per group) Stimulation of H4IIE cells with rhIL-6 (50ng/mL) also activated Tyk2 in a time-dependent manner in the absence of changes of total Tyk2 expression in these cells (Figure 4 9a, n=4 per group), increased pTyk2 expression being detected at 2 mins reaching a maximal response at 40 mins (Figure 4 9a, upper panel, n=4 per group) Recombinant human IL-6 (50ng/mL) also stimulated Tyk2 activation in cultured hepatocytes (Figure 4 9b, n=4 per group), increased pTyk2 expression being detected at 2 mins and a maximal response occurring between 60-120 mins (Figure 4 9b, upper panel, n=4 per group) Treatment of hepatocytes with rhIL-6 did not alter the expression of total Tyk2 (Figure 4 9b, lower panel, n=4 per group)

Cell lysates from H4IIE cells and cultured rat hepatocytes were next analysed for total STAT3 and active (pSTAT3) expression by Western blot In H4IIE cells 50ng/mL rhIL-6 caused a time dependent increase in pSTAT3 expression, an increase being detected 5 mins after addition and a maximal response occurring between 40 and 60 mins, followed by a decrease in expression at 2h (Figure 4 10a, upper panel, n=4 per group) Changes in pSTAT3 expression following rhIL-6 addition occurred in the absence of changes in total STAT3 expression throughout the time course (Figure 4 10a, lower panel, n=4 per group) In cultured hepatocytes, treatment with rhIL-6 again led to increases in STAT3 activation in the absence of changes in total STAT3 expression (Figure 4 10b, n=4 per group) As with H4IIE cells, STAT3 activation occurred within 5 mins of addition and a maximal change in activity was detected between 40 and 60 mins (Figure 4 10b, upper panel, n=4 per group) To assess optimal

(a) H4IIE



(b) Hepatocytes

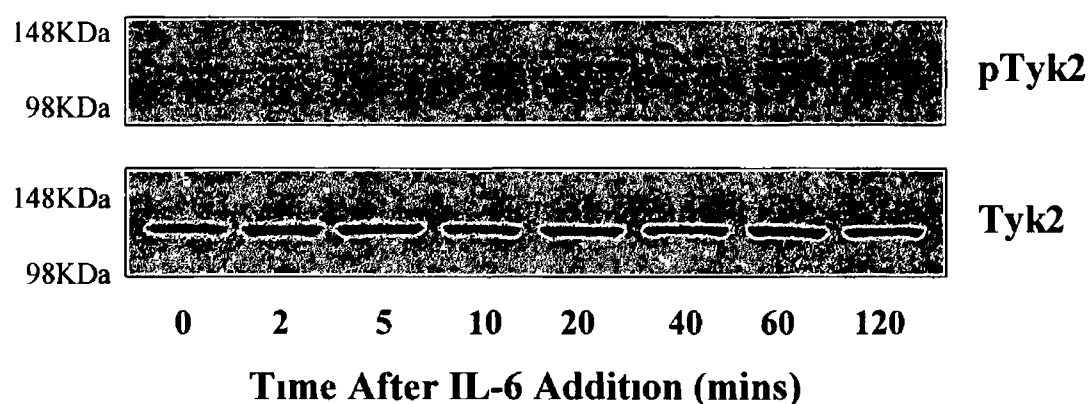
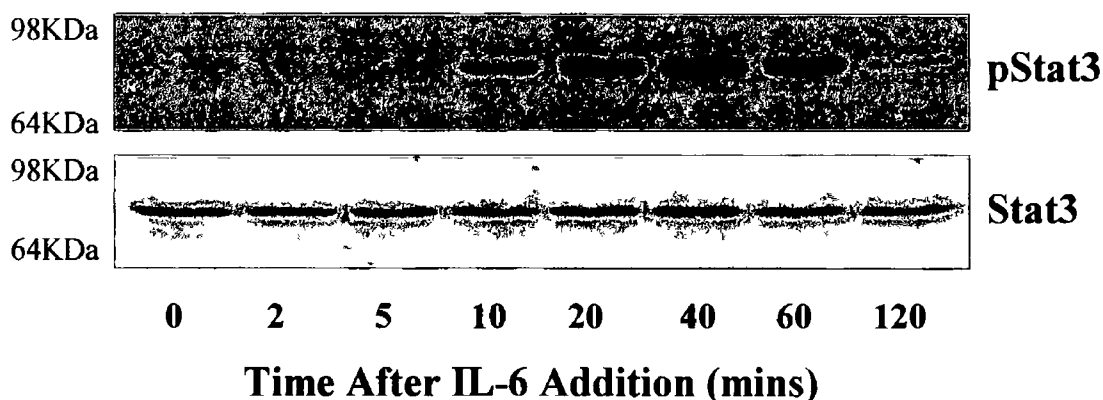


Figure 4 9 RhIL-6 stimulates Tyk2 activity in H4IIE (HCC) cells and isolated cultured rat hepatocytes in a time dependent manner in the absence of changes in total Tyk2 expression *in vitro* a) Representative Western blot analysis performed on cell lysate samples prepared from cultured H4IIE cells using an antibody specific against active (phospho-) Tyk2 (pTyk2, upper panel) or total Tyk2 (lower panel) H4IIE cells were isolated and purified from *in vivo* HCC tissue and cultured prior to treatment with rhIL-6 (50ng/ml) in serum free media for varying time periods (0-120 mins) b) Representative Western blot analysis performed on cell lysate samples prepared from isolated cultured rat hepatocytes using an antibody specific against active (phospho-) Tyk2 (pTyk2, upper panel) or total Tyk2 (lower panel) Hepatocyte cell populations were isolated from normal rat livers by perfusion Following attachment, hepatocytes were placed in serum free media prior to treatment with rhIL-6 (50ng/ml) for varying time periods (0-120 mins)

(a) H4IIE



(b) Hepatocytes

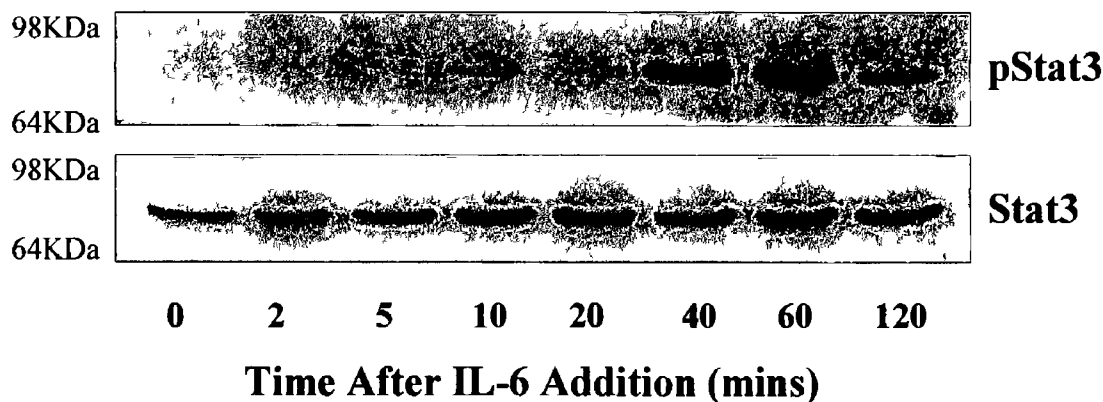


Figure 4.10 RhIL-6 stimulates STAT3 activity in H4IIE (HCC) cells and isolated cultured rat hepatocytes in a time dependent manner in the absence of changes in total STAT3 expression *in vitro* a) Representative Western blot analysis performed on cell lysate samples prepared from cultured H4IIE cells using an antibody specific against active (phospho-) STAT3 (pSTAT3, upper panel) or total STAT3 (lower panel) H4IIE cells were isolated and purified from *in vivo* HCC tissue and cultured prior to treatment with rhIL-6 (50ng/ml) in serum free media for varying time periods (0-120 mins) b) Representative Western blot analysis performed on cell lysate samples prepared from isolated cultured rat hepatocytes using an antibody specific against active (phospho-) STAT3 (pSTAT3, upper panel) or total STAT3 (lower panel) Hepatocyte cell populations were isolated from normal rat livers by perfusion Following attachment, hepatocytes were placed in serum free media prior to treatment with rhIL-6 (50ng/ml) for varying time periods (0-120 mins)

doses of IL-6, H4IIE cells and cultured hepatocytes were next treated with rhIL-6 (0-50ng/mL) for 60 mins. These data demonstrated dose dependent increases in pSTAT3 expression in both cell types, increases in STAT3 activation occurring at 1-5ng/ml and a maximal response being detected at 50ng/mL (Figure 4 11a and 4 11b, upper panel, n=4 per group). In both instances no differences in total STAT3 expression were detected at any of the doses employed (Figure 4 11a and 4 11b, lower panel, n=4 per group).

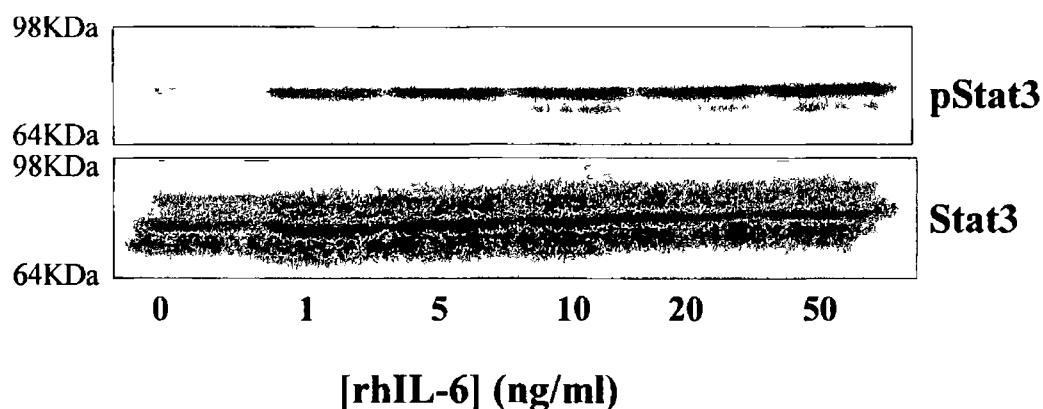
4 3 3 Effect of IL-6 on MEK Activity in H4IIE Cells and Hepatocytes *In Vitro*

To investigate the involvement of a MAPK pathway in intracellular IL-6 signalling in H4IIE cells and hepatocytes, cells were treated with 50ng/mL rhIL-6 for different time periods and cell lysates prepared for Western blot analysis of total and activated (phosphorylated) ERK 1/2 expression. In both cell types total ERK expression did not change throughout the experimental period (Figure 4 12a and 4 12b, lower panel, n=4 per group). In H4IIE cells, rhIL-6 caused a biphasic change in ERK 1/2 activity, an initial activation occurring between 2 and 5 mins before decreasing back to baseline, followed by a second period of stimulation between 40 and 60 mins (Figure 4 12a, upper panel, n=4 per group). In contrast, in hepatocytes, while increases in pERK 1/2 detection occurred 5 mins after rhIL-6 addition, ERK 1/2 activity was maintained for 20-40 mins before returning towards basal levels at 60 and 120 mins (Figure 4 12b, upper panel, n=4 per group).

4 3.4 Downstream Effects of IL-6 signalling in H4IIE Cells and Hepatocytes

Having determined that IL-6 stimulates STAT3 and ERK 1/2 intracellular signalling pathways in normal and transformed hepatic cells, the effect of IL-6 receptor activation

(a) H4IIE



(b) Hepatocytes

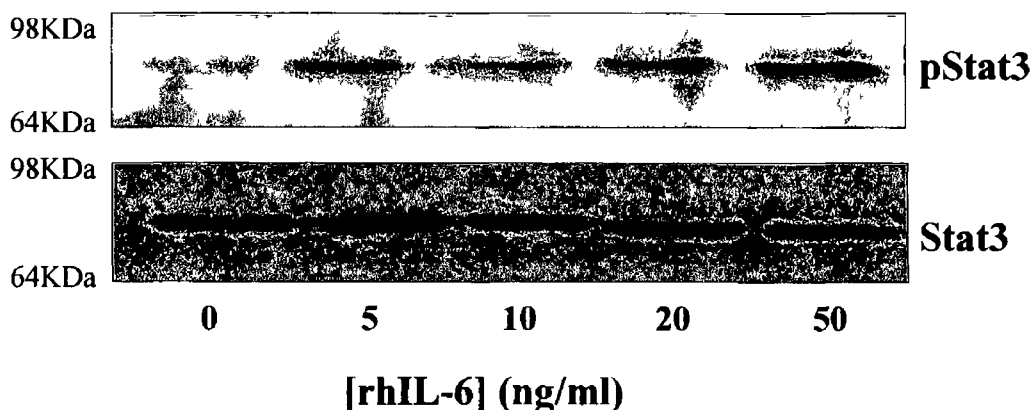
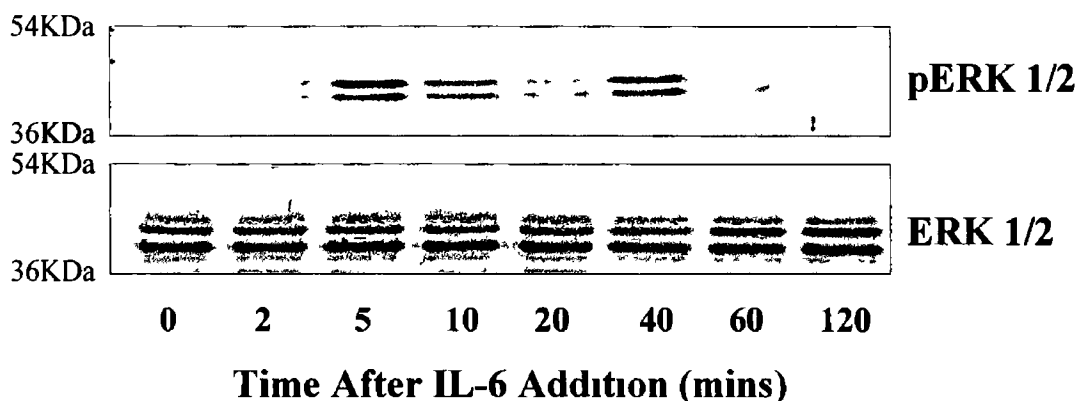


Figure 4 11 RhIL-6 stimulates STAT3 activity in H4IIE (HCC) cells and isolated cultured rat hepatocytes in a dose dependent manner in the absence of changes in total STAT3 expression *in vitro* a) Representative Western blot analysis performed on cell lysate samples prepared from cultured H4IIE cells using an antibody specific against active (phospho-) STAT3 (pSTAT3, upper panel) or total STAT3 (lower panel) H4IIE cells were isolated and purified from *in vivo* HCC tissue and cultured prior to treatment with rhIL-6 (0-50ng/ml) in serum free media for 60 mins b) Representative Western blot analysis performed on cell lysate samples prepared from isolated cultured rat hepatocytes using an antibody specific against active (phospho-) STAT3 (pSTAT3, upper panel) or total STAT3 (lower panel) Hepatocyte cell populations were isolated from normal rat livers by perfusion Following attachment, hepatocytes were placed in serum free media prior to treatment with rhIL-6 (0-50ng/ml) for 60 mins

(a) H4IIE



(b) Hepatocytes

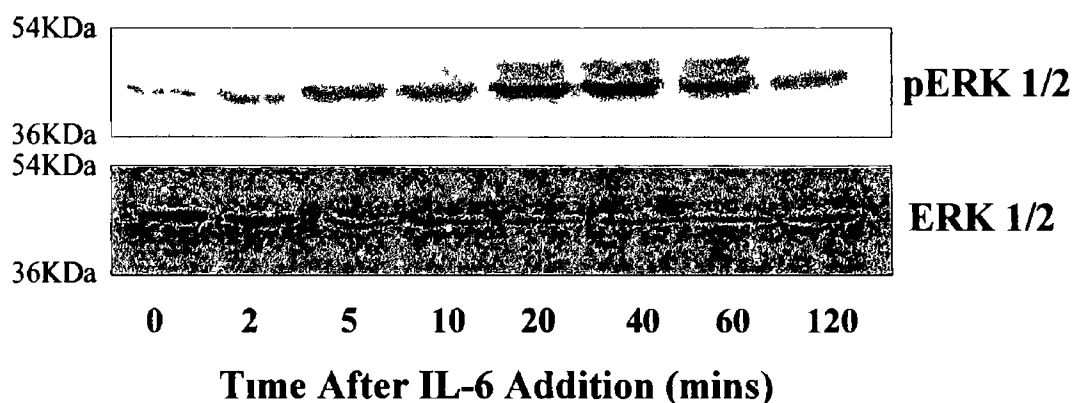


Figure 4 12 RhIL-6 stimulates MEK activity in H4IIE (HCC) cells and isolated cultured rat hepatocytes in a time-dependent manner in the absence of changes in total ERK expression *in vitro*. a) Representative Western blot analysis performed on cell lysates prepared from cultured H4IIE cells using an antibody specific against active ERK 1/2 (pERK 1/2, upper panel) or total ERK 1/2 (lower panel) H4IIE cells were isolated and purified from *in vivo* HCC tissue and cultured prior to treatment with rhIL-6 (50ng/ml) in serum free media for varying time periods (0-120 mins) b) Representative Western blot analysis performed on cell lysates prepared from isolated cultured rat hepatocytes using an antibody specific against active ERK 1/2 (pERK 1/2, upper panel) or total ERK 1/2 (lower panel) Hepatocyte cell populations were isolated from normal rat livers by perfusion Following attachment, hepatocytes were placed in serum free media prior to treatment with rhIL-6 (50ng/ml) in low serum media for varying time periods (0-120 mins)

on nuclear signalling pathways involved in cell proliferation was assessed. H4IIE cells and rat hepatocytes were cultured as previously and treated with 50ng/mL rhIL-6 over a 24h time period. Cell lysates were prepared for both untreated and treated cells at varying time points.

The expression of cyclins involved in the progression through the G1 restriction point was determined by Western blot analysis. Immunoblotting with antibodies specific against cyclin D1, D3 and A was carried out on cell lysates from H4IIE cells treated with rhIL-6 (50ng/mL). No differences in expression of cyclin A (Figure 4 13a, n=4), cyclin D1 (Figure 4 13b, n=4) or cyclin D3 (Figure 4 13c, n=4) were detected in rhIL-6 treated H4IIE cells compared to untreated cells at any of the time points. Furthermore, expression of each of these cyclins was not altered over the course of this experiment in either treatment group. Analysis of hepatocyte cell lysates following rhIL-6 treatment demonstrated both cyclin A (Figure 4 14a, n=4) and cyclin D3 (Figure 4 14c, n=4) were increased at 24h in both the untreated and rhIL-6 treated cells. There was however no difference in cyclin A or cyclin D3 expression between rhIL-6 treated and untreated hepatocytes at any of the time points assayed. Western blot analysis for cyclin D1 expression in hepatocytes also indicated increased expression of this protein at 24h in untreated cells (Figure 4 14b, n=4). Treatment of hepatocytes with rhIL-6 (50ng/mL) suppressed this increase in cyclin D1 expression at 24h (Figure 4 14b, n=4).

Having established cyclin expression in H4IIE cells and rat hepatocytes, the expression of cyclin dependent kinases (cdk) was next determined. Cdk2 and cdk4 are key factors during transition through the G1 cell cycle restriction point while cdc2 p34 is an important regulator of passage through the G2/M stages of the cell cycle (Morgan, 1995). Immunoblotting using antibodies specific against cdc2 p34, cdk2 and cdk4 was

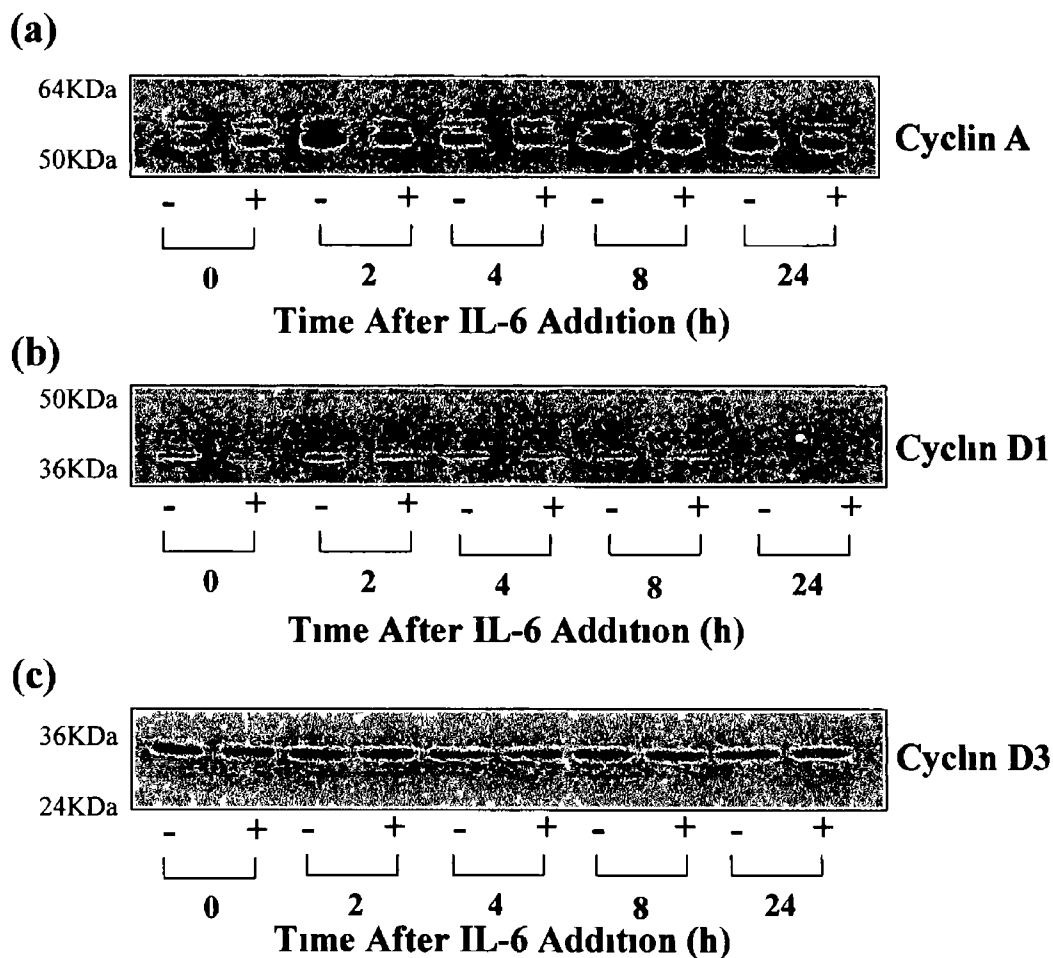


Figure 4 13 RhIL-6 treatment does not alter the expression of cyclins A, D1 and D3 in H4IIE (HCC) cells *in vitro*. Representative Western blot analysis performed on cell lysates prepared from cultured H4IIE cells using an antibody specific against a) cyclin A, b) cyclin D1 and c) cyclin D3. H4IIE cells were isolated and purified from *in vivo* HCC tissue and cultured prior to treatment (+) with rhIL-6 (50ng/ml) in serum free media for varying time periods (0-24h). Cell lysates from untreated (-) H4IIE cells were used as controls.

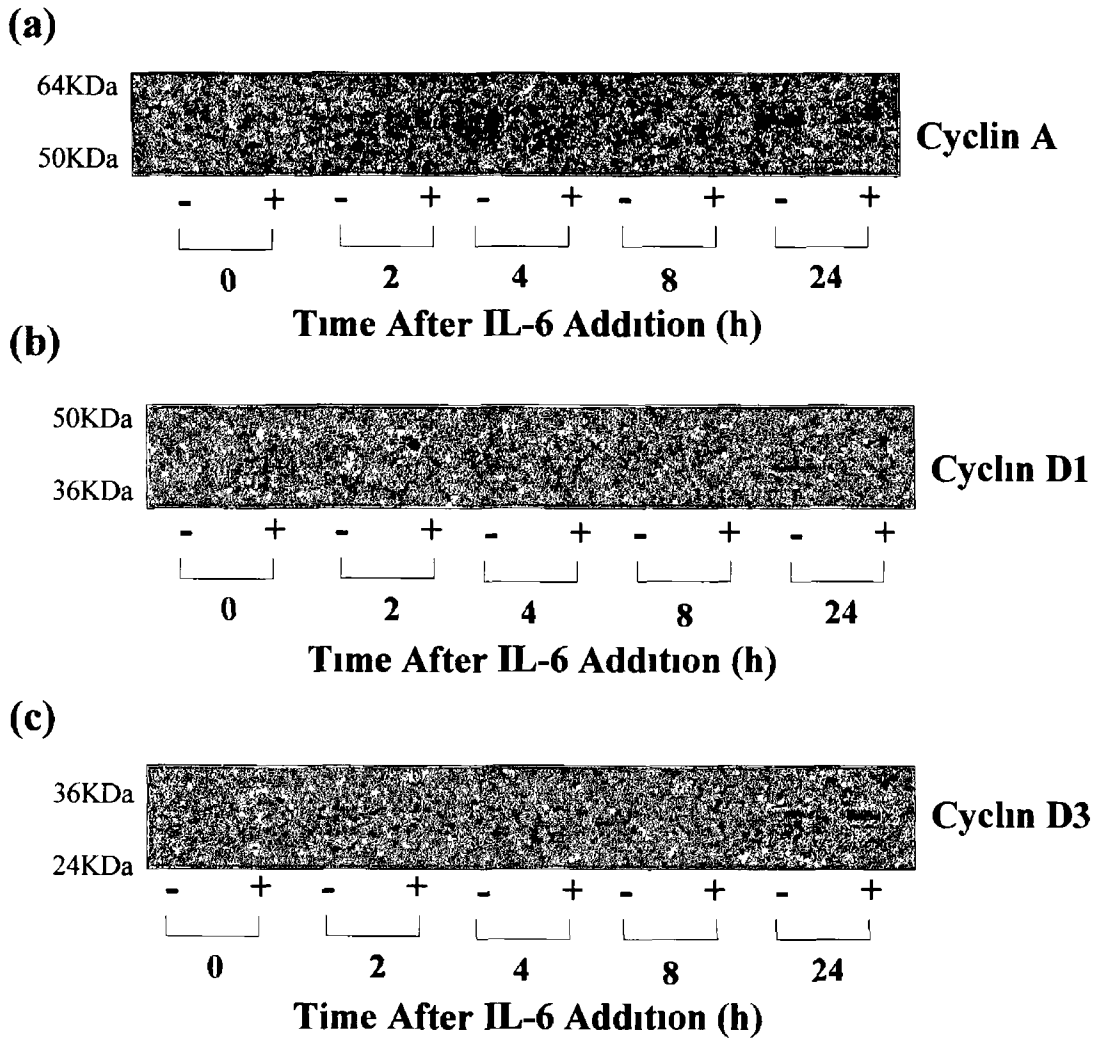


Figure 4 14 RhIL-6 treatment does not alter the expression of cyclins A and D3 but does suppress cyclin D1 expression in isolated cultured rat hepatocytes *in vitro*. Representative Western blot analysis performed on cell lysates prepared from isolated cultured rat hepatocytes using an antibody specific against a) cyclin A, b) cyclin D1 and c) cyclin D3. Hepatocyte cell populations were isolated from normal rat livers by perfusion. Following attachment, hepatocytes were placed in serum free media prior to treatment (+) with rhIL-6 (50ng/ml) for varying time periods (0-24h). Cell lysates from untreated (-) hepatocytes were used as controls.

performed on lysates from rhIL-6 (50ng/mL) treated and untreated H4IIE cells and rat hepatocytes collected over a 24h time period. No changes in cdc2 p34 (Figure 4 15a, n=4), cdk2 (Figure 4 15b, n=4) or cdk4 (Figure 4 15c, n=4) expression between rhIL-6 treated and control H4IIE cells was detected following IL-6 treatment. The treatment of hepatocytes with rhIL-6 did not alter the expression of either cdc2 p34 (Figure 4 16a, n=4), cdk2 (Figure 4 16b, n=4) or cdk4 (Figure 4 16c, n=4) when compared with untreated controls. Expression of cdk4 was decreased at 8h and 24h in both rhIL-6 treated and untreated hepatocytes (Figure 4 16c, n=4).

Expression of the cell cycle regulator proliferating cell nuclear antigen (PCNA) was next examined in rhIL-6 (50ng/mL) treated H4IIE cells and rat hepatocytes. Immunoblotting with an antibody specific for PCNA demonstrated that rhIL-6 treatment in H4IIE cells or hepatocytes had no effect on PCNA expression as compared to untreated controls over the experimental time period (Figure 4 17, n=4). Expression of PCNA increased, though not significantly at 24h in both treated and untreated hepatocytes (Figure 4 17b, n=4).

H4IIE cells and rat hepatocytes were next analysed for p21^{waf1/cip1} and p27^{Kip1} expression following rhIL-6 (50ng/mL) treatment by Western blot analysis. These data demonstrated time dependent increases in p21^{waf1/cip1} and p27^{Kip1} expression in H4IIE cells. Increased p21^{waf1/cip1} was detected 4h after rhIL-6 addition before peaking at 8h and returning to baseline levels after 24h (Figure 4 18a, n=4). In contrast, p27^{Kip1} expression did not increase until 8h after treatment, elevated expression being maintained up to 24h after IL-6 treatment (Figure 4 19a, n=4). Expression levels of p21^{waf1/cip1} and p27^{Kip1} in isolated hepatocytes did not change following rhIL-6 treatment throughout the time course assayed (Figure 4 18b and 4 19b, n=4).

Having established that the expression of cdk inhibitors p21^{waf1/cip1} and p27^{Kip1} was elevated by rhIL-6 treatment in H4IIE cells, the expression of pRb/ppRb was

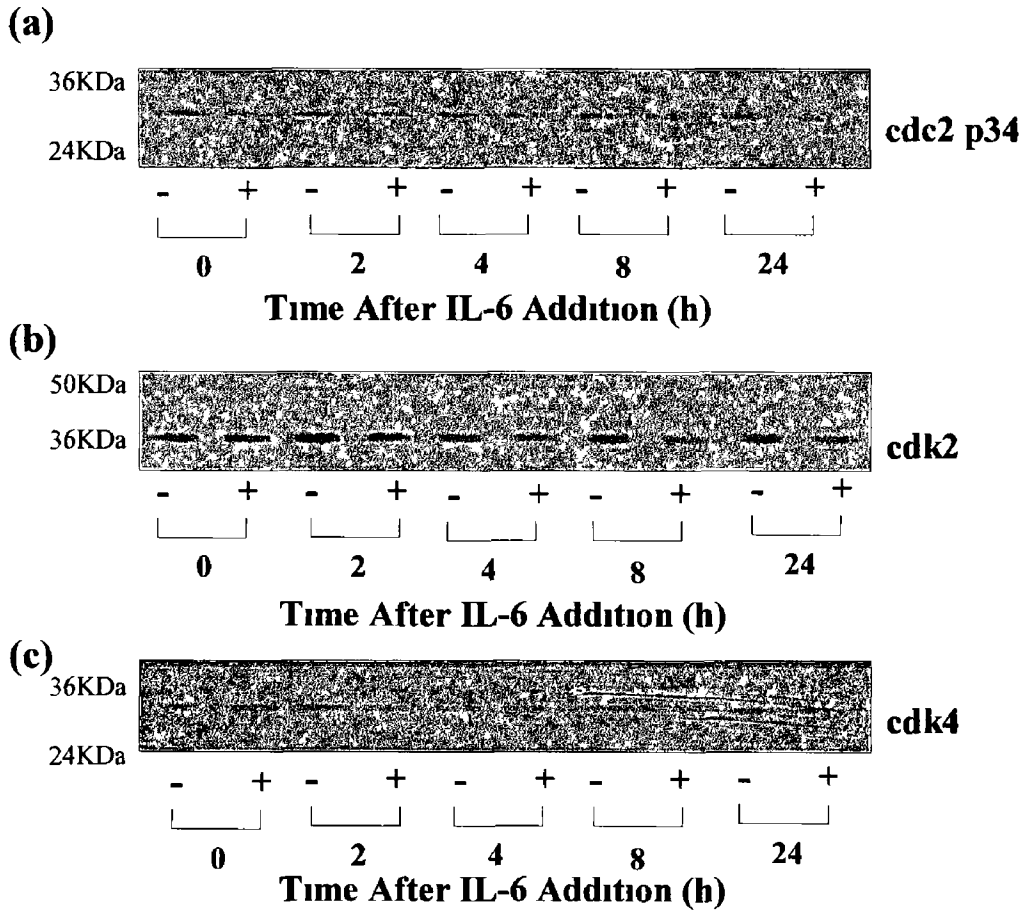


Figure 4 15 RhIL-6 treatment does not alter the expression of cyclin dependent kinases cdc2 p34, cdk2 and cdk4 in H4IIE (HCC) cells *in vitro* Representative Western blot analysis performed on cell lysates prepared from cultured H4IIE cells using an antibody specific against a) cdc2 p34, b) cdk2 and c) cdk4 H4IIE cells were isolated and purified from *in vivo* HCC tissue and cultured prior to treatment (+) with rhIL-6 (50ng/ml) in serum free media for varying time periods (0-24h) Cell lysates from untreated (-) H4IIE cells were used as controls

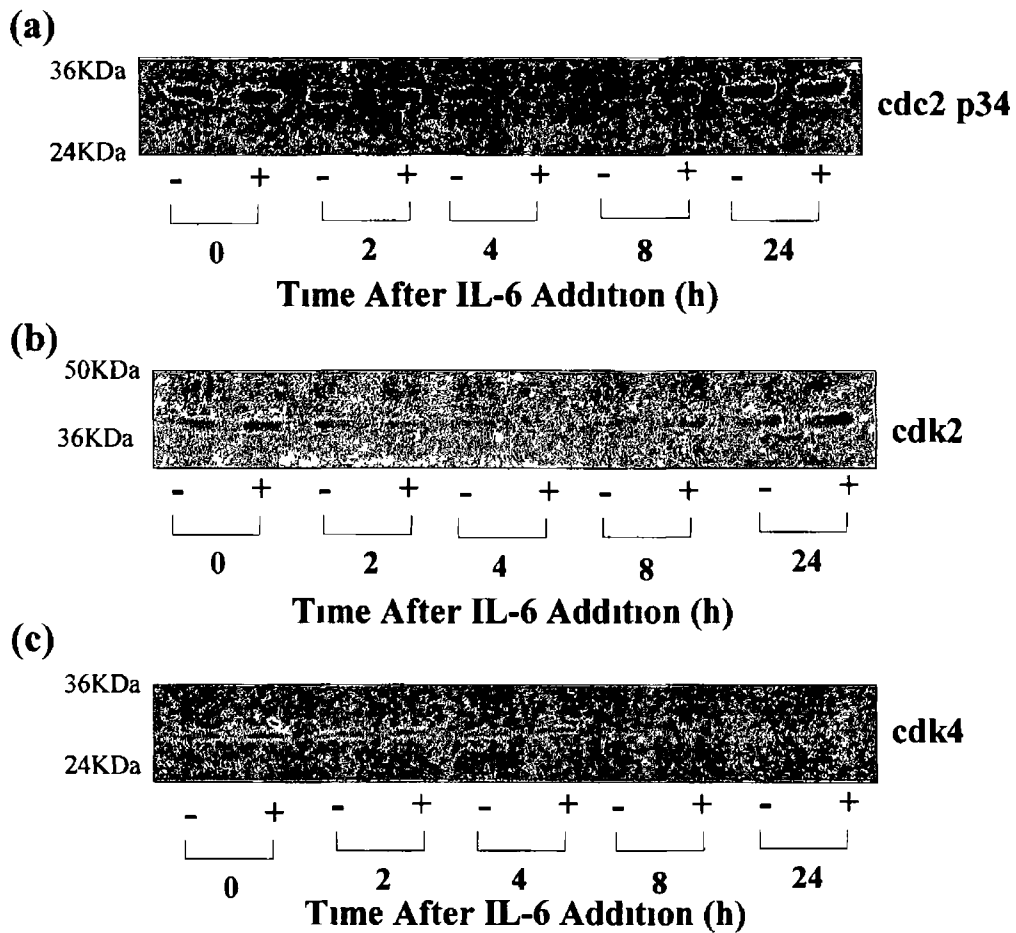
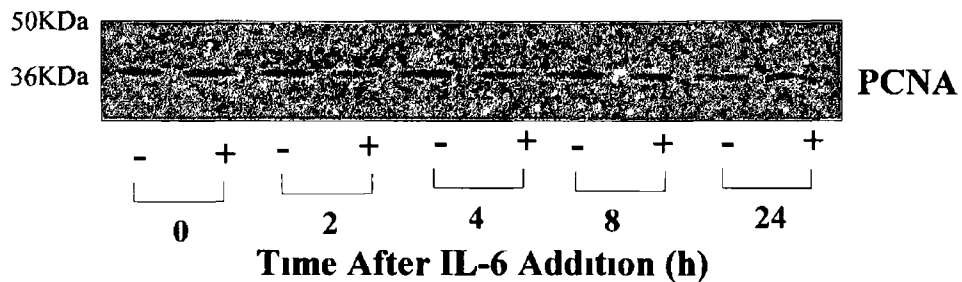


Figure 4.16 RhIL-6 treatment does not alter the expression of cyclin dependent kinases cdc2 p34, cdk2 and cdk4 in isolated cultured rat hepatocytes *in vitro*. Representative Western blot analysis performed on cell lysates prepared from isolated cultured rat hepatocytes using an antibody specific against a) cdc2 p34, b) cdk2 and c) cdk4. Hepatocyte cell populations were isolated from normal rat livers by perfusion. Following attachment, hepatocytes were placed in serum free media prior to treatment (+) with rhIL-6 (50ng/ml) for varying time periods (0-24h). Cell lysates from untreated (-) hepatocytes were used as controls.

(a) H4IIE



(b) Hepatocytes

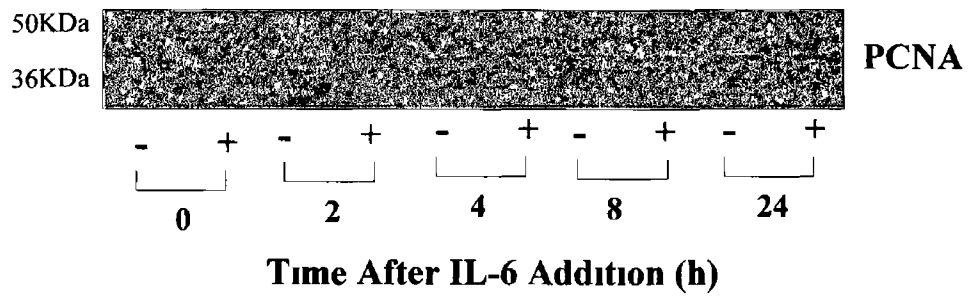
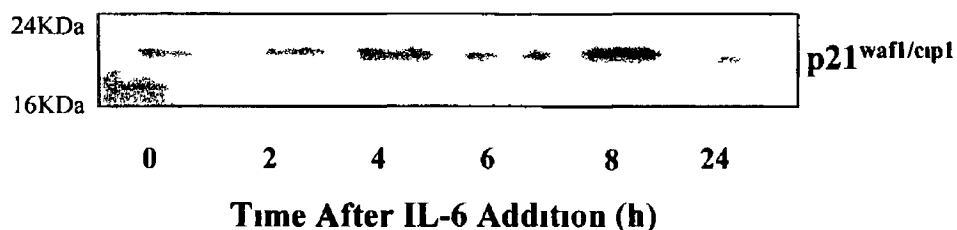


Figure 4.17 RhIL-6 treatment does not alter the expression of PCNA in H4IIE (HCC) cells or isolated cultured rat hepatocytes *in vitro* a) Representative Western blot analysis performed on cell lysates prepared from cultured H4IIE cells using an antibody specific against PCNA. H4IIE cells were isolated and purified from *in vivo* HCC tissue and cultured prior to treatment (+) with rhIL-6 (50ng/ml) in serum free media for varying time periods (0-24h). Cell lysates from untreated (-) H4IIE cells were used as controls. b) Representative Western blot analysis performed on cell lysates prepared from isolated cultured rat hepatocytes using an antibody specific against PCNA. Hepatocyte cell populations were isolated from normal rat livers by perfusion. Following attachment, hepatocytes were placed in serum free media prior to treatment (+) with rhIL-6 (50ng/ml) for varying time periods (0-24h). Cell lysates from untreated (-) hepatocytes were used as controls.

(a) H4IIE



(b) Hepatocytes

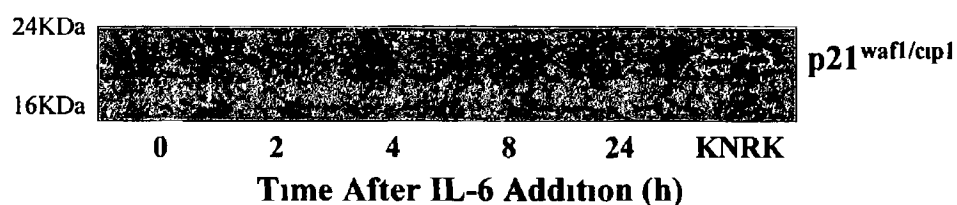
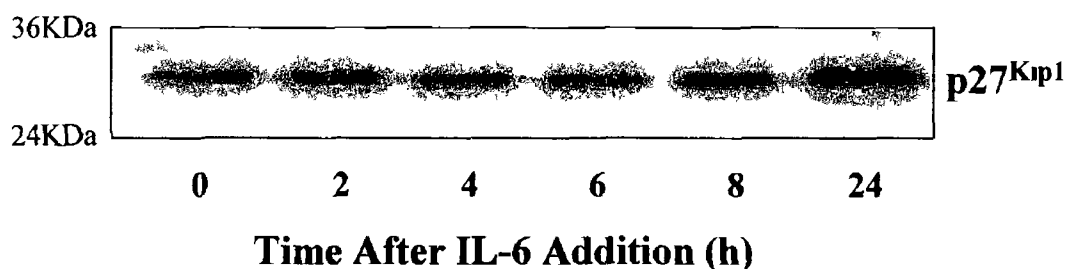


Figure 4.18 RhIL-6 stimulates expression of the cyclin dependent kinase inhibitor p21^{waf1/cip1} in H4IIE (HCC) but does not alter its expression in isolated cultured rat hepatocytes *in vitro*. a) Representative Western blot analysis performed on cell lysates prepared from cultured H4IIE cells using an antibody specific against p21^{waf1/cip1}. H4IIE cells were isolated and purified from *in vivo* HCC tissue and cultured prior to treatment with rhIL-6 (50ng/ml) in serum free media for varying time periods (0-24h) b) Representative Western blot analysis performed on cell lysates prepared from isolated cultured rat hepatocytes using an antibody specific against p21^{waf1/cip1}. Hepatocyte cell populations were isolated from normal rat livers by perfusion. Following attachment, hepatocytes were placed in serum free media prior to treatment with rhIL-6 (50ng/ml) for varying time periods (0-24h). KNRK nuclear extract was loaded as a positive control for p21^{waf1/cip1} expression.

(a) H4IIE



(b) Hepatocytes

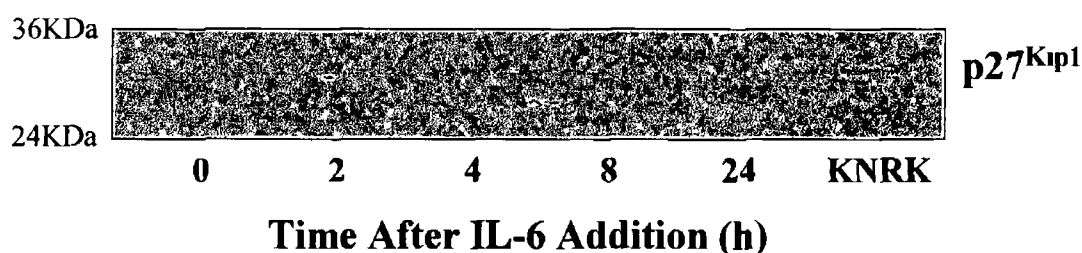


Figure 4 19 RhIL-6 stimulates expression of the cyclin dependent kinase inhibitor p27^{Kip1} in H4IIE (HCC) but does not alter its expression in isolated cultured rat hepatocytes *in vitro*. a) Representative Western blot analysis performed on cell lysates prepared from cultured H4IIE cells using an antibody specific against p27^{Kip1}. H4IIE cells were isolated and purified from *in vivo* HCC tissue and cultured prior to treatment with rhIL-6 (50ng/ml) in serum free media for varying time periods (0-24h) b) Representative Western blot analysis performed on cell lysates prepared from isolated cultured rat hepatocytes using an antibody specific against p27^{Kip1}. Hepatocyte cell populations were isolated from normal rat livers by perfusion. Following attachment, hepatocytes were placed in serum free media prior to treatment with rhIL-6 (50ng/ml) for varying time periods (0-24h). KNRK nuclear extract was loaded as a positive control for p27^{Kip1} expression.

measured as a marker of cdk activity at the G1 restriction point. Hypophosphorylated Rb (pRb) acts as an inhibitor of premature entry of the cell into the S-phase of the cell cycle and is a target for cdk dependent phosphorylation. These data demonstrated that 4h after rhIL-6 treatment the levels of ppRB expression, the hyperphosphorylated form of Rb, were decreased as compared to untreated H4IIE cells (Figure 4 20, n=4). Throughout the remainder of the time course, ppRb expression remained significantly higher in untreated cells than cells treated with IL-6.

Given that p21^{waf1/cip1} and p27^{Kip1} expression was increased and Rb phosphorylation was decreased in IL-6 treated H4IIE cells, cdk activity was next determined in these cells. Cultured H4IIE cells were treated with rhIL-6 (50ng/mL) over a 24h period. Cyclin dependent kinase 2 and cdk4 were immunoprecipitated from cell lysates collected at varying time points in IL-6 treated and untreated cells. The activity of cdk2 was determined using a kinase reaction with Histone H1 as a substrate. IL-6 decreased the level of cdk2 activity as evidenced by decreased phosphorylation of the Histone H1 substrate at 8h and 24h compared to untreated controls (Figure 4 21, n=4). Kinase reactions to measure cdk4 activity, using the Rb-C fusion protein as a substrate, also demonstrated decreased kinase activity at 8h after IL-6 treatment *versus* untreated cells (Figure 4 22, n=4).

4 3.5 Pharmacological Inhibition of IL-6 Stimulated ERK Activation *In Vitro*

To determine the intracellular signalling pathway responsible for rhIL-6 stimulated p21^{waf1/cip1} and p27^{Kip1} upregulation in H4IIE cells, PD98059, a selective MEK inhibitor, was used to abrogate IL-6 dependent ERK 1/2 activation. H4IIE cells were cultured as previously and pretreated with PD98059 (20µM) for 1h prior to treatment with rhIL-6 (50ng/mL). Control cells were pretreated for 1h with DMSO (1µL/mL) followed by rhIL-6 (50ng/mL). Cell lysates were then collected at varying time points

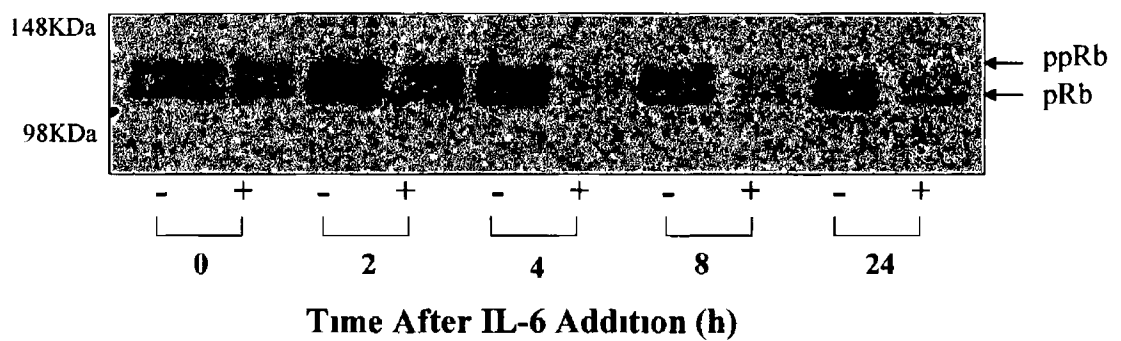


Figure 4 20 RhIL-6 treatment in H4IIE (HCC) cells is associated with a decreased level of phosphorylation of the retinoblastoma protein *in vitro*. Representative Western blot analysis performed on cell lysates prepared from cultured H4IIE cells using an antibody specific against the phosphorylated and hyperphosphorylated forms of Rb protein (pRb and ppRb respectively). H4IIE cells were isolated and purified from *in vivo* HCC tissue and cultured prior to treatment (+) with rhIL-6 (50ng/ml) in serum free media for varying time periods (0-24h). Cell lysates from untreated (-) H4IIE cells were used as controls. Increased pRb versus ppRb represents increased ability to suppress entry of the cell into the S-phase of the cell cycle.

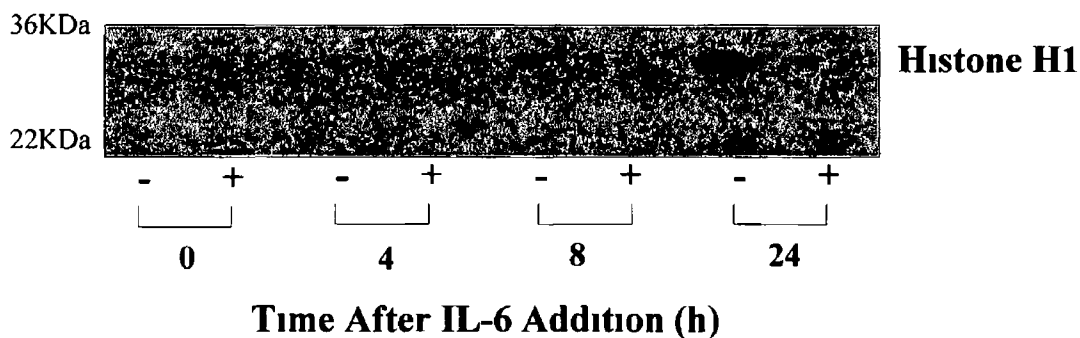


Figure 4.21 RhIL-6 treatment of H4IIE (HCC) cells is associated with a decreased level of cdk2 activity *in vitro*. Representative kinase assay analysis performed on cell lysates prepared from cultured H4IIE cells using Histone H1 as substrate. H4IIE cells were isolated and purified from *in vivo* HCC tissue and cultured prior to treatment (+) with rhIL-6 (50ng/ml) in serum free media for varying time periods (0-24h). Cell lysates from untreated (-) H4IIE cells were used as controls. Cdk2 was immunoprecipitated from these lysates and used in an *in vitro* kinase reaction in the presence of radioactive γ -P³² labelled ATP.

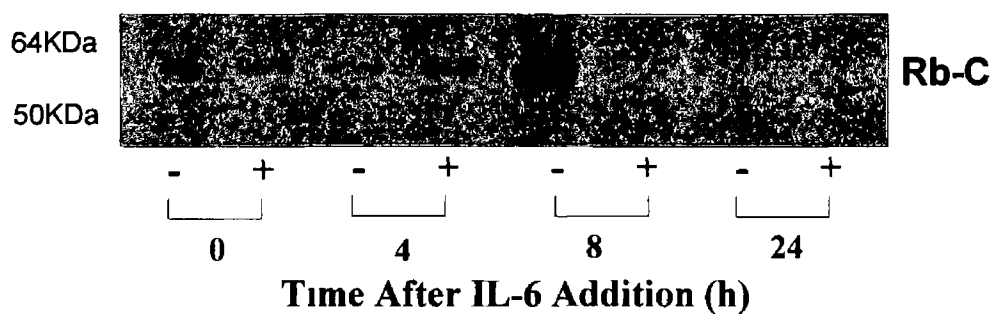


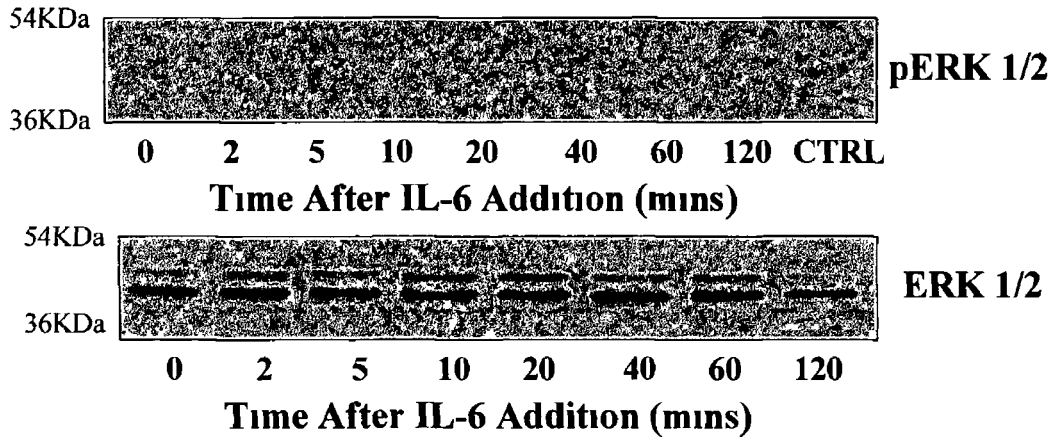
Figure 4 22 RhIL-6 treatment of H4IIE (HCC) cells is associated with a decreased level of cdk4 activity *in vitro* Representative kinase assay analysis performed on cell lysates prepared from cultured H4IIE cells using Rb-C fusion protein as substrate. H4IIE cells were isolated and purified from *in vivo* HCC tissue and cultured prior to treatment (+) with rhIL-6 (50ng/ml) in serum free media for varying time periods (0-24h). Cell lysates from untreated (-) H4IIE cells were used as controls. Cdk4 was immunoprecipitated from these lysates and used in an *in vitro* kinase reaction in the presence of radioactive γ - P^{32} labelled ATP.

up to 24h Previous data demonstrates rhIL-6 stimulates ERK 1/2 activity in a biphasic manner, an initial increase being detected 2-5 mins after addition followed by a second, sustained activation 40-60 mins later (Figure 4 12a) Treatment of cells with DMSO abrogated initial, early ERK 1/2 activation but did not alter the second phase of the ERK activation profile (Figure 4 23b, n=4) Treatment with PD98059 abolished ERK 1/2 activity at all time points assayed following rhIL-6 addition (Figure 4 23a, n=4) In contrast, treatment with either PD98059 or vehicle (DMSO) did not affect STAT3 activation profiles in H4IIE cells following rhIL-6 stimulation (Figure 4 24, n=4) Having determined that PD98059 treatment abolishes ERK 1/2 activation in the absence of changes in STAT3 activity, p21^{waf1/cip1} and p27^{Kip1} expression was next assayed following inhibition of ERK 1/2 activity using PD98059 The addition of rhIL-6 in vehicle pretreated cells resulted in increased p21^{waf1/cip1} and p27^{Kip1} expression 4h and 8h respectively after addition (Figure 4 25b, n=4) The expression of both p21^{waf1/cip1} and p27^{Kip1} was similar to that observed in the absence of DMSO (Figure 4 18a and 4 19a, n=4) Immunoblotting for both p21^{waf1/cip1} and p27^{Kip1} in cell lysates from PD98059 pretreated rhIL-6 stimulated H4IIE cells demonstrated both p21^{waf1/cip1} and p27^{Kip1} expression increased in response to rhIL-6 despite the absence of ERK 1/2 activation (Figure 4 25a, n=4) P21^{waf1/cip1} expression was increased 4h after rhIL-6 addition reaching a maximal expression after 8h (Figure 4 25a, upper panel, n=4) and p27^{Kip1} expression was increased at 8h and further increased up to 24h following rhIL-6 treatment (Figure 4 25a, lower panel, n=4)

4 3 6 Inhibition of IL-6 Stimulated STAT3 Activation *In Vitro*

Having established that inhibition of a MEK-ERK signalling pathway did not alter rhIL-6 stimulated p21^{waf1/cip1} and p27^{Kip1} expression in H4IIE cells, inhibition of STAT3 activation was next addressed In an initial attempt to inhibit STAT3, an

(a) PD98059



(b) DMSO

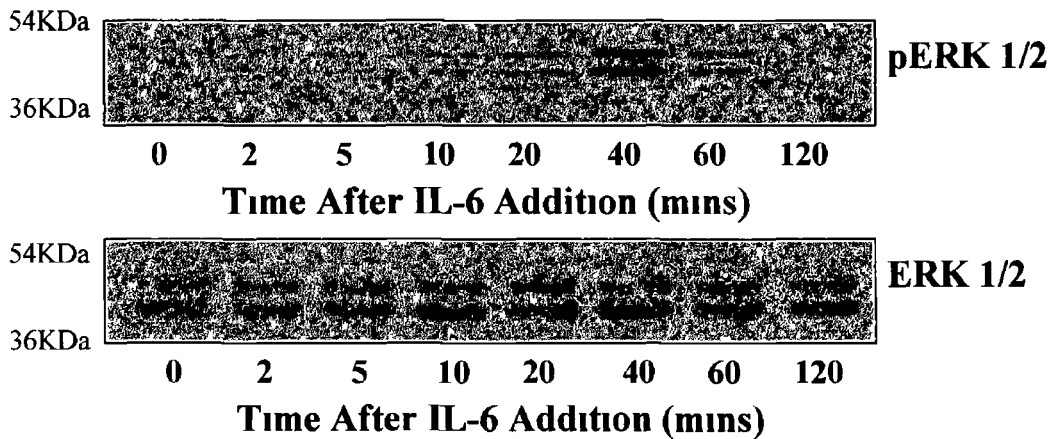
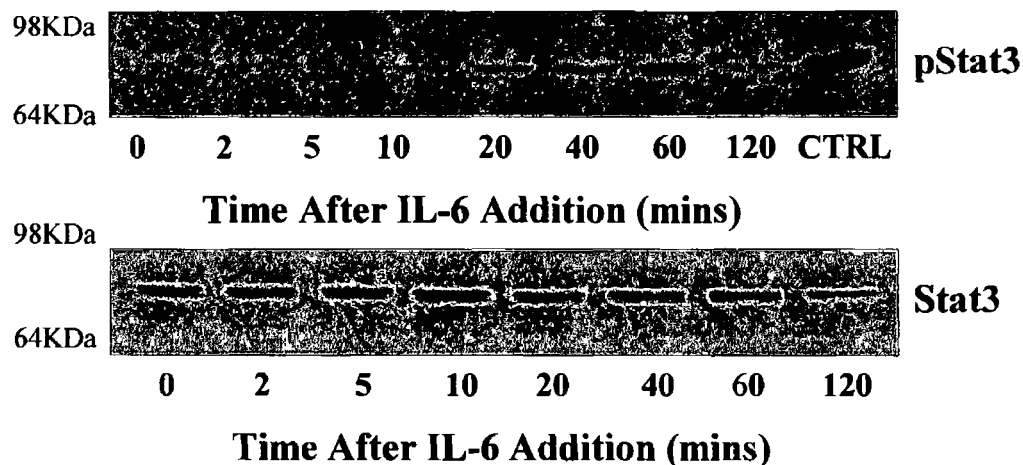


Figure 4.23 PD98059 (MEK inhibitor) treatment of H4IIE (HCC) cells abolishes rhIL-6 stimulation of MEK activity *in vitro* a) Representative Western blot analysis performed on cell lysates prepared from cultured H4IIE cells in the a) presence or b) absence of PD98059 using an antibody specific against active (phospho-) ERK 1/2 (pERK 1/2, upper panel) or total ERK 1/2 (lower panel) H4IIE cells were isolated and purified from *in vivo* HCC tissue and cultured prior to treatment with a) PD98059 (20 μ M) or b) DMSO (control, 1 μ L/mL) in serum free media for 1h. Cells were then treated with rhIL-6 (50ng/mL) for varying time periods (0-120 mins). Cell lysate from quiesced H4IIE cells stimulated for 10 mins with serum was used as positive control (CTRL) for pERK 1/2.

(a) PD98059



(b) DMSO

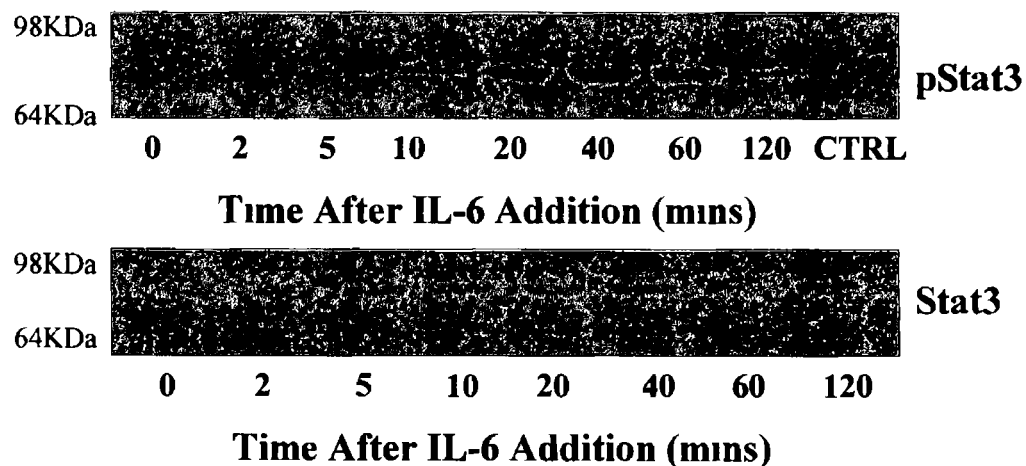
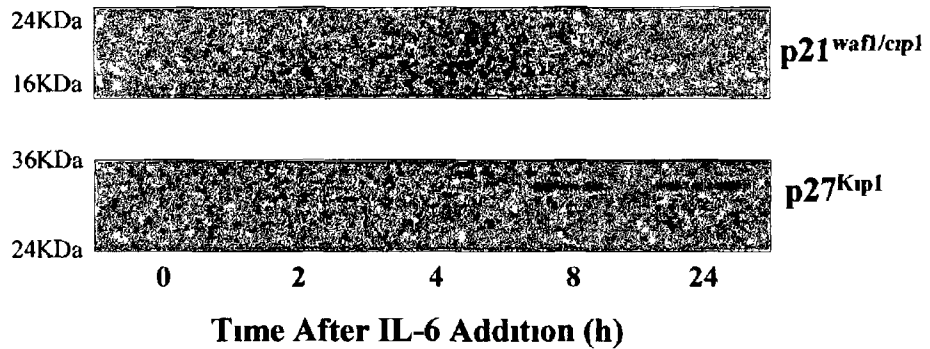


Figure 4 24 RhIL-6 stimulation of STAT3 activity is not altered by PD98059 (MEK inhibitor) treatment of H4IIE (HCC) cells *in vitro*. a) Representative Western blot analysis performed on cell lysates prepared from cultured H4IIE cells in the a) presence or b) absence of PD98059 using an antibody specific against active (phospho) STAT3 (pSTAT3, upper panel) or total STAT3 (lower panel). H4IIE cells were isolated and purified from *in vivo* HCC tissue and cultured prior to treatment with a) PD98059 (20 μ M) or b) DMSO (control, 1 μ L/mL) in serum free media for 1h. Cells were then treated with rhIL-6 (50ng/mL) for varying time periods (0-120 mins). Cell lysate from H4IIE cells stimulated for 1h with rhIL-6 was used as positive control (CTRL) for pSTAT3.

(a) PD98059



(b) DMSO

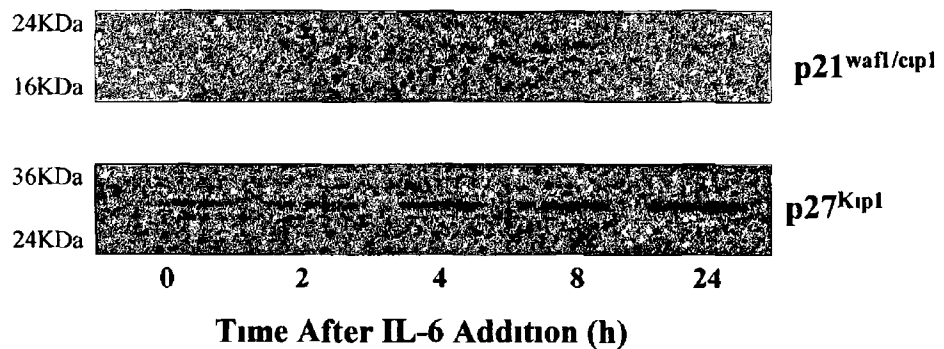
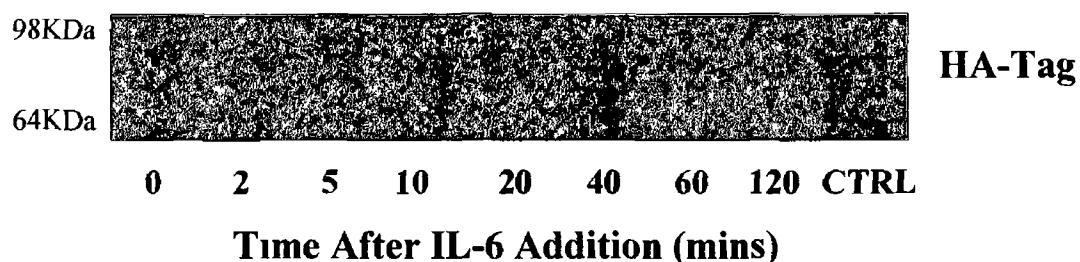


Figure 4 25 PD98059 (MEK inhibitor) treatment of H4IIE (HCC) cells does not inhibit the rhIL-6 stimulated expression of p21^{waf1/cip1} and p27^{Kip1} *in vitro*. a) Representative Western blot analysis performed on cell lysates prepared from cultured H4IIE cells in the a) presence or b) absence of PD98059 using an antibody specific against p21^{waf1/cip1} (upper panel) or p27^{Kip1} (lower panel) H4IIE cells were isolated and purified from *in vivo* HCC tissue and cultured prior to treatment with a) PD98059 (20 μ M) or b) DMSO (control, 1 μ L/mL) in serum free media for 1h Cells were then treated with rhIL-6 (50ng/mL) for varying time periods (0-24h)

overexpression vector for dominant negative STAT3 was transiently transfected into H4IIE cells. pEFHASTAT3F expresses an HA tagged STAT3 (STAT3F) in which the tyrosine residue at position 705 has been replaced with a phenylalanine residue preventing its phosphorylation/activation. Control cells were transfected with the expression vector pEFHASTAT3 containing cDNA coding for HA tagged wild type STAT3. The optimum method for H4IIE transfection had been previously determined in our laboratory using a series of luciferase transfections and these parameters were used in these experiments. Highest levels of transfection were previously obtained using 20µg lipofectamine/6µg of plasmid DNA/reaction in 1mL of media on an 80-90% confluent well in 6 well plates. In previous experiments, cells were incubated with this mixture for a period of 20h prior to addition of high serum media (HSM). Maximum luciferase activity was observed 48h post HSM addition. H4IIE cells were cultured as previously and transiently transfected with pEFHASTAT3F or pEFHASTAT3 expression vectors under these conditions. High levels of cell death (~80-90%) occurred when H4IIE cells were incubated with transfection mixture for a period of 20h. In all subsequent experiments an incubation of 5h with plasmid DNA/lipofectamine was used prior to addition of HSM. This minimised cell death (~10-15% total cell death) in the H4IIE population. Once transfected, cells were maintained in HSM for 40h prior to quiescing for 24h in serum free media. Cells were then treated with rhIL-6 (50ng/mL) and cell lysates collected at varying time points. Immunoblotting specific against the HA-tag was then performed on cell lysates to determine if the cells were expressing the dominant negative or wild type STAT3. Despite continued efforts, the HA-Tag could not be detected in the H4IIE lysates from cells transfected with either pEFHASTAT3F (Figure 4.26a, n=5) or pEFHASTAT3 (Figure 4.26b, n=5). Furthermore, Western blotting for active STAT3 in these lysates indicated that STAT3 was activated by rhIL-6 stimulation with no differences in

(a) HASTAT3F Transfected



(b) HASTAT3 Transfected

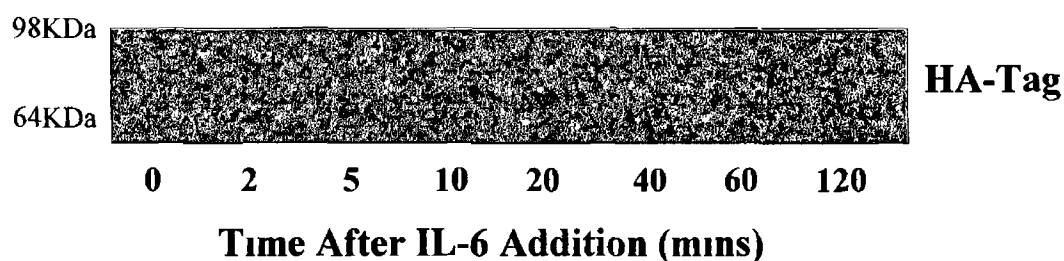


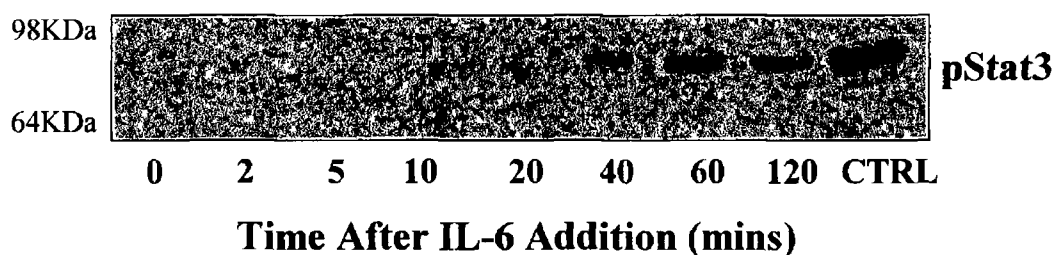
Figure 4 26 HA-Tag was not detectable in cell lysates of H4IIE (HCC) cells transfected with HA-tagged wild type expressing or HA-tagged dominant negative expressing STAT3 plasmids *in vitro* Representative Western blot analysis performed on cell lysates prepared from a) pEFHASTAT3F transfected (STAT3 dominant negative expression vector) or b) pEFHASTAT3 transfected (STAT3 wild type expression vector) H4IIE cells using an antibody specific against active HA-Tag H4IIE cells were isolated and purified from *in vivo* HCC tissue and cultured prior to transfection with pEFHASTAT3F or pEFHASTAT3 expression vectors After 40h in culture cells were quiesced in SFM for 24h and then treated with rhIL-6 (50ng/mL) for varying time periods (0-120 mins) Non transfected H4IIE cell lysates were loaded as control (CTRL)

expression profile being observed between dominant negative and wild type transfectants (Figure 4.27, n=4). Due to the low efficiency and the inherent difficulties associated with the transfection of this cell type, other means to STAT3 inhibition were sought.

To counter the problems associated with transfection AG490, a specific inhibitor of Jak activity, was next used to inhibit rhIL-6 stimulation of STAT3 in H4IIE cells *in vitro*. To establish the parameters for optimum STAT3 inhibition, H4IIE cells were pretreated with AG490 (0-150 μ M) for 1h prior to stimulation of cells with rhIL-6 (50ng/mL). Cell lysates were collected 1h post-rhIL-6 treatment, equalised for protein content and then analysed for pSTAT3 expression by Western blot. AG490 abrogated rhIL-6 dependent STAT3 activation, decreases in pSTAT3 detection being observed at a concentration of 50 μ M AG490 and decreasing further to 19.20 \pm 9.57% of untreated at 100 μ M (Figure 4.28, n=4). Pretreatment of H4IIE cells with the highest dose of AG490 (150 μ M) altered cell morphology and was not used. H4IIE cells were cultured as previously and pretreated with AG490 or DMSO (0.6 μ L/mL; vehicle) for 1h followed by rhIL-6 over a 24h period. Cell lysates were collected at varying time points and analysed for STAT3 and ERK activation and p21^{waf1/cip1} and p27^{Kip1} expression by Western blot analysis. Treatment with rhIL-6 in the presence of DMSO increased STAT3 activation at 5 mins, reaching a maximal response at 40 to 60 mins in the absence of changes in total STAT3 expression (Figure 4.29b, n=4). In contrast, rhIL-6 treatment in AG490 pretreated H4IIE cells led to an ablated phosphorylation of STAT3 following the same activation profile (Figure 4.29a, upper panel, n=4). AG490 treatment did not alter total STAT3 expression (Figure 4.29a, lower panel).

Immunoblotting for pERK 1/2 was next performed to establish the effects of AG490 on its activation profile following rhIL-6 treatment. Recombinant human IL-6 stimulated ERK 1/2 activation in the presence of DMSO (0.6 μ L/mL; Figure 4.30b,

(a) HASTAT3F Transfected



(b) HASTAT3 Transfected

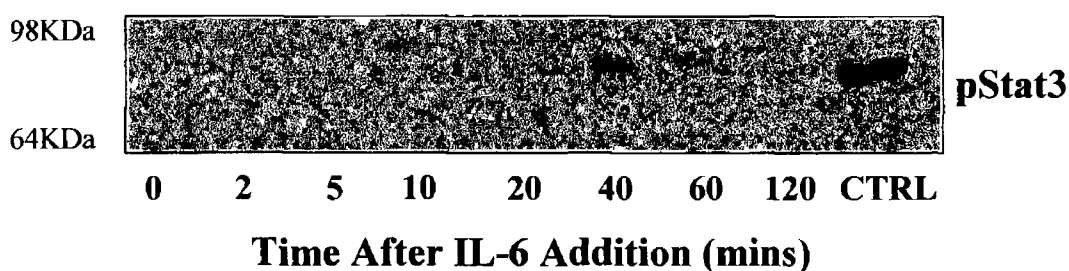


Figure 4 27 Transfection of H4IIE (HCC) cells with a plasmid expressing dominant negative STAT3 failed to inhibit rhIL-6 stimulation of STAT3 activity *in vitro* a) Representative Western blot analysis performed on cell lysates prepared from cultured pEFHASTAT3F transfected (STAT3 dominant negative expression vector) H4IIE cells using an antibody specific against active (phospho-) STAT3 (pSTAT3) H4IIE cells were isolated and purified from *in vivo* HCC tissue and cultured prior to transfection with pEFHASTAT3F After 40h *in culture* cells were quiesced in SFM for 24h and then treated with rhIL-6 (50ng/mL) for varying time periods (0-120 mins) b) Representative Western blot analysis performed on cell lysate samples prepared from cultured pEFHASTAT3 transfected (STAT3 wild type expression vector) H4IIE cells using an antibody specific against active (phospho-) STAT3 (pSTAT3) H4IIE cells were isolated and purified from *in vivo* HCC tissue and cultured prior to transfection with pEFHASTAT3 After 60h *in culture* cells were treated with rhIL-6 (50ng/mL) for varying time periods (0-120 mins) Cell lysate from H4IIE cells stimulated for 1h with rhIL-6 was used as positive control (CTRL) for pSTAT3

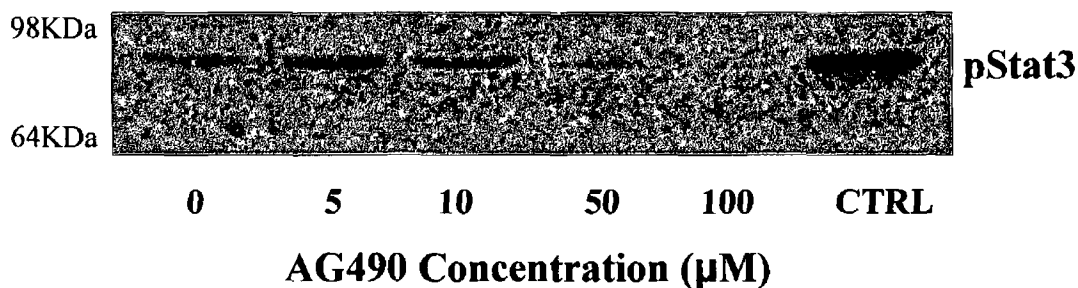
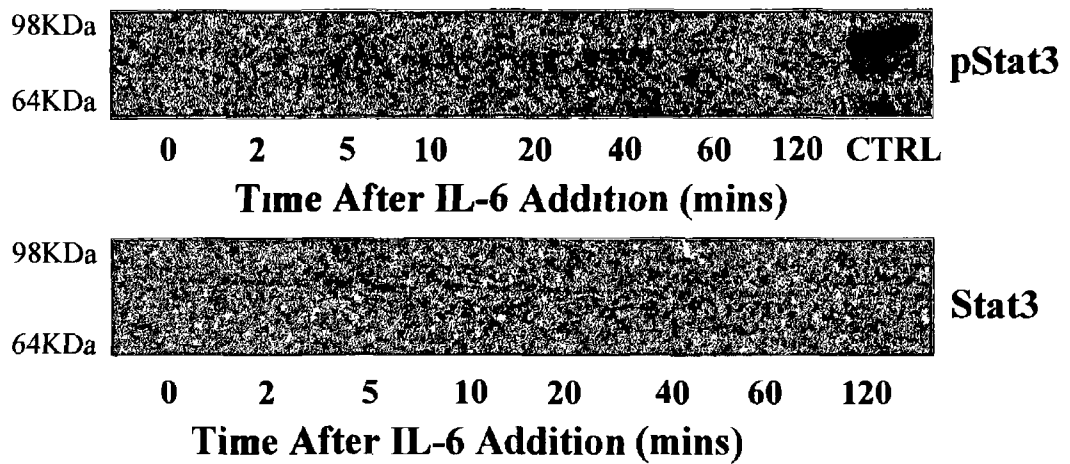


Figure 4 28 AG490 inhibits rhIL-6 stimulation of STAT3 activity in a dose dependent manner *in vitro*. Representative Western blot analysis performed on cell lysates prepared from cultured H4IIE cells in the presence of varying concentrations of AG490 using an antibody specific against active (phospho-) STAT3 (pSTAT3) H4IIE cells were isolated and purified from *in vivo* HCC tissue and cultured prior to treatment with varying concentrations of AG490 (0-100 μM) in serum free media for 1h Cells were then treated with rhIL-6 (50ng/mL) for 1h Cell lysate from H4IIE cells stimulated for 1h with rhIL-6 was used as positive control (CTRL) for pSTAT3

(a) AG490



(b) DMSO

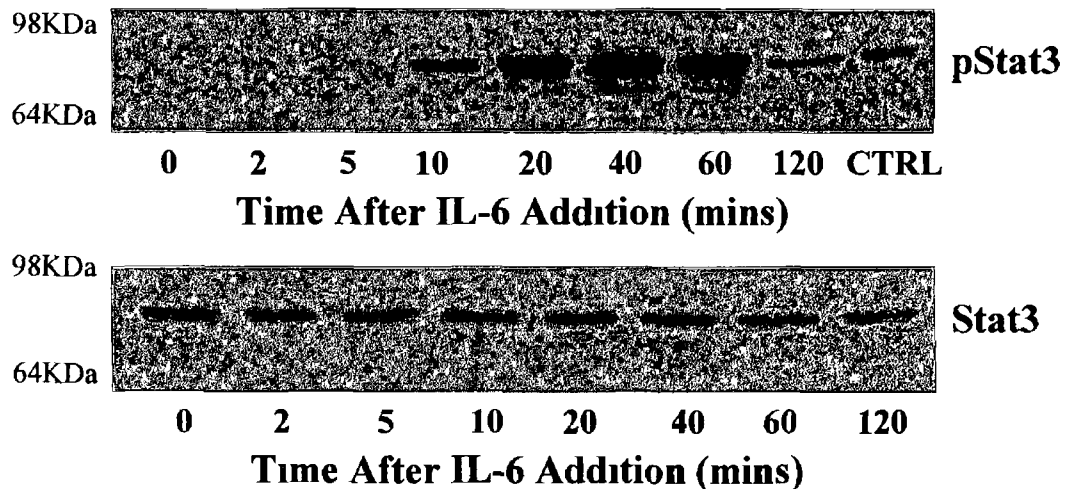
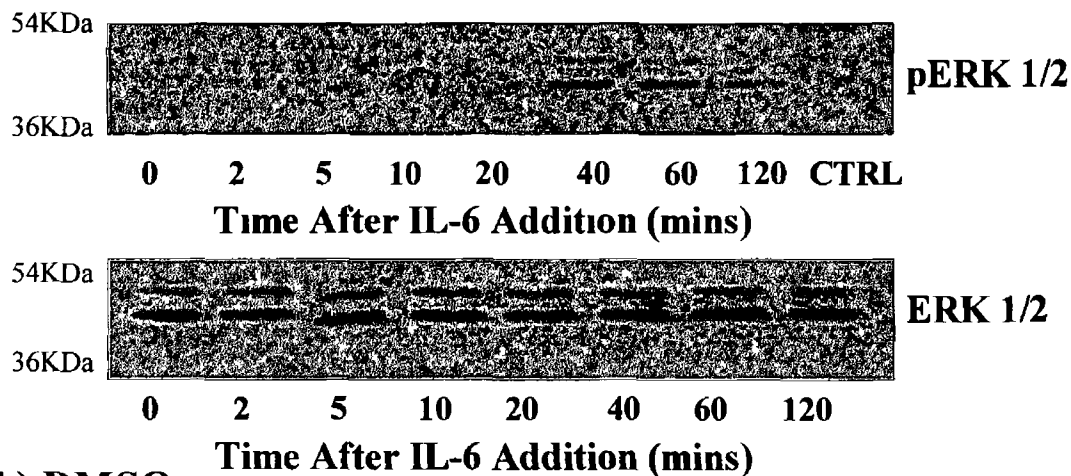


Figure 4.29 RhIL-6 stimulation of STAT3 activity is ablated by AG490 (Jak inhibitor) treatment of H4IIE (HCC) cells *in vitro*. a) Representative Western blot analysis performed on cell lysates prepared from cultured H4IIE cells in the a) presence or b) absence of AG490 using an antibody specific against active (phospho-) STAT3 (pSTAT3, upper panel) or total STAT3 (lower panel) H4IIE cells were isolated and purified from *in vivo* HCC tissue and cultured prior to treatment with a) AG490 (100 μ M) or b) DMSO (control, 0 6 μ L/mL) in serum free media for 1h Cells were then treated with rhIL-6 (50ng/mL) for varying time periods (0-120 mins) Cell lysate from H4IIE cells stimulated for 1h with rhIL-6 was used as positive control (CTRL) for pSTAT3

(a) AG490



(b) DMSO

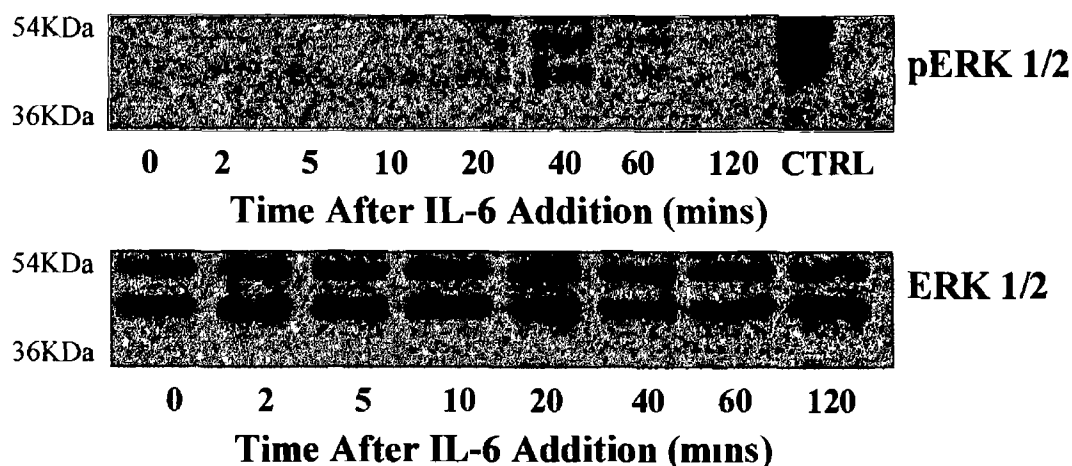
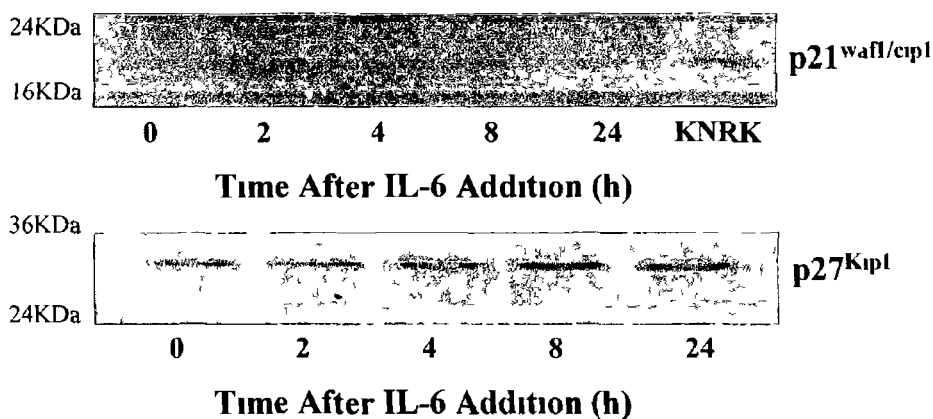


Figure 4 30 RhIL-6 ability to stimulate MEK activity is not altered by AG490 (Jak inhibitor) treatment of H4IIE (HCC) cells *in vitro*. a) Representative Western blot analysis performed on cell lysates prepared from cultured H4IIE cells in the a) presence or b) absence of AG490 using an antibody specific against active (phospho-) ERK 1/2 (pERK 1/2, upper panel) or total ERK 1/2 (lower panel) H4IIE cells were isolated and purified from *in vivo* HCC tissue and cultured prior to treatment with a) AG490 (100 μ M) or b) DMSO (control, 0.6 μ L/mL) in serum free media for 1h. Cells were then treated with rhIL-6 (50ng/mL) for varying time periods (0-120 mins). Cell lysate from quiesced H4IIE cells stimulated for 10 mins with serum was used as positive control (CTRL) for pERK 1/2.

n=4) was similar to that previously established in DMSO pretreated H4IIE cells (1 μ l/mL, Figure 4 24b) The early phase of ERK 1/2 activation (2-5 mins) was again abolished in the presence of DMSO while pERK 1/2 expression was increased at 40 mins returning towards baseline expression by 60 mins post IL-6 treatment (Figure 4 30b, upper panel, n=4) DMSO did not alter the expression of total ERK 1/2 (Figure 4 30b, lower panel, n=4) Recombinant human IL-6 stimulation of AG490 pretreated H4IIE cells also resulted in increased levels of pERK 1/2 at 40 mins However, in these cells the increased ERK activity was sustained and remained upregulated up to 2h after rhIL-6 treatment (Figure 4 30a, upper panel, n=4) Total ERK 1/2 expression remained unchanged throughout this time period (Figure 4 30a, lower panel, n=4)

Expression of p21^{waf1/cip1} and p27^{Kip1} was next compared in AG490 pretreated and control (DMSO pretreated) H4IIE cells Immunoblotting of cell lysates using antibodies specific against p21^{waf1/cip1} in control H4IIE cells demonstrated that DMSO did not affect rhIL-6 stimulated p21^{waf1/cip1} expression (Figure 4 31b, upper panel, n=4) As observed in cells treated in the absence of DMSO (Figure 4 18a), rhIL-6 caused an upregulation of p21^{waf1/cip1} at 4h which was further increased at 8h before returning to baseline expression at 24h (Figure 4 31b, upper panel, n=4) Similarly, the upregulation of p27^{Kip1} expression in response to rhIL-6 stimulation was maintained in DMSO pretreated cells, increased levels being detected at 8h and 24h after rhIL-6 stimulation (Figure 4 31b, lower panel, n=4) Treatment of H4IIE cells with AG490 prior to rhIL-6 stimulation blocked the upregulation in p21^{waf1/cip1} observed in control cells (Figure 4 31a, upper panel, n=4) In contrast, AG490 treatment did not alter rhIL-6 stimulated p27^{Kip1} expression induced by rhIL-6 stimulation as compared to control cells (Figure 4 31a, lower panel, n=4)

(a) AG490



(b) DMSO

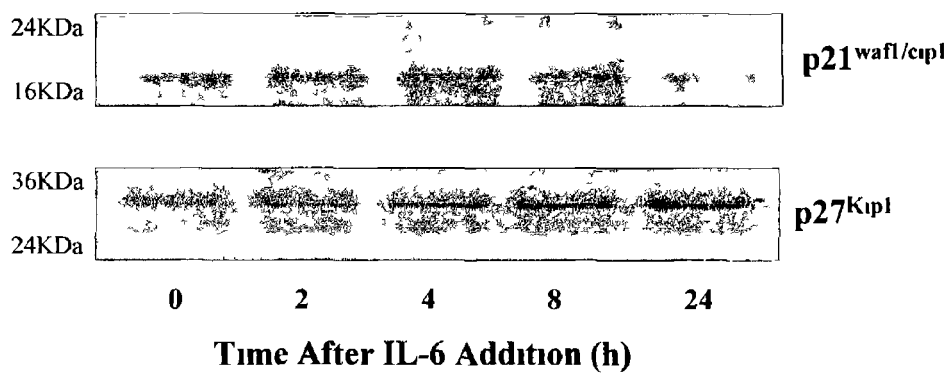


Figure 4 31 AG490 (Jak inhibitor) treatment of H4IIE (HCC) cells inhibits the rhIL-6 stimulated expression of p21^{waf1/cip1} but does not affect the expression of p27^{Kip1} *in vitro* a) Representative Western blot analysis performed on cell lysates prepared from cultured H4IIE cells in the a) presence or b) absence of AG490 using an antibody specific against p21^{waf1/cip1} (upper panel) or p27^{Kip1} (lower panel) H4IIE cells were isolated and purified from *in vivo* HCC tissue and cultured prior to treatment with a) AG490 (100μM) or b) DMSO (control, 0.6μL/mL) in serum free media for 1h Cells were then treated with rhIL-6 (50ng/mL) for varying time periods (0-24h) KNRK nuclear extract was used as a positive control for both p21^{waf1/cip1}

4.4 Discussion

Previous studies have established a critical role for IL-6 signalling during hepatocyte proliferation (Streetz et al , 2000, Fausto, 2000) In contrast, the role of IL-6 in HCC remains controversial and poorly defined Data included in these studies establishes clear differences between IL-6 signalling pathways in HCC cells as compared to isolated cultured hepatocytes IL-6 signalling initiates Jak-STAT and Ras-MAPK signalling cascades in both normal and transformed liver cells While the Jak-STAT pathway was similarly activated in both cell types, IL-6 had a distinctive biphasic effect on ERK activity in HCC cells *versus* normal hepatocytes Furthermore, IL-6 treatment suppressed Cyclin D1 expression in hepatocytes but did not effect the expression of any of the other cell cycle regulatory proteins examined (cyclins, cdks and PCNA) In HCC cells, cyclin, cdk and PCNA expression was not affected by IL-6 stimulation however IL-6 treatment did result in the upregulation of the cdk inhibitors, p21^{waf1/cip1} and p27^{Kip1}, an effect unseen in hepatocytes This increase in cdk inhibitor expression was associated with decreased cdk2 and cdk4 activity and reduced phosphorylation of their primary substrate, the retinoblastoma protein (Rb) IL-6 stimulated p21^{waf1/cip1} expression was abrogated by inhibition of STAT3 activity, while p27^{Kip1} expression was not affected by inhibition of the MAPK pathway or partial inhibition of the Jak-STAT signalling cascade

Normally hepatocytes are long lived and rarely divide *in vivo* yet retain the ability to proliferate in response to infection and toxic injury (Taub, 2004, Fausto, 2000) Two-thirds partial hepatectomy (the removal of approximately 70% of the liver) induces synchronised cell cycle entry of approximately 95% of hepatic cells resulting in the complete replacement of the resected organ mass (Taub, 2004) Unlike cells of proliferative tissues, hepatocytes are generally quiescent and rest in the G0 phase of the cell cycle (Fausto, 2000) In liver regeneration, hepatocytes are primed to exit G0 and

enter the G1 phase of the cell cycle in preparation for DNA synthesis and mitosis. The primed hepatocytes then respond to a variety of growth factors including transforming growth factor- α (TGF- α), hepatocyte growth factor (HGF) and epidermal growth factor (EGF) which stimulate the hepatocytes to overcome the G1 restriction point and commit to DNA replication (Fausto, 2000, Streetz et al, 2000, Taub, 2004). IL-6 is a key cytokine in this priming process. Reduced liver mass causes increased serum TNF- α levels which stimulate IL-6 expression and downstream STAT3 activation. STAT3 activation, in collaboration with additional transcription factors such as C/EBP β , enhance the expression of other factors such as NF-IL-6, c-myc, c-fos, Jun-B, IRF-1, and others, enabling the resting hepatocytes to progress into cell proliferation (Streetz et al, 2000, Fausto, 2000). Activation of STAT3 and early gene expression is absent in IL-6 $^{-/-}$ mice in which defective regeneration is reported following partial hepatectomy (Cressman et al, 1996). Further reports demonstrate that the MAPK pathway activated during liver regeneration is stimulated by IL-6 signalling and is linked to G1 progression (Li et al, 2001, Talarmin et al, 1999). More recently, Zimmers et al report that IL-6 can act as a complete mitogen in the liver. In this model circulating IL-6 levels were increased in nude mice using a transfected CHO cell line, leading to dramatic hepatomegaly and hepatocyte hyperplasia in the absence of liver injury (Zimmers et al, 2003). In support of this observation, previous research using double transgenic mice expressing human IL-6 and human soluble IL-6R under liver specific promoters also demonstrate hepatomegaly, hepatic hyperplasia and the presence of hepatic adenomas (Maione et al, 1998, Schirmacher et al, 1998).

Previous studies have demonstrated that the process of hepatocyte isolation (collagenase digestion) primes hepatocytes for replication as evidenced by expression of immediate early genes such as the proto-oncogenes, *c-fos* and *c-jun*, resulting in the entry of these cells into the G1 phase of the cell cycle. The presence of growth factors

is required to stimulate the hepatocytes into DNA replication (S phase entry) *in vitro* reflecting the *in vivo* model of liver regeneration (Albrecht and Hansen, 1999, Loyer et al , 1996) Growth factors such as EGF- α and TGF- α lead to the orderly activation of key cell cycle regulatory proteins that control the transition through the G1 restriction point after which hepatocytes are fully committed to mitogen independent DNA synthesis and mitosis (Fausto, 2000, Streetz et al , 2000, Loyer et al , 1996) The expression of hepatocyte cyclin D1 mRNA increases at the G1 restriction point while cyclin A, cdk2, cdc2 p34 and cyclin D3 mRNA becomes detectable, or increase, in late G1/early S phase following mitogen stimulation In the absence of growth factors, expression of these proteins (except cyclin D3 and cdk4) does not occur (Loyer et al , 1996, Albrecht and Hansen, 1999) Surprisingly, in the current study, expression of cyclin D1, cyclin A and cyclin D3 were all increased at 44h after plating in hepatocyte cultures in the absence of growth factors While these all serve as markers of cell cycle entry, the expression of cyclin D1 alone has been shown to be sufficient for passage through the G1 restriction point in hepatocytes (Albrecht and Hansen, 1999) If indeed these hepatocytes are proliferating, the source of growth stimuli is unclear The presence of FBS during the first four hours of culture has previously been shown not to stimulate DNA synthesis in hepatocytes (Loyer et al , 1996) Furthermore collagenase treatment, cell washing or cell seeding in culture medium do not induce cyclin D1 expression (Loyer et al , 1996) It is worth noting that much of the previous research has been performed on hepatocyte populations which have been isolated by collagenase digestion and then further purified using a Percoll gradient (Loyer et al , 1996, Albrecht and Hansen, 1999) In the current set of experiments the hepatocyte population from collagenase digestion without further purification was used The population of non parenchymal cells such as stellate and Kupffer cells can reach up to 20% of these cultures Further enrichment of hepatocyte cultures with non parenchymal cells and

incubation of hepatocytes with media from non parenchymal cell cultures have been shown to increase hepatocyte DNA synthesis (Hasmall et al , 2000) *In vivo*, non parenchymal cells act as the main source of hepatic cytokines and growth factors such as HGF and TNF- α (Taub, 2004) It is possible that secretion of growth factors by other cell populations in these cultures gave rise to the increased cell cycle activity observed Furthermore, it is worth noting that IL-6 treatment was capable of suppressing cyclin D1 expression *in vitro* in the absence of effects on other cell cycle regulatory proteins studied While previous studies indicate a stimulatory role for IL-6 in the proliferation of cultured hepatocytes (Kuma et al , 1990), several others report an inhibitory effect of IL-6 on DNA synthesis, even after growth factor stimulation *in vitro* (Sato and Yamazaki, 1992, Kordula et al , 1991) The exact mechanisms behind the inhibition of cyclin D1 expression by IL-6 in this study is unclear however, it may be associated with an inhibitory effect on hepatocyte proliferation in this culture system

Progression through the cell cycle is tightly controlled by cyclin dependent kinases (cdks) (Morgan, 1995) Cyclins associate with cdks and are the primary regulators of cdk activity (Sherr and Roberts, 1999, Morgan, 1995) The activation of cdk4 plays an important role in the passage through the G1 restriction point when the cell becomes committed to proceed through the cell cycle, while cdk2 activation plays an essential role in the transition into S phase and DNA synthesis Cyclin D1 expression, which is induced during G1 phase in response to various mitogens, complexes with and activates cdk4 Cyclin dependent kinase 2 is regulated primarily by cyclin E and cyclin A during G1/S transition and S phase respectively (Sherr and Roberts, 1999, Morgan, 1995, Sherr and Roberts, 1995) Retinoblastoma protein (Rb) is the major target for cyclin dependent kinase activity and is phosphorylated by both cyclin D dependent kinases and by cdk2 Hyperphosphorylation of the Rb protein disrupts its association with E2F transcription factors which, once released, stimulates

the expression of a series of genes required for DNA synthesis (Sherr and Roberts, 1999, Morgan, 1995, Sherr and Roberts, 1995) In the present study IL-6 stimulation resulted in decreased phosphorylation of Rb protein when compared to untreated HCC cells 4h after treatment which was maintained for up to 24h following addition Analysis of G1/S phase cyclin and cdk expression demonstrated no significant change in these regulatory proteins following IL-6 addition Increased levels of the cyclin dependent kinase inhibitor p21^{waf1/cip1} were detected at 4h before peaking at 8h following IL-6 treatment corresponding with the decreases in hyperphosphorylated Rb protein detection Increased p27^{Kip1} expression was detected at both 8h and 24h after IL-6 addition P27^{Kip1} and p21^{waf1/cip1} are members of the Cip/Kip family of cdk inhibitors that can affect the activity of cyclin D-, E- and A-dependent kinases through binding of both the cyclin and cdk subunits (Sherr and Roberts, 1999) Further analysis of cdk activity in the current model demonstrates that IL-6 in HCC cells reduces the activity of both cdk2 and cdk4 *in vitro* Collectively this data suggests an inhibitory effect of IL-6 treatment on cell cycle progression in these HCC cells Indeed, several other reports have identified a similar inhibitory effect of IL-6 in other cancer cells which have been further associated with the upregulation of p27^{Kip1} and p21^{waf1/cip1} (Kortylewski et al , 1999, Klausen et al , 2000, Florenes et al , 1999, Bellido et al , 1998)

The addition of exogenous IL-6 activates identical intracellular signalling pathways (JAK-STAT and Ras-MAPK) in both transformed H4IIE cells and primary hepatocytes in culture Despite these apparent similarities in signalling pathways, treatment of cells with IL-6 only results in increased expression of the cdk inhibitors p21^{waf1/cip1} and p27^{Kip1} in transformed hepatic cells In this study ERK 1/2 activation in H4IIE cells and cultured primary rat hepatocytes was observed following IL-6 stimulation However, the temporal patterns of ERK phosphorylation differed greatly between these two cell types A distinctive transient biphasic phosphorylation of ERK

1/2 was observed in H4IIE cells as compared to the monophasic phosphorylation/activation in primary hepatocytes. Several reports have now identified the critical temporal profile of ERK activation in mediating cell differentiation versus cellular proliferation (Weber et al., 1997; Meloche et al., 1992; Cook and McCormick, 1996; Tamemoto et al., 1992) whereby sustained ERK activation is implicated in ERK regulated cellular proliferation (Cook and McCormick, 1996; Meloche et al., 1992).

Both the Jak-STAT and MAPK pathways have been implicated in upregulating p21^{waf1/cip1} and p27^{Kip1} in response to IL-6 in other cell types (Kortylewski et al., 1999; Klausen et al., 2000; Florenes et al., 1999; Bellido et al., 1998). Furthermore, expression of p21^{waf1/cip1} and p27^{Kip1} has been linked to STAT3 activation (Bellido et al., 1998; Johannessen et al., 1999; de Koning et al., 2000; Kortylewski et al., 1999) and ERK 1/2 activity (Bottazzi et al., 1999; Dixon et al., 2002; Klausen et al., 2000) stimulated by other ligands. In H4IIE cells inhibition of IL-6 stimulated ERK 1/2 activity using PD98059 had no effect on p21^{waf1/cip1} or p27^{Kip1} expression. Initially, in an effort to elucidate the involvement of the STAT3 pathway in this model, H4IIE cells were transiently transfected with a dominant negative STAT3 (HASTAT3F) expression vector. In this mutant STAT3, the tyrosine residue at position 705 has been mutated to phenylalanine (Nakajima et al., 1996). Phosphorylation of Tyr705 is required for dimerisation and nuclear translocation. Despite continued efforts this mutant form of STAT3 was not detectable in H4IIE cell lysates and IL-6 continued to stimulate STAT3 activity in the transfected cells. Further work carried out in our research laboratory has demonstrated through the use of LacZ detection systems that maximum achievable transient transfection efficiency could not be increased past 1% of the total cell population in this cell type. This would explain the lack of HASTAT3F expression in the current study. Ideally stable transfections would prove more useful in this work

however this expression vector, in its current state, lacks selection markers for animal cell culture and hence could not be used in this way

AG490, an inhibitor of Jak activity, was used as an alternative method to inhibit the IL-6 induced STAT3 pathway. While complete abolishment of STAT3 activity was not possible in these cells, AG490 did allow a partial inhibition of STAT3 activity. Phosphorylated STAT3 levels in AG490 pretreated cells decreased by approximately 80% *versus* untreated cells following IL-6 treatment. It is worth noting that AG490 mediated inhibition of STAT3 phosphorylation was accompanied by altered pERK 1/2 expression. Phosphorylation of ERK 1/2 was sustained up to 2h after stimulation in AG490 pretreated cells compared to a peak in phosphorylation at 40–60 mins observed in untreated cells after IL-6 addition. Similar changes in ERK 1/2 activation have been reported when STAT3 activity is inhibited by AG490 or genetic means. In other models, this effect being potentially linked to both decreased SOCS expression and decreased expression of phosphatases such as mitogen activated protein kinase phosphatase 1 (Ernst et al, 2001, Sandberg et al, 2004). The AG490 mediated reduction in STAT3 activation was sufficient to ablate p21^{waf1/cip1} expression indicating that the IL-6 stimulated activation of STAT3 is responsible for its upregulation in H4IIE cells. Interestingly, IL-6 stimulated increases in p27^{Kip1} expression in H4IIE cells were maintained despite decreased pSTAT3. The underlying mechanism by which p27^{Kip1} expression is modulated in this cell type after IL-6 addition remains unclear. Potentially, lower levels of active STAT3 are sufficient for p27^{Kip1} upregulation, however, this could only be proved by complete inhibition of STAT3 activity which was not possible in the current studies. Furthermore, other pathways may be regulated by IL-6 addition in this cell type. STAT3 and MAPK are the primary targets after IL-6 stimulation however STAT5 (Klausen et al, 2000), PI3K (Chen et al, 1999) and STAT1 (Kortylewski et al, 1999) have been shown to be activated in other models.

Furthermore, both PI3K and STAT5 have the ability to alter p27^{Kip1} expression (Klausen et al , 2000, Banerji et al , 2001, Zhu et al , 2003, Barata et al , 2004) Overall, a more efficient system for STAT3 inhibition, in addition to further research on other potential activation targets for IL-6 within these cells, is required to fully establish the mechanism involved in the upregulation of p27^{Kip1}

H4IIE cells grown in culture do retain characteristics observed *in vivo* even with continual passaging H4IIE cells express decreased levels of both components of the IL-6 receptor *in vitro* The observed alterations in expression of IL-6 signalling components in resected tumours (chapter 3) led to the current study in which IL-6 signalling in H4IIE cells and hepatocytes *in vitro* was compared and contrasted It has been established that IL-6 can activate similar pathways in both cell types however with different activation profiles Furthermore, it has been observed that IL-6 upregulated the expression of the cdk inhibitors p21^{waf1/cip1} and p27^{Kip1} in H4IIE cells, an effect that was unseen in hepatocytes This increase in cdk inhibitors also correlated with decreased cdk activity and reduced levels of phosphorylation of their target, Rb Taken together, these data are suggestive of an inhibitory effect of IL-6 on cell cycle progression in H4IIE cells

Chapter 5: Growth Regulatory Effects of IL-6 in HCC

5.1 Introduction

HCC is characterised by altered expression of components of the IL-6 signalling cascade *in vivo* and *in vitro* (chapters 3 & 4) This includes downregulated expression of IL-6 receptor components and upregulated IL-6 production and secretion Nevertheless, IL-6 treatment of HCC cells *in vitro* activates Jak-STAT and Ras-MAPK pathways leading to increased expression of the cdk inhibitors, p21^{waf1/cip1} and p27^{Kip1} (chapter 4) Decreased phosphorylation of the Rb protein and attenuated cdk activity were observed concomitant with this upregulation Collectively, these events are potentially inhibitory on cell cycle progression in H4IIE cells, however, the consequences for cell proliferation remain to be determined

Interleukin-6 has been identified as a growth factor for several cancer cell types including renal cell carcinoma (Miki et al , 1989), multiple myeloma (Kawano et al , 1988) and plasmacytoma (Nordan et al , 1987) In contrast, IL-6 is reported to inhibit the growth of other cancer cells Growth arrest and terminal differentiation is induced in M1 myeloid leukaemia cells, an effect that is blocked by the expression of dominant negative forms of STAT3 (Minami et al , 1996, Fukada et al , 1996) In addition, IL-6 induces an anti-proliferative effect in early stage human melanoma cells associated with STAT-mediated transcriptional up-regulation of p27^{Kip1} (Kortylewski et al , 1999) and p21^{waf1/cip1} (Florenes et al , 1999) Similarly, IL-6-induced growth inhibition has been reported in prostate cancer (LNCaP) (Spiotto and Chung, 2000), human breast carcinoma cells (Novick et al , 1992, Chen et al , 1988) and a number of leukaemia/lymphoma cell lines (Chen et al , 1988) In hepatoma cells the effects of IL-

6 on downstream effector pathways and cell proliferation remains uncertain. Stimulation of the IL-6R α in human HepG2 cells results in the accumulation of p27^{Kip1} and growth arrest in the G1 phase (Klausen et al , 2000) an inhibitory effect similar to that observed by Kim et al in the H-35 rat hepatoma cell line however the underlying mechanism of this inhibition was not determined (Kim and Baumann, 1999) In contrast IL-6 has been indicated as an autocrine growth factor in hepatoma cells where IL-6 producing HCC-M hepatoma cell proliferation is inhibited following IL-6 antisense treatment (Kumagai et al , 2002) Interleukin-6 is also implicated in cell survival during hepatic injury and inhibits TGF- β -induced apoptosis in the human hepatoma derived Hep3B cell line (Chen et al , 1999)

The elucidation of IL-6 signalling pathways and their downstream effects in H4IIE cells has established an upregulation of cdk inhibitors p21^{waf1/cip1} and p27^{Kip1} and a downregulation of cdk activity (chapter 4) The expression of both p21^{waf1/cip1} and p27^{Kip1} has been linked to IL-6 induced cell cycle arrest in other tumour cells (Klausen et al , 2000, Kortylewski et al , 1999, Florenes et al , 1999) In the current studies, the effects of IL-6 treatment on cell proliferation were examined

5.2 Methods

5.2.1 Nuclear Thymidine Incorporation

5.2.1.1 Materials

Recombinant human IL-6 (rhIL-6), phosphate buffered saline (PBS) and prime foetal bovine serum (FBS) were purchased from Biosource International (Camarillo, CA, USA) Thymidine methyl- $[^3\text{H}]$ was purchased from Perkin Elmer Life Sciences (Boston, MA, USA) Scintisafe Econo-1 scintillation fluid and scintillation vials were purchased from Fisher Scientific (Pittsburgh, PA, USA) Ether, ethanol, trichloroacetic acid and sodium hydroxide were purchased from Sigma-Aldrich (St Louis, MO, USA)

5.2.1.2 Method

H4IIE cells were isolated and cultured as described in section 2.2 Cells were seeded in 24 well plates and grown to approximately 80% confluency in high serum media (HSM) Cells were washed twice with PBS (37°C, pH 7.4) and then quiesced for 24h in serum free media (SFM) SFM was then removed and replaced with media containing incremental increases in FBS levels (0.1-10% (v/v) FBS) for 20h At this point $[^3\text{H}]$ thymidine (1 $\mu\text{Ci}/\text{ml}$) was added to each well for a further 4h For the IL-6 treated group, parallel experiments were performed with the exception that cells were pretreated with rhIL-6 (20ng/ml) for 4h prior to replacement of SFM with media containing incremental increases in FBS levels (0.1-10% (v/v) FBS) and rhIL-6 (20ng/ml) After incubation with $[^3\text{H}]$ thymidine, cells were washed three times in 10% (v/v) trichloroacetic acid followed by 3 washes in ether:ethanol (2:1) and allowed to dry Cells were then solubilised in 500 μL 1M NaOH 100 μL of this solution was added to 5mL of scintillation fluid Counts per minute (cpm) for all samples were determined using a Beckman LS6000SC scintillation counter (Fullerton, CA, USA)

5.2.2 Alamar Blue Proliferation Assay

5 2 2 1 Materials

Alamar Blue was purchased from Biosource International (Camarillo, CA, USA) Microplate reader (μ Quant) was purchased from Biotek Instruments (Winooski, VT, USA)

5 2 2 2 Method

H4IIE cells were isolated and cultured as described in section 2.2 Cells were seeded in 96 well plates at 5×10^3 cells/well and grown overnight in HSM Cells were washed twice with PBS (37°C, pH 7.4) and then quiesced in SFM for 24h Cells were next pretreated with rhIL-6 (50ng/ml) for a period of 4h prior to FBS stimulation (1% (v/v) FBS) Media (with or without IL-6) was refreshed daily After 48h, 10% of cell culture media in each well was replaced with Alamar Blue and 2h later the absorbance at 570nm and 600nm was measured using a μ Quant microplate reader Negative control wells were established in the absence of cells (media with Alamar Blue alone) Percentage reduction of Alamar Blue was calculated using the following equation where $\lambda_1=570\text{nm}$ and $\lambda_2=600\text{nm}$

$$\% \text{Reduced} = \frac{(\epsilon_{ox} \lambda_2)(A \lambda_1) - (\epsilon_{ox} \lambda_1)(A \lambda_2)}{(\epsilon_{red} \lambda_1)(A' \lambda_2) - (\epsilon_{red} \lambda_2)(A' \lambda_1)} \times 100$$

Where

$(\epsilon_{red} \lambda_1) = 155,677$ (Molar extinction coefficient of reduced Alamar Blue at 570nm)

$(\epsilon_{red} \lambda_2) = 14,652$ (Molar extinction coefficient of reduced Alamar Blue at 600nm)

$(\epsilon_{ox} \lambda_1) = 80,586$ (Molar extinction coefficient of oxidised Alamar Blue at 570nm)

$(\epsilon_{ox} \lambda_2) = 117,216$ (Molar extinction coefficient of oxidised Alamar Blue at 600nm)

$(A \lambda_1) =$ Absorbance of test wells at 570nm

$(A \lambda_2) =$ Absorbance of test wells at 600nm

$(A' \lambda_1) =$ Absorbance of negative control wells at 570nm

$(A' \lambda_2) =$ Absorbance of negative control wells at 600nm

5.2.3 Cell Counting

5.2.3.1 Materials

Haemocytometer was purchased from Hausser Scientific (Horsham, PA, USA)

Trypsin-EDTA was purchased from Sigma-Aldrich (St Louis, MO, USA)

5.2.3.2 Method

H4IIE cells were isolated and cultured as described in section 2.2. Cells were plated in 12 well plates in HSM and allowed to attach and proliferate until 30-35% confluency was achieved. At this point HSM was removed, the cells were washed twice with PBS (37°C, pH 7.4) and SFM was added for 24h. At the end of this period, plates were separated into two groups and left either untreated or were treated with rhIL-6 (50ng/ml) for 4h. SFM was then removed from all wells and 1% (v/v) FBS media or 1% (v/v) FBS media containing 50ng/ml rhIL-6 was added to each well daily. At 24h intervals, media was removed from three wells and the cells were detached using trypsin-EDTA. Cell suspensions from each of the three wells were then combined and manually counted using a haemocytometer. This procedure was repeated over a three

day period and was repeated a minimum of four separate times per experimental condition

5.2.4 FACS Cell Cycle Analysis

5.2.4.1 Materials

Bovine Serum Albumin (BSA) was purchased from Fisher Scientific (Pittsburgh, PA, USA) RNase A, propidium iodide and sodium citrate were purchased from Sigma-Aldrich (St Louis, MO, USA) BD FACSCalibur flow cytometer and Modfit LT version 3.0 software was purchased from BD Biosciences (San Jose, CA, USA)

5.2.4.2 Method

H4IIE cells were isolated and cultured as described in section 2.2. Cells were seeded in 6 well plates and grown to approximately 80% confluency in high serum media (HSM). Cells were washed twice with PBS (37°C, pH 7.4) and then synchronised in SFM (media refreshed every 2 days) for 7 days. At the end of this period, plates were separated into two groups and left either untreated or were treated with rhIL-6 (50ng/ml) for 2h. SFM was then removed from all wells and 2.5% (v/v) FBS media or 2.5% (v/v) FBS media containing 50ng/ml rhIL-6 was added to each well. Samples for cell cycle analysis were collected at varying time points (0-46h). At each time point cells were trypsinised, pelleted at 2500 x g and then resuspended in PBS containing 0.1% (v/v) BSA. Cells were washed twice in PBS/0.1% (v/v) BSA and then cell concentration was adjusted to 1.5×10^6 cells/mL. Cells were fixed with ice cold absolute ethanol (3mL ethanol added to 1mL of cells) and rested on ice for 15 mins prior to storage at 4°C. Cells were centrifuged at 1000 x g and ethanol was removed. Cell pellet was next resuspended in 250µL of RNase A (0.7mg/mL) and then

incubated at 37°C for 15 mins. Cells were then treated with 250µL of propidium iodide (50µg/mL) and incubated at room temperature in darkness for 1h. PBS (500µL) was added to each sample prior to FACS analysis. Cells were passed through a BD FACScalibur flow cytometer and gated based on side light scatter (particle density) vs forward light scatter (particle size) plots in addition to further gating based on FL2-A (total fluorescence) vs FL2-W (transit time) plots to discriminate single cell viable populations from aggregates and debris. FL2-A data was modelled using Modfit LT version 3.0 cell cycle analysis software.

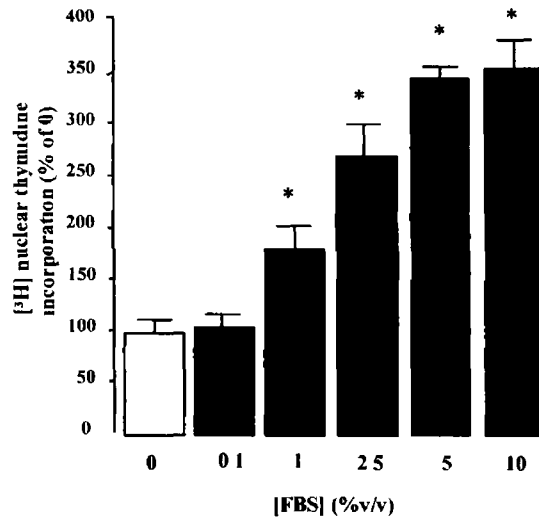
5.3 Results

5.3.1 Effect of rhIL-6 on HCC Cell Proliferation *In Vitro*

To determine the effects of rhIL-6 on HCC cell proliferation H4IIE cells were isolated, grown in culture and treated with rhIL-6 (20-50ng/ml). Nuclear [³H] thymidine incorporation, Alamar Blue reduction and cell numbers were then assayed as indices of cellular proliferation. Treatment of quiescent H4IIE cells with FBS led to a dose dependent increase in nuclear [³H] thymidine incorporation, a significant increase being detected following treatment with 1% (v/v) FBS rising to a maximal effect with the use of 5-10% (v/v) FBS media (345±17% versus 0 1% (v/v) FBS media, n=4 per group, p<0.05, Figure 5.1a). In parallel experiments, cells were pretreated with 20ng/ml rhIL-6 for 4h. At the end of this period, media FBS concentrations were adjusted to those used previously. Under these conditions, 20ng/ml rhIL-6 significantly inhibited FBS stimulated nuclear [³H] thymidine incorporation at all doses (0.1-10% v/v) of FBS employed (Figure 5.1b, p<0.05, n=4 per group).

To confirm these data an Alamar Blue assay was next used to determine the metabolic rate of cells as an index of proliferation. The Alamar Blue assay is a colourimetric assay in which oxidised Alamar Blue (blue) is converted to its reduced form (red) in the presence of proliferating cells. In this set of experiments 1% (v/v) FBS was used to stimulate proliferation of H4IIE cells. Higher concentrations of FBS caused greater levels of proliferation which resulted in an inversion of the colour change in this assay, the underlying cause of this effect was not determined. These data demonstrated a significantly reduced level of proliferation of H4IIE cells in the presence of rhIL-6 as assessed by the decreased presence of the reduced (red) form of Alamar Blue. These data demonstrated decreased Alamar Blue reduction in HCC cells pretreated with rhIL-6 followed by 1% (v/v) FBS as compared to 1% (v/v) FBS treated alone (94.28±0.9%

(a)



(b)

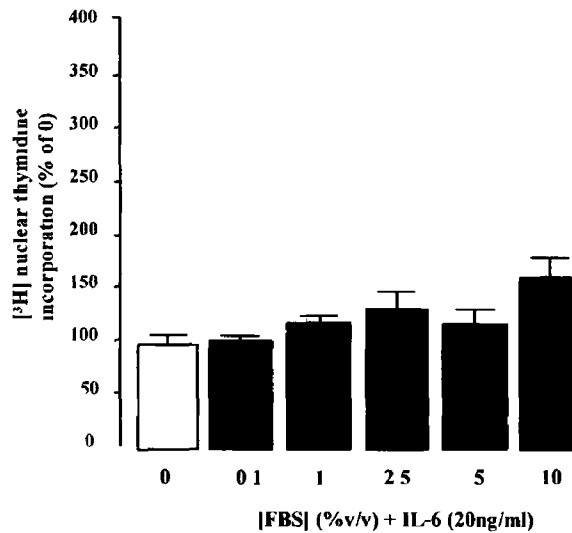


Figure 5 1 rhIL-6 inhibits DNA synthesis in H4IIE (HCC) cells *in vitro* Nuclear [³H] thymidine incorporation was determined as a measure of *de novo* DNA synthesis in H4IIE HCC cells in culture as a marker of cellular proliferation a) H4IIE cells were isolated from *in vivo* HCC tissue, cultured and quiesced for 24h (SFM) prior to treatment with culture media containing varying amounts of FBS (0-10% v/v) for 24h (n=4 per group, *p<0.05) b) H4IIE cells were isolated from *in vivo* HCC tissue, cultured and quiesced for 24h (SFM) prior to treatment with rhIL-6 (20ng/ml) for 4h. At this point media was replaced with culture media containing varying amounts of FBS (0-10% v/v) and rhIL-6 (20ng/ml) for 24h (n=4 per group)

versus $105.37 \pm 0.21\%$ respectively, values are given as percentage reduction versus control cells (untreated), $p < 0.05$, $n=4$ per group, Figure 5.2)

Finally, sequential cell count experiments were performed in which cells were treated with either 1% (v/v) FBS or 1% (v/v) FBS and 50ng/ml rhIL-6. These data demonstrated significantly increasing cell numbers 1-3 days after addition of 1% (v/v) FBS as compared to day 0 (Figure 5.3, $n=4$ per group, $p < 0.05$). Furthermore, throughout the three day experimental period, cell numbers were significantly higher in FBS alone as compared to FBS and rhIL-6 (Figure 5.3, $n=4$ per group, $p < 0.05$).

5.3.2 Effect of rhIL-6 on HCC Cell Cycle Progression *In Vitro*

To determine the effects of rhIL-6 on HCC cell cycle progression H4IIE cells were isolated, grown in culture and treated with rhIL-6 (50ng/ml). These cells were stained with propidium iodide and DNA content was measured by flow cytometry. In order to acquire an accurate analysis of cell cycle events the cells were first synchronised by serum deprivation as initially described by Pardee (Pardee, 1974). This procedure synchronises cells in the G₀/G₁ phase of the cell cycle. In order to examine the effect of serum deprivation on H4IIE cell cycle progression and to establish the ideal length of time required to sufficiently synchronise these cells, H4IIE cells were cultured in SFM for varying time periods (2-8 days). The percentage population of H4IIE cells in the G₀/G₁ phase of the cell cycle was analysed at each time point. After culturing for 2 days in SFM, $48.01 \pm 1.0\%$ of the H4IIE cells were in the G₀/G₁ phase of the cell cycle (Table 5.1, $n=4$). Extended serum deprivation significantly increased the cell population in the G₀/G₁ phase reaching $64.78 \pm 2.0\%$ ($n=4$, $p < 0.05$ versus 2 days) and $78.12 \pm 0.98\%$ ($n=7$, $p < 0.05$ versus 2 days) after 6 and 7 days culture in SFM respectively. While further culturing of H4IIE cells in SFM did significantly enhance the G₀/G₁ cell population ($80.1 \pm 0.23\%$ at 8 days, $n=4$, $p < 0.05$ versus 7 days) the

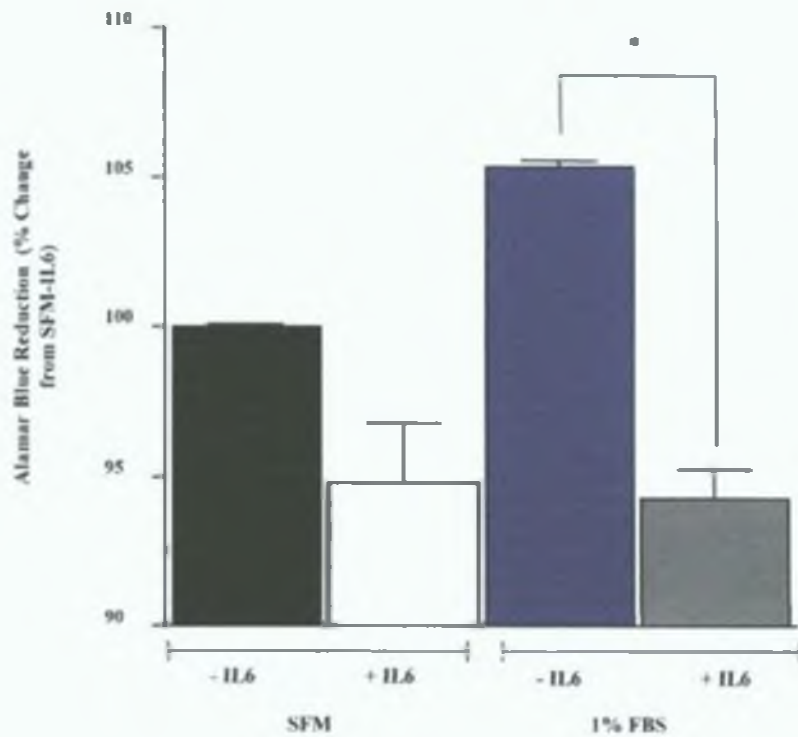


Figure 5.2 rhIL-6 inhibits H4IIE (HCC) cell proliferation as evidenced by Alamar Blue reduction *in vitro*. The ability of H4IIE cells to reduce Alamar Blue was determined using a colourimetric assay as a marker of cellular proliferation. H4IIE cells were isolated from *in vivo* HCC tissue, cultured in 96-well plates and quiesced for 24h (SFM) prior to treatment with culture media that was either serum free or contained 1% (v/v) FBS in the absence (-) or presence (+) of rhIL-6 (50ng/ml) for 48h (n=4 per group. *p<0.05).

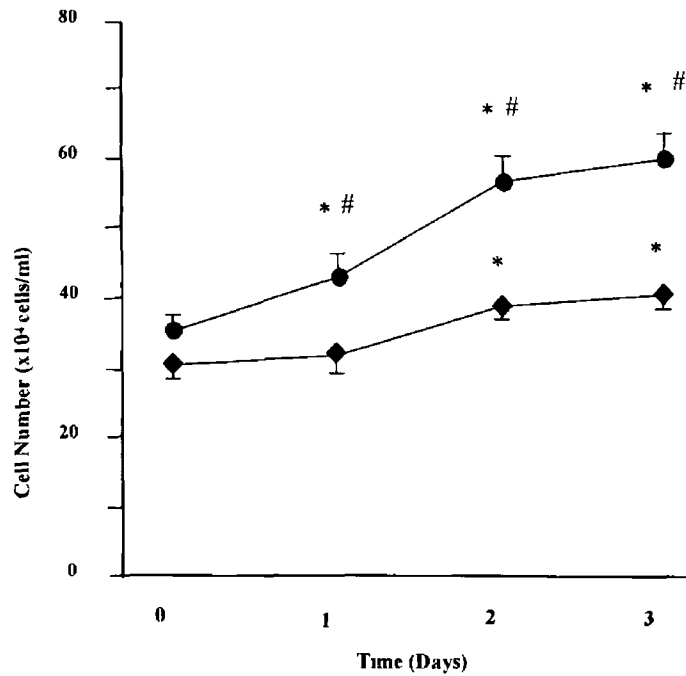


Figure 5.3 RhIL-6 inhibits H4IIE (HCC) cell proliferation as evidenced by cell counting *in vitro* To determine the net effect of rhIL-6 on H4IIE HCC cell proliferation, H4IIE cells were isolated from *in vivo* HCC tumours, seeded on 12-well plates and allowed to grow to 35% confluence. At this point media was removed and cells quiesced for 24h (SFM). At the end of this period, media was removed and replaced with fresh media containing either 1% (v/v) FBS (●) or 1% (v/v) FBS + rhIL-6 (50ng/ml) (◆). Cells were then cultured for a further 3 days and cell counts performed at days 0, 1, 2 & 3 (n=4 separate experiments per group, *p<0.05 versus day 0, #p<0.05 FBS versus FBS+rhIL-6 for corresponding time points).

Days Quiesced	G0/G1	S	G2/M
2	48.01±1.00	46.80±0.25	5.20±0.77
6	64.78±2.00	22.47±0.65	12.75±1.37
7	78.12±0.98	15.40±0.74	6.48±0.29
8	80.1±0.23	16.37±0.77	3.53±0.54

Table 5.1 Effect of serum deprivation on cell cycle progression in H4IIE (HCC) cells. Serum deprivation retards H4IIE cells in the G0/G1 phase of the cell cycle. H4IIE cells were isolated and cultured prior to quiescing for varying time (2-8 days) in SFM. Cells were stained with propidium iodide and analysed for DNA content by flow cytometry. Data represents the mean±SEM of n=4 experiments for 2 days, 6 days and 8 days and n=7 experiments for 7 days.

differences were not pronounced, as a result, 7 days of serum deprivation was considered sufficient for H4IIE cell cycle analysis. Synchronised H4IIE cells were next treated with 2.5% (v/v) FBS to release the cells from this G0/G1 arrest and initiate DNA synthesis. Analysis of DNA content demonstrated that FBS treatment induced the exit of H4IIE cells from the G0/G1 phase of the cell cycle with a significant decrease in the G0/G1 cell population being observed at 20h ($15.09 \pm 0.35\%$ decrease in G0/G1 population, $n=4$, $p < 0.05$ versus time 0, Figure 5.4 & 5.5) after FBS stimulation reaching a maximal decrease at 28h ($19.72 \pm 0.02\%$ decrease in G0/G1 population, $n=4$, $p < 0.05$ versus time 0, Figure 5.4 & 5.5). This occurred concomitant with increases in the S phase population (Figure 5.4, $n=4$). Similar treatment of H4IIE cells with FBS in the presence of rhIL-6 (50ng/mL) resulted in significantly reduced exit of cells from the G0/G1 phase of the cell cycle compared to untreated controls. At 20h, treatment with FBS in the presence of rhIL-6 resulted in the exit of $9.86 \pm 0.16\%$ of H4IIE cells from the G0/G1 phase of the cell cycle (Figure 5.5, $n=4$, $p < 0.05$ versus untreated control at 20h). At 28h after FBS stimulation in the presence of rhIL-6 (50ng/mL) the population of cells exited from the G0/G1 phase of the cell cycle was increased further but not significantly ($11.53 \pm 0.23\%$, $n=4$, Figure 5.5). After 46h, G0/G1 population of rhIL-6 treated and untreated H4IIE cells increased to levels above those observed at 0h (Figure 5.4, $n=4$).

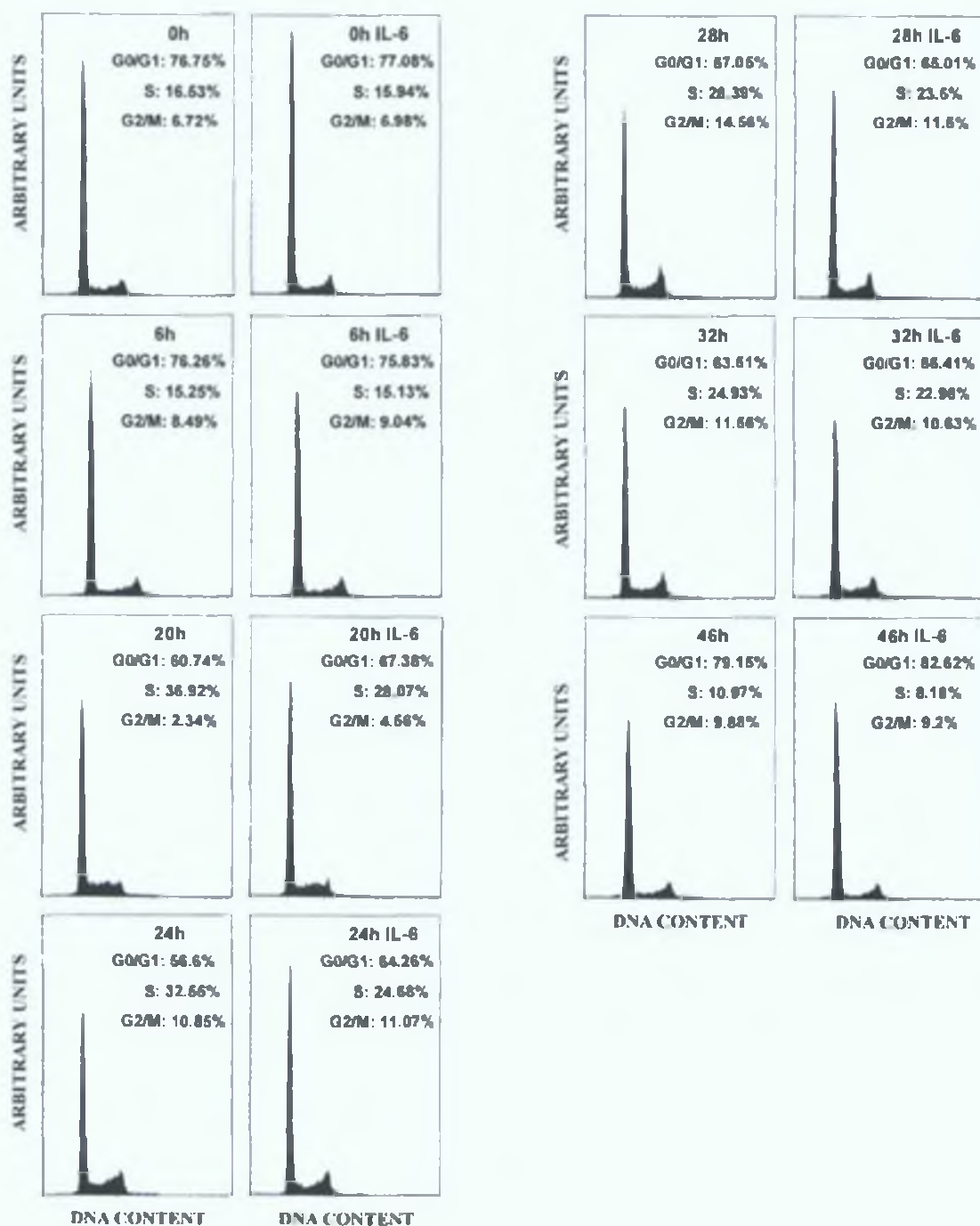


Figure 5.4 RhIL-6 induces a G0/G1 growth arrest in H4IIE cells *in vitro*. Representative flow cytometric histograms of DNA content in H4IIE cells at varying time points after treatment with IL-6. H4IIE cells were isolated and cultured prior to quiescing for 7 days in SFM. At the end of this period, media was removed and replaced with fresh media containing either 2.5% (v/v) FBS or 2.5% (v/v) FBS + rhIL-6 (50ng/ml). Cells were stained with propidium iodide and analysed for DNA content by flow cytometry at varying time points.

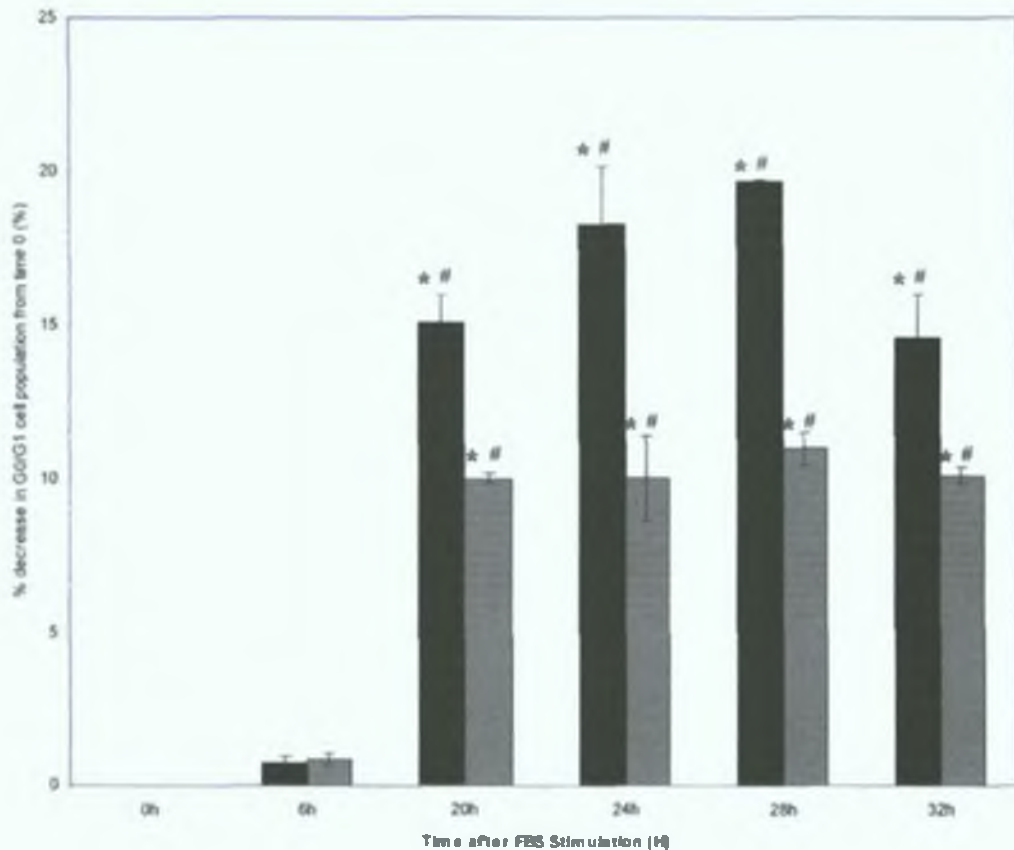


Figure 5.5 RhIL-6 inhibits exit from G0/G1 phase of the H4IIE cell cycle *in vitro*. H4IIE cells were isolated and cultured prior to quiescing for 7 days in SFM. At the end of this period, media was removed and replaced with fresh media containing either 2.5% (v/v) FBS (black) or 2.5% (v/v) FBS + rhIL-6 (50ng/ml) (shaded). Cells were stained with propidium iodide and analysed for DNA content by flow cytometry at varying time points (*p<0.05% versus 0h, n=4 per group; #p<0.05 FBS versus FBS+rhIL-6 for corresponding time points, n=4 per group).

5.4 Discussion

Interleukin-6 treatment in H4IIE (HCC) cells leads to increased expression of the cdk inhibitors p21^{waf1/cip1} and p27^{Kip1} and an associated decreased activity of both cdk2 and cdk4. This is further correlated with a decreased level of phosphorylation of the cdk target, Rb (chapter 4). The current study established that IL-6 treatment inhibits the proliferation of H4IIE cells *in vitro*. Further analysis demonstrated that IL-6 induces a G0/G1 growth arrest in these cells.

Previous reports identify IL-6 as a critical cytokine in the initiation phase of liver regeneration (Streetz et al, 2000, Fausto, 2000). Reduced liver mass causes increased serum TNF- α levels followed by increased IL-6 and STAT3 activation. STAT3 activation, in collaboration with additional transcription factors such as C/EBP β , enhance the expression of additional factors, such as NF-IL-6, c-myc, c-fos, IRF-1 and others, enabling the resting hepatocytes to progress into cell proliferation (Streetz et al, 2000, Fausto, 2000). More recently, Zimmers et al report the potential of IL-6 to act as a complete mitogen in the liver. In this model circulating IL-6 levels were elevated in nude mice using a transfected CHO cell line leading to dramatic hepatomegaly and hepatocyte hyperplasia in the absence of liver injury (Zimmers et al, 2003). In support of this observation, double transgenic mice expressing human IL-6 and human soluble IL-6R under liver specific promoters demonstrate hepatomegaly, hepatic hyperplasia and the presence of hepatic adenomas (Maione et al, 1998, Schurmacher et al, 1998). IL-6 treatment of hepatocytes *in vitro* however has resulted in both stimulation and inhibition of DNA synthesis (Kordula et al, 1991, Kuma et al, 1990, Satoh and Yamazaki, 1992).

In contrast to its role in normal hepatocyte proliferation, the current study identifies a growth inhibitory effect of IL-6 treatment in HCC cells *in vitro*. This correlates with previous research which demonstrates decreased proliferation in both

human (Klausen et al , 2000) and rat (Kim and Baumann, 1999, Lai et al , 1999) hepatoma cell lines in response to IL-6. The reduced proliferation of human HepG2 cells in response to IL-6 is linked to a MAPK dependent increase of p27^{Kip1} in addition to mildly enhanced p21^{waf1/cip1} levels (Klausen et al , 2000). Conversely, IL-6 induced growth inhibition of H-35 rat HCC cells did not involve altered expression of either of these cdk inhibitors (Kim and Baumann, 1999, Lai et al , 1999). In the current model an over expression of both p21^{waf1/cip1} and p27^{Kip1}, which is at least partially STAT3 dependent, was correlated with IL-6 mediated inhibition of HCC cell proliferation. Collectively these data suggest that the mechanisms of IL-6 induced growth inhibition in HCC are varied and cell type specific. Furthermore, roles for IL-6 as an autocrine growth factor (Kumagai et al , 2002) and survival factor (Chen et al , 1999) have been demonstrated in human HCC cell lines, HCC-M and Hep3B, respectively. This highlights distinct biological outcomes of IL-6 signalling in different HCC cell types. Similarly, IL-6 has been shown to act as a paracrine growth inhibitor in certain prostate cancer cell lines and an autocrine growth stimulator in others (Spiotto and Chung, 2000). Moreover, studies show that IL-6 can also switch from acting as a paracrine growth inhibitor to an autocrine growth stimulator during the progression of human melanoma (Lu and Kerbel, 1993, Florenes et al , 1999). Taking into consideration that IL-6 is produced and secreted by H4IIE cells (chapter 3), these data suggest a role for IL-6 as an autocrine negative growth regulator in the current HCC model. Indeed IL-6 has been established to have similar autocrine growth inhibitory effects in human meningioma (Todo et al , 1994) and lung cancer cells (Takizawa et al , 1993). In the latter case, the cells have a relatively low IL-6 sensitivity when compared with noncarcinogenic human bronchial epithelial cells suggesting that escape from growth regulation of this inhibitory factor may be involved in lung oncogenesis. Similarly, H4IIE cells are characterised by decreased expression of IL-6 receptor components.

(chapters 3 & 4) supporting potentially evasive cell mechanisms from IL-6 growth inhibition. Autocrine negative growth regulation by other cytokines such as TGF- β in other cancer models has been established while the development of multicytokine resistance during the process of oncogenesis has been linked to clonal dominance of primary tumours by metastatically competent cells (Lu et al, 1992, Kerbel, 1992, Wu et al, 1992). Overall the proliferation of neoplastic cells is dependent on the interaction and balance between both stimulatory and inhibitory factors.

Interleukin-6 treatment of H4IIE (HCC) cells blocked cell cycle progression in the G0/G1 phase. H4IIE cells were synchronised by serum deprivation for 7 days prior to the determination of the effects of IL-6 on cell cycle progression. This resulted in accumulation of H4IIE cells in the G0/G1 phase of the cell cycle. While this was an extended period of serum starvation, past research confirms that H4IIE cells enter a quiescent state and can remain viable for up to 7 days in the absence of serum (Squinto et al, 1989). The cells promptly re-enter the cell cycle once serum stimulated. The current study demonstrates that IL-6 inhibits the entry of H4IIE cells into the S phase of the cell cycle. Interleukin-6 stimulation in H4IIE cells results in an upregulation of the cdk inhibitors p21^{waf1/cip1} and p27^{Kip1} which occurs concomitant with a decreased activity of cdk2 and cdk4 in addition to decreased levels of Rb phosphorylation (chapter 4). Progression through the cell cycle is tightly controlled by cdks (Morgan, 1995). Cyclins associate with cdks and are the primary regulators of cdk activity (Sherr and Roberts, 1999, Morgan, 1995). The activation of cdk4 plays an important role in the passage through the G1 restriction point when the cell becomes committed to proceed through the cell cycle, while cdk2 activation plays an essential role in the transition into S phase and DNA synthesis. Cyclin D1 expression is induced during G1 phase in response to various mitogens, complexes with and activates cdk4. Cyclin dependent kinase 2 is regulated primarily by cyclin E and cyclin A during G1/S

transition and S phase respectively (Sherr and Roberts, 1999, Morgan, 1995, Sherr and Roberts, 1995) Retinoblastoma protein is the major target for cyclin dependent kinase activity and is phosphorylated by both cyclin D dependent kinases and by cdk2. Hyperphosphorylation of the Rb protein disrupts its association with E2F transcription factors which once released can stimulate the expression of a series of genes required for DNA synthesis (Sherr and Roberts, 1999, Morgan, 1995, Sherr and Roberts, 1995). Cyclin dependent kinase inhibitors further regulate the activity of these cyclin/cdk complexes. p27^{Kip1} and p21^{waf1/cip1} are members of the Cip/Kip family of cdk inhibitors that can affect the activity of cyclin D-, E- and A- dependent kinases through binding of both the cyclin and cdk subunits (Sherr and Roberts, 1999). Overall, increased cdk inhibitor expression leading to decreased cdk activity and a resulting reduction in Rb phosphorylation in response to IL-6 treatment gives a direct mechanism for the observed G0/G1 growth arrest in H4IIE cells.

In conclusion, exogenous addition of IL-6 inhibits the proliferation of H4IIE HCC cells *in vitro* through the induction of an arrest in the G0/G1 phase of the cell cycle. Interleukin-6 treatment increases both p21^{waf1/cip1} and p27^{Kip1} in H4IIE cells, leading to decreased cdk2 and cdk4 activity and a subsequent decrease in Rb phosphorylation. Ultimately this sequence of events results in reduced entry of H4IIE cells into the S phase of the cell cycle and as a result decreased cell proliferation *in vitro*. This may suggest an autocrine negative growth regulatory function for IL-6 when considered in light of results demonstrating that H4IIE cells produce both IL-6 and the IL-6 receptor. However, dysregulated expression of various IL-6 signalling components and in particular decreased levels of IL-6 receptor expression may suggest that mechanisms are present in H4IIE cells to evade the growth inhibitory effects of IL-6.

Chapter 6: Microencapsulation of Engineered CHO Cells for IL-6 Delivery *In Vivo*

6.1 Introduction

HCC is characterised by dysregulated expression of components of the IL-6 signalling cascade both *in vivo* and *in vitro* (chapters 3 & 4) This includes downregulated expression of the IL-6 receptor in addition to upregulated IL-6 production and secretion Nevertheless, IL-6 treatment of HCC cells *in vitro* leads to the activation of Jak-STAT and Ras-MAPK pathways resulting in increased expression of the cdk inhibitors, p21^{waf1/cip1} and p27^{Kip1} (chapter 4) Decreased phosphorylation of the Rb protein and attenuated cdk activity were observed concomitant with this upregulation Collectively, these events induce a G0/G1 growth arrest in H4IIE HCC cells *in vitro* (chapter 5) However, the effects of IL-6 administration on HCC progression *in vivo* remain to be determined

A growth inhibitory effect of IL-6 treatment has been demonstrated in H4IIE HCC cells *in vitro* (chapter 5) This correlates with previous research which has demonstrated decreased proliferation in both human (Klausen et al , 2000) and rat (Kim and Baumann, 1999, Lai et al , 1999) hepatoma cell lines in response to IL-6 However, roles for IL-6 as an autocrine growth factor (Kumagai et al , 2002) and survival factor (Chen et al , 1999) have also been demonstrated in the human HCC cell lines, HCC-M and Hep3B, respectively The effects of IL-6 on HCC progression *in vivo* remain

poorly defined. The overexpression of IL-6 in a rat hepatocellular carcinoma cell line was linked to an increase in metastatic potential (Reichner et al, 1998) while the transfection of an IL-6 expression vector in a murine liver tumour cell line was inhibitory on tumour growth *in vivo* (Kang et al, 1999). Previous reports demonstrate the potential of systemic IL-6 administration to decrease tumour burden of other cancers *in vivo*. Human IL-6 administered to mice with transplantable acute myeloid leukaemia (AML) and irradiation/dexamethasone induced AML results in reduced leukaemia development and increased animal survival (Givon et al, 1992). This may be due to direct effects on tumour cells and/or through an enhancement of the host immune system. Recombinant IL-6 administration also reduces the number of established metastases from colon adenocarcinoma and fibrosarcoma tumours *in vivo*, an effect mediated *via* the enhancement of tumour specific CD8⁺ cytotoxic T lymphocyte (CTL) activity (Eisenthal et al, 1993, Mule et al, 1992). Furthermore, IL-6 administration in combination with cyclophosphamide, a chemotherapeutic agent, ameliorates the majority of C57BL/6 mice with advanced, 10 day subcutaneous or pulmonary sarcoma tumour nodules (Mule et al, 1992). Similarly other cytokines have been administered as potential cancer therapeutics. Interferon- α (IFN- α) has been the most successfully administered cytokine demonstrating anti-tumour effects in several haematological malignancies and solid tumours and also reducing the risk of malignant melanoma recurrence after surgical resection of localized lymph node metastases (Group, 1997, Kirkwood et al, 1996). Interleukin-2 (IL-2) administered systemically at high doses can mediate renal carcinoma and melanoma tumour regression in some patients (Fyfe et al, 1995, Rosenberg et al, 1993). However, the infusion of defined cytokines is often associated with severe side effects and dose limiting toxicities (Fyfe et al, 1995, Rosenberg et al, 1993, Lienard et al, 1992, Atkins et al, 1997). Despite its involvement with several inflammatory disease states and systemic

lymphoproliferative disorders, administration of high doses of IL-6 in mice does not result in discernible side effects or toxicity (Eisenthal et al , 1993, Givon et al , 1992, Mule et al , 1992)

Systemically administered cytokines have a short half life *in vivo* ^{125}I -IL6 injected into rats is cleared with a plasma half life of approximately two minutes (Castell et al , 1988, Castell et al , 1990a) As a result it is difficult and expensive to maintain sustained high cytokine levels *in vivo* The microencapsulation of cells engineered to secrete cytokines and their subsequent implantation in animals offers a more economical and sustainable method of cytokine delivery *in vivo* The principle of microencapsulation is to create a physical semi-permeable barrier between the encapsulated cells and the host immune system This membrane allows diffusion of oxygen and nutrients to the encapsulated cells while preventing contact with host immune cells or large molecules such as immunoglobulins (Uludag et al , 2000) Alginate, an unbranched polysaccharide mainly extracted from brown algae, is used extensively for the encapsulation of many cell types Alginate is composed of 1,4-linked α -L guluronic acids (G) and β -D mannuronic acids (M) which crosslink on contact with divalent cations (Ba^{2+} and Ca^{2+}) to form a gel matrix (Uludag et al , 2000) Cells are suspended in an iso-osmolar sodium alginate solution and are forced by a syringe through a nozzle forming droplets of alginate containing cells which then fall into an iso-osmolar solution of Ba^{2+} or Ca^{2+} The divalent cations cause gelation of the alginate resulting in spherical beads containing live encapsulated cells (Smidsrod and Skjak-Braek, 1990) In many cases the beads are next suspended in a poly-L-lysine (PLL) solution to enhance the perm-selective properties and strength of the alginate encapsulated structures Poly-L-lysine coated calcium crosslinked alginate beads can then be further modified by liquefaction of the alginate core using calcium chelators such as citrate (Uludag et al , 2000) Encapsulated cells have been successfully used to

deliver biotherapeutic substances *in vivo* such as Factor IX for haemophilia therapy (Hortelano et al , 1996), parathyroid hormone for the treatment of hypoparathyroidism (Hasse et al , 1997) and dopamine in experimental models of Parkinson's disease (Aebischer et al , 1994) Furthermore, encapsulated allogeneic and xenogeneic pancreatic islets have been successfully used to establish normoglycaemia in diabetic rodents (O'Shea and Sun, 1986), dogs (Soon-Shiong et al , 1992), monkeys (Sun et al , 1996) and in a human diabetic patient (Soon-Shiong et al , 1994) In regard to cancer therapy, alginate encapsulation has been utilised as a method of delivery for many potentially therapeutic substances Anti-angiogenic factors such as endostatin and angiostatin delivered using encapsulated genetically modified cells result in decreased tumour volume and increased survival in the treatment of rat glioma and murine melanoma respectively (Read et al , 2001, Cirone et al , 2003) Microencapsulated iNOS expressing cells have also been used to suppress tumour growth of colon and ovarian carcinomas *in vivo* (Xu et al , 2002) Another group has developed a system using microencapsulated genetically engineered myoblasts expressing IL-2 linked to the Fv region of a humanized antibody with affinity to tumours over-expressing the oncogene ERB2/HER2/NEU to specifically suppress tumour growth (Cirone et al , 2002)

The aim of the current study was to microencapsulate rhIL-6 expressing CHO cells for rhIL-6 delivery *in vivo* and determine its effect on HCC progression

6.2 Methods

6.2.1 Tumour Model

The rat HCC tumour model was established by direct injection of H4IIE cells into the left liver lobe of male ACI rats (200-250g) as described in section 2.3. Tumour volumes (mm^3) were calculated ($\frac{1}{2}L \times W \times H$) from measurements of length (L), width (W) and height (H) of tumour cross section.

6.2.2 CHO Cell Culture

CHO-IL6, a CHO cell line stably expressing IL-6 and a mock transfected CHO cell line (CHO-CTRL) were used in these experiments. These lines were generated by introduction of a plasmid vector containing the human IL-6 complementary DNA (CHO-IL6) or empty vector (CHO-CTRL) into DHFR-deficient CHO-DUXX cells by protoplast fusion followed by methotrexate selection. Cells were cultured as described in section 2.2.

6.2.3 Alginate Microencapsulation of CHO Cells

6.2.3.1 Materials

Pronova ultrapure sodium alginate LVG was purchased from Pronova (Drammen, Norway). CaCl_2 , hepes, NaCl and glucose were purchased from Sigma Aldrich (St. Louis, MO, USA). R3603 Tygon autoclavable tubing, Nalgene filter holders, Corning suspension culture dishes (150mm x 25mm), Cytostir stirrer culture flasks, Stereomaster Zoom stereo microscope and sterile 5mL syringes were purchased from Fisher Scientific (Pittsburgh, PA, USA). Polypropylene mesh filters were purchased from Spectrum Laboratories (Rancho Dominguez, CA, USA). PHD 2000

syringe pump was purchased from Harvard Apparatus (Holliston, MA, USA) Air pressure meter was purchased from Cole Parmer (Vernon Hills, IL, USA) Millex 0.2µm vent air filter units were purchased from Millipore (Bedford, MA, USA) Coaxial spray atomiser was purchased from Spraying Systems (Wheaton, IL, USA) AMEM was purchased from Biosource (Camarillo, CA, USA)

6.2.3.2 Cell Encapsulation

The apparatus was assembled as illustrated in figure 6.1 and 6.2. Briefly, a 5ml syringe mounted on a syringe pump was connected *via* tubing (1/8" inner diameter Tygon) to the liquid inlet on a coaxial spray atomiser. The gas inlet on the atomiser was connected to an air line (1/4" inner diameter Tygon). Air was pumped at a rate of 6L/min through a Millex (0.2µm) in line filter to the atomiser. The atomiser was mounted 20cm above the surface level of 150mL of a 1.5% (w/v) CaCl₂ solution (1.5% (w/v) CaCl₂, 13mM hepes, 0.2µM sterile filtered) contained in a sterile 150mm cell culture suspension dish. This solution was placed on a magnetic stirrer plate and agitated gently using a sterile magnetic stirrer.

CHO cells were cultured, trypsinised and then resuspended in PBS. Cells were seeded at a concentration of 1×10^6 cells/mL in a 1.7% (w/v) sodium alginate solution (1.7% (w/v) ultrapure sodium alginate LVG, 0.9% (w/v) NaCl, 2.2mM hepes, 150mg/L glucose, pH 7.4, stirred overnight and then 0.2µm sterile filtered). Alginate/cell suspension (1×10^6 cells/mL) was placed in a syringe and fed to the atomiser at a rate of 1.0mL/min. Alginate beads formed on contact with CaCl₂ solution and were agitated gently for 5 mins. Beads were initially filtered through a 500µm polypropylene mesh filter and then the filtrate was passed through a 297µm polypropylene mesh filter. Alginate beads were washed in place on the 297µm mesh filter using AMEM cell culture media (no antibiotics or buffers added). Alginate beads on the mesh filter were

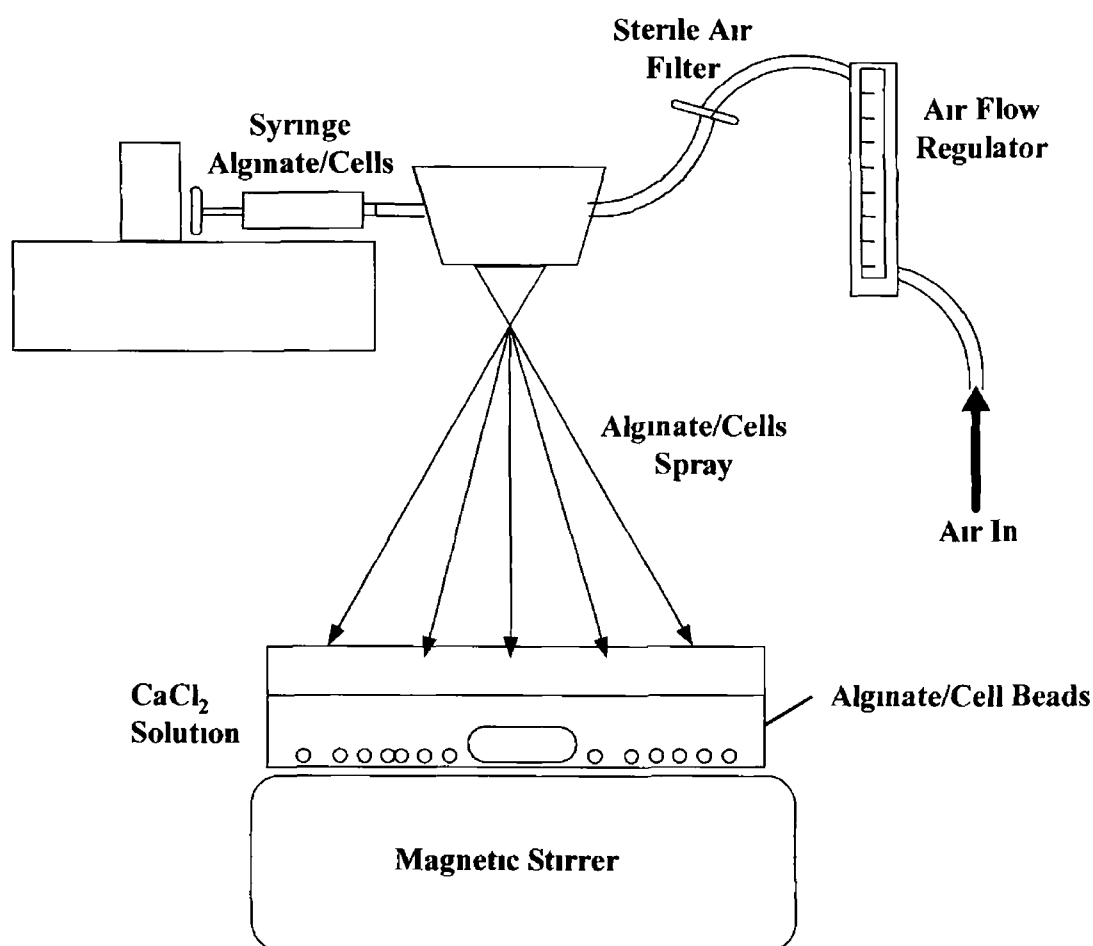


Figure 6.1 Illustrated representation of the apparatus used for alginate cell encapsulation CHO cells suspended in a 1.7% (w/v) sodium alginate solution were fed to a spray atomiser at a rate of 1.0 mL/min using a syringe mounted on a syringe pump. Air was pumped through a sterile filter to the spray atomiser at a rate of 6 L/min which was controlled using an air flow regulator. Alginate/cell mix was sprayed into a CaCl₂ solution which was agitated using a magnetic stirrer. Alginate polymerised on contact with the CaCl₂ solution resulting in beads containing encapsulated cells. Beads were cultured in high serum media at 37°C in a humidified incubator in the presence of 5% CO₂.

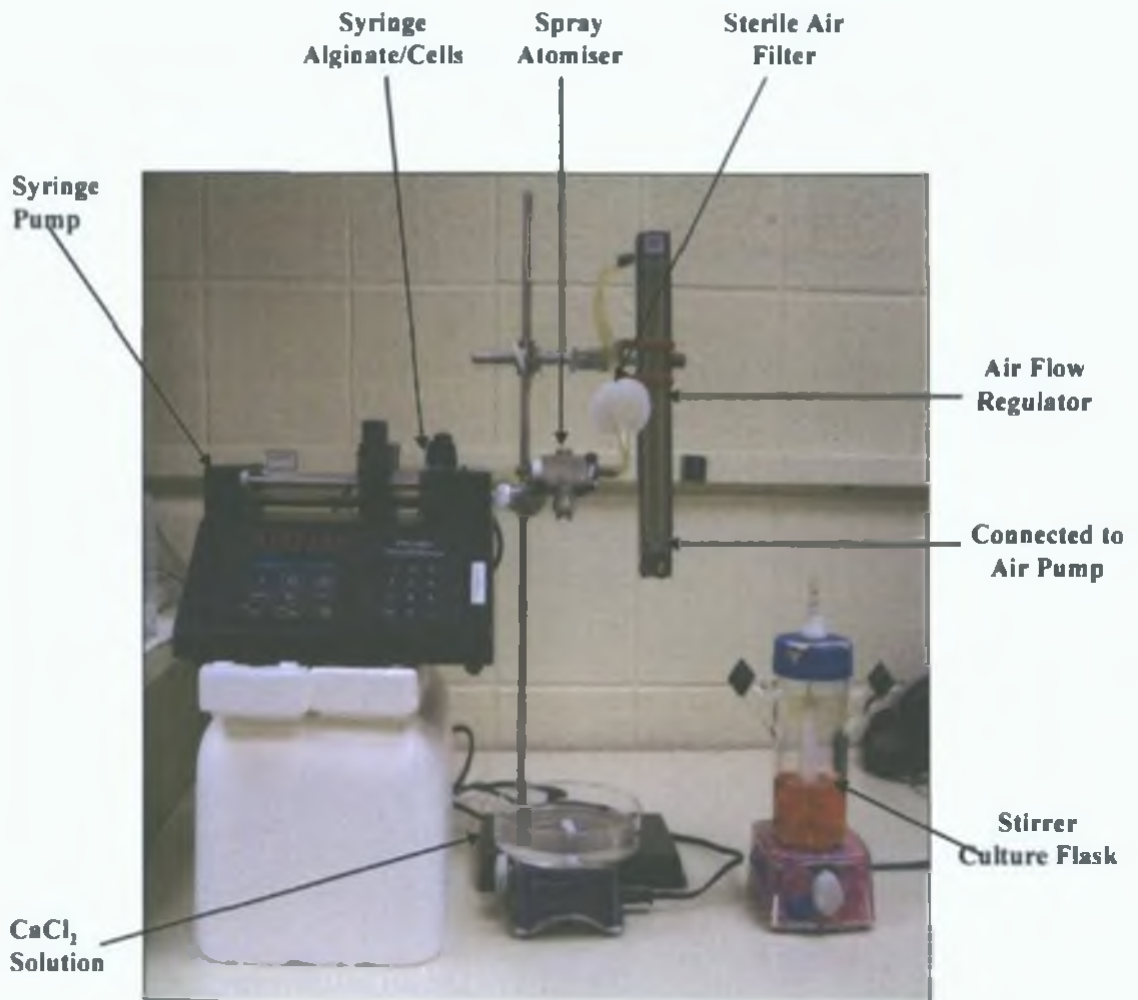


Figure 6.2 Photograph of the apparatus used for alginate cell encapsulation. CHO cells suspended in a 1.7% (w/v) sodium alginate solution were fed to a spray atomiser at a rate of 1.0mL/min using a syringe mounted on a syringe pump. Air was pumped through a sterile filter to the spray atomiser at a rate of 6L/min which was controlled using an air flow regulator. Alginate/cell mix was sprayed into a 1.5% (w/v) CaCl₂ solution which was agitated using a magnetic stirrer. Alginate polymerised on contact with the CaCl₂ solution resulting in beads containing encapsulated cells. Beads were washed and cultured in high serum media in stirrer culture flasks at 37°C in a humidified incubator in the presence of 5% CO₂.

then placed in 100mL CHO high serum media (HSM, section 2.2) in a Cytostir stirrer culture flask (100mL) and incubated with gentle agitation in a 37°C humidified incubator in the presence of 5% CO₂. 80mL of media was replaced every 2 days with fresh HSM. Agitation was ceased and beads were allowed to settle for at least 15 mins prior to changing the media. Bead size and shape was estimated by visualisation of beads using a stereo microscope.

6.2.3.3 Poly-L-lysine Coating of Alginate Beads

CHO-IL6 encapsulated beads were removed from culture and washed twice in buffered saline (0.9% (w/v) NaCl, 2.2mM hepes, pH 7.4). Beads were then suspended in 0.05% (v/v) poly-L-lysine (PLL) for 6 mins with stirring. Beads were collected and washed twice in buffered saline and next suspended in 0.06% (w/v) sodium alginate (0.06% (w/v) sodium alginate, 0.9% (w/v) NaCl) for 4 mins with stirring. Beads were washed twice in buffered saline followed by two successive treatments with 1.5% (w/v) sodium citrate for 7 mins each. Beads were then washed 3 times in buffered saline, resuspended in HSM and then incubated in stirrer culture at 37°C in a humidified incubator in the presence of 5% CO₂.

6.2.4 IL-6 ELISA

6.2.4.1 Plasma Preparation for IL-6 ELISA

Blood (5-7mL) was collected from male ACI rats *via* cardiac puncture using a 27 gauge needle and syringe containing 50 units heparin (Fisher Scientific, Pittsburgh, PA, USA). Blood was centrifuged at 1000 x g for 10 mins (4°C). Plasma was separated and stored at -20°C prior to analysis.

6.2.4.2 Culture Media Preparation for IL-6 ELISA

CHO cells were grown in culture as described in section 2.2. Media samples (300 μ L) were removed daily and stored at -20°C prior to analysis. Cell number was calculated at each sample time point by direct cell counting using a haemocytometer.

Encapsulated CHO cells were placed in culture in 6 well plates (6mL media per well). Media samples (300 μ L) were removed daily and stored at -20°C prior to analysis. Bead number in each well was determined by direct microscopic counting.

6.2.4.3 IL-6 ELISA

ELISA for human IL-6 was performed on cell culture media and rat plasma using a BD OPTeia ELISA set as described in section 2.6.

6.2.5 Live/Dead Cell Viability Assay

6.2.5.1 Materials

Live/Dead Viability/Cytotoxicity Kit containing Calcein AM and ethidium homodimer (EthD-1) was purchased from Molecular Probes (Eugene, OR, USA). Phosphate buffered saline (PBS) was purchased from Biosource (Camarillo, CA, USA). Nunc 4 well tissue culture plates were purchased from Fisher Scientific (Pittsburgh, PA, USA).

6.2.5.2 Method

Sample (1mL) of alginate beads was removed from stirred culture and allowed to settle in an eppendorf tube for 5 mins. Excess media was discarded and beads (in approximately 50 μ L media) were placed in a 4 well tissue culture plate. 250 μ L of Live/Dead working reagent (2 μ M Calcein AM, 4 μ M EthD-1, PBS) was added and beads were incubated in darkness for 45 mins. Beads were visualised using a Fluoview

FV500 IX70 confocal laser scanning biological microscope and Fluoview FV500 version 4.3 image processing software (Olympus America, Melville, NY, USA). Calcein AM is enzymatically converted to green fluorescent calcein by the ubiquitous intracellular esterase activity in living cells. Dead cells appear red due to the binding of EthD-1 to nucleic acids in cells which have damaged membranes.

6.2.6 Alginate Bead Implantation

Alginate Beads were removed from stirrer culture and allowed to settle in 50mL sterile tubes for 10 mins. Excess media was discarded and alginate beads were placed in 15mL sterile centrifuge tubes. Beads were washed 3 times in AMEM media (no antibiotics/buffers) and allowed to settle. Excess AMEM was removed.

Beads were implanted intraperitoneally in tumour burdened male ACI rats (200-250g) under anaesthesia (isoflurane gas/oxygen mix). Rats were allowed to recover and were maintained with food and water *ad libitum* and exposure to a light-dark (12h/12h) cycle. Rats were weighed daily. At the end of the experimental period animals were sacrificed and a peritoneal lavage was performed using AMEM to retrieve transplanted beads. The liver was removed and weighed and resected liver tissue was snap frozen in liquid nitrogen prior to storage at -80°C.

6.2.7 Preparation of Tissue Lysates

Tumour and normal liver tissue lysates for protein analysis were prepared as described in section 2.4.3.

6.2.8 Immunoblotting

Western blots were performed as described in section 2.5. Antisera specific against gp130 (M-20), IL-6R α (M-20), IL-6 (M-19), PCNA (PC-10), ERK2 (K-23) and

STAT3 (H-190) were all purchased from Santa Cruz Biotechnology (Santa Cruz, CA, USA) Antisera specific against Phospho-STAT3 (Tyr705) and Phospho-p42/44 MAPK were purchased from Cell Signaling Technology (Beverly, MA, USA) All primary antibodies were diluted 1 1000 in 5% (w/v) non fat dry milk (NFDM)/0.1% (v/v) Tween/tris buffered saline (TBS) except for Phospho-STAT3 (1 2000) Horseradish peroxidase conjugated goat anti-rabbit Ig and goat anti-mouse Ig were supplied by Jackson Immunoresearch Laboratories (West Grove, PA, USA) and were used as secondary detection antibodies at a dilution of 1 5000 in 5% (w/v) NFDM/0.1% (v/v) Tween/TBS

6.3 Results

6.3.1 Encapsulation of CHO-IL6 and CHO-CTRL Cells

CHO-IL6 and CHO-CTRL cells were grown in culture. Microscopic analysis demonstrated that these cell lines differed morphologically (Figure 6.3a and 6.3b). CHO-CTRL cells appear more elongated and larger than the rhIL-6 expressing CHO cells. Both cell types proliferated rapidly in culture. ELISA for human IL-6 performed on media from CHO-IL6 and CHO-CTRL cells removed at 3 and 4 days after seeding in culture demonstrated that CHO-IL6 media but not CHO-CTRL media was positive for human IL-6 (Table 6.1). The average production of IL-6 per CHO-IL6 cell over a 24h period was determined as 35.16 ± 5.79 pg/mL ($n=4$ per group) and 31.26 ± 4.07 pg/mL ($n=4$ per group) at 3 and 4 days after cell seeding respectively. IL-6 production rate per cell on successive days was not significantly different ($n=4$ per group).

Trial and error experiments involving the alteration of three factors (air flow rate, height of the atomiser from the CaCl_2 solution and alginate flow rate) were next performed to establish optimal parameters for alginate encapsulation. The apparatus was assembled as illustrated in Figure 6.1 and 6.2. The air flow rate was adjusted using an air flow regulator and the rate of alginate delivery to the atomiser was altered using a syringe pump. The atomiser was clamped on a buret stand and height adjusted accordingly. Experiments were performed using a 1.7% (w/v) sodium alginate solution in the absence of cells which was sprayed into a 1.5% (w/v) CaCl_2 solution. Size, sphericity and uniformity of alginate beads produced were estimated by visualisation using a stereo microscope. Parameters were altered in order to obtain $\sim 500\mu\text{m}$ diameter spherical beads. Increasing the distance between the atomiser and the CaCl_2 surface decreased the bead size and resulted in a more spherical bead (Table 6.2). At 5cm from the liquid surface the atomiser produced irregularly shaped beads which were typically

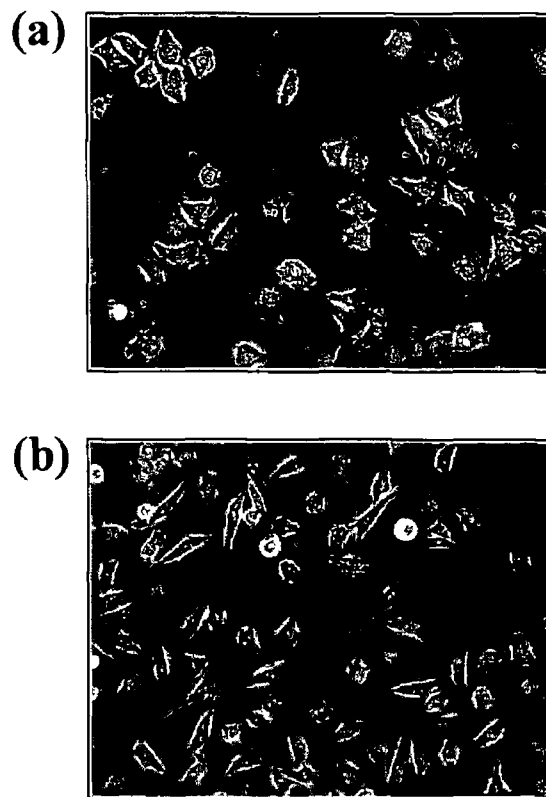


Figure 6.3 Photomicrographs of cultured **CHO-IL6** and **CHO-CTRL** cells. a) CHO-IL6 and b) CHO-CTRL cells were grown overnight in high serum media in adherent tissue culture flasks. Cells were fixed with methanol and viewed microscopically (40x) using an inverted light microscope.

Days After Seeding in Culture	CHO-IL6 cells Average IL-6 produced (pg/cell/day)	CHO-CTRL cells Average IL-6 produced (pg/cell/day)
3	35.16 +/- 5.79	ND
4	31.26 +/- 4.07	ND

Table 6.1 Human IL-6 production by CHO-IL6 and CHO-CTRL cells *in vitro*
 ELISA for human IL-6 was performed on media removed from CHO-CTRL and CHO-IL6 cells at 3 and 4 days after initial seeding in culture. Cells were counted using a haemocytometer and average rate of IL-6 production per cell over 24h was established (n=4 per group). Concentrations below detectable level of this ELISA were denoted not detectable (ND).

Height (cm)	Air Flow Rate (L/min)	Fluid Flow Rate (mL/min)	Bead Diameter/ Bead Shape (Sphericity)
5	2	0.1	>>1mm/irregular
	4	0.1	~1mm/irregular
	5	0.1	~1mm/irregular
	5.5	0.1	~1mm/irregular
	5.5	0.25	>1mm/irregular
	5.5	0.5	>1mm/irregular
	6	1.0	>1mm/irregular
	6.5	0.1	>1mm/irregular
15	5.5	1.0	~500 μ m/irregular
	6	1.0	~500 μ m/irregular
20	5.5	1.0	~700 μ m/regular
	6	1.0	~500 μ m/regular
	6	1.5	~500 μ m/regular
	6.5	1.0	<500 μ m/regular
	7.5	0.5	<<500 μ m/regular
	7.5	1.0	<<500 μ m/regular
25	6	1.0	<500 μ m/regular

Table 6.2 Effects of physical parameters on alginate bead size and sphericity. A 1.7% (w/v) sodium alginate solution was sprayed into a 1.5% (w/v) CaCl₂ solution using a spray atomiser resulting in bead formation. The height of the atomiser from the CaCl₂ solution surface, the gas and alginate flow rates were adjusted in a series of trial and error experiments to determine the optimum parameters for bead production. Bead size and shape were estimated visually by stereo microscopy after alteration of each parameter.

above 1mm diameter despite the use of different air and/or alginate flow rates. When the atomiser was moved to 15cm from the liquid surface the bead diameter was on average approximately 500 μ m however the beads were still irregularly shaped. Sphericity of the beads was improved when the atomiser was moved to 20cm from the liquid surface. At 20cm from the liquid surface, increasing the air flow rate above 6L/min decreased the size of the alginate beads to below 500 μ m while increasing the alginate flow rate past 1mL/min had no noticeable effect on either bead diameter or bead shape. At 20cm, an air flow rate of 6L/min and an alginate flow rate of 1mL/min the beads were spherical with a diameter of ~500 μ m. These parameters were determined to be optimal for the encapsulation process.

Despite this optimisation procedure a large proportion of the alginate beads produced were determined to deviate considerably from the average diameter of ~500 μ m. In an effort to obtain a more uniformly sized population of beads, polypropylene mesh filters were used in a two step filtration process to limit the bead size to between 297 μ m to 500 μ m diameter. The alginate beads were initially passed through a 500 μ m mesh filter to remove all beads greater than 500 μ m diameter (Figure 6 4a). The filtrate was then passed through a 297 μ m filter to remove all beads below 297 μ m diameter (Figure 6 4b). The retentate from the 297 μ m filter was used in all subsequent experiments (Figure 6 4c).

CHO-IL6 and CHO-CTRL cells were next encapsulated in alginate beads (297 μ m-500 μ m diameter) and cultured for over two weeks. Live/Dead assays were performed to determine cell viability in these beads at varying times during culture. CHO-CTRL and CHO-IL6 cell viability was high in alginate beads at 1 day after encapsulation and remained high up to 17 days in culture as demonstrated by the presence of predominantly green staining cells in these beads (Figure 6 5). When observed 1 day after encapsulation both CHO-CTRL and CHO-IL6 cells were

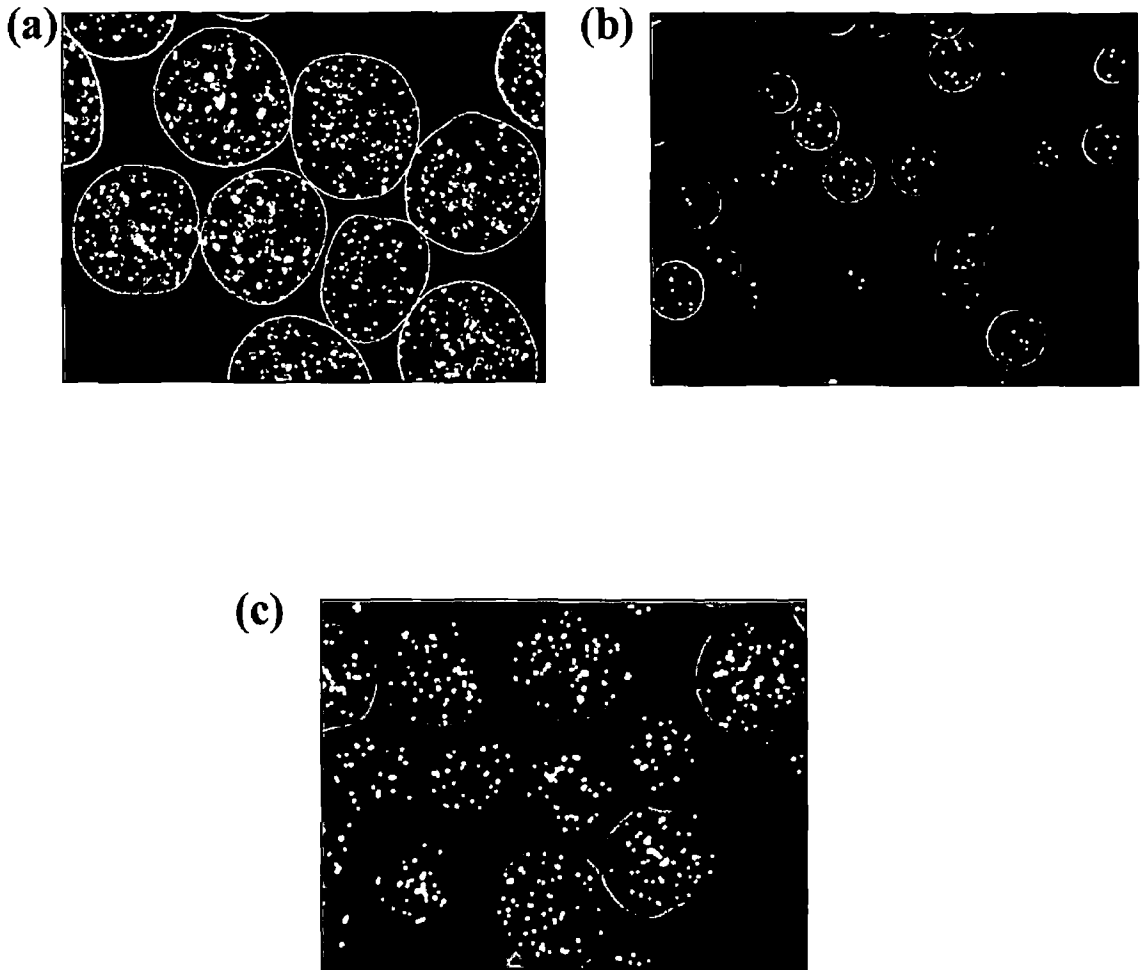


Figure 6 4 Two step filtration of beads results in a uniform sized bead population. In order to obtain a uniformly sized bead population, beads (CHO-CTRL beads shown) were a) filtered through a 500µm polypropylene filter to remove beads greater than 500µm diameter Retained beads were photomicrographed (4x) b) Filtrate from the 500µm filtration step was passed through a 297µm polypropylene filter to remove beads smaller than 297µm diameter Filtrate was photomicrographed (4x) c) Beads retained on the 297µm filter were dispersed in culture media and photomicrographed (4x)

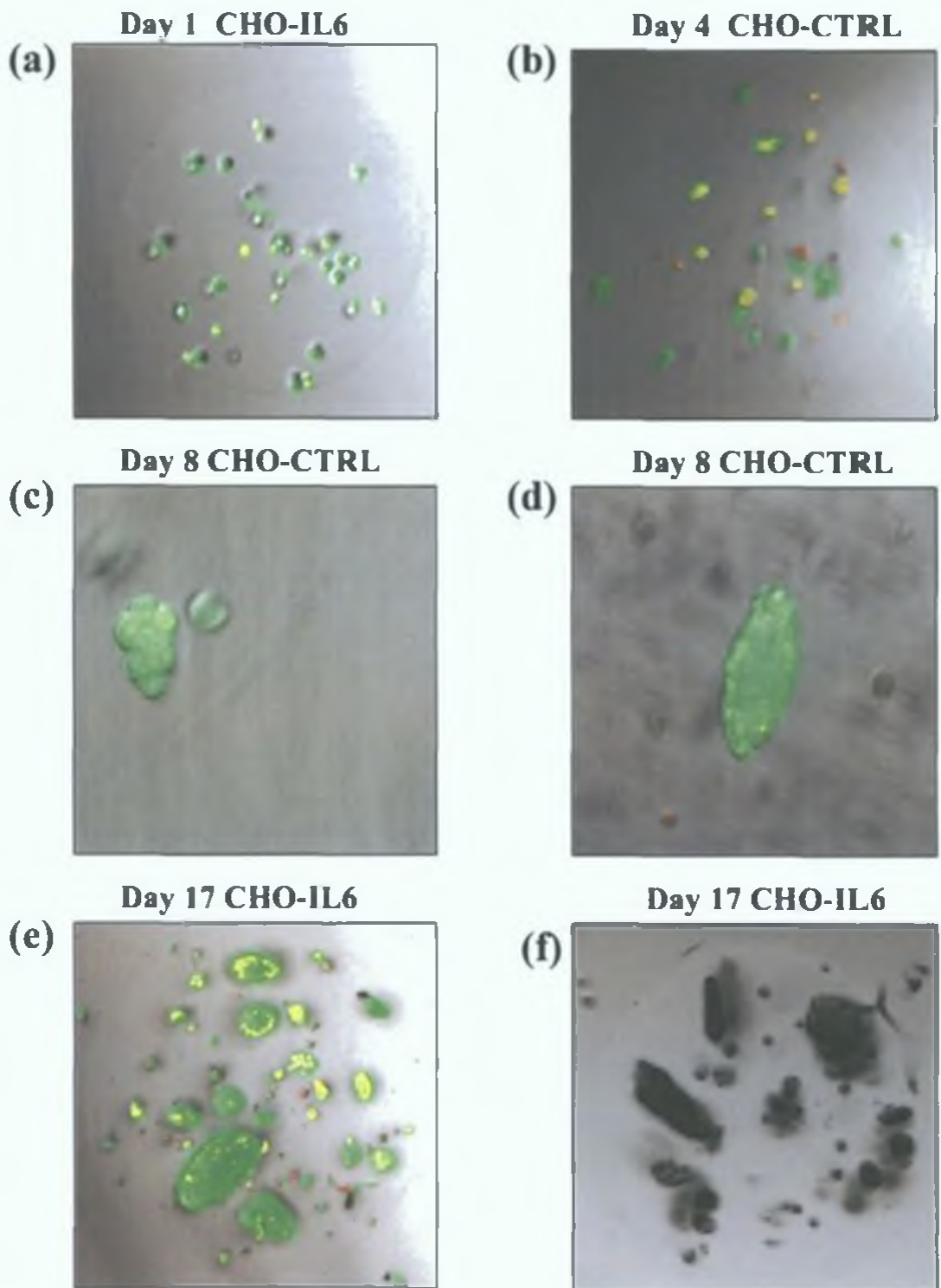


Figure 6.5 Encapsulated CHO-IL6 and CHO-CTRL cell viability and colony morphology *in vitro*. (a-e) Representative composite confocal images of alginate encapsulated CHO-IL6 (a,f,e) and CHO-CTRL (b,c,d) beads after live-dead staining at varying times throughout culture *in vitro*. Live cells fluoresce green and dead cells appear red. All images captured at 10x magnification except c & d which were captured at 40x to display colony morphology. f) Composite confocal image of a representative CHO-IL6 bead removed from culture 17 days after culture *in vitro*. Image represents an extended focus view (10x) of 1800 individual slices.

dispersed throughout the alginate beads and typically appeared as single cells (Figure 6 4a) As the culture progressed the CHO-CTRL and CHO-IL6 cells grew in colonies within the alginate beads (Figure 6 4b-f) After approximately 7 days of culture both CHO-IL6 and CHO-CTRL cells were capable of escaping the beads Beads were viewed microscopically and demonstrated escaping cells from colonies adjacent to the bead wall (Figure 6 6a-d) When 7 day old beads were placed in tissue culture plates in the presence of HSM, the escaping cells attached to the plate surface and continued to grow normally (Figure 6 6e)

In order to reduce CHO cell escape alginate beads were next PLL coated and the bead core was liquefied using sodium citrate in order to allow more centralised cell growth within the beads While this procedure did cause the CHO cell colonies to disperse (Figure 6 7a-d) and did not alter cell viability, the process considerably altered bead sphericity (Figure 6 7b) Furthermore, the PLL coating procedure caused bead aggregation (Figure 6 7a) and in some cases bead rupture resulting in cell release (Figure 6 7b) Beads were not PLL coated for subsequent experiments due to these effects

ELISA for human IL-6 was performed on media from beads removed from culture at varying time points throughout the course of the experiment to determine if the encapsulated CHO-IL6 cells could still produce and release rhIL-6 CHO-IL6 and CHO-CTRL beads were removed from stirrer culture and placed in tissue culture plates in the presence of HSM IL-6 production over a 24h period was determined and related to bead number CHO-IL6 cells successfully produced and released human IL-6 into the culture media Rate of IL-6 production by encapsulated CHO-IL6 cells significantly increased with time from 431.7 ± 148.2 pg/bead/day on Day 1 to 3622.5 ± 273.4 pg/bead/day and 5494.8 ± 777.8 pg/bead/day at 7 and 12 days in culture respectively (Table 6 3 & Figure 6 8, n=4 per group, $p < 0.05$, Day 7 *versus* Day 1,

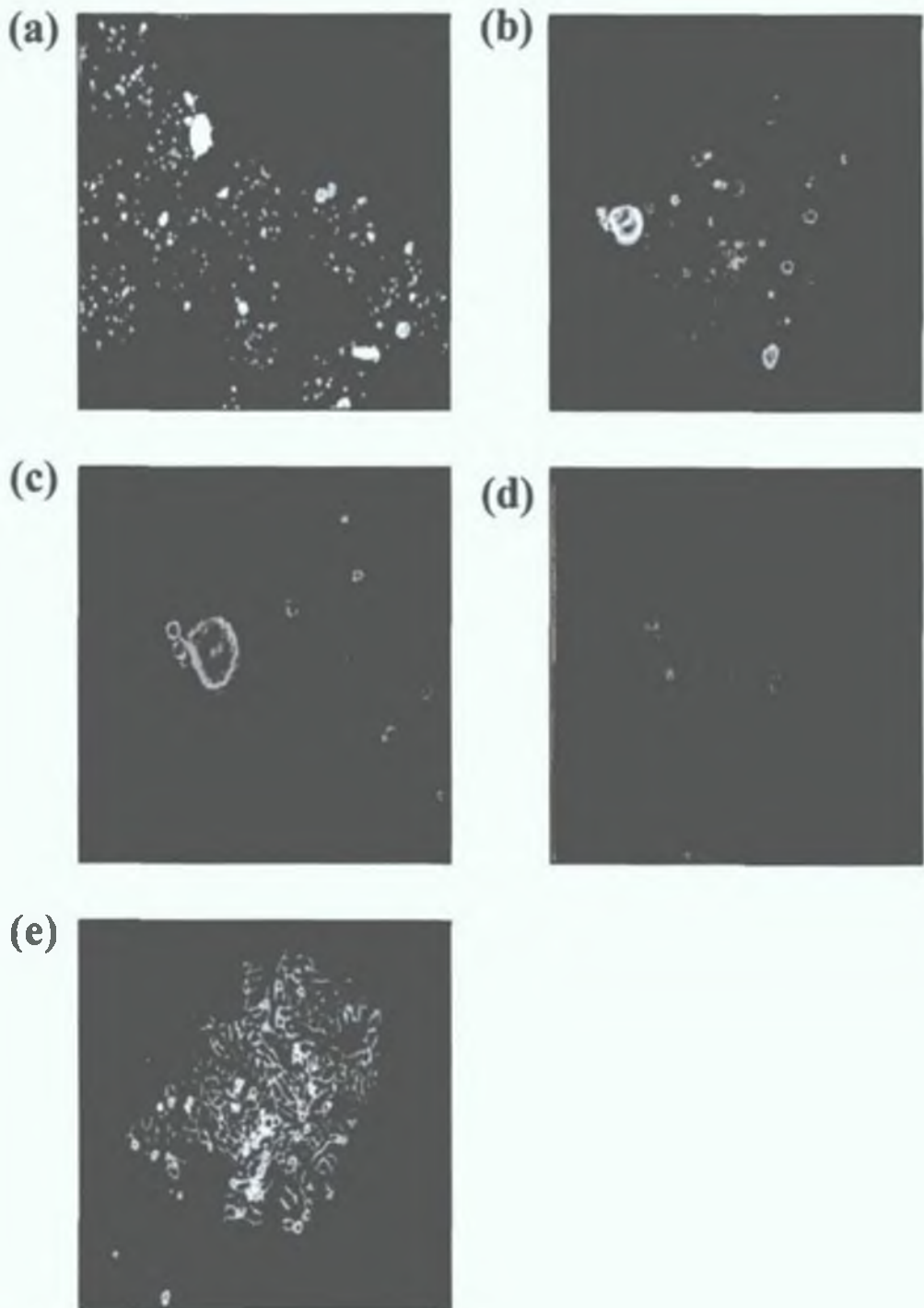


Figure 6.6 CHO cells escape from alginate beads after 7 days culture *in vitro*. Representative phase contrast micrographs of CHO-IL6 beads 7 days after culture *in vitro*. a) Alginate encapsulated CHO-IL6 cells were grown in culture for 7 days and then viewed microscopically (4x). b-d) Representative Alginate encapsulated CHO-IL6 cell bead was viewed at b) 10x, c) 20x and d) 40x magnification demonstrating cell escape through the bead wall. e) Escaped CHO-IL6 cells grew adherently on the plate surface as demonstrated by microscopy (20x).

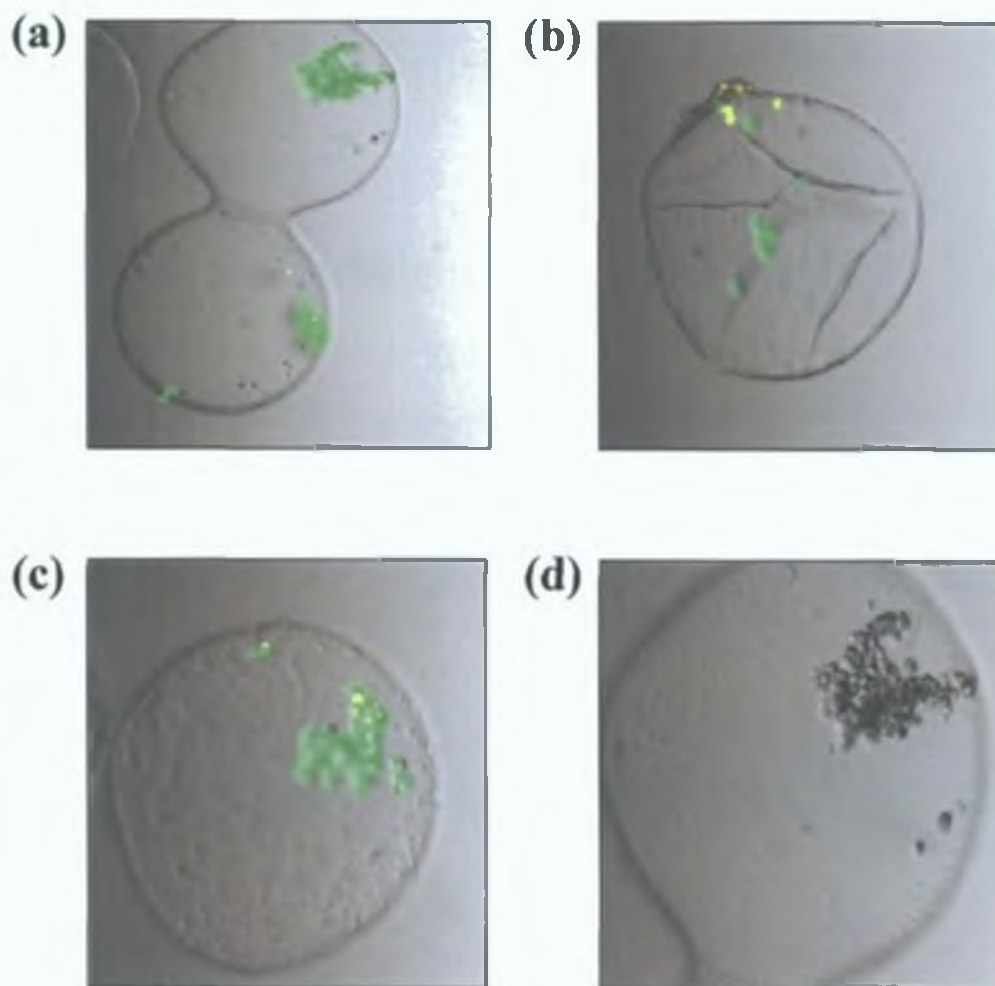


Figure 6.7 Poly-L-lysine (PLL) coating of encapsulated CHO cell beads diminishes bead integrity. Representative images of PLL coated CHO-IL6 alginate beads. a-c) CHO-IL6 cell alginate beads were coated with PLL, the alginate core was then liquefied using citrate and beads were finally recoated with an outer layer of alginate. Live/Dead staining was performed and confocal images were captured (10x). Live cells fluoresce green and dead cells appear red. d) Confocal image of PLL coated alginate bead demonstrating dispersal of CHO-IL6 colony.

Days in Culture	CHO-IL6 cells Average IL-6 produced (pg/bead/day)	CHO-CTRL cells Average IL-6 produced (pg/bead/day)
1	431.7 +/- 148.2	ND
7	3622.5 +/- 273.4	ND
12	5494.8 +/- 777.8	ND

Table 6.3 IL-6 production by alginate encapsulated CHO-IL6 and CHO-CTRL cells *in vitro*. CHO-IL6 and CHO-CTRL cells were encapsulated in alginate and cultured *in vitro*. Beads were removed from culture at varying time points and grown in HSM in separate wells for a 24h period. Human IL-6 production was determined by performing ELISA on the culture media removed from these wells (n=4 per group). IL-6 concentrations below detectable levels were denoted not detectable (ND).

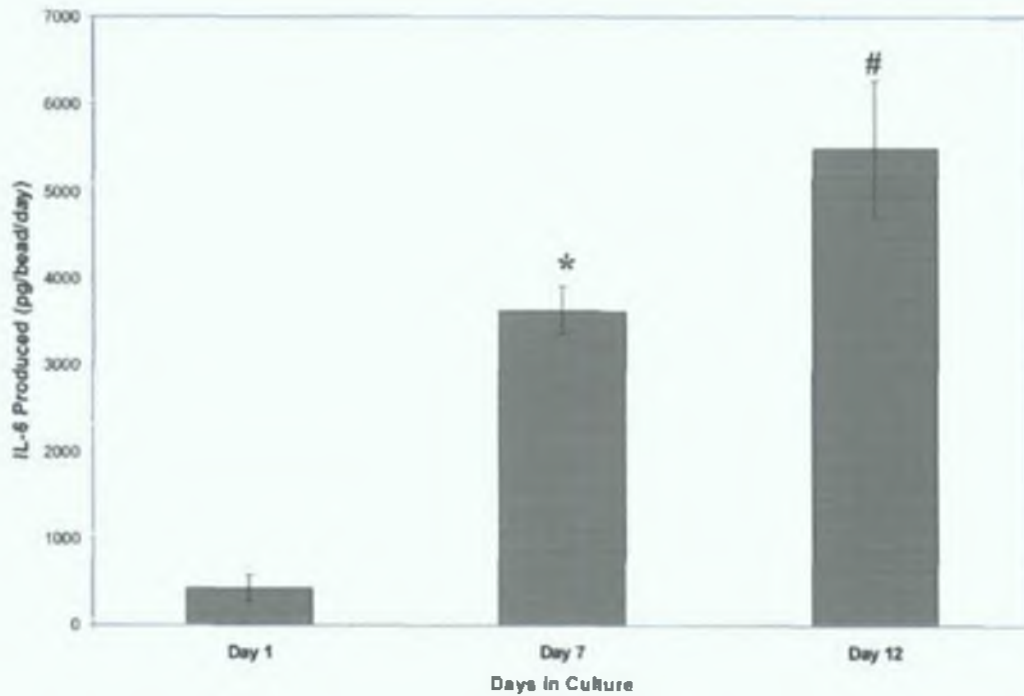


Figure 6.8 IL-6 production by alginate encapsulated CHO-IL6 and CHO-CTRL cells *in vitro*. CHO-IL6 and CHO-CTRL cells were encapsulated in alginate and cultured *in vitro*. Beads were removed from culture at varying time points and grown in HSM in separate wells for a 24h period. Human IL-6 production was determined by performing ELISA on the culture media removed from these wells (n=4 per group, *p<0.05, Day 7 versus Day 1; # p<0.05 Day 12 versus Day7).

p<0.05, Day 12 *versus* Day 7) Human IL-6 was not detectable in the media of CHO-CTRL beads (Table 6.3)

6.3.2 Rat Implantation of Microencapsulated CHO-IL6 and CHO-CTRL Cells

CHO-IL6 and CHO-CTRL cells were microencapsulated and cultured for four days *in vitro* prior to implantation intraperitoneally in male ACI rats. Animals were maintained for 4 or 7 days at which point the animals were sacrificed. A peritoneal lavage was performed on each animal after sacrifice to retrieve alginate beads. Recovered beads were then washed in AMEM and the viability of encapsulated CHO cells was examined using a Live/Dead assay. Peritoneal lavage released fibrotic tissue from both CHO-CTRL and CHO-IL6 implanted rats at 4 days after implantation (Figure 6.9a-d). Microscopic examination demonstrated that alginate beads were trapped within this fibrotic tissue (Figure 6.9b-d). Viability of encapsulated CHO cells was high in beads trapped within these tissues recovered 4 days after implantation (Figure 6.9c). Live/Dead assays performed on encapsulated CHO-IL6 and CHO-CTRL cells recovered from rats after 4 days demonstrated the presence of large viable CHO colonies in each bead type (Figure 6.10). Cells, most likely of immunological origin, were also attached to the outside of all recovered CHO-CTRL and CHO-IL6 beads recovered at 4 days after implantation. CHO-IL6 and CHO-CTRL beads recovered 7 days after implantation did not contain viable CHO cells as determined by the presence of predominantly red staining cells within these beads in Live/Dead assays (Figure 6.11a & b). Microscopic analysis demonstrated the presence of living cells accumulated on the outer surface of the washed CHO-IL6 and CHO-CTRL beads after recovery at 7 days (Figure 6.11a & b).

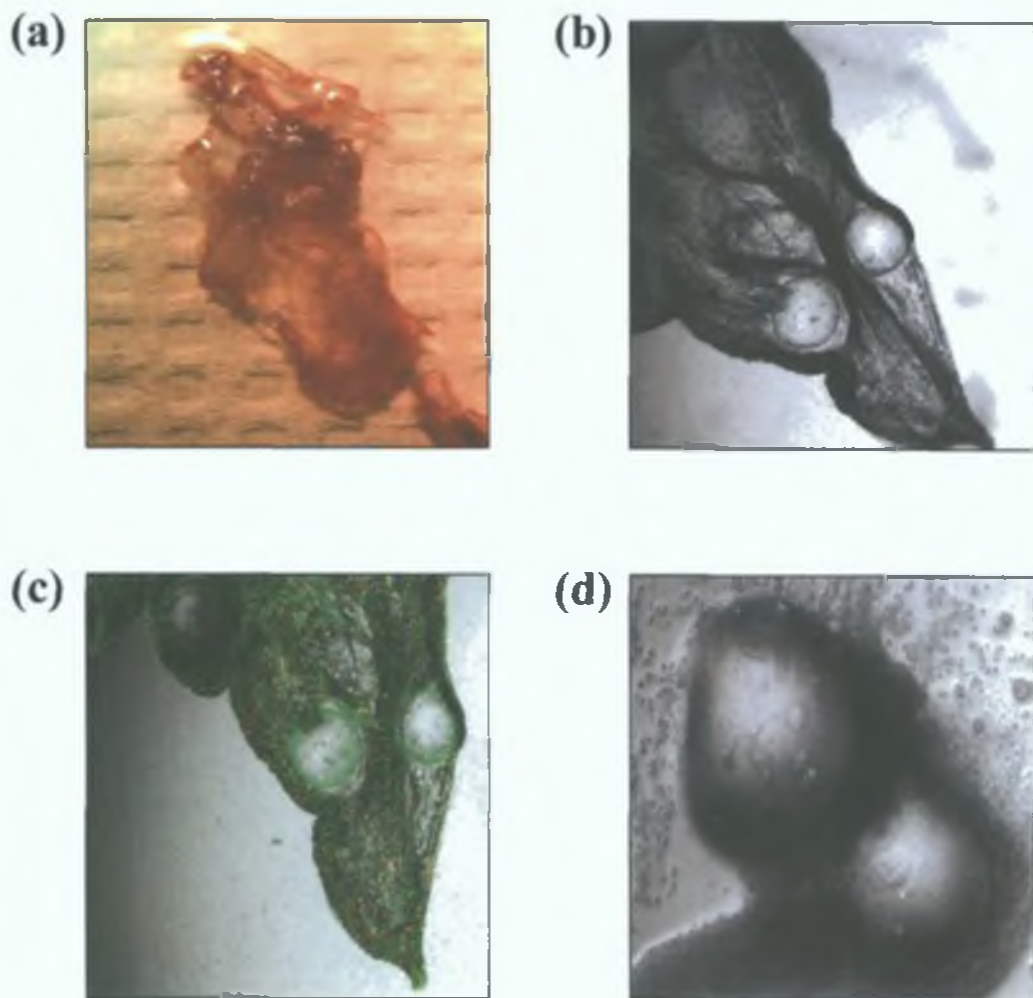


Figure 6.9 Fibrotic overgrowth present on CHO-CTRL and CHO-IL6 beads retrieved from rats 4 days after implantation. CHO-IL6 and CHO-CTRL alginate beads were implanted in rats. After 4 days, peritoneal lavage was performed. Fibrotic overgrowth was isolated and visualised. a) Representative photographic image of fibrotic overgrowth surrounding CHO-IL6 encapsulated beads retrieved 4 days after implantation in rats. b,c) Representative confocal images (4x) of b) unstained and c) Live/Dead stained fibrotic tissue surrounding CHO-IL6 beads retrieved from rats 4 days after implantation. After Live/Dead staining, live cells fluoresce green and dead cells appear red. d) Representative confocal image (10x) of fibrotic overgrowth surrounding CHO-CTRL encapsulated cells retrieved 4 days after implantation in rats.

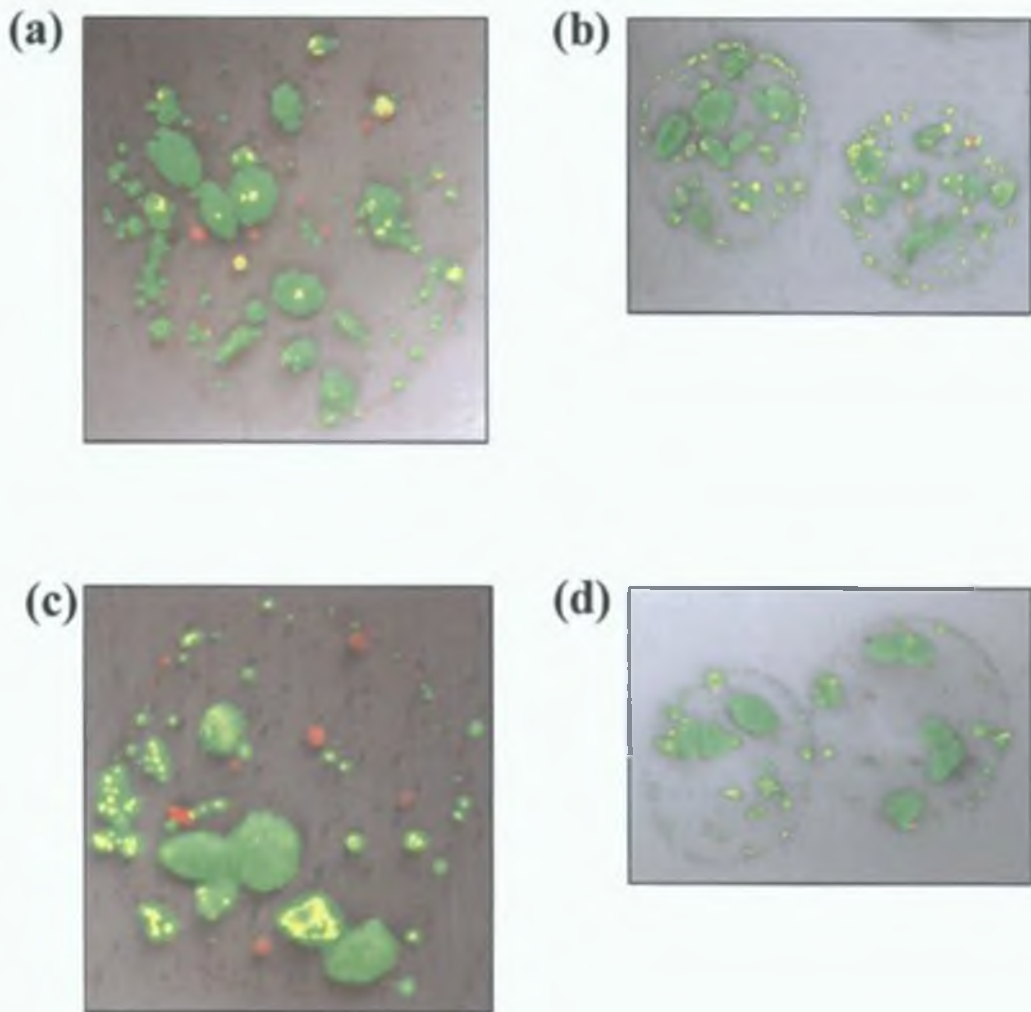


Figure 6.10 Appearance of CHO-IL6 and CHO-CTRL beads retrieved from rats 4 days after implantation. CHO-IL6 and CHO-CTRL alginate beads were implanted in rats. After 4 days, peritoneal lavage was performed. Beads were Live/Dead stained and visualised on a confocal microscope. After Live/Dead staining, live cells fluoresce green and dead cells appear red. a,b) Representative composite confocal images (10x) of CHO-IL6 beads retrieved by peritoneal lavage 4 days after implantation. c,d) Composite confocal images (10x) of CHO-CTRL beads retrieved by peritoneal lavage 4 days after implantation.

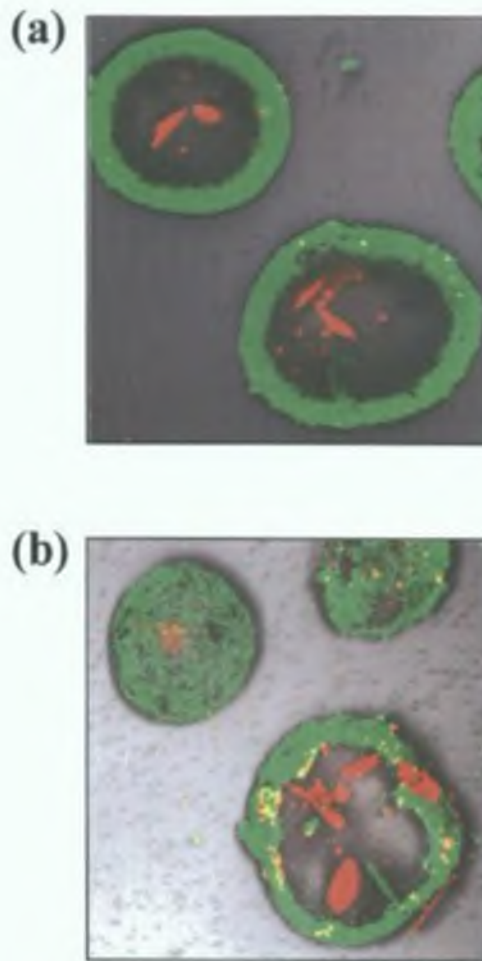


Figure 6.11 Appearance of CHO-IL6 and CHO-CTRL beads retrieved from rats 7 days after implantation. CHO-IL6 and CHO-CTRL alginate beads were implanted in rats. After 7 days, peritoneal lavage was performed. Beads were Live/Dead stained and visualised on a confocal microscope. After Live/Dead staining, live cells fluoresce green and dead cells appear red. a,b) Representative composite confocal images (10x) of CHO-IL6 beads retrieved by peritoneal lavage 7 days after implantation. c,d) Composite confocal images (10x) of CHO-CTRL beads retrieved by peritoneal lavage 7 days after implantation.

Taking into consideration that cells attached to the outside of CHO-CTRL and CHO-IL6 beads were most likely of immune origin it was next established whether alginate alone in the absence of cells could stimulate a similar response after implantation in rats. Alginate beads were prepared and implanted for 4 or 7 days in male ACI rats. Beads were recovered by peritoneal lavage, washed in AMEM and examined microscopically after Live/Dead staining for the presence of externally attached cells. Cells were not detected on the outer surface of these empty beads after either 4 or 7 days in the animals (Figure 6.12a-c).

Plasma was separated from blood collected from alginate bead implanted animals at 4 and 7 days after implantation. ELISA for human IL-6 was performed on these samples. Human IL-6 was detectable in the plasma of CHO-IL6 bead implanted rats at 4 days but not at 7 days after implantation (Table 6.4). 0.25mL packed volume of CHO-IL6 beads resulted in a plasma level of human IL-6 of 0.92 ± 0.18 pg/mL/g rat body weight (n=4) while plasma concentration of IL-6 in animals implanted with 0.5mL packed volume of beads increased further to 4.95 ± 0.39 pg/mL/g rat body weight (n=4) at 4 days after implantation. Human IL-6 was not detectable in the plasma of CHO-CTRL bead or empty bead implanted rats at either 4 or 7 days after surgery (Table 6.4, n=4). Beads retrieved from implanted animals were next washed and placed in culture in the presence of HSM. The production rate of IL-6 over a 24h period was determined using a human IL-6 ELISA performed on the cell culture media. Human IL-6 was detectable in the media removed from CHO-IL6 beads retrieved 4 days after surgery but not from cultures of CHO-IL6 beads recovered from rats at 7 days (Table 6.5). Average rate of IL-6 production by these recovered CHO-IL6 beads (4 day) in culture was 2075.9 ± 287.6 pg/bead/day (n=4). Human IL-6 was not detectable in media from cultured CHO-CTRL or empty beads removed either at 4 or 7 days after implantation (Table 6.5).

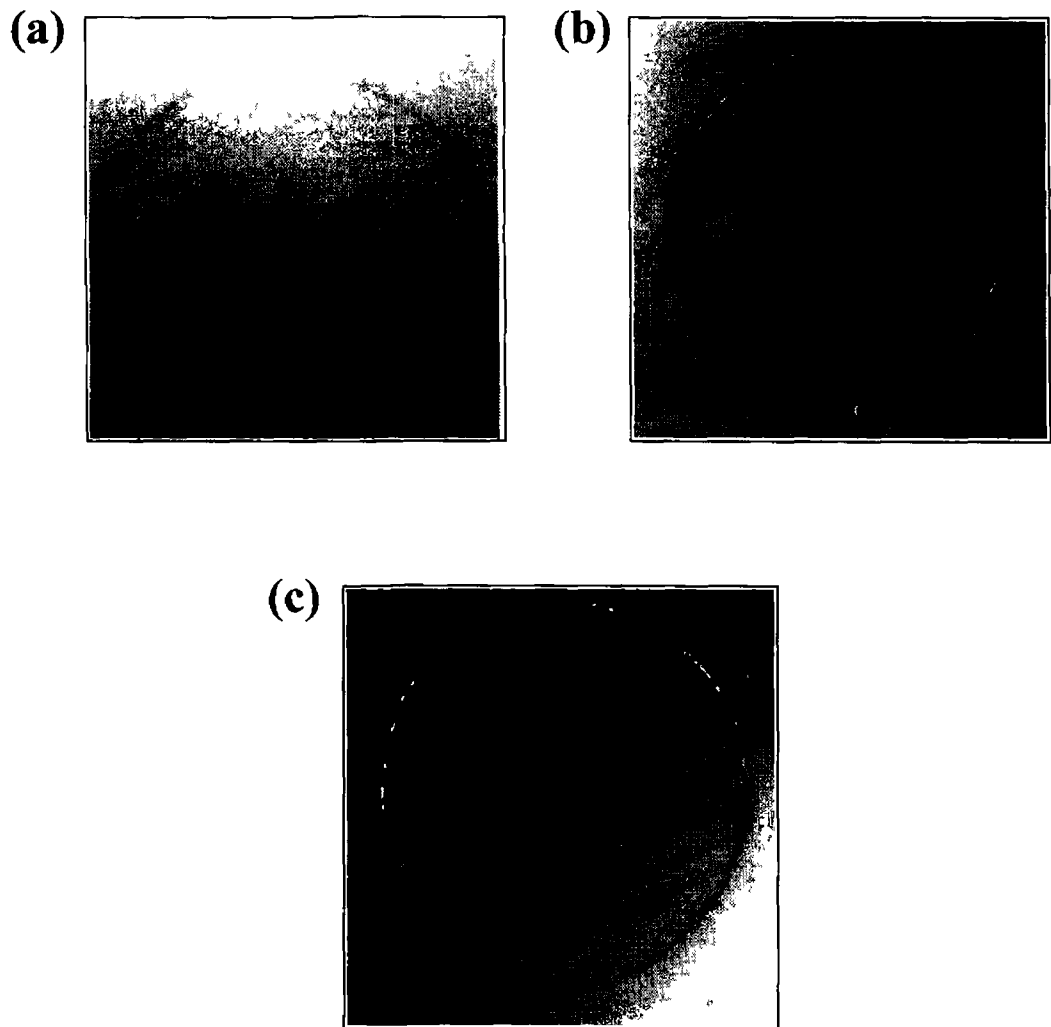


Figure 6 12 Empty alginate beads do not induce fibrotic overgrowth *in vivo*. Empty alginate beads were implanted in rats. Peritoneal lavages were performed 4 and 7 days after implantation. Beads were Live/Dead stained and visualised on a confocal microscope. After Live/Dead staining, live cells fluoresce green and dead cells appear red. a-c) Representative composite confocal images (10x) of empty beads a) before implantation, b) retrieved by peritoneal lavage 4 days or c) 7 days after implantation.

Days after Implantation	Packed Volume of Beads (mL)	CHO-IL6 Beads Implanted (pg/mL/g rat body weight)	CHO-CTRL Beads Implanted (pg/mL/g rat body weight)	Empty Beads Implanted (pg/mL/g rat body weight)
4	0.25	0.92±0.18	ND	ND
	0.5	4.95±0.39	ND	ND
7	0.25	ND	ND	ND

Table 6.4 Plasma IL-6 levels in CHO-IL6, CHO-CTRL and empty bead implanted rats. CHO-IL6, CHO-CTRL and empty alginate beads were implanted in male ACI rats. Plasma was separated from blood withdrawn by cardiac puncture 4 and 7 days after implantation. Concentration of human IL-6 in collected plasma was determined by ELISA (n=4 per group). Plasma IL-6 concentrations below detectable levels were denoted not detectable (ND).

Days after Implantation	CHO-IL6 cells Average IL-6 produced (pg/bead/day)	CHO-CTRL cells Average IL-6 produced (pg/bead/day)	Empty Beads Average IL-6 produced (pg/bead/day)
4	2075.9 ± 287.6	ND	ND
7	ND	ND	ND

Table 6.5 IL-6 production by CHO-IL6, CHO-CTRL and empty beads retrieved from rats *in vitro*. CHO-IL6, CHO-CTRL and empty alginate beads were implanted in male ACI rats. Beads were retrieved from rats 4 or 7 days after implantation and grown in HSM in separate wells for a 24h period. Human IL-6 production was determined by performing ELISA on the culture media removed from these wells (n=4 per group). IL-6 concentrations below detectable levels were denoted not detectable (ND).

6 3 3 Effects of IL-6 on Liver and HCC Tumour Growth *In Vivo*

Preliminary experiments to establish the effects of IL-6 administration on liver and HCC tumour growth *in vivo* were next performed. HCC tumours were established in male ACI rats by direct injection of H4IIE cells into the left hepatic lobe. Ten days after surgery, 0.5 mL packed volume of empty, CHO-CTRL or CHO-IL6 alginate beads were implanted intraperitoneally in these rats for 4 days. At this point the beads were retrieved by peritoneal lavage and the liver was removed and weighed. Tumours were then resected and samples of normal and tumour liver tissues were snap frozen on liquid nitrogen for western blot analysis.

Body weight of rats in all treatment groups did not change significantly over the course of the experiment. Liver weight was significantly increased in rats with CHO-IL6 bead implants (37.1 ± 1.7 mg liver wt/g body wt) compared to empty bead implanted littermates (31.2 ± 1.4 mg liver wt/g body wt, Table 6.6 & Figure 6.13, n=4 per group, p<0.05). Liver weight was also higher in CHO-IL6 bead implanted animals compared to CHO-CTRL bead implanted animals (32.8 ± 0.9 mg liver wt/g body wt, n=4) but not significantly. CHO-CTRL bead and empty bead implanted rat liver weights were not significantly different (Table 6.6 & Figure 6.13, n=4 per group). Tumour volume was highly variable even within treatment groups and no conclusions could be reached as to the effect of IL-6 treatment on tumour size (Table 6.6 & 6.7).

Western blot analysis of lysates prepared from tumour and normal liver samples demonstrated that IL-6 was detectable in normal and tumour liver tissues from CHO-IL6 bead implanted rats (Figure 6.14, n=4). In contrast, IL-6 was not detectable in tumour or normal liver tissues from CHO-CTRL bead or empty bead implanted rats. Immunoblot analysis for gp130 expression demonstrated that gp130 expression in tumour and normal liver tissues was not altered by IL-6 administration *in vivo* when compared with liver tissues resected from CHO-CTRL bead and empty bead implanted

Beads Implanted	Liver Weight to Body Weight Ratio (mg/g)	Tumour Volume (mm³)
Empty Beads	31.2 +/- 1.4	604.6 +/- 265
CHO-CTRL Beads	32.8 +/- 0.9	504.4 +/- 305.3
CHO-IL6 Beads	37.1 +/- 1.7	485 +/- 174.3

Table 6.6 Effects of CHO-CTRL, CHO-IL6 and empty alginate bead implantation on HCC tumour volume and rat liver weight. CHO-IL6, CHO-CTRL and empty alginate beads were implanted in tumour burdened male ACI rats 10 days after tumour inoculation. Rat body and liver weights were determined 4 days after bead implantation (n=4 per group). Length, width and height of HCC tumour mass were determined and used to calculate the tumour volume (n=4 per group).

RAT	Liver to Body Weight Ratio (mg/g)	Tumour Volume (mm³)
Empty Rat 1	35.2	1380
Empty Rat 2	29.2	216
Empty Rat 3	30.0	319
Empty Rat 4	30.4	504
CTRL Rat 1	31.4	525
CTRL Rat 2	34.2	33
CTRL Rat 3	31.0	100
CTRL Rat 4	34.7	1360
IL-6 Rat 1	39.1	525
IL-6 Rat 2	35.9	945
IL-6 Rat 3	32.7	120
IL-6 Rat 4	40.6	350

Table 6.7 Effects of CHO-CTRL, CHO-IL6 and empty alginate bead implantation on HCC tumour volume and rat liver weight CHO-IL6, CHO-CTRL and empty alginate beads were implanted in tumour burdened male ACI rats 10 days after tumour inoculation. Rat body and liver weights were determined 4 days after bead implantation. Length, width and height of HCC tumour mass were determined and used to calculate the tumour volume.

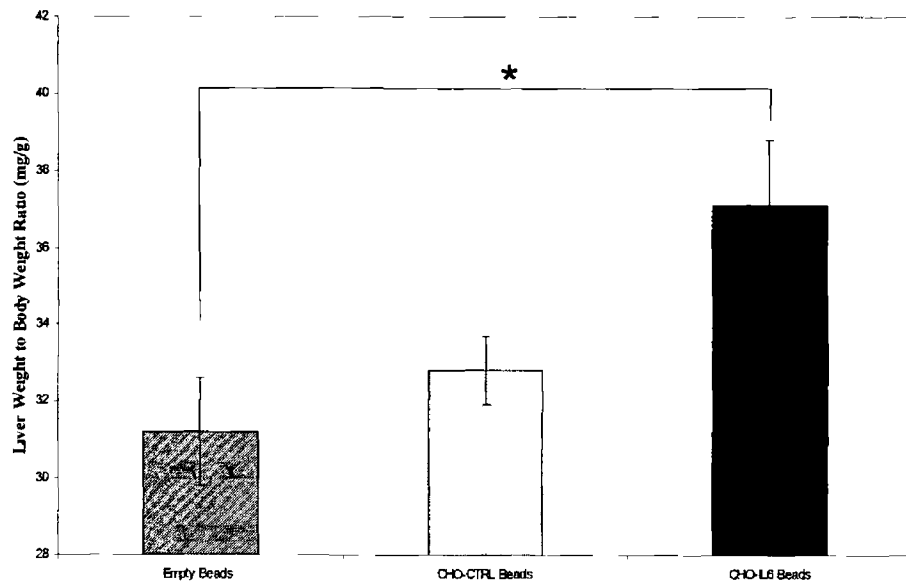


Figure 6.13 Effects of CHO-CTRL, CHO-IL6 and empty alginate bead implantation on rat liver weight CHO-IL6, CHO-CTRL and empty alginate beads were implanted in tumour burdened male ACI rats 10 days after tumour inoculation. Rat body and liver weights were determined 4 days after bead implantation (*p<0.05, n=4 per group)

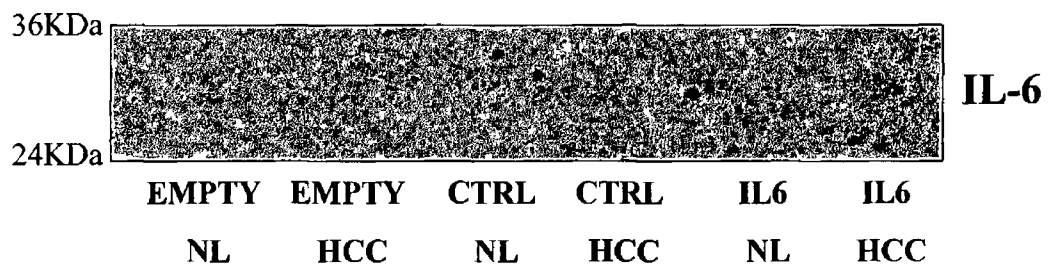


Figure 6 14 IL-6 was detectable in HCC and normal liver tissues resected from CHO-IL6 implanted rats. Representative Western blot analysis performed on lysates prepared from normal liver (NL) and HCC tissues resected from empty bead (EMPTY), CHO-CTRL bead (CTRL) and CHO-IL6 (IL6) bead implanted rats using an antibody specific against IL-6. HCC tumours were established by direct injection of H4IIE cells into the left hepatic lobe of male ACI rats. Alginate beads were implanted 10 days after tumour inoculation. Liver tissues were resected 4 days after bead implantation.

rats (Figure 6 15, n=4) Expression of gp130 was decreased in tumour tissues as compared to pair matched normal livers tissue as previously established (chapter 3) Western blotting for IL-6R α demonstrated that IL-6R α expression was elevated but not significantly in normal liver tissues from CHO-IL6 bead implanted rats *versus* CHO-CTRL bead and empty bead implanted rat liver tissues (Figure 6 16) IL-6R α expression was not significantly different between CHO-CTRL and empty bead implanted rat normal or tumour liver tissues IL-6R α expression was significantly lower in tumour tissues compared to pair matched normal liver tissues as previously determined (chapter 3)

Immunoblotting using antisera specific against pSTAT3 demonstrated that STAT3 was activated in normal and tumour liver tissues resected from CHO-IL6 implanted rats in the absence of changes in total STAT3 expression (Figure 6 17, n=4, p<0 05) Phospho-STAT3 expression was higher in HCC tissues compared to pair matched normal liver tissues resected from CHO-CTRL bead or empty bead implanted rats as previously described (chapter 3) IL-6 treatment *in vivo* increased pSTAT3 expression in HCC tissue Western blotting for pERK 1/2 determined that pERK 1/2 expression was not significantly different in normal or tumour liver tissues from CHO-IL6 bead implanted rats compared to CHO-CTRL bead or empty bead implanted rats (Figure 6 18) Total ERK 1/2 and pERK1/2 expression was elevated in HCC tumours compared to pair matched normal liver tissues from all rats studied as previously described (McKillop et al , 1997) Immunoblotting for PCNA demonstrated higher PCNA expression in HCC when compared with normal pair matched liver tissue in all animals studied (Figure 6 19) PCNA expression was not significantly different in normal liver tissue (Figure 6 19a, n=4) or HCC tumour tissue (Figure 6 19b, n=4) resected from CHO-IL6 bead implanted rats compared to CHO-CTRL or empty bead implanted rats

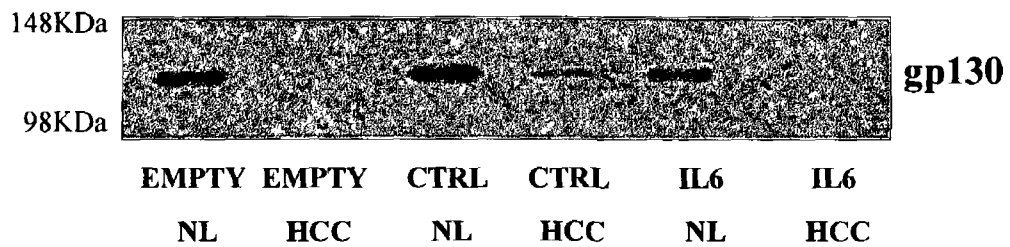


Figure 6.15 Gp130 expression in HCC and normal liver tissues resected from CHO-IL6, CHO-CTRL and empty bead implanted rats Representative Western blot analysis performed on lysates prepared from normal liver (NL) and HCC tissues resected from empty bead (EMPTY), CHO-CTRL bead (CTRL) and CHO-IL6 (IL6) bead implanted rats using an antibody specific against gp130. HCC tumours were established by direct injection of H4IIE cells into the left hepatic lobe of male ACI rats. Alginate beads were implanted 10 days after tumour inoculation. Liver tissues were resected 4 days after bead implantation.

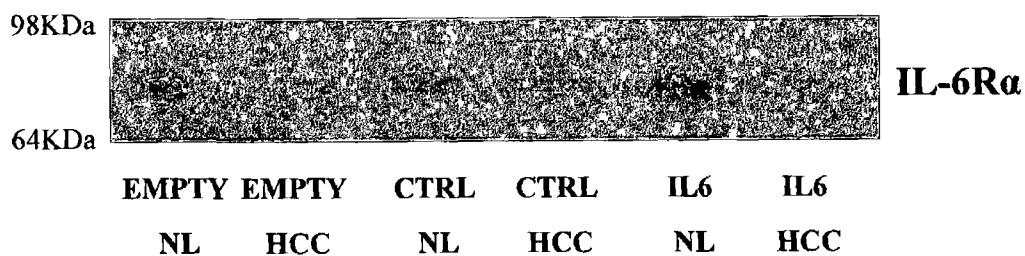


Figure 6 16 IL-6R α expression in HCC and normal liver tissues resected from CHO-IL6, CHO-CTRL and empty bead implanted rats Representative Western blot analysis performed on lysates prepared from normal liver (NL) and HCC tissues resected from empty bead (EMPTY), CHO-CTRL bead (CTRL) and CHO-IL6 (IL6) bead implanted rats using an antibody specific against IL-6R α . HCC tumours were established by direct injection of H4IIE cells into the left hepatic lobe of male ACI rats. Alginate beads were implanted 10 days after tumour inoculation. Liver tissues were resected 4 days after bead implantation.

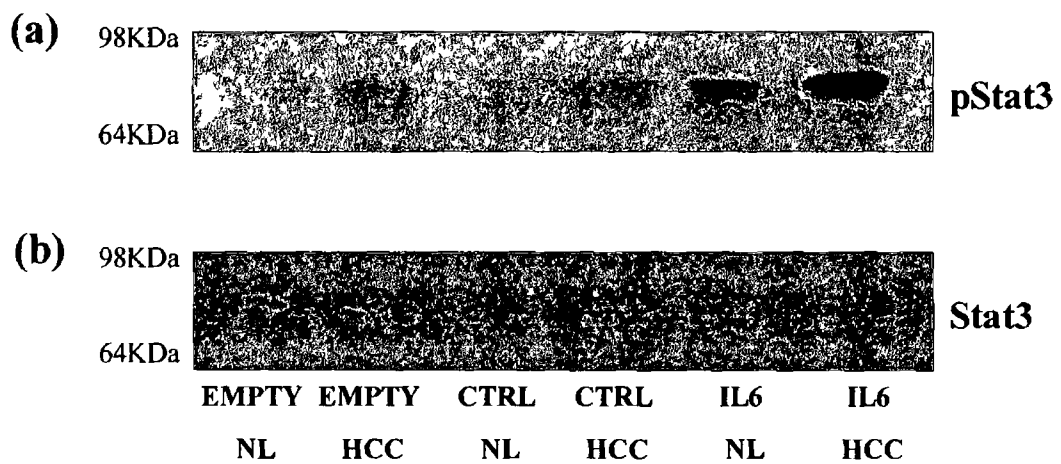


Figure 6 17 PSTAT3 expression was increased in HCC and normal liver tissues resected from CHO-IL6 implanted rats Representative Western blot analysis performed on lysates prepared from normal liver (NL) and HCC tissues resected from empty bead (EMPTY), CHO-CTRL bead (CTRL) and CHO-IL6 (IL6) bead implanted rats using antibodies specific against a) pSTAT3 and b) total STAT3. HCC tumours were established by direct injection of H4IIE cells into the left hepatic lobe of male ACI rats. Alginate beads were implanted 10 days after tumour inoculation. Liver tissues were resected 4 days after bead implantation.

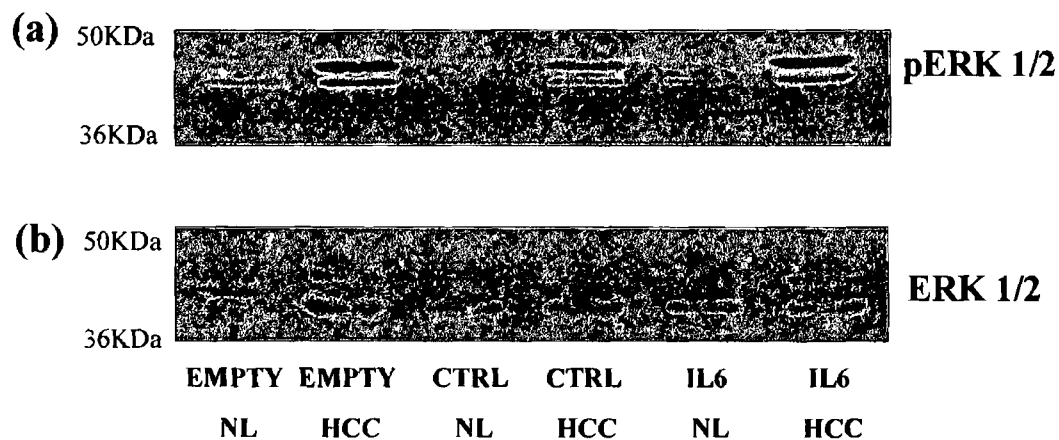


Figure 6.18 PERK 1/2 expression in HCC and normal liver tissues resected from CHO-IL6, CHO-CTRL and empty bead implanted rats Representative Western blot analysis performed on lysates prepared from normal liver (NL) and HCC tissues resected from empty bead (EMPTY), CHO-CTRL bead (CTRL) and CHO-IL6 (IL6) bead implanted rats using antibodies specific against a) pERK 1/2 and b) total ERK 1/2. HCC tumours were established by direct injection of H4IIE cells into the left hepatic lobe of male ACI rats. Alginate beads were implanted 10 days after tumour inoculation. Liver tissues were resected 4 days after bead implantation.

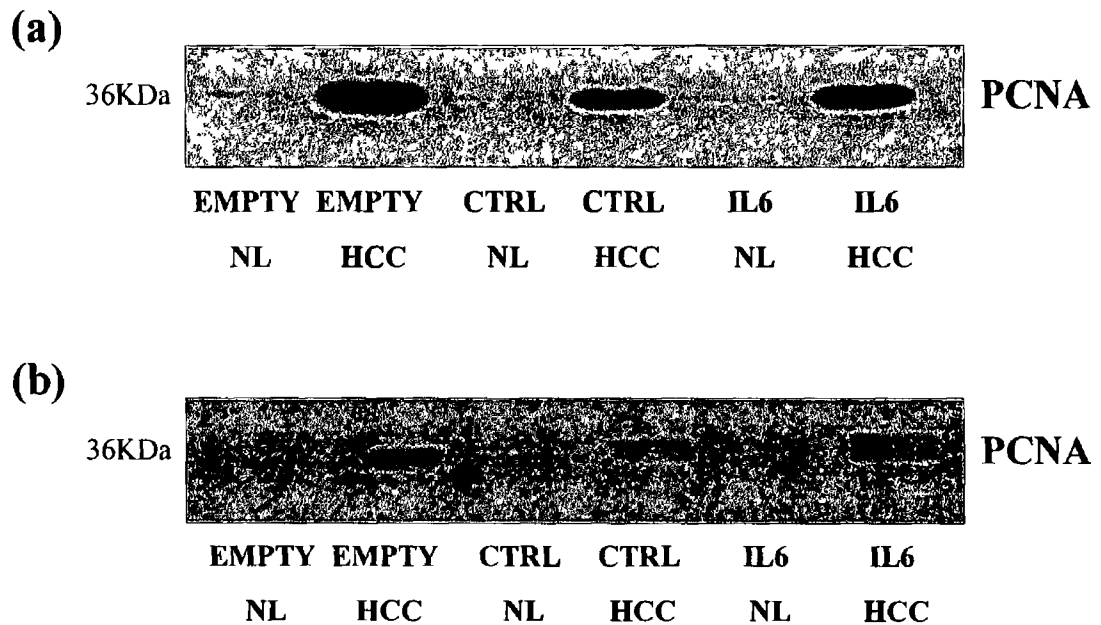


Figure 6 19 PCNA expression in HCC and normal liver tissues resected from CHO-IL6, CHO-CTRL and empty bead implanted rats Representative Western blot analysis performed on lysates prepared from normal liver (NL) and HCC tissues resected from empty bead (EMPTY), CHO-CTRL bead (CTRL) and CHO-IL6 (IL6) bead implanted rats using an antibody specific against PCNA a) Western blot demonstrating PCNA expression in NL tissues b) Western blot demonstrating PCNA expression in HCC tissues HCC tumours were established by direct injection of H4IIE cells into the left hepatic lobe of male ACI rats Alginate beads were implanted 10 days after tumour inoculation Liver tissues were resected 4 days after bead implantation

6.4 Discussion

Microencapsulation of recombinant cells and their subsequent implantation in animals offers the possibility of sustained delivery of biotherapeutic substances *in vivo* (Uludag et al , 2000) In the current study alginate encapsulated IL-6 expressing CHO cells were used to deliver human IL-6 in an immune competent rat model of HCC Encapsulated IL-6 expressing and control CHO cells remain viable and form large colonies in alginate beads up to 17 days after encapsulation *in vitro* Encapsulated CHO-IL6 cells retain the ability to produce and secrete high levels of human IL-6 Implantation of encapsulated CHO cells intraperitoneally in rats results in an accumulation of living cells on the outer surfaces of beads, fibrotic overgrowth and complete loss of bead viability by 7 days However, at 4 days after implantation CHO cells remain viable and actively secrete human IL-6 resulting in high plasma IL-6 levels Increased plasma rhIL-6 in CHO-IL6 bead implanted rats is associated with increased STAT3 activity in both normal liver and HCC tissues ERK 1/2 activity was not altered in normal and HCC tissues from CHO-IL6 bead implanted rats compared to controls IL-6R α expression was elevated in normal liver tissues from CHO-IL6 implanted rats but not significantly Total liver weight was significantly increased in CHO-IL6 bead implanted rats compared to empty bead implanted rats Liver weight was also increased compared to CHO-CTRL bead implanted rats however not significantly HCC tumour volume was highly variable within groups and hence no conclusion on the effect of IL-6 on HCC tumour progression can be drawn

Alginate encapsulation is a single step process which is carried out under mild conditions making it suitable for microencapsulation of living cells (Uludag et al , 2000) In the current study CHO-IL6 and CHO-CTRL cells were encapsulated in alginate beads which were crosslinked using Ca²⁺ Cell viability was retained in these capsules and large colonies of CHO cells developed within these beads *in vitro*

demonstrating the suitability of this environment to sustain cell growth and allow transfer of both nutrients and oxygen to these cells. However, noticeable leakage of CHO-IL6 and CHO-CTRL cells was observed from these beads at day 7 post-encapsulation. Living cells were capable of escaping the beads and could begin further growth outside of the bead environment. In an effort to limit this cell shedding the beads were PLL coated, followed by the reliquefaction of the alginate core using citrate. Liquefaction of the core did allow dispersal of the growing CHO cell colonies and provided more space for cell proliferation however the bead integrity was diminished by this procedure. Previous reports have demonstrated cell shedding from alginate beads in particular when cells with high proliferation rates, such as recombinant cell lines, are used (Visted et al , 2003, Rokstad et al , 2003, Rokstad et al , 2002). Proliferating cells can disrupt the alginate network resulting in bead rupture and cell escape (Rokstad et al , 2003). Strengthening the beads with PLL without subsequent liquefaction may assist in the prevention of bead rupture (Thu et al , 1996b, Thu et al , 1996a). Furthermore, the use of Ba^{2+} in the place of Ca^{2+} in the encapsulation process has been reported to result in a stronger bead due to a higher degree of crosslinking within the alginate structure (Gaumann et al , 2001, Visted et al , 2003, Uludag et al , 2000). Inhomogeneous beads have also proved to be more stable and are less permeable thereby reducing cell escape. These beads have a higher alginate concentration at the bead surface than in the core. To create these beads alginate is dropped into a low Ca^{2+} concentration solution which results in alginate diffusion towards the surface of the bead due to its affinity for the rare Ca^{2+} ions (Thu et al , 1996b, Thu et al , 1996a, Visted et al , 2003). In addition to these modifications other reports have suggested the potential to reduce the proliferative capacity of encapsulated cells as a method to prevent cell leakage (Rokstad et al , 2003). This can be achieved through the transfection of a multicistronic expression unit for a cell cycle arrest gene.

and the gene of the product of interest under the control of a regulatory promoter (Fux et al , 2001, Mazur et al , 1999) or through the use of genetically engineered primary cells such as myoblasts that differentiate to a non proliferative state while still expressing the protein of interest (Cirone et al , 2002, Garcia-Martin et al , 2002) The use of contact inhibited cells (Ritt et al , 2000, Takahashi and Suzuki, 1996) for encapsulation offers another possible method to minimise bead rupture due to cells with high proliferative capacity These techniques may help to minimise the cell leakage observed in the current model allowing the development of a more suitable structure for implantation *in vivo*

Successful implantation of microencapsulated cells *in vivo* requires the avoidance of the detrimental effects of the host immune response and fibrotic overgrowth (Uludag et al , 2000) Beads which are not biocompatible result in fibrotic overgrowth which interferes with the diffusion of nutrients and oxygen to the encapsulated cells In general, the alginate composition, bead size, smoothness and integrity determine the biocompatibility of implanted beads (de Groot et al , 2004) Tails and craters in the bead outer structure, the presence of impurities in alginate and cell shedding have all been linked to decreased biocompatibility *in vivo* (De Vos et al , 1993, De Vos et al , 1997, De Vos et al , 1996) In the current model fibrotic overgrowth was apparent on beads retrieved at 4 days and increased further at 7 days after implantation In general this appeared as the build up of living cells on the exterior surface of individual beads however gross presentation of vascularised fibrotic tissue surrounding multiple beads was also observed in peritoneal lavages from several implanted animals Graft failure was apparent at 7 days post-implantation The encapsulation process in the current study was optimised to provide uniform spherical beads within a desired size range (diameter 297-500µm) Furthermore, the beads were manufactured from commercially available ultrapure sodium alginate optimised for cell

encapsulation by the removal of endotoxins Empty alginate beads produced using this optimised procedure in the current study do not initiate a foreign body response after implantation in rats which excludes bead composition and integrity as causative factors for the observed fibrotic overgrowth This suggests that in the current study the presence of encapsulated cells is the most important factor leading to decreased biocompatibility *in vivo* Cell leakage and antigen shedding from the encapsulated cells are the most probable initiators of this foreign body response (de Groot et al , 2004) Macrophages act as the main cell type recruited to the bead surface after initiation of the host response resulting from graft disruption of host vasculature or passive antigen shedding from encapsulated cells (Uludag et al , 2000, de Groot et al , 2004) Macrophages secrete cytokines such as interleukin-1 β (IL-1 β), TNF- α and interferon- γ (IFN- γ), nitric oxide (NO) and oxygen radicals which diffuse into the beads resulting in encapsulated cell death (Gray, 2001, Omer et al , 2003, King et al , 2000) Furthermore, fibroblasts migrate to the bead surface and mediate matrix production coupled with a neo-vascularisation response (Uludag et al , 2000) This ultimately leads to the ensheathing of the implant in fibrous materials and glycosaminoglycans The fibrotic build up prevents diffusion of oxygen and nutrients to the encapsulated cells and leads to cell necrosis The current model utilises a xenograft implanted intraperitoneally in rats The implantation of encapsulated xenogeneic cells has been shown to pose greater problems than those seen after allograft implantation (de Groot et al , 2004) Virtually every protein shed from xenogeneic cells is different than the host These xenoantigens not only attract macrophages but also are presented to responder T cells *via* an indirect pathway resulting in the initiation of an immune response against the graft Past studies demonstrate CD3⁺ T cells and MHCII expressing macrophages constitute the most prominent cell types present in the peritoneum during xenotransplantation indicating the specific recognition of the xenograft despite the capsule (Siebers et al , 1999)

Prevention of cell shedding as described above will assist in the minimisation of these host responses however, no method currently exists to prevent antigen shedding from the encapsulated CHO cells. This makes sustained survival of encapsulated cells difficult to achieve *in vivo*. The use of genetically modified allogeneic rather than xenogeneic cells may assist in overcoming these problems. Other research suggests the genetic engineering of cells to acquire resistance to deleterious molecules such as cytokines and NO through the forced expression of anti-apoptotic proteins as a method to avoid xenograft rejection (Rabinovitch et al, 1999, Contreras et al, 2001). The potential for co-encapsulation with other cells such as Sertoli cells which are capable of inducing local immuno-suppressive effects has also been proposed to extend graft survival *in vivo* (Yang and Wright, 1999).

Sustained IL-6 delivery greater than 4 days was not possible using the current system *in vivo*. However, high plasma levels of human IL-6 were achieved 4 days after implantation in rats. Furthermore, increased levels of plasma human IL-6 were associated with an increase in detectable IL-6 in both normal and tumour liver tissues. This was further correlated with increased STAT3 activity in both normal and tumour liver tissues. This data demonstrates that CHO-IL6 encapsulated cells can produce and deliver biologically active human IL-6 in a rat model. Moreover, this data indicates that H4IIE tumour cells respond to IL-6 *in vivo* despite decreased receptor expression. While the IL-6 receptors are downregulated in HCC tissue compared to normal liver, the cells do express the receptor and hence can retain responsiveness to IL-6. In the current study, tumour cells were inoculated directly into the liver parenchyma. After 10 days, CHO-IL6, CHO-CTRL or empty beads were implanted in these animals. Characterisation of the H4IIE tumour model *in vivo* has shown that the mean latent period following injection of 1×10^6 H4IIE cells into male ACI rats is 8-10 days (Evans and Kovacs, 1977). As a result, 10 days after inoculation was considered an appropriate

time for implantation of encapsulated CHO cells as this is the beginning of the exponential tumour growth phase *in vivo*. While no tumour mass was visible at the time of intraperitoneal implantation of the alginate beads, the current study based the time of bead implantation on a study performed using a subcutaneous injection site on the back of male ACI rats rather than the liver as the site of tumour development (Evans and Kovacs, 1977). The kinetics and efficiency of tumour development in the liver differs from the site studied in past research. Indeed, in the current study, tumour volumes were considered to be highly variable within treatment groups and as a result no direct effects on tumour volume attributed to IL-6 treatment could be concluded. Tumour size variability was not reported as being considerably high at the subcutaneous tumour site (Evans and Kovacs, 1977). The reasons for selection of the liver as a site of tumour formation rather than a subcutaneous site in this study are twofold. The current research aims to provide a more physiologically relevant analysis of liver tumour development *in vivo* which it is believed could not be achieved at a subcutaneous site. Secondly, the current approach recognises that the liver is the site of the highest levels of IL-6 *in vivo* due to its role in IL-6 degradation. Past research has demonstrated that injected IL-6 is cleared efficiently with a plasma half life of approximately 2 minutes and that after 20 minutes approximately 80% of the administered IL-6 is located in the liver (Castell et al , 1988, Castell et al , 1990a)

Despite the inability to draw conclusions on the effects of sustained high levels of rhIL-6 on HCC tumour development *in vivo*, the current study did determine an increase in liver weight in CHO-IL6 implanted rats, which could not be accounted for by tumour volume. IL-6 is a key cytokine in injury stimulated liver regeneration where increased IL-6 levels prime resting hepatocytes to respond to growth factors such as epidermal growth factor, hepatocyte growth factor and transforming growth factor- α (Fausto, 2000). Sustained systemic administration of IL-6 using CHO-IL6 cell tumours

in a nude mouse model resulted in dramatic hepatomegaly and hepatocyte hyperplasia in the absence of liver injury (Zimmers et al , 2003) This was associated with increased STAT3 and ERK2 activity in addition to increased PCNA expression in the liver Furthermore IL-6R α expression was increased in this model while gp130 expression remained unchanged In the current model sustained rhIL-6 administration in an immune competent rat also resulted in increased STAT3 activity It is worth noting that PCNA expression was elevated in normal liver tissues from two of the four animals treated with IL-6 in the current study Furthermore IL-6R α expression was elevated but not significantly in all of the CHO-IL6 implanted rat normal liver tissues compared to control animals This may be suggestive of the initiation of similar phenomena as that observed in the nude mouse model (Zimmers et al , 2003) The aim of this study was to optimise the procedure for rhIL-6 delivery *in vivo* The results demonstrating the effects of rhIL-6 on normal liver and HCC growth can only be considered preliminary data and taking into consideration the variability associated with the *in vivo* environment do not incorporate a sufficient sample size to draw clear conclusions However, these initial findings suggest that this model constitutes a potentially useful method to study the effects of IL-6 on normal liver growth in the absence of HCC in immune competent animals However, increased graft survival is required to sustain IL-6 delivery over longer periods to fully establish these effects

In conclusion, microencapsulation of recombinant CHO cells constitutes an effective method for systemic IL-6 delivery *in vivo* However, modifications to prolong graft survival are required in order to extend the delivery period This includes the development of techniques to prevent cell shedding, to strengthen the integrity of the bead and to decrease the responsiveness of these cells to host defence mechanisms Ultimately these alterations should decrease the intensity and effectiveness of the host response and prolong the survival of the encapsulated cells *in vivo* While the

variability of H4IIE tumour size prevented the determination of the effects of IL-6 on HCC tumour progression *in vivo*, this method of IL-6 delivery does have potential application in the study of normal liver growth

Chapter 7: Discussion

7.1 The Role of Interleukin-6 in Hepatocellular Carcinoma Progression

Hepatocellular carcinoma (HCC) is the most common malignant tumour of the liver (Parkin et al , 2001) This cancer usually arises from defined causal factors the most common of which are viral hepatitis, aflatoxin exposure and chronic alcohol abuse (Kew, 2002, Okuda, 2000) Despite the identification of these aetiological agents hepatocarcinogenesis remains poorly understood Currently surgical resection or liver transplantation offer the best treatment for HCC however, these therapies are hindered by tumour recurrence and/or donor shortages (Kew, 2002, Okuda, 2000) A better understanding of the molecular mechanisms involved in initiation and progression of HCC is essential to our understanding of HCC and in the potential design of new therapeutic strategies targeting this malignancy

Interleukin-6 is a pleiotropic cytokine with diverse biological functions IL-6 acts as a key cytokine in normal hepatocyte proliferation during the process of injury stimulated liver regeneration (Fausto, 2000) Furthermore, a mitogenic role for IL-6 in hepatocyte proliferation in the absence of liver injury has been reported (Zimmers et al , 2003) Double transgenic mice expressing human IL-6 and human soluble IL-6R under liver specific promoters also indicate hepatomegaly, hepatic hyperplasia and the emergence of hepatic adenomas (Maione et al , 1998, Schirmacher et al , 1998) Hepatic adenomas are considered an absolute precursor of hepatocyte transformation

(Takayama et al , 1990) Taking into consideration the links between IL-6 signalling and hepatocyte proliferation the current studies proposed to examine the relationship between IL-6 and HCC, a malignancy characterised by dysregulated proliferation of transformed hepatocytes

Previous research has determined growth inhibitory and stimulatory effects of IL-6 in HCC cells (Kim and Baumann, 1999, Lai et al , 1999, Klausen et al , 2000, Kumagai et al , 2002) Furthermore, IL-6 has been linked to increased survival (Chen et al , 1999) and increased metastatic potential (Reichner et al , 1998) in HCC cells The current study aimed to establish the relationship between IL-6 signalling and HCC progression using complimentary *in vitro* and *in vivo* rat models An *in vivo* tumour model was established by the direct inoculation of H4IIE rat hepatoma cells into the liver parenchyma of male ACI rats Tissues from these tumours were characterised for components of the IL-6 signalling cascade and compared with expression in normal liver tissue Cells isolated from HCC tumours were then used *in vitro* to establish the effects of IL-6 signalling in these cells

This study identified differences in expression of IL-6 signalling cascade components between normal and HCC tissues HCC is characterised by decreased IL-6 receptor expression and increased IL-6 expression compared to normal liver tissue Furthermore, STAT3 activity is increased in these tumours *versus* normal liver tissue SOCS-1 expression is upregulated while SOCS-3 expression is downregulated in HCC compared to normal liver tissue Analysis of downstream effectors of IL-6 signalling demonstrates that p21^{waf1/cip1} and p27^{Kip1} expression are upregulated in HCC tissue IL-6 treatment of cells isolated from these tumours activates Jak-STAT and Ras-MAPK intracellular signalling pathways These pathways are also activated in isolated hepatocytes While the Jak-STAT pathway is activated similarly in each cell type, the Ras-MAPK pathway has a different activation profile after IL-6 treatment in H4IIE

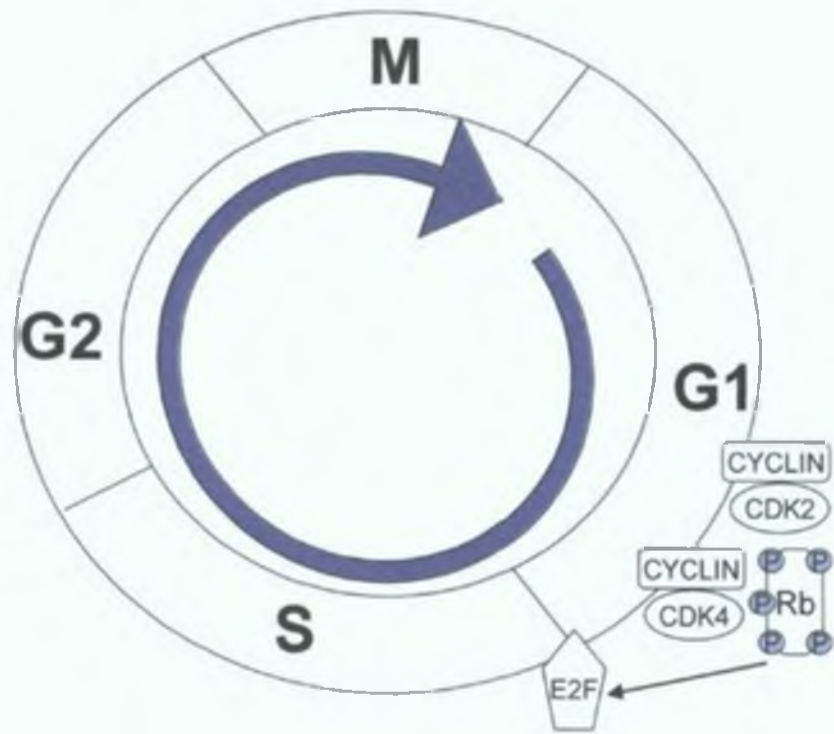
HCC cells than in isolated hepatocytes. Interleukin-6 treatment in H4IIE cells stimulates the expression of the cdk inhibitors p21^{waf1/cip1} and p27^{Kip1}, an effect which is not observed in isolated hepatocytes. Inhibition of the Jak-STAT and Ras-MAPK pathways in H4IIE cells established that p21^{waf1/cip1} expression is STAT dependent however the pathway responsible for upregulated p27^{Kip1} expression after IL-6 treatment remains to be determined. The expression of cdk inhibitors occurs concomitant with decreased cyclin dependent kinase 2 (cdk2) and cyclin dependent kinase 4 (cdk4) activity in addition to decreased phosphorylation of Retinoblastoma protein (Rb). Ultimately this sequence of events results in reduced entry of H4IIE cells into the S phase of the cell cycle and as a result decreased cell proliferation *in vitro*.

Interleukin-6 treatment of H4IIE (HCC) cells blocks cell cycle progression in the G0/G1 phase. Progression through the cell cycle is tightly controlled by cdks (Morgan, 1995). Cyclins associate with cdks and are the primary regulators of cdk activity (Sherr and Roberts, 1999, Morgan, 1995). The activation of cdk4 plays an important role in the passage through the G1 restriction point when the cell becomes committed to proceed through the cell cycle while cdk2 activation plays an essential role in the transition into S phase and DNA synthesis. Cyclin D1 expression is induced during G1 phase in response to various mitogens, complexes with and activates cdk4 (Morgan, 1995). Cyclin dependent kinase 2 is regulated primarily by cyclin E and cyclin A during G1/S transition and S phase respectively (Sherr and Roberts, 1999, Morgan, 1995, Sherr and Roberts, 1995). Retinoblastoma is the major target for cyclin dependent kinase activity and is phosphorylated by both cyclin D dependent kinases and by cdk2. Hyperphosphorylation of the Rb protein disrupts its association with E2F transcription factors which once released can stimulate the expression of a series of genes required for DNA synthesis (Sherr and Roberts, 1999, Morgan, 1995, Sherr and Roberts, 1995). Cyclin dependent kinase inhibitors further regulate the activity of these

cyclin/cdk complexes p27^{Kip1} and p21^{waf1/cip1} are members of the Cip/Kip family of cdk inhibitors that can affect the activity of cyclin D-, E- and A- dependent kinases through binding of both the cyclin and cdk subunits (Sherr and Roberts, 1999) Taking into consideration the roles of each of these regulatory proteins in cell cycle progression, a mechanism for IL-6 induced growth arrest in H4IIE cells has been proposed (Figure 7 1) IL-6 treatment results in increased p21^{waf1/cip1} and p27^{Kip1} protein expression which can then proceed to bind cyclin-cdk2 and cyclin-cdk4 complexes This results in decreased cdk2 and cdk4 kinase activity which is manifested in reduced Rb phosphorylation This prevents the release of E2F transcription factors required for DNA synthesis and thereby inhibits the exit of these cells from the G0/G1 phase of the cell cycle In order to further clarify the role of p21^{waf1/cip1} and p27^{Kip1} in this process it is recommended that further experimentation be performed While increased p21^{waf1/cip1} and p27^{Kip1} expression has been previously linked to similar G0/G1 growth arrests after IL-6 treatment in other transformed cells, the mechanisms of action may vary (Kortylewski et al , 1999, Klausen et al , 2000, Florenes et al , 1999, Bellido et al , 1998) Immunoprecipitation of p21^{waf1/cip1} and p27^{Kip1} from IL-6 treated H4IIE cell lysates and subsequent immunoblotting for cyclins and cdks would establish the particular cyclin-cdk complexes to which these inhibitors bind Furthermore, through the use of siRNA technology it may be possible to knockdown the expression of these cdk inhibitors and thereby establish the individual contribution of each to this growth arrest Overall, these experiments should provide a greater insight into the interactions of cell cycle regulatory proteins after IL-6 stimulation in HCC

The current study aimed to establish the differences in intracellular signalling pathways activated in normal and malignant hepatocytes The activation of Jak-STAT pathways in normal hepatocytes and HCC cells followed a similar profile However, the ERK activation profile differed in each cell type A characteristic biphasic

(a)



(b)

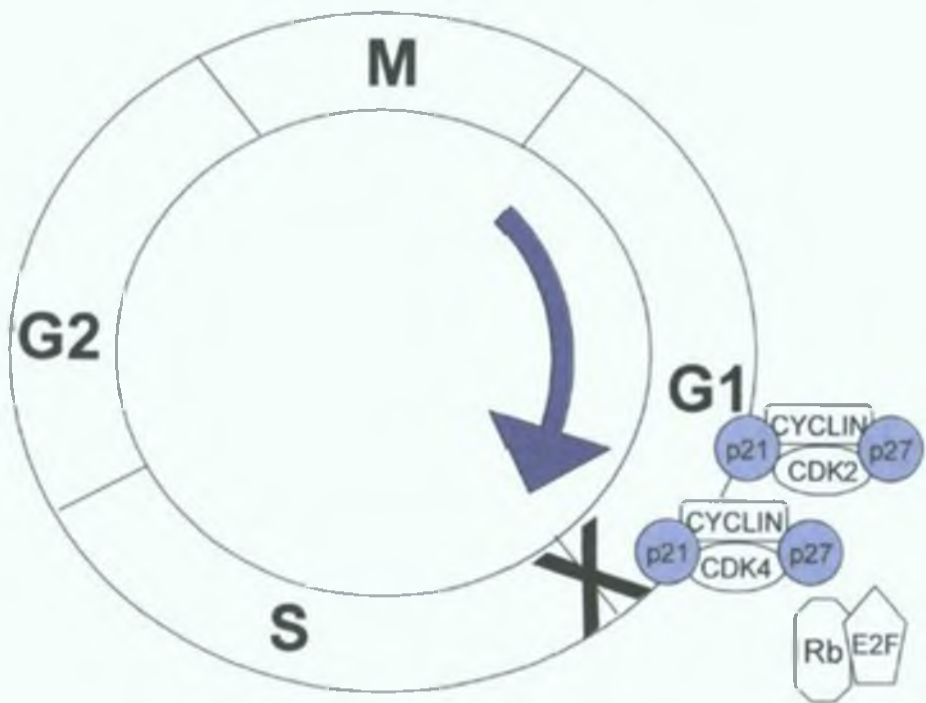


Figure 7.1 Proposed mechanism for IL-6 induced growth arrest in H4IIE cells. a) Passage through the G1 restriction point is controlled by cyclin-cdk complexes which phosphorylate Rb resulting in the release of E2F transcription factors which can then stimulate the expression of genes required for DNA synthesis. b) IL-6 treatment of H4IIE cells results in upregulated expression of p21^{waf1/cip1} and p27^{Kip1} which can then bind and inhibit cyclin-cdk2 and cyclin-cdk4 complexes. Phosphorylation of Rb is reduced preventing the release of E2F transcription factors and blocking entry into the S phase of the cell cycle.

activation of ERK was observed in HCC cells compared to a monophasic activation of ERK in isolated hepatocytes. Taking into consideration that the expression of p21^{waf1/cip1} and p27^{Kip1} following IL-6 treatment was limited to HCC cells it was considered possible that the observed alterations in ERK activation may account for these differences. However, inhibition of the Ras-MAPK pathway in HCC cells did not alter the expression of either p21^{waf1/cip1} or p27^{Kip1}. Pharmacological inhibition of the Jak-STAT pathway did however ablate p21^{waf1/cip1} expression but had no effect on p27^{Kip1} expression. This demonstrates that the altered ERK activation profile in HCC cells was not responsible for the differences in cdk inhibitor expression observed between the normal and malignant cell type. The current studies did not establish the responsible pathway for increased p27^{Kip1} expression after IL-6 treatment in HCC cells. Pharmacological inhibition of the Jak-STAT pathway using AG490 in these cells does not result in complete inhibition of STAT3 activation while transient transfection of a dominant negative STAT3 into H4IIE cells did not alter STAT3 activation. As such it is not possible to completely discount the potential involvement of this pathway in the expression of p27^{Kip1}. Stable transfection of H4IIE cells with dominant negative STAT3 expression vectors may enhance the level of inhibition in the current model. Furthermore, other pathways may be activated by IL-6 treatment in this cell type. STAT3 and MAPK are the primary targets after IL-6 stimulation however STAT5 (Klausen et al, 2000), PI3K (Chen et al, 1999) and STAT1 (Kortylewski et al, 1999) have been shown to be activated in other models. Furthermore, both PI3K and STAT5 have the ability to modulate p27^{Kip1} expression (Klausen et al, 2000, Banerji et al, 2001, Zhu et al, 2003, Barata et al, 2004). The possible involvement of these pathways during IL-6 treatment of H4IIE cells warrants further study.

Taking into consideration that IL-6 is inhibitory on the proliferation of H4IIE cells it is perhaps surprising that H4IIE cells secrete IL-6 and express the components

of the IL-6 receptor. However, IL-6 receptor expression is decreased in this HCC tissue. STAT3 is constitutively activated in these tumours *in vivo*. Furthermore, SOCS-1 is upregulated in HCC while SOCS-3 is downregulated in HCC. These alterations in IL-6 signalling may decrease the responsiveness of HCC cells to IL-6. While the SOCS-1 and SOCS-3 genes are silenced in many malignancies including some human HCCs (Watanabe *et al*, 2004, Yoshikawa *et al*, 2001a, He *et al*, 2003), overexpression has been identified in other tumours and has been linked to cytokine resistance (Raccurt *et al*, 2003, Sakai *et al*, 2002, Tannapfel *et al*, 2003). Downregulated SOCS-3 expression identified in these tumours may account for constitutive STAT3 activity due to inadequate negative regulation of Jak-STAT signalling. Interestingly, the constitutive activation of STAT3 in murine plasmacytomas and hybridomas is associated with the acquisition of an IL-6 independent phenotype (Rawat *et al*, 2000). Despite these changes the cells remain responsive to IL-6 both *in vitro* and *in vivo*.

Alterations in IL-6 signalling components identified in HCC tumours may be due to persistent autocrine stimulation in the tumour cells. H4IIE cells proliferate rapidly in culture despite the presence of endogenous IL-6. Analysis of tumour tissue demonstrates these HCC tumours have increased p21^{waf1/cip1} and p27^{Kip1} expression. IL-6 signalling could be the reason for constitutive STAT3 activation. Downregulation of SOCS-3 expression could function to prolong STAT3 activation during this process. Given that p21^{waf1/cip1} and p27^{Kip1} are downstream targets of IL-6 signalling in H4IIE cells *in vitro*, and that SOCS-1 is also upregulated by IL-6 signalling in other cells, it is possible that IL-6 signalling ultimately results in the observed alterations in expression of these downstream proteins. Indeed, autocrine IL-6 stimulation has been identified as the underlying mechanism for constitutive STAT3 activation in multiple myeloma cells (Bromberg, 2001). IL-6 has also been demonstrated to downregulate gp130 and IL-

6R α expression, adding further support for this potential mechanism of action for IL-6 in HCC (Zohlhofer et al , 1992, Wang et al , 1998) Both p21^{waf1/cip1} and p27^{Kip1} genes contain STAT responsive elements and can be modulated by IL-6 type cytokines (Bellido et al , 1998, Kortylewski et al , 1999, de Koning et al , 2000) however, they are also subject to regulation *via* other factors P21^{waf1/cip1} and p27^{Kip1} are cyclin dependent kinase inhibitors that inhibit G1 associated cyclin complexes such as cdk4/cyclin D and cdk2/Cyclin E and, in doing so, inhibit cell cycle progression At low stoichiometric concentrations p21^{waf1/cip1} and p27^{Kip1} may serve as assembly factors for active cyclin-cdk complexes (LaBaer et al , 1997) and have been implicated as regulators of hepatocyte proliferation in the liver following partial hepatectomy where they determine the rate of progression through the G1 phase of the cell cycle (Albrecht et al , 1998) This evidence implies that the presence or absence of these cdk inhibitors is less important than the relative ratio between them and cyclin-cdk complexes Overexpression of both p21^{waf1/cip1} and p27^{Kip1} has been previously observed in human HCC specimens (Qin and Ng, 2001) Taking into consideration that H4IIE cells proliferate rapidly *in vivo* forming large tumour masses, the increased expression of p21^{waf1/cip1} and p27^{Kip1} does not appear to be inhibitory on their proliferation While p21^{waf1/cip1} and p27^{Kip1} could have a role in cyclin-cdk complex assembly *in vivo*, the treatment of H4IIE cells with IL-6 *in vitro* may result in an imbalance of p21^{waf1/cip1} and p27^{Kip1} expression resulting in the inhibition of cdk-cyclin complexes

These data could also suggest a role for IL-6 as an autocrine negative growth regulator in the current HCC model IL-6 has been demonstrated to be an autocrine growth inhibitor in human meningioma (Todo et al , 1994) and lung cancer cells (Takizawa et al , 1993) In the latter case, the cells have a relatively low IL-6 sensitivity as compared with noncarcinogenic human bronchial epithelial cells suggesting that escape from growth regulation of this inhibitory factor may be involved in lung

oncogenesis. Similarly, H4IIE cells are characterised by decreased IL-6 receptor expression supporting potentially evasive cellular mechanisms from IL-6 growth inhibition. Interestingly, IL-6 does not induce complete inhibition of H4IIE cell proliferation. This raises the possibility that subpopulations of treated H4IIE cells have resistance to IL-6 induced growth arrest. The mechanism by which these cells achieve this resistance to growth inhibition is not completely clear however it may be associated with even further decreases in receptor expression compared to their IL-6 sensitive counterparts. Autocrine negative growth regulation by cytokines in other cancer models has been established. Transforming growth factor- β has growth inhibitory effects on low grade gliomas yet stimulates the growth of high grade gliomas (Jennings et al, 1991). The acquisition of multicytokine resistance during the process of oncogenesis has also been linked to clonal dominance of primary tumours by metastatically competent cells (Lu et al, 1992, Kerbel, 1992, Wu et al, 1992). Interleukin-6 has a similar effect in melanoma cells, acting as a growth inhibitor in early stage melanoma and a growth factor for late stage melanoma (Florenes et al, 1999, Lu et al, 1992, Lu and Kerbel, 1993). In the case of melanoma, as seen with TGF- β , the development of IL-6 resistance coincides with the acquisition of metastatic competence. Overall the proliferation of neoplastic cells is dependent on the interaction and balance between both growth stimulatory and inhibitory factors. During the process of tumour progression, the cells which are most adapted to growth at the primary tumour site and in other foreign environments of the body become the dominant clones of primary tumours (Kerbel, 1992).

Other functions of endogenously produced IL-6 in the current model are possible. Interleukin-6 stimulates the expression of anti-apoptotic proteins (Chen et al, 1999) and has been associated with an increase in metastatic potential (Reichner et al, 1998) in other HCC models. However, IL-6 is associated with multiple roles in the

progression of a variety of other cancers. In addition to its function as a growth regulatory factor in many malignancies (Miki et al , 1989, Nordan et al , 1987, Kawano et al , 1988, Jernberg et al , 1991, Levy et al , 1991, Okuno et al , 1992, Miles et al , 1990, Novick et al , 1992, Chen et al , 1988) IL-6 is involved in the processes of angiogenesis, tumour invasion and the development of multidrug resistance. IL-6 stimulates the expression of vascular endothelial growth factor, a specific mitogen for vascular endothelial cells, demonstrating a role during neo-angiogenesis (Cohen et al , 1996, Dankbar et al , 2000). The expression of matrix metalloproteinases is also modulated by IL-6 in several tumours (Kossakowska et al , 1999, To et al , 2002). These enzymes degrade extracellular matrix components allowing tumour invasion and are associated with clinical aggressiveness of many malignancies (Folgueras et al , 2004). IL-6 mediates an anti-apoptotic effect in many cancer cells including multiple myeloma and has been linked to the development of chemotherapy resistance (Lichtenstein et al , 1995). Furthermore, autocrine production of IL-6 in breast cancer cells stimulates multidrug resistance protein 1 expression and subsequent resistance to chemotherapeutic agents (Conze et al , 2001). In several human cervical carcinoma cell lines IL-6 production is increased while IL-6 receptors are decreased resulting in abrogation of constitutive monocyte chemoattractant protein-1 expression (Hess et al , 2000). This may constitute an immune escape mechanism for the tumour. Overall, it is clear that IL-6 has diverse effects on tumour progression. Further experimentation is required to establish the function of IL-6 in the current model. Inhibition of IL-6 expression by siRNA or antisense in H4IIE cells would allow a better understanding of the progression and tumour formation of these cells both *in vitro* and *in vivo*.

Serum levels of IL-6 are often increased in human HCC patients (Goydos et al , 1998, Giannitrapani et al , 2002) and have been shown to correlate with the stage of HCC progression (Giannitrapani et al , 2002). Furthermore, IL-6 production in human

HCC cells has been linked to the degree of cell differentiation. Interleukin-6 is not constitutively produced by the well differentiated human HCC HepG2 cell line or the moderately differentiated human HCC L17A cell line. However, IL-6 is constitutively synthesised by scarcely differentiated HA22T/VGH human hepatoma cells (Paroli et al, 1993). H4IIE cells are poorly differentiated rat HCC cells which were originally derived from the well differentiated H-35 hepatoma cell line (Evans and Kovacs, 1977). The cytokine expression profile for H-35 cells has not been reported. However, H-35 cell proliferation is inhibited by IL-6 treatment albeit through mechanisms which do not involve increased expression of p21^{waf1/cip1} or p27^{Kip1} (Kim and Baumann, 1999, Lai et al, 1999). The determination of IL-6 expression in H-35 cells would give a greater insight into whether this tumour model correlates with that observed in human HCC in relation to level of differentiation and IL-6 expression. In any case, these data demonstrate the heterogeneity in expression and function of IL-6 in HCC.

In conclusion, IL-6 treatment of H4IIE HCC cells is inhibitory on cell cycle progression *in vitro*. Nevertheless, H4IIE cells secrete IL-6 and express the IL-6 receptor. The effects of autocrine IL-6 stimulation in these cells remain to be determined. The data presented suggests a possible role for IL-6 in autocrine negative growth regulation of H4IIE cells where it could potentially “select” cells with the highest levels of resistance to the growth inhibitory effects of IL-6. Tumour progression is associated with the acquisition of dominance by the most aggressive cell type. In HCC this is further correlated with decreased differentiation. A relationship between the level of differentiation and IL-6 expression in HCC implies that further studies on IL-6 signalling in HCC must incorporate cell types from various stages of HCC progression as the effects may vary. It is tempting to speculate that IL-6 may have different roles in HCC progression at various stages throughout HCC tumour formation. Further studies using rodent tumour models as used in this study will better

the understanding of the role of IL-6 in hepatocarcinogenesis. Ultimately this research should be performed in human HCC cells using the knowledge gained from these models. The complete characterisation of the role of IL-6 in HCC will allow the potential for manipulation of this pathway as a means of therapeutic intervention in HCC.

7.2 Cell Microencapsulation for IL-6 Delivery *In Vivo*

In order to deliver sustained high levels of IL-6 in a rat model of HCC, rhIL-6 expressing CHO cells (CHO-IL6) were encapsulated in sodium alginate and implanted in HCC tumour burdened male ACI rats. CHO cells remained viable and formed large colonies in alginate beads up to 17 days after encapsulation *in vitro*. Encapsulated CHO-IL6 cells retained the ability to secrete rhIL-6. Beads were implanted intraperitoneally in male ACI rats. Viability of encapsulated cells was sustained up to 4 days after implantation resulting in high serum levels of rhIL-6. However, analysis of beads retrieved 7 days after implantation demonstrated complete loss of encapsulated cell viability accompanied by the accumulation of living cells on the outer surface of the beads. Fibrotic overgrowth was observed 4 days after encapsulation however this did not appear to affect cell viability. Empty alginate beads did not stimulate a host response at 4 or 7 days after encapsulation. At 4 days after implantation rhIL-6 was detectable in normal and HCC liver tissues. This resulted in the activation of the Jak-STAT signalling pathway in normal and HCC liver tissues. Analysis of IL-6 receptor expression demonstrated IL-6R α was increased but not significantly in normal liver tissue from CHO-IL6 implanted rats while gp130 expression was not affected by rhIL-6 treatment. Liver weight of CHO-IL6 implanted animals was increased compared to

control animals Tumour volume was highly variable and as a result no conclusions on the effect of rhIL-6 on HCC progression *in vivo* could be determined

Alginate, derived from brown algae, has ideal characteristics for cell encapsulation Alginate forms an extensive gel network on contact with divalent cations allowing encapsulation of cells in the absence of extreme heat or harsh chemicals (Uludag et al , 2000) Furthermore, ultrapure alginates are not immunoreactive allowing safe implantation *in vivo* The principle of microencapsulation is to create a physical semi-permeable barrier between the encapsulated cells and the host immune system This membrane allows diffusion of oxygen and nutrients to the encapsulated cells while preventing contact with host immune cells or large molecules such as immunoglobulins (Uludag et al , 2000) Alginate microencapsulation systems have been used effectively as therapy in many models of disease Most notably alginate encapsulation of xenogeneic and allogeneic pancreatic islets has been used to establish normoglycemia in diabetic rodents (O'Shea and Sun, 1986), dogs (Soon-Shiong et al , 1992), monkeys (Sun et al , 1996) and in a human diabetic patient (Soon-Shiong et al , 1994) In diabetes therapy the alginate membrane allows the free transport of glucose and insulin providing a system that is highly responsive to the host plasma glucose levels Similarly, alginate encapsulated cells have been successfully used to deliver biotherapeutic substances *in vivo* such as Factor IX for haemophilia therapy (Hortelano et al , 1996), parathyroid hormone for the treatment of hypoparathyroidism (Hasse et al , 1997) and dopamine in experimental models of Parkinson's disease (Aebischer et al , 1994)

The aim of the current study was to deliver systemically high levels of rhIL-6 in HCC tumour burdened rats using alginate microencapsulated CHO-IL6 cells This study has established an inhibitory effect of rhIL-6 on H4IIE HCC cell proliferation *in vitro*, as a result the effects of IL-6 administration on HCC tumour progression *in vivo*

were of particular interest Encapsulated CHO-IL6 and CHO-CTRL (mock transfected CHO cells) cells exhibited long term survival and proliferation *in vitro* Implantation of these beads *in vivo* however resulted in complete loss of viability 7 days after implantation Closer examination demonstrated the presence of living cells on the outer surface of these beads Furthermore, fibrotic overgrowth of many beads retrieved 4 and 7 days after implantation was observed Typically macrophages are the main cell type recruited to the bead surface after initiation of the host response resulting from graft disruption of host vasculature or passive antigen shedding from encapsulated cells (Uludag et al , 2000, de Groot et al , 2004) Macrophages secrete cytokines such as interleukin-1 β (IL-1 β), TNF- α and interferon- γ (IFN- γ), nitric oxide (NO) and oxygen radicals which diffuse into the beads resulting in encapsulated cell death (Gray, 2001, Omer et al , 2003, King et al , 2000) Furthermore, fibroblasts migrate to the bead surface and mediate matrix production coupled with a neo-vascularisation response (Uludag et al , 2000) This ultimately leads to ensheathing of the implant in fibrous materials and glycosaminoglycans The fibrotic build up prevents diffusion of oxygen and nutrients to the encapsulated cells and leads to cell necrosis

The microencapsulation system used for rhIL-6 delivery in this study requires optimisation to improve cell viability *in vivo* Ultimately this should involve alterations that minimise the host's foreign body/immune response after implantation Empty alginate beads did not elicit a noticeable host response suggesting that in the current study the presence of encapsulated cells is the most important factor leading to decreased biocompatibility *in vivo* The use of CHO cells for this encapsulation process presents at least two major problems, CHO cells proliferate rapidly in these beads and once implanted in rats constitute a xenograft *in vivo* Examination of CHO-IL6 and CHO-CTRL beads after encapsulation demonstrated that these cells can escape through the walls of the alginate beads The proliferative capacity of these cells is a major factor

leading to cell leakage. Two approaches could potentially be used to remedy this problem. Strengthening of the alginate beads could possibly prevent bead rupture and thereby reduce cell escape. Various methods to enhance the strength of these beads are currently in use including the use of Ba^{2+} as crosslinking cations rather than Ca^{2+} which were used in the current model (Gaumann et al , 2001, Visted et al , 2003, Uludag et al , 2000), poly-L-lysine coating of alginate beads (Thu et al , 1996b, Thu et al , 1996a) and the use of inhomogenous beads in place of the standard homogenous beads used in the current study (Thu et al , 1996b, Thu et al , 1996a, Visted et al , 2003). The second approach is to reduce the proliferative capacity of the encapsulated cells as a method to reduce cell leakage. This can be achieved through the transfection of a multicistronic expression unit for a cell cycle arrest gene and the gene of the product of interest under the control of a regulatory promoter (Fux et al , 2001, Mazur et al , 1999) or through the use of genetically engineered primary cells such as myoblasts that differentiate to a non proliferative state while still expressing the therapeutic protein of interest (Cirone et al , 2002, Garcia-Martin et al , 2002). The use of contact inhibited cells (Ritt et al , 2000, Takahashi and Suzuki, 1996) for encapsulation offers another possible method to minimise bead rupture due to cells with high proliferative capacity. However, this delivery system constitutes a xenograft in rats which is associated with a stronger host response than is typically seen with similar implantation of allografts *in vivo* (de Groot et al , 2004). Virtually every protein shed from xenogeneic cells differs from that of the host. These xenoantigens allow recognition of the xenograft despite the presence of the alginate capsule (Siebers et al , 1999). Prevention of cell shedding as described above will assist in the minimisation of these host responses however, no method exists to prevent antigen shedding from the encapsulated CHO cells. This makes sustained survival of these encapsulated cells difficult to achieve *in vivo*. The use of genetically modified allogeneic rather than xenogeneic cells may assist in overcoming these

problems. Other research suggests the genetic engineering of cells to acquire resistance to deleterious molecules such as cytokines and NO through the forced expression of anti-apoptotic proteins as a method to avoid xenograft rejection (Rabinovitch et al , 1999, Contreras et al , 2001). The potential for co-encapsulation with other cells such as Sertoli cells which are capable of inducing local immuno-suppressive effects has also been proposed to extend graft survival *in vivo* (Yang and Wright, 1999).

Microencapsulated cells have been successfully used to administer anti-cancer agents such as angiostatin, endostatin and iNOS *in vivo* (Read et al , 2001, Cirone et al , 2003, Xu et al , 2002). This method is particularly suited for the delivery of biologically active agents such as cytokines which typically display short plasma half lives and are relatively expensive for continual administration. However, administration of cytokines is often associated with dose limiting toxicities (Fyfe et al , 1995, Rosenberg et al , 1993, Lienard et al , 1992, Atkins et al , 1997). Previous reports demonstrate the potential of systemic IL-6 administration to decrease tumour burden of other cancers *in vivo* in the absence of discernible side effects or toxicity (Eisenthal et al , 1993, Givon et al , 1992, Mule et al , 1992). Human IL-6 administered to mice with transplantable acute myeloid leukaemia (AML) and irradiation/dexamethasone induced AML results in reduced leukaemia development and increased animal survival (Givon et al , 1992). This may be due to direct effects on tumour cells and/or through an enhancement of the host immune system. Recombinant IL-6 administration also reduces the number of established metastases from colon adenocarcinoma and fibrosarcoma tumours *in vivo*, an effect mediated *via* the enhancement of tumour specific CD8⁺ cytotoxic T lymphocyte (CTL) activity (Eisenthal et al , 1993, Mule et al , 1992). Furthermore, IL-6 administration in combination with cyclophosphamide, a chemotherapeutic agent, ameliorates the majority of C57BL/6 mice with advanced, 10 day subcutaneous or pulmonary sarcoma tumour nodules (Mule et al , 1992). The effect

of systemic administration of IL-6 on HCC progression in the current model is unclear. Tumour size was highly variable making it difficult to ascertain the effects due to IL-6 alone. It was clear that biologically active IL-6 was released *in vivo* up to 4 days after implantation resulting in activation of the Jak-STAT pathway in both normal and tumour liver tissues. This data indicates that H4IIE tumour cells respond to IL-6 *in vivo* despite decreased receptor expression. While the IL-6 receptors are downregulated in HCC tissue compared to normal liver, the cells do express the receptor and hence can retain responsiveness to IL-6. Cell cycle analysis using propidium iodide staining and subsequent FACS analysis on IL-6 treated tumour tissue may help to determine the effects of IL-6 on cell cycle progression *in vivo*. It is worth noting that IL-6 treatment of H4IIE cells *in vitro* does not result in complete inhibition of proliferation. Subpopulations of H4IIE cells do appear to be resistant to IL-6 induced growth arrest which may become a relevant factor *in vivo*. Furthermore, the *in vivo* environment is complex comprising multiple cell types and the presence of multiple cytokines and growth regulatory agents. The interplay between IL-6 signalling and other growth regulatory pathways will need to be established *in order to ascertain the full effects of* IL-6 treatment on HCC. For example, IL-6 has been shown to inhibit transforming growth factor- β (TGF- β) induced apoptosis in hepatoma cells (Chen et al, 1999) while TGF- β can augment IL-6 induced STAT3 activity in HCC cells (Yamamoto et al, 2001). Investigation using H4IIE cells implanted subcutaneously would provide an easier method to measure tumour volume during IL-6 treatment and should have higher reproducibility due in part to a less complex cytokine profile associated with this environment. However, this will be less physiologically relevant. Ultimately, the use of microencapsulated cells to deliver IL-6 as a potential therapeutic in HCC appears difficult to regulate and may be associated with complications due to HCC cell resistance and the complex HCC environment.

Administration of high sustained levels of rhIL-6 in a nude mouse model using CHO-IL6 tumours results in massive hepatomegaly and liver growth in the absence of liver injury (Zimmers et al , 2003) Plasma levels of rhIL-6 were elevated in these mice to 80ng/mL This increase in liver growth did not involve other growth factors such as epidermal growth factor or hepatocyte growth factor and was the first demonstration of IL-6 acting as a complete mitogen for liver growth This effect was accompanied by an increase in STAT3 and ERK 2 activity in addition to increased PCNA and IL-6R α expression in liver tissues These effects have not yet been demonstrated in an immune competent animal In the current study a significant increase in liver weight which could not be accounted for by tumour volume was observed in rhIL-6 treated animals compared to controls It is worth noting that PCNA expression was elevated in normal liver tissues from two of the four animals treated with IL-6 in the current study Furthermore IL-6R α expression was elevated but not significantly in all of the CHO-IL6 implanted rat normal liver tissues compared to control animals This data correlates with events in the nude mouse model (Zimmers et al , 2003) and is suggestive of similar phenomena in immune competent animals during sustained rhIL-6 delivery Taking into consideration the variability associated with the *in vivo* environment, these preliminary results demonstrating the effects of rhIL-6 on normal liver and HCC growth do not incorporate a sufficient sample size to draw clear conclusions However, these initial findings suggest the use of encapsulated cells as an ideal method to study the effects of sustained high levels of rhIL-6 on normal liver growth Moreover, the highest levels of liver growth during rhIL-6 treatment were observed between 8 and 16 days after inoculation with CHO-IL6 cells in nude mice, as a result it is necessary to extend the survival of encapsulated CHO cells greater than 4 days to fully establish the effects of rhIL-6 on normal liver growth in the current model Furthermore, rat plasma levels of rhIL-6 in the current model reached approximately 1 25ng/mL This is less

than levels used in the nude mouse study. Implantation of encapsulated CHO-IL6 in immune competent mice instead of rats should allow greater levels of circulating rhIL-6 *in vivo*.

In conclusion, alginate beads can sustain the growth of encapsulated CHO cells *in vitro*. This system to administer rhIL-6 requires further optimisation to sustain cell viability *in vivo*. This should include methods to reduce cell proliferative capacity, strengthening of the bead structure and the use of allogeneic cells. Overall, this system may have limited application in HCC therapy however may prove useful for the study of normal liver and HCC tumour growth *in vivo*.

References

- Aebischer, P., Goddard, M , Signore, A. P and Timpson, R L. (1994) Functional recovery in hemiparkinsonian primates transplanted with polymer-encapsulated PC12 cells *Experimental Neurology*, 126(2), 151-8.
- Aguayo, A and Patt, Y. Z. (2001) Nonsurgical treatment of hepatocellular carcinoma *Clinics in Liver Disease*, 5(1), 175-89
- Albrecht, J H and Hansen, L K (1999) Cyclin D1 promotes mitogen-independent cell cycle progression in hepatocytes *Cell Growth & Differentiation*, 10(6), 397-404
- Albrecht, J H , Poon, R. Y , Ahonen, C L , Rieland, B M , Deng, C. and Crary, G S. (1998) Involvement of p21 and p27 in the regulation of CDK activity and cell cycle progression in the regenerating liver *Oncogene*, 16(16), 2141-50
- Andus, T., Geiger, T., Hirano, T., Northoff, H , Ganter, U , Bauer, J , Kishimoto, T and Heinrich, P C (1987) Recombinant human B cell stimulatory factor 2 (BSF-2/IFN-beta 2) regulates beta-fibrinogen and albumin mRNA levels in Fao-9 cells *FEBS Letters*, 221(1), 18-22
- Arakawa, M , Kage, M , Sugihara, S , Nakashima, T., Suenaga, M and Okuda, K. (1986) Emergence of malignant lesions within an adenomatous hyperplastic nodule in a cirrhotic liver Observations in five cases *Gastroenterology*, 91(1), 198-208
- Atkins, M B , Robertson, M J , Gordon, M , Lotze, M T , DeCoste, M., DuBois, J S , Ritz, J , Sandler, A B , Edington, H. D , Garzone, P. D., et al (1997) Phase I evaluation of intravenous recombinant human interleukin 12 in patients with advanced malignancies. *Clinical Cancer Research*, 3(3), 409-17.
- Banerji, L , Glassford, J , Lea, N C , Thomas, N S , Klaus, G G and Lam, E W (2001) BCR signals target p27(Kip1) and cyclin D2 via the PI3-K signalling pathway to mediate cell cycle arrest and apoptosis of WEHI 231 B cells *Oncogene*, 20(50), 7352-67
- Barata, J T , Silva, A , Brandao, J G , Nadler, L M., Cardoso, A A and Boussiotis, V. A. (2004) Activation of PI3K is indispensable for interleukin 7-mediated viability, proliferation, glucose use, and growth of T cell acute lymphoblastic leukemia cells. *Journal of Experimental Medicine*, 200(5), 659-69.
- Barut, B., Chauhan, D., Uchiyama, H and Anderson, K C. (1993) Interleukin-6 functions as an intracellular growth factor in hairy cell leukemia in vitro. *Journal of Clinical Investigation*, 92(5), 2346-52.

Beasley, R P , Hwang, L. Y., Lin, C C and Chien, C S. (1981) Hepatocellular carcinoma and hepatitis B virus. A prospective study of 22 707 men in Taiwan *Lancet*, 2(8256), 1129-33.

Belhdo, T., O'Brien, C A , Roberson, P. K. and Manolagas, S. C. (1998) Transcriptional activation of the p21(WAF1,CIP1,SDI1) gene by interleukin-6 type cytokines A prerequisite for their pro-differentiating and anti-apoptotic effects on human osteoblastic cells *Journal of Biological Chemistry*, 273(33), 21137-44

Bergsland, E K and Venook, A P (2000) Hepatocellular carcinoma *Current Opinion in Oncology*, 12(4), 357-61

Bonta, I. L and Ben-Efraim, S (1993) Involvement of inflammatory mediators in macrophage antitumor activity *Journal of Leukocyte Biology*, 54(6), 613-26

Bosch, F X , Ribes, J. and Borrás, J (1999) Epidemiology of primary liver cancer. *Seminars in Liver Disease*, 19(3), 271-85.

Bottazzi, M. E., Zhu, X , Bohmer, R M. and Assoian, R K (1999) Regulation of p21(cip1) expression by growth factors and the extracellular matrix reveals a role for transient ERK activity in G1 phase *Journal of Cell Biology*, 146(6), 1255-64

Bowman, T , Garcia, R , Turkson, J. and Jove, R (2000) STATs in oncogenesis *Oncogene*, 19(21), 2474-88

Brandt, S J., Bodine, D M., Dunbar, C E and Nienhuis, A W (1990) Dysregulated interleukin 6 expression produces a syndrome resembling Castleman's disease in mice *Journal of Clinical Investigation*, 86(2), 592-9.

Breborowicz, J , Mackiewicz, A. and Breborowicz, D (1981) Microheterogeneity of alpha-fetoprotein in patient serum as demonstrated by lectin affinity-electrophoresis *Scandinavian Journal of Immunology*, 14(1), 15-20.

Bromberg, J and Chen, X (2001) STAT proteins: signal transducers and activators of transcription *Methods Enzymol*, 333:138-51

Bromberg, J F. (2001) Activation of STAT proteins and growth control *Bioessays*, 23(2), 161-9

Bromberg, J F , Horvath, C. M., Besser, D , Lathem, W. W. and Darnell, J E , Jr (1998) Stat3 activation is required for cellular transformation by v-src *Molecular & Cellular Biology*, 18(5), 2553-8

Bromberg, J F., Wrzeszczynska, M. H , Deygan, G , Zhao, Y , Pestell, R G., Albanese, C and Darnell, J E , Jr (1999) Stat3 as an oncogene *Cell*, 98(3), 295-303

Bruix, J. and Llovet, J. M (2002) Prognostic prediction and treatment strategy in hepatocellular carcinoma. *Hepatology*, 35(3), 519-24

- Bruix, J , Sherman, M., Llovet, J M., Beaugrand, M., Lencioni, R , Burroughs, A. K , Christensen, E , Pagliaro, L , Colombo, M., Rodes, J., et al (2001) Clinical management of hepatocellular carcinoma. Conclusions of the Barcelona-2000 EASL conference. European Association for the Study of the Liver *Journal of Hepatology*, 35(3), 421-30.
- Buetow, K H , Sheffield, V C , Zhu, M., Zhou, T , Shen, F M , Hino, O , Smith, M , McMahon, B J , Lanier, A. P , London, W. T , et al. (1992) Low frequency of p53 mutations observed in a diverse collection of primary hepatocellular carcinomas *Proceedings of the National Academy of Sciences of the United States of America*, 89(20), 9622-6
- Burger, R , Neipel, F., Fleckenstein, B , Savino, R., Ciliberto, G., Kalden, J R. and Gramatzki, M. (1998) Human herpesvirus type 8 interleukin-6 homologue is functionally active on human myeloma cells *Blood*, 91(6), 1858-63
- Cadoret, A , Ovejero, C , Saadi-Kheddouci, S., Souil, E , Fabre, M , Romagnolo, B , Kahn, A and Perret, C (2001) Hepatomegaly in transgenic mice expressing an oncogenic form of beta-catenin *Cancer Research*, 61(8), 3245-9
- Calvisi, D F , Factor, V M , Loi, R. and Thorgeirsson, S S. (2001) Activation of beta-catenin during hepatocarcinogenesis in transgenic mouse models relationship to phenotype and tumor grade. *Cancer Research*, 61(5), 2085-91.
- Camargo, C A., Jr., Madden, J. F., Gao, W , Selvan, R S. and Clavien, P. A (1997) Interleukin-6 protects liver against warm ischemia/reperfusion injury and promotes hepatocyte proliferation in the rodent *Hepatology*, 26(6), 1513-20
- Castell, J , Klapproth, J , Gross, V., Walter, E , Andus, T , Snyers, L , Content, J. and Heinrich, P. C. (1990a) Fate of interleukin-6 in the rat. Involvement of skin in its catabolism *European Journal of Biochemistry*, 189(1), 113-8
- Castell, J V , Geiger, T., Gross, V , Andus, T., Walter, E , Hirano, T , Kishimoto, T and Heinrich, P C. (1988) Plasma clearance, organ distribution and target cells of interleukin-6/hepatocyte-stimulating factor in the rat. *European Journal of Biochemistry*, 177(2), 357-61
- Castell, J V., Gomez-Lechon, M. J., David, M., Fabra, R., Trullenque, R and Heinrich, P. C (1990b) Acute-phase response of human hepatocytes regulation of acute-phase protein synthesis by interleukin-6 *Hepatology*, 12(5), 1179-86
- Catlett-Falcone, R., Landowski, T H., Oshiro, M M., Turkson, J , Levitzki, A , Savino, R., Ciliberto, G., Moscinski, L., Fernandez-Luna, J L., Nunez, G., et al (1999) Constitutive activation of Stat3 signaling confers resistance to apoptosis in human U266 myeloma cells *Immunity*, 10(1), 105-15
- Chang, L and Karin, M. (2001) Mammalian MAP kinase signalling cascades. *Nature*, 410(6824), 37-40.

- Chang, M H., Chen, C J , Lai, M S , Hsu, H M , Wu, T C , Kong, M S , Liang, D C , Shau, W Y and Chen, D S (1997) Universal hepatitis B vaccination in Taiwan and the incidence of hepatocellular carcinoma in children Taiwan Childhood Hepatoma Study Group *New England Journal of Medicine*, 336(26), 1855-9
- Chaubert, P , Gayer, R , Zimmermann, A , Fontollet, C., Stamm, B., Bosman, F and Shaw, P (1997) Germ-line mutations of the p16INK4(MTS1) gene occur in a subset of patients with hepatocellular carcinoma. *Hepatology*, 25(6), 1376-81.
- Chen, L , Mory, Y , Zilberstein, A and Revel, M. (1988) Growth inhibition of human breast carcinoma and leukemia/lymphoma cell lines by recombinant interferon-beta 2 *Proceedings of the National Academy of Sciences of the United States of America*, 85(21), 8037-41
- Chen, R H , Chang, M C , Su, Y. H., Tsai, Y T. and Kuo, M L (1999) Interleukin-6 inhibits transforming growth factor-beta-induced apoptosis through the phosphatidylinositol 3-kinase/Akt and signal transducers and activators of transcription 3 pathways *Journal of Biological Chemistry*, 274(33), 23013-9
- Chiu, C P and Lee, F (1989) IL-6 is a differentiation factor for M1 and WEHI-3B myeloid leukemic cells *Journal of Immunology*, 142(6), 1909-15
- Chung, C. D , Liao, J , Liu, B , Rao, X., Jay, P., Berta, P and Shuai, K. (1997) Specific inhibition of Stat3 signal transduction by PIAS3 *Science*, 278(5344), 1803-5
- Cichy, J , Rose-John, S , Pryjma, J. and Travis, J. (1996) Effect of soluble interleukin-6 receptor on interleukin-6 synthesis in human skin fibroblasts *Biochemical & Biophysical Research Communications*, 227(2), 318-21
- Cirone, P , Bourgeois, J M , Austin, R C. and Chang, P. L. (2002) A novel approach to tumor suppression with microencapsulated recombinant cells. *Human Gene Therapy*, 13(10), 1157-66
- Cirone, P , Bourgeois, J M and Chang, P. L. (2003) Antiangiogenic cancer therapy with microencapsulated cells *Human Gene Therapy*, 14(11), 1065-77
- Clavien, P A , Camargo, C A , Jr , Gorczynski, R , Washington, M K , Levy, G A , Langer, B and Greig, P D (1996) Acute reactant cytokines and neutrophil adhesion after warm ischemia in cirrhotic and noncirrhotic human livers *Hepatology*, 23(6), 1456-63
- Cohen, T , Nahari, D , Cerem, L W., Neufeld, G and Levi, B Z (1996) Interleukin 6 induces the expression of vascular endothelial growth factor *Journal of Biological Chemistry*, 271(2), 736-41.
- Contreras, J L., Bilbao, G , Smyth, C , Eckhoff, D E , Xiang, X L , Jenkins, S , Cartner, S , Curiel, D T , Thomas, F T and Thomas, J M (2001) Gene transfer of the Bcl-2 gene confers cytoprotection to isolated adult porcine pancreatic islets exposed to xenoreactive antibodies and complement *Surgery*, 130(2), 166-74

- Conze, D., Weiss, L , Regen, P. S , Bhushan, A , Weaver, D , Johnson, P and Rincon, M (2001) Autocrine production of interleukin 6 causes multidrug resistance in breast cancer cells *Cancer Research*, 61(24), 8851-8
- Cook, S J and McCormick, F (1996) Kinetic and biochemical correlation between sustained p44ERK1 (44 kDa extracellular signal-regulated kinase 1) activation and lysophosphatidic acid-stimulated DNA synthesis in Rat-1 cells. *Biochemical Journal*, 320(Pt 1), 237-45
- Cressman, D. E., Diamond, R H and Taub, R (1995) Rapid activation of the Stat3 transcription complex in liver regeneration *Hepatology*, 21(5), 1443-9.
- Cressman, D. E., Greenbaum, L E., DeAngelis, R. A., Ciliberto, G., Furth, E E , Poli, V and Taub, R. (1996) Liver failure and defective hepatocyte regeneration in interleukin-6-deficient mice *Science*, 274(5291), 1379-83
- Crocker, B A., Krebs, D L , Zhang, J G , Wormald, S., Willson, T A., Stanley, E. G , Robb, L , Greenhalgh, C J., Forster, I , Clausen, B E., et al (2003) SOCS3 negatively regulates IL-6 signaling in vivo *Nature Immunology*, 4(6), 540-5
- Dankbar, B , Padro, T., Leo, R , Feldmann, B , Kropff, M , Mesters, R M , Serve, H , Berdel, W E and Kienast, J. (2000) Vascular endothelial growth factor and interleukin-6 in paracrine tumor-stromal cell interactions in multiple myeloma *Blood*, 95(8), 2630-6.
- Day, C P (1996) Is necroinflammation a prerequisite for fibrogenesis? *Hepato-Gastroenterology*, 43(7), 104-20
- de Groot, M., Schuurs, T. A. and van Schilfgaarde, R (2004) Causes of limited survival of microencapsulated pancreatic islet grafts. *Journal of Surgical Research*, 121(1), 141-50
- de Koning, J P , Soede-Bobok, A A., Ward, A. C , Schelen, A M , Antonissen, C , van Leeuwen, D , Lowenberg, B and Touw, I P (2000) STAT3-mediated differentiation and survival of myeloid cells in response to granulocyte colony-stimulating factor role for the cyclin-dependent kinase inhibitor p27(Kip1) *Oncogene*, 19(29), 3290-8
- De Vos, P , De Haan, B , Wolters, G H and Van Schilfgaarde, R (1996) Factors influencing the adequacy of microencapsulation of rat pancreatic islets *Transplantation*, 62(7), 888-93
- De Vos, P., De Haan, B J., Wolters, G H , Strubbe, J H and Van Schilfgaarde, R (1997) Improved biocompatibility but limited graft survival after purification of alginate for microencapsulation of pancreatic islets. *Diabetologia*, 40(3), 262-70.
- De Vos, P , Wolters, G H., Fritschy, W M. and Van Schilfgaarde, R (1993) Obstacles in the application of microencapsulation in islet transplantation *International Journal of Artificial Organs*, 16(4), 205-12.
- Di Maio, M., De Maio, E , Perrone, F , Pignata, S and Daniele, B (2002) Hepatocellular carcinoma systemic treatments *Journal of Clinical Gastroenterology*, 35(5 Suppl 2), S109-14

- Dittrich, E., Rose-John, S , Gerhartz, C , Mullberg, J , Stoyan, T , Yasukawa, K , Heinrich, P C and Graeve, L (1994) Identification of a region within the cytoplasmic domain of the interleukin-6 (IL-6) signal transducer gp130 important for ligand-induced endocytosis of the IL-6 receptor. *Journal of Biological Chemistry*, 269(29), 19014-20.
- Dixon, B. S , Evanoff, D , Fang, W B. and Dennis, M J (2002) Bradykinin B1 receptor blocks PDGF-induced mitogenesis by prolonging ERK activation and increasing p27Kip1. *American Journal of Physiology - Cell Physiology*, 283(1), C193-203
- Dougherty, G J , Thacker, J D , Lavey, R S , Beldegrun, A and McBride, W H (1994) Inhibitory effect of locally produced and exogenous interleukin-6 on tumor growth in vivo *Cancer Immunology & Immunotherapy*, 38(5), 339-45
- Edamoto, Y , Hara, A , Biernat, W , Terracciano, L , Cathomas, G , Riehle, H M , Matsuda, M , Fujii, H , Scoazec, J Y and Ohgaki, H (2003) Alterations of RB1, p53 and Wnt pathways in hepatocellular carcinomas associated with hepatitis C, hepatitis B and alcoholic liver cirrhosis. *International Journal of Cancer*, 106(3), 334-41
- Eisenthal, A., Kashtan, H., Rabau, M., Ramakrishna, V., Chaitchik, S. and Skornick, Y. (1993) Antitumor effects of recombinant interleukin-6 expressed in eukaryotic cells *Cancer Immunology, Immunotherapy*, 36(2), 101-7.
- el-Serag, H. B (2001) Epidemiology of hepatocellular carcinoma *Clinics in Liver Disease*, 5(1), 87-107
- Endo, T A , Masuhara, M , Yokouchi, M , Suzuki, R., Sakamoto, H , Mitsui, K , Matsumoto, A , Tanimura, S., Ohtsubo, M , Misawa, H , et al (1997) A new protein containing an SH2 domain that inhibits JAK kinases. *Nature*, 387(6636), 921-4.
- Ernst, M., Inglese, M , Waring, P , Campbell, I K , Bao, S , Clay, F J , Alexander, W S , Wicks, I P , Tarlinton, D M , Novak, U , et al (2001) Defective gp130-mediated signal transducer and activator of transcription (STAT) signaling results in degenerative joint disease, gastrointestinal ulceration, and failure of uterine implantation. *Journal of Experimental Medicine*, 194(2), 189-203
- Evans, M. J. and Kovacs, C J (1977) Properties of the H-4-II-E tumor cell system. I Growth and cell proliferation kinetics of an experimental hepatoma. *Cell and Tissue Kinetics*, 10(3), 233-43
- Fattori, E , Cappelletti, M , Costa, P., Sellitto, C., Cantoni, L., Carelli, M., Faggioni, R , Fantuzzi, G., Ghezzi, P and Poli, V. (1994) Defective inflammatory response in interleukin 6-deficient mice *Journal of Experimental Medicine*, 180(4), 1243-50
- Fausto, N. (2000) Liver regeneration. *Journal of Hepatology*, 32(1 Suppl), 19-31.
- Feitelson, M A , Sun, B , Satiroglu Tufan, N L , Liu, J , Pan, J and Lian, Z (2002) Genetic mechanisms of hepatocarcinogenesis *Oncogene*, 21(16), 2593-604

- Feng, J , Witthuhn, B A., Matsuda, T., Kohlhuber, F , Kerr, I M and Ihle, J. N (1997) Activation of Jak2 catalytic activity requires phosphorylation of Y1007 in the kinase activation loop *Molecular & Cellular Biology*, 17(5), 2497-501
- Florenes, V. A., Lu, C , Bhattacharya, N , Rak, J , Sheehan, C , Slingerland, J M. and Kerbel, R S. (1999) Interleukin-6 dependent induction of the cyclin dependent kinase inhibitor p21WAF1/CIP1 is lost during progression of human malignant melanoma *Oncogene*, 18(4), 1023-32
- Folgueras, A. R , Pendas, A M., Sanchez, L. M and Lopez-Otin, C (2004) Matrix metalloproteinases in cancer: from new functions to improved inhibition strategies *International Journal of Developmental Biology*, 48(5-6), 411-24
- Forns, X , Bukh, J and Purcell, R. H (2002) The challenge of developing a vaccine against hepatitis C virus. *Journal of Hepatology*, 37(5), 684-95.
- Fukada, T , Hibi, M., Yamanaka, Y , Takahashi-Tezuka, M , Fujitani, Y , Yamaguchi, T , Nakajima, K and Hirano, T (1996) Two signals are necessary for cell proliferation induced by a cytokine receptor gp130 involvement of STAT3 in anti-apoptosis *Immunity*, 5(5), 449-60
- Fux, C , Moser, S , Schlatter, S., Rimann, M., Bailey, J. E and Fussenegger, M (2001) Streptogramin- and tetracycline-responsive dual regulated expression of p27(Kip1) sense and antisense enables positive and negative growth control of Chinese hamster ovary cells. *Nucleic Acids Research*, 29(4), E19
- Fyfe, G , Fisher, R I , Rosenberg, S A , Sznol, M , Parkinson, D R and Louie, A C (1995) Results of treatment of 255 patients with metastatic renal cell carcinoma who received high-dose recombinant interleukin-2 therapy. *Journal of Clinical Oncology*, 13(3), 688-96.
- Gaillard, J P , Bataille, R , Brailly, H , Zuber, C., Yasukawa, K , Attal, M , Maruo, N , Taga, T , Kishimoto, T and Klein, B (1993) Increased and highly stable levels of functional soluble interleukin-6 receptor in sera of patients with monoclonal gammopathy. *European Journal of Immunology*, 23(4), 820-4.
- Gajewski, T. F., Renauld, J C , Van Pel, A and Boon, T (1995) Costimulation with B7-1, IL-6, and IL-12 is sufficient for primary generation of murine antitumor cytolytic T lymphocytes in vitro. *Journal of Immunology*, 154(11), 5637-48.
- Galun, E and Axelrod, J H. (2002) The role of cytokines in liver failure and regeneration potential new molecular therapies. *Biochimica et Biophysica Acta*, 1592(3), 345-58
- Ganapathi, M. K , Weizer, A K , Borsellino, S , Bukowski, R M , Ganapathi, R., Rice, T , Casey, G and Kawamura, K (1996) Resistance to interleukin 6 in human non-small cell lung carcinoma cell lines role of receptor components *Cell Growth & Differentiation*, 7(7), 923-9.

- Garcia-Martin, C , Chuah, M K , Van Damme, A , Robinson, K E., Vanzielegheem, B , Saint-Remy, J M , Gallardo, D , Ofosu, F A , Vandendriessche, T and Hortelano, G (2002) Therapeutic levels of human factor VIII in mice implanted with encapsulated cells potential for gene therapy of haemophilia A *Journal of Gene Medicine*, 4(2), 215-23
- Gauldie, J , Richards, C , Harnish, D , Lansdorp, P and Baumann, H (1987) Interferon beta 2/B-cell stimulatory factor type 2 shares identity with monocyte-derived hepatocyte-stimulating factor and regulates the major acute phase protein response in liver cells. *Proceedings of the National Academy of Sciences of the United States of America*, 84(20), 7251-5
- Gaumann, A., Laudes, M , Jacob, B , Pommersheim, R , Laue, C., Vogt, W and Schrezenmeir, J. (2001) Xenotransplantation of parathyroids in rats using barium-alginate and polyacrylic acid multilayer microcapsules *Experimental & Toxicologic Pathology*, 53(1), 35-43
- Gerhartz, C , Heesel, B., Sasse, J., Hemmann, U , Landgraf, C , Schneider-Mergener, J., Horn, F , Heinrich, P. C and Graeve, L (1996) Differential activation of acute phase response factor/STAT3 and STAT1 via the cytoplasmic domain of the interleukin 6 signal transducer gp130 I Definition of a novel phosphotyrosine motif mediating STAT1 activation *Journal of Biological Chemistry*, 271(22), 12991-8
- Ghosh, A K , Steele, R., Meyer, K , Ray, R. and Ray, R B (1999) Hepatitis C virus NS5A protein modulates cell cycle regulatory genes and promotes cell growth. *Journal of General Virology*, 80(Pt 5), 1179-83
- Giannitrapani, L , Cervello, M , Soresi, M , Notarbartolo, M , La Rosa, M , VIRRUSO, L , D'Alessandro, N and Montalto, G (2002) Circulating IL-6 and sIL-6R in patients with hepatocellular carcinoma. *Annals of the New York Academy of Sciences*, 96346-52
- Girasole, G , Jilka, R L , Passeri, G , Boswell, S., Boder, G , Williams, D C and Manolagas, S C (1992) 17 beta-estradiol inhibits interleukin-6 production by bone marrow-derived stromal cells and osteoblasts in vitro a potential mechanism for the antiosteoporotic effect of estrogens *Journal of Clinical Investigation*, 89(3), 883-91
- Givon, T., Slavin, S., Haran-Ghera, N , Michalevycz, R. and Revel, M. (1992) Antitumor effects of human recombinant interleukin-6 on acute myeloid leukemia in mice and in cell cultures *Blood*, 79(9), 2392-8
- Goydos, J S , Brumfield, A M., Frezza, E., Booth, A , Lotze, M T and Carty, S. E (1998) Marked elevation of serum interleukin-6 in patients with cholangiocarcinoma validation of utility as a clinical marker *Annals of Surgery*, 227(3), 398-404
- Gray, D W. (2001) An overview of the immune system with specific reference to membrane encapsulation and islet transplantation *Annals of the New York Academy of Sciences*, 944226-39

- Grossman, R M , Krueger, J , Yourish, D , Granelli-Piperno, A , Murphy, D. P., May, L T , Kupper, T S , Sehgal, P. B and Gottlieb, A B (1989) Interleukin 6 is expressed in high levels in psoriatic skin and stimulates proliferation of cultured human keratinocytes. *Proceedings of the National Academy of Sciences of the United States of America*, 86(16), 6367-71
- Group , C M L T C (1997) Interferon alfa versus chemotherapy for chronic myeloid leukemia a meta-analysis of seven randomized trials Chronic Myeloid Leukemia Trialists' Collaborative Group *Journal of the National Cancer Institute*, 89(21), 1616-20.
- Hakovirta, H., Syed, V., Jegou, B and Parvinen, M (1995) Function of interleukin-6 as an inhibitor of meiotic DNA synthesis in the rat seminiferous epithelium. *Molecular & Cellular Endocrinology*, 108(1-2), 193-8
- Hasmall, S C , West, D. A., Olsen, K and Roberts, R A (2000) Role of hepatic non-parenchymal cells in the response of rat hepatocytes to the peroxisome proliferator nafenopin m vitro. *Carcinogenesis*, 21(12), 2159-65.
- Hasse, C , Zielke, A., Klock, G , Schlosser, A , Zimmermann, U and Rothmund, M (1997) Isotransplantation of microencapsulated parathyroid tissue in rats *Experimental & Clinical Endocrinology & Diabetes*, 105(1), 53-6
- Hayashi, J , Aoki, H , Kajino, K., Moriyama, M , Arakawa, Y and Hino, O (2000) Hepatitis C virus core protein activates the MAPK/ERK cascade synergistically with tumor promoter TPA, but not with epidermal growth factor or transforming growth factor alpha *Hepatology*, 32(5), 958-61.
- He, B , You, L , Uematsu, K , Zang, K , Xu, Z , Lee, A Y., Costello, J F , McCormick, F and Jablons, D M (2003) SOCS-3 is frequently silenced by hypermethylation and suppresses cell growth in human lung cancer *Proceedings of the National Academy of Sciences of the United States of America*, 100(24), 14133-8
- Heinrich, P C , Behrmann, I , Muller-Newen, G , Schaper, F and Graeve, L. (1998) Interleukin-6-type cytokine signalling through the gp130/Jak/STAT pathway. *Biochemical Journal*, 334(Pt 2), 297-314
- Hess, S., Smola, H., Sandaradura De Silva, U., Hadaschik, D , Kube, D , Baldus, S E , Flucke, U. and Pfister, H (2000) Loss of IL-6 receptor expression in cervical carcinoma cells inhibits autocrine IL-6 stimulation. abrogation of constitutive monocyte chemoattractant protein-1 production *Journal of Immunology*, 165(4), 1939-48.
- Hibi, M., Murakami, M , Saito, M , Hirano, T , Taga, T and Kishimoto, T. (1990) Molecular cloning and expression of an IL-6 signal transducer, gp130 *Cell*, 63(6), 1149-57
- Hill, R J., Warren, M. K., Stenberg, P., Levin, J., Corash, L , Drummond, R , Baker, G , Levin, F. and Mok, Y. (1991) Stimulation of megakaryocytopoiesis in mice by human recombinant interleukin-6 *Blood*, 77(1), 42-8

Hirano, T., Yasukawa, K., Harada, H., Taga, T., Watanabe, Y., Matsuda, T., Kashiwamura, S., Nakajima, K., Koyama, K., Iwamatsu, A., et al. (1986) Complementary DNA for a novel human interleukin (BSF-2) that induces B lymphocytes to produce immunoglobulin. *Nature*, 324(6092), 73-6.

Holgado-Madruga, M., Emlet, D. R., Moscatello, D. K., Godwin, A. K. and Wong, A. J. (1996) A Grb2-associated docking protein in EGF- and insulin-receptor signalling. *Nature*, 379(6565), 560-4.

Honda, M., Yamamoto, S., Cheng, M., Yasukawa, K., Suzuki, H., Saito, T., Osugi, Y., Tokunaga, T. and Kishimoto, T. (1992) Human soluble IL-6 receptor: its detection and enhanced release by HIV infection. *Journal of Immunology*, 148(7), 2175-80.

Hortelano, G., Al-Hendy, A., Ofosu, F. A. and Chang, P. L. (1996) Delivery of human factor IX in mice by encapsulated recombinant myoblasts: a novel approach towards allogeneic gene therapy of hemophilia B. *Blood*, 87(12), 5095-103.

Huo, T. I., Wang, X. W., Forgues, M., Wu, C. G., Spillare, E. A., Giannini, C., Brechot, C. and Harris, C. C. (2001) Hepatitis B virus X mutants derived from human hepatocellular carcinoma retain the ability to abrogate p53-induced apoptosis. *Oncogene*, 20(28), 3620-8.

Ihara, S., Nakajima, K., Fukada, T., Hibi, M., Nagata, S., Hirano, T. and Fukui, Y. (1997) Dual control of neurite outgrowth by STAT3 and MAP kinase in PC12 cells stimulated with interleukin-6. *EMBO Journal*, 16(17), 5345-52.

Ikeda, K., Saitoh, S., Kobayashi, M., Suzuki, Y., Suzuki, F., Tsubota, A., Arase, Y., Murashima, N., Chayama, K. and Kumada, H. (2001) Long-term interferon therapy for 1 year or longer reduces the hepatocellular carcinogenesis rate in patients with liver cirrhosis caused by hepatitis C virus: a pilot study. *Journal of Gastroenterology and Hepatology*, 16(4), 406-15.

Ikeda, K., Saitoh, S., Koida, I., Arase, Y., Tsubota, A., Chayama, K., Kumada, H. and Kawanishi, M. (1993) A multivariate analysis of risk factors for hepatocellular carcinogenesis: a prospective observation of 795 patients with viral and alcoholic cirrhosis. *Hepatology*, 18(1), 47-53.

Imada, K. and Leonard, W. J. (2000) The Jak-STAT pathway. *Molecular Immunology*, 37(1-2), 1-11.

Jee, S. H., Chiu, H. C., Tsai, T. F., Tsai, W. L., Liao, Y. H., Chu, C. Y. and Kuo, M. L. (2002) The phosphatidylinositol 3-kinase/Akt signal pathway is involved in interleukin-6-mediated Mcl-1 upregulation and anti-apoptosis activity in basal cell carcinoma cells. *Journal of Investigative Dermatology*, 119(5), 1121-7.

Jennings, M. T., Maciunas, R. J., Carver, R., Bascom, C. C., Juneau, P., Misulis, K. and Moses, H. L. (1991) TGF beta 1 and TGF beta 2 are potential growth regulators for low-grade and malignant gliomas in vitro: evidence in support of an autocrine hypothesis. *International Journal of Cancer*, 49(1), 129-39.

- Jernberg, H , Pettersson, M , Kishimoto, T. and Nilsson, K. (1991) Heterogeneity in response to interleukin 6 (IL-6), expression of IL-6 and IL-6 receptor mRNA in a panel of established human multiple myeloma cell lines *Leukemia*, 5(3), 255-65
- Jilka, R. L., Hangoc, G., Girasole, G., Passeri, G., Williams, D. C., Abrams, J S., Boyce, B , Broxmeyer, H and Manolagas, S C (1992) Increased osteoclast development after estrogen loss mediation by interleukin-6 *Science*, 257(5066), 88-91
- Johannessen, L E., Knardal, S L. and Madshus, I. H (1999) Epidermal growth factor increases the level of the cyclin-dependent kinase (CDK) inhibitor p21/CIP1 (CDK-interacting protein 1) in A431 cells by increasing the half-lives of the p21/CIP1 transcript and the p21/CIP1 protein *Biochemical Journal*, 337(Pt 3), 599-606
- Johnson, P J (2000) In *Comprehensive Clinical Hepatology*(Eds, O'Grady, J , Lake, J and Howdle, P) Mosby, London, pp 25 1-25 18
- Kallen, K J (2002) The role of transsignalling via the agonistic soluble IL-6 receptor in human diseases *Biochimica et Biophysica Acta*, 1592(3), 323-43.
- Kang, H S., Cho, D. H , Kim, S. S , Pyun, K. H and Choi, I (1999) Antitumor effects of IL-6 on murine liver tumor cells in vivo *Journal of Biomedical Science*, 6(2), 142-4
- Katso, R., Okkenhaug, K , Ahmadi, K., White, S , Timms, J. and Waterfield, M D. (2001) Cellular function of phosphoinositide 3-kinases implications for development, homeostasis, and cancer. *Annual Review of Cell & Developmental Biology*, 17615-75.
- Kawano, M., Hirano, T , Matsuda, T , Taga, T , Horn, Y., Iwato, K , Asaoku, H , Tang, B , Tanabe, O , Tanaka, H., et al (1988) Autocrine generation and requirement of BSF-2/IL-6 for human multiple myelomas *Nature*, 332(6159), 83-5
- Keller, E T , Wanagat, J and Ershler, W B (1996) Molecular and cellular biology of interleukin-6 and its receptor *Frontiers in Biosciences*, 1d340-57
- Kerbel, R. S (1992) Expression of multi-cytokine resistance and multi-growth factor independence in advanced stage metastatic cancer Malignant melanoma as a paradigm *American Journal of Pathology*, 141(3), 519-24
- Kew, M C. (2002) Epidemiology of hepatocellular carcinoma *Toxicology*, 181-18235-8
- Kim, C. M , Koike, K , Saito, I , Miyamura, T and Jay, G. (1991) HBx gene of hepatitis B virus induces liver cancer in transgenic mice. *Nature*, 351(6324), 317-20
- Kim, H and Baumann, H (1999) Dual signaling role of the protein tyrosine phosphatase SHP-2 in regulating expression of acute-phase plasma proteins by interleukin-6 cytokine receptors in hepatic cells *Molecular & Cellular Biology*, 19(8), 5326-38

- Kimura, H , Kagawa, K , Deguchi, T., Nakajima, T , Kakusui, M , Ohkawara, T., Katagishi, T , Okanoue, T , Kashima, K and Ashihara, T. (1996) Cytogenetic analyses of hepatocellular carcinoma by in situ hybridization with a chromosome-specific DNA probe *Cancer*, 77(2), 271-7
- King, A , Andersson, A. and Sandler, S (2000) Cytokine-induced functional suppression of microencapsulated rat pancreatic islets in vitro. *Transplantation*, 70(2), 380-3
- Kirkwood, J. M , Strawderman, M H., Ernstoff, M. S , Smith, T. J , Borden, E. C and Blum, R. H. (1996) Interferon alfa-2b adjuvant therapy of high-risk resected cutaneous melanoma the Eastern Cooperative Oncology Group Trial EST 1684 [see comment] *Journal of Clinical Oncology*, 14(1), 7-17
- Klausen, P , Pedersen, L , Jurlander, J and Baumann, H. (2000) Oncostatin M and interleukin 6 inhibit cell cycle progression by prevention of p27kip1 degradation in HepG2 cells *Oncogene*, 19(32), 3675-83
- Kordula, T , Rokita, H , Koj, A., Fiers, W., Gauldie, J. and Baumann, H. (1991) Effects of interleukin-6 and leukemia inhibitory factor on the acute phase response and DNA synthesis in cultured rat hepatocytes. *Lymphokine & Cytokine Research*, 10(1-2), 23-6
- Kortylewski, M , Heinrich, P. C., Mackiewicz, A , Schmiertshauer, U , Klingmuller, U., Nakajima, K , Hirano, T., Horn, F and Behrmann, I (1999) Interleukin-6 and oncostatin M-induced growth inhibition of human A375 melanoma cells is STAT-dependent and involves upregulation of the cyclin-dependent kinase inhibitor p27/Kip1 *Oncogene*, 18(25), 3742-53.
- Kossakowska, A E , Edwards, D. R., Prusinkiewicz, C., Zhang, M C , Guo, D , Urbanski, S J , Grogan, T , Marquez, L A. and Janowska-Wieczorek, A. (1999) Interleukin-6 regulation of matrix metalloproteinase (MMP-2 and MMP-9) and tissue inhibitor of metalloproteinase (TIMP-1) expression in malignant non-Hodgkin's lymphomas *Blood*, 94(6), 2080-9
- Kotake, S , Sato, K , Kim, K J , Takahashi, N., Udagawa, N., Nakamura, I , Yamaguchi, A , Kishimoto, T , Suda, T and Kashiwazaki, S (1996) Interleukin-6 and soluble interleukin-6 receptors in the synovial fluids from rheumatoid arthritis patients are responsible for osteoclast-like cell formation *Journal of Bone & Mineral Research*, 11(1), 88-95.
- Kovacs, C J., Evans, M. J and Hopkins, H. A (1977) Properties of the H-4-II-E tumor cell system II In vitro characteristics of an experimental tumor cell line *Cell and Tissue Kinetics*, 10(3), 245-54.
- Kuma, S , Inaba, M., Ogata, H., Inaba, K , Okumura, T , Saito, K , Yamamoto, M and Ikehara, S (1990) Effect of human recombinant interleukin-6 on the proliferation of mouse hepatocytes in the primary culture *Immunobiology*, 180(2-3), 235-42.

- Kumagai, N , Tsuchimoto, K , Tsunematsu, S , Toda, K., Takeuchi, O , Saito, H., Morizane, T , Tsuchiya, M and Ishii, H. (2002) Inhibition of growth of human hepatoma cells by dual-function antisense IL-6 oligonucleotides. *Hepatology Research*, 22(2), 119-126
- Kurihara, N., Bertolini, D , Suda, T , Akiyama, Y. and Roodman, G D. (1990) IL-6 stimulates osteoclast-like multinucleated cell formation in long term human marrow cultures by inducing IL-1 release. *Journal of Immunology*, 144(11), 4226-30
- Kuromatsu, R., Tanaka, M., Shimauchi, Y , Shimada, M , Tanikawa, K , Watanabe, K. and Yokoo, T (1997) Usefulness of ED036 kit for measuring serum PIVKA-II levels in small hepatocellular carcinoma *Journal of Gastroenterology*, 32(4), 507-12
- LaBaer, J., Garrett, M D , Stevenson, L F., Slingerland, J. M , Sandhu, C , Chou, H S , Fattaey, A and Harlow, E. (1997) New functional activities for the p21 family of CDK inhibitors *Genes & Development*, 11(7), 847-62
- Lai, C F., Ripperger, J , Wang, Y , Kim, H , Hawley, R B and Baumann, H (1999) The STAT3-independent signaling pathway by glycoprotein 130 in hepatic cells *Journal of Biological Chemistry*, 274(12), 7793-802
- Levy, Y , Tsapis, A and Brouet, J C (1991) Interleukin-6 antisense oligonucleotides inhibit the growth of human myeloma cell lines *Journal of Clinical Investigation*, 88(2), 696-9
- Li, W., Liang, X , Leu, J I , Kovalovich, K , Ciliberto, G. and Taub, R (2001) Global changes in interleukin-6-dependent gene expression patterns in mouse livers after partial hepatectomy *Hepatology*, 33(6), 1377-86
- Lichtenstein, A., Tu, Y., Fady, C , Vescio, R and Berenson, J (1995) Interleukin-6 inhibits apoptosis of malignant plasma cells *Cellular Immunology*, 162(2), 248-55.
- Lienard, D , Ewalenko, P , Delmotte, J J , Renard, N and Lejeune, F J (1992) High-dose recombinant tumor necrosis factor alpha in combination with interferon gamma and melphalan in isolation perfusion of the limbs for melanoma and sarcoma. *Journal of Clinical Oncology*, 10(1), 52-60
- Lim, I. K (2002) Spectrum of molecular changes during hepatocarcinogenesis induced by DEN and other chemicals in Fischer 344 male rats. *Mechanisms of Ageing & Development*, 123(12), 1665-80.
- Liu, B , Liao, J , Rao, X , Kushner, S A , Chung, C D , Chang, D D and Shuai, K (1998) Inhibition of Stat1-mediated gene activation by PIAS1. *Proceedings of the National Academy of Sciences of the United States of America*, 95(18), 10626-31
- Lok, A. S (2000) Hepatitis B infection pathogenesis and management *Journal of Hepatology*, 32(1 Suppl), 89-97

- Lotz, M , Jirik, F , Kabouridis, P., Tsoukas, C , Hirano, T , Kishimoto, T and Carson, D. A (1988) B cell stimulating factor 2/interleukin 6 is a costimulant for human thymocytes and T lymphocytes *Journal of Experimental Medicine*, 167(3), 1253-8
- Lou, W , Ni, Z., Dyer, K , Tweardy, D J and Gao, A C (2000) Interleukin-6 induces prostate cancer cell growth accompanied by activation of stat3 signaling pathway *Prostate*, 42(3), 239-42
- Loyer, P , Cariou, S., Glaise, D., Bilodeau, M., Baffet, G. and Guguen-Guillouzo, C (1996) Growth factor dependence of progression through G1 and S phases of adult rat hepatocytes in vitro Evidence of a mitogen restriction point in mid-late G1 *Journal of Biological Chemistry*, 271(19), 11484-92
- Lu, C. and Kerbel, R S (1993) Interleukin-6 undergoes transition from paracrine growth inhibitor to autocrine stimulator during human melanoma progression *Journal of Cell Biology*, 120(5), 1281-8
- Lu, C., Vickers, M F and Kerbel, R S. (1992) Interleukin 6. a fibroblast-derived growth inhibitor of human melanoma cells from early but not advanced stages of tumor progression *Proceedings of the National Academy of Sciences of the United States of America*, 89(19), 9215-9.
- Luger, T A., Krutmann, J , Kirnbauer, R., Urbanski, A , Schwarz, T., Klappacher, G., Kock, A , Micksche, M., Malejczyk, J., Schauer, E , et al. (1989) IFN-beta 2/IL-6 augments the activity of human natural killer cells *Journal of Immunology*, 143(4), 1206-9
- Lutticken, C , Wegenka, U M., Yuan, J , Buschmann, J , Schindler, C , Ziemiecki, A., Harpur, A. G , Wilks, A. F., Yasukawa, K., Taga, T , et al (1994) Association of transcription factor APRF and protein kinase Jak1 with the interleukin-6 signal transducer gp130 *Science*, 263(5143), 89-92.
- Maddrey, W. C (2001) Hepatitis B--an important public health issue *Clinical Laboratory*, 47(1-2), 51-5.
- Maione, D , Di Carlo, E., Li, W , Musiani, P , Modesti, A., Peters, M , Rose-John, S , Della Rocca, C , Tripodi, M , Lazzaro, D , et al (1998) Coexpression of IL-6 and soluble IL-6R causes nodular regenerative hyperplasia and adenomas of the liver *EMBO Journal*, 17(19), 5588-97.
- Marusawa, H , Hijikata, M , Chiba, T and Shimotohno, K. (1999) Hepatitis C virus core protein inhibits Fas- and tumor necrosis factor alpha-mediated apoptosis via NF-kappaB activation *Journal of Virology*, 73(6), 4713-20.
- Matsuda, T., Yamanaka, Y. and Hirano, T (1994) Interleukin-6-induced tyrosine phosphorylation of multiple proteins in murine hematopoietic lineage cells *Biochemical & Biophysical Research Communications*, 200(2), 821-8

- May, L T., Ghrayeb, J , Santhanam, U , Tatter, S. B., Sthoeger, Z , Helfgott, D C , Chiorazzi, N , Grienering, G and Sehgal, P B (1988a) Synthesis and secretion of multiple forms of beta 2-interferon/B-cell differentiation factor 2/hepatocyte-stimulating factor by human fibroblasts and monocytes *Journal of Biological Chemistry*, 263(16), 7760-6
- May, L T , Santhanam, U , Tatter, S B , Bhardwaj, N , Ghrayeb, J and Sehgal, P B (1988b) Phosphorylation of secreted forms of human beta 2-interferon/hepatocyte stimulating factor/interleukin-6 *Biochemical & Biophysical Research Communications*, 152(3), 1144-50
- Mazur, X , Eppenberger, H M , Bailey, J E. and Fussenegger, M (1999) A novel autoregulated proliferation-controlled production process using recombinant CHO cells. *Biotechnology & Bioengineering*, 65(2), 144-50.
- McKillop, I H., Schmidt, C M., Cahill, P A and Sitzmann, J V (1997) Altered expression of mitogen-activated protein kinases in a rat model of experimental hepatocellular carcinoma. *Hepatology*, 26(6), 1484-91
- Meloche, S , Seuwen, K , Pages, G. and Pouyssegur, J (1992) Biphasic and synergistic activation of p44mapk (ERK1) by growth factors: correlation between late phase activation and mitogenicity *Molecular Endocrinology*, 6(5), 845-54
- Miki, S , Iwano, M , Miki, Y , Yamamoto, M , Tang, B., Yokokawa, K , Sonoda, T , Hirano, T and Kishimoto, T (1989) Interleukin-6 (IL-6) functions as an in vitro autocrine growth factor in renal cell carcinomas *FEBS Letters* , 250(2), 607-10
- Miles, S. A , Rezaei, A R , Salazar-Gonzalez, J F , Vander Meyden, M , Stevens, R H , Logan, D M , Mitsuyasu, R T , Taga, T , Hirano, T., Kishimoto, T., et al (1990) AIDS Kaposi sarcoma-derived cells produce and respond to interleukin 6 *Proceedings of the National Academy of Sciences of the United States of America*, 87(11), 4068-72
- Minami, M , Inoue, M , Wei, S., Takeda, K., Matsumoto, M., Kishimoto, T and Akira, S (1996) STAT3 activation is a critical step in gp130-mediated terminal differentiation and growth arrest of a myeloid cell line *Proceedings of the National Academy of Sciences of the United States of America*, 93(9), 3963-6
- Mizuhara, H., O'Neill, E., Seki, N , Ogawa, T , Kusunoki, C., Otsuka, K , Satoh, S , Niwa, M , Senoh, H and Fujiwara, H. (1994) T cell activation-associated hepatic injury mediation by tumor necrosis factors and protection by interleukin 6 *Journal of Experimental Medicine*, 179(5), 1529-37
- Moore, P. S , Boshoff, C , Weiss, R A and Chang, Y. (1996) Molecular mimicry of human cytokine and cytokine response pathway genes by KSHV *Science*, 274(5293), 1739-44
- Morgan, D. O. (1995) Principles of CDK regulation *Nature*, 374(6518), 131-4

Moriya, K., Fujie, H., Shintani, Y., Yotsuyanagi, H , Tsutsumi, T , Ishibashi, K , Matsuura, Y , Kimura, S , Miyamura, T and Koike, K (1998) The core protein of hepatitis C virus induces hepatocellular carcinoma in transgenic mice *Nature Medicine*, 4(9), 1065-7

Mouawad, R., Benhammouda, A , Rixe, O , Antoine, E C , Borel, C , Weil, M., Khayat, D and Soubrane, C. (1996) Endogenous interleukin 6 levels in patients with metastatic malignant melanoma correlation with tumor burden *Clinical Cancer Research*, 2(8), 1405-9

Mule, J J., Custer, M C., Travis, W D. and Rosenberg, S A. (1992) Cellular mechanisms of the antitumor activity of recombinant IL-6 in mice. *Journal of Immunology*, 148(8), 2622-9

Muraguchi, A., Hirano, T , Tang, B , Matsuda, T., Horii, Y., Nakajima, K. and Kishimoto, T (1988) The essential role of B cell stimulatory factor 2 (BSF-2/IL-6) for the terminal differentiation of B cells *Journal of Experimental Medicine*, 167(2), 332-44.

Murakami, M , Hibi, M , Nakagawa, N , Nakagawa, T., Yasukawa, K., Yamanishi, K , Taga, T and Kishimoto, T (1993) IL-6-induced homodimerization of gp130 and associated activation of a tyrosine kinase *Science*, 260(5115), 1808-10

Muto, Y., Moriwaki, H , Nmomiya, M , Adachi, S , Saito, A., Takasaki, K. T , Tanaka, T , Tsurumi, K , Okuno, M , Tomita, E , et al (1996) Prevention of second primary tumors by an acyclic retinoid, polyprenoic acid, in patients with hepatocellular carcinoma. Hepatoma Prevention Study Group *New England Journal of Medicine*, 334(24), 1561-7.

Naka, T , Narazaki, M , Hirata, M , Matsumoto, T , Minamoto, S., Aono, A , Nishimoto, N , Kajita, T., Taga, T , Yoshizaki, K., et al. (1997) Structure and function of a new STAT-induced STAT inhibitor *Nature*, 387(6636), 924-9

Naka, T , Nishimoto, N and Kishimoto, T (2002) The paradigm of IL-6 from basic science to medicine *Arthritis Research*, 4(Suppl 3), S233-42

Nakajima, K., Yamanaka, Y., Nakae, K , Kojima, H , Ichiba, M., Kiuchi, N , Kitaoka, T , Fukada, T , Hibi, M and Hirano, T (1996) A central role for Stat3 in IL-6-induced regulation of growth and differentiation in M1 leukemia cells *EMBO Journal*, 15(14), 3651-8

Nakashima, Y , Nakashima, O., Hsia, C. C., Kojiro, M and Tabor, E. (1999) Vascularization of small hepatocellular carcinomas correlation with differentiation *Liver*, 19(1), 12-8

Narazaki, M , Witthuhn, B A , Yoshida, K., Silvennoinen, O., Yasukawa, K., Ihle, J N , Kishimoto, T and Taga, T (1994) Activation of JAK2 kinase mediated by the interleukin 6 signal transducer gp130 *Proceedings of the National Academy of Sciences of the United States of America*, 91(6), 2285-9

Narazaki, M., Yasukawa, K , Saito, T , Ohsugi, Y., Fukui, H , Koishihara, Y , Yancopoulos, G D , Taga, T and Kishimoto, T. (1993) Soluble forms of the interleukin-6 signal-transducing receptor component gp130 in human serum possessing a potential to inhibit signals through membrane-anchored gp130 *Blood*, 82(4), 1120-6.

Navarro, S , Dehli, N , Le Couedic, J P , Klein, B., Breton-Gorius, J , Doly, J and Vainchenker, W. (1991) Interleukin-6 and its receptor are expressed by human megakaryocytes in vitro effects on proliferation and endoreplication *Blood*, 77(3), 461-71.

Nesbitt, J E and Fuller, G M (1992) Differential regulation of interleukin-6 receptor and gp130 gene expression in rat hepatocytes *Molecular Biology of the Cell*, 3(1), 103-12.

Nordan, R P , Pumphrey, J G. and Rudikoff, S. (1987) Purification and NH₂-terminal sequence of a plasmacytoma growth factor derived from the murine macrophage cell line P388D1. *Journal of Immunology* , 139(3), 813-7

Northemann, W., Braciak, T A., Hattori, M., Lee, F and Fey, G H (1989) Structure of the rat interleukin 6 gene and its expression in macrophage-derived cells *Journal of Biological Chemistry*, 264(27), 16072-82.

Novick, D., Engelmann, H., Wallach, D and Rubinstein, M (1989) Soluble cytokine receptors are present in normal human urine *Journal of Experimental Medicine*, 170(4), 1409-14.

Novick, D., Shulman, L M., Chen, L and Revel, M. (1992) Enhancement of interleukin 6 cytostatic effect on human breast carcinoma cells by soluble IL-6 receptor from urine and reversion by monoclonal antibody *Cytokine*, 4(1), 6-11

Oh, J. W , Katz, A , Harroch, S., Eisenbach, L , Revel, M and Chebath, J (1997) Unmasking by soluble IL-6 receptor of IL-6 effect on metastatic melanoma: growth inhibition and differentiation of B16-F10.9 tumor cells *Oncogene*, 15(5), 569-77

Okabe, H , Satoh, S , Kato, T , Kitahara, O , Yanagawa, R , Yamaoka, Y , Tsunoda, T , Furukawa, Y and Nakamura, Y (2001) Genome-wide analysis of gene expression in human hepatocellular carcinomas using cDNA microarray identification of genes involved in viral carcinogenesis and tumor progression. *Cancer Research*, 61(5), 2129-37

Okazaki, I., Wada, N., Nakano, M., Saito, A , Takasaki, K., Doi, M., Kameyama, K , Otani, Y , Kubochi, K , Nuoka, M., et al. (1997) Difference in gene expression for matrix metalloproteinase-1 between early and advanced hepatocellular carcinomas *Hepatology*, 25(3), 580-4

Okuda, K (2000) Hepatocellular carcinoma *Journal of Hepatology*, 32(1 Suppl), 225-37.

Okuno, Y , Takahashi, T , Suzuki, A., Fukumoto, M., Nakamura, K., Fukui, H , Koishihara, Y , Ohsugi, Y and Imura, H (1992) Acquisition of growth autonomy and tumorigenicity by an interleukin 6-dependent human myeloma cell line transfected with interleukin 6 cDNA. *Experimental Hematology*, 20(4), 395-400

Omer, A., Keegan, M , Czismadia, E., De Vos, P., Van Rooijen, N., Bonner-Weir, S and Weir, G C (2003) Macrophage depletion improves survival of porcine neonatal pancreatic cell clusters contained in alginate macrocapsules transplanted into rats *Xenotransplantation*, 10(3), 240-51

O'Shea, G M. and Sun, A M (1986) Encapsulation of rat islets of Langerhans prolongs xenograft survival in diabetic mice *Diabetes*, 35(8), 943-6

Ozturk, M (1991) p53 mutation in hepatocellular carcinoma after aflatoxin exposure *Lancet*, 338(8779), 1356-9

Pardee, A. B (1974) A restriction point for control of normal animal cell proliferation *Proceedings of the National Academy of Sciences of the United States of America*, 71(4), 1286-90

Parkin, D M , Bray, F , Ferlay, J. and Pisani, P (2001) Estimating the world cancer burden Globocan 2000 *International Journal of Cancer*, 94(2), 153-6

Paroli, M , Carloni, G., Alfani, E., De Petrillo, G and Barnaba, V (1993) Interleukin-6 production by human hepatoma lines is related to a low degree of cell differentiation *Research in Virology*, 144(4), 323-6

Peters, M , Jacobs, S , Ehlers, M., Vollmer, P , Mullberg, J, Wolf, E , Brem, G., Meyer zum Buschenfelde, K. H and Rose-John, S (1996) The function of the soluble interleukin 6 (IL-6) receptor in vivo: sensitization of human soluble IL-6 receptor transgenic mice towards IL-6 and prolongation of the plasma half-life of IL-6 *Journal of Experimental Medicine*, 183(4), 1399-406

Pitot, H. C., Peraino, C , Morse, P A , Jr and Potter, V R (1964) Hepatomas in tissue culture compared with adapting liver in vivo *National Cancer Institute Monographs*, 13229-45

Poli, V , Balena, R , Fattori, E , Markatos, A , Yamamoto, M , Tanaka, H , Ciliberto, G , Rodan, G. A and Costantini, F. (1994) Interleukin-6 deficient mice are protected from bone loss caused by estrogen depletion *EMBO Journal*, 13(5), 1189-96

Qin, L. F. and Ng, I O. (2001) Expression of p27(KIP1) and p21(WAF1/CIP1) in primary hepatocellular carcinoma: clinicopathologic correlation and survival analysis *Human Pathology*, 32(8), 778-84

Rabinovitch, A , Suarez-Pinzon, W , Strynadka, K , Ju, Q , Edelstein, D., Brownlee, M , Korbitt, G S. and Rajotte, R V. (1999) Transfection of human pancreatic islets with an anti-apoptotic gene (bcl-2) protects beta-cells from cytokine-induced destruction *Diabetes*, 48(6), 1223-9.

Raccurt, M., Tam, S. P., Lau, P., Mertani, H. C., Lambert, A., Garcia-Caballero, T., Li, H., Brown, R. J., McGuckin, M. A., Morel, G., et al. (2003) Suppressor of cytokine signalling gene expression is elevated in breast carcinoma. *British Journal of Cancer*, 89(3), 524-32.

Ramadori, G. and Christ, B. (1999) Cytokines and the hepatic acute-phase response. *Seminars in Liver Disease*, 19(2), 141-55.

Rawat, R., Rainey, G. J., Thompson, C. D., Frazier-Jessen, M. R., Brown, R. T. and Nordan, R. P. (2000) Constitutive activation of STAT3 is associated with the acquisition of an interleukin 6-independent phenotype by murine plasmacytomas and hybridomas. *Blood*, 96(10), 3514-21.

Ray, A., Sassone-Corsi, P. and Sehgal, P. B. (1989) A multiple cytokine- and second messenger-responsive element in the enhancer of the human interleukin-6 gene: similarities with c-fos gene regulation. *Molecular & Cellular Biology*, 9(12), 5537-47.

Ray Kim, W. (2002) Global epidemiology and burden of hepatitis C. *Microbes & Infection*, 4(12), 1219-25.

Ray, R. B., Lagging, L. M., Meyer, K., Steele, R. and Ray, R. (1995) Transcriptional regulation of cellular and viral promoters by the hepatitis C virus core protein. *Virus Research*, 37(3), 209-20.

Read, T. A., Sorensen, D. R., Mahesparan, R., Enger, P. O., Timpl, R., Olsen, B. R., Hjelstuen, M. H., Haraldseth, O. and Bjerkvig, R. (2001) Local endostatin treatment of gliomas administered by microencapsulated producer cells.[see comment]. *Nature Biotechnology*, 19(1), 29-34.

Reichner, J. S., Mulligan, J. A., Spisni, R., Sotomayor, E. A., Albina, J. E. and Bland, K. I. (1998) Effect of IL-6 overexpression on the metastatic potential of rat hepatocellular carcinoma cells. *Ann Surg Oncol*, 5(3), 279-86.

Renauld, J. C., Vink, A. and Van Snick, J. (1989) Accessory signals in murine cytolytic T cell responses. Dual requirement for IL-1 and IL-6. *Journal of Immunology*, 143(6), 1894-8.

Ritt, M. G., Mayor, J., Wojcieszyn, J., Smith, R., Barton, C. L. and Modiano, J. F. (2000) Sustained nuclear localization of p21/WAF-1 upon growth arrest induced by contact inhibition. *Cancer Letters*, 158(1), 73-84.

Rokstad, A. M., Holtan, S., Strand, B., Steinkjer, B., Ryan, L., Kulseng, B., Skjak-Braek, G. and Espevik, T. (2002) Microencapsulation of cells producing therapeutic proteins: optimizing cell growth and secretion. *Cell Transplantation*, 11(4), 313-24.

Rokstad, A. M., Strand, B., Rian, K., Steinkjer, B., Kulseng, B., Skjak-Braek, G. and Espevik, T. (2003) Evaluation of different types of alginate microcapsules as bioreactors for producing endostatin. *Cell Transplantation*, 12(4), 351-64.

Romeo, R. and Colombo, M. (2002) The natural history of hepatocellular carcinoma. *Toxicology*, 181-182:39-42.

Rosenberg, S. A., Lotze, M. T., Yang, J. C., Topalian, S. L., Chang, A. E., Schwartzentruber, D. J., Aebbersold, P., Leitman, S., Linehan, W. M., Seipp, C. A., et al. (1993) Prospective randomized trial of high-dose interleukin-2 alone or in conjunction with lymphokine-activated killer cells for the treatment of patients with advanced cancer. [erratum appears in J Natl Cancer Inst 1993 Jul 7;85(13):1091]. *Journal of the National Cancer Institute*, 85(8), 622-32.

Rust, C. and Gores, G. J. (2001) Locoregional management of hepatocellular carcinoma. Surgical and ablation therapies. *Clinics in Liver Disease*, 5(1), 161-73.

Sakai, I., Takeuchi, K., Yamauchi, H., Narumi, H. and Fujita, S. (2002) Constitutive expression of SOCS3 confers resistance to IFN-alpha in chronic myelogenous leukemia cells. *Blood*, 100(8), 2926-31.

Sakamoto, K., Arakawa, H., Mita, S., Ishiko, T., Ikei, S., Egami, H., Hisano, S. and Ogawa, M. (1994) Elevation of circulating interleukin 6 after surgery: factors influencing the serum level. *Cytokine*, 6(2), 181-6.

Sakamuro, D., Furukawa, T. and Takegami, T. (1995) Hepatitis C virus nonstructural protein NS3 transforms NIH 3T3 cells. *Journal of Virology*, 69(6), 3893-6.

Sandberg, E. M., Ma, X., VonDerLinden, D., Godeny, M. D. and Sayeski, P. P. (2004) Jak2 tyrosine kinase mediates angiotensin II-dependent inactivation of ERK2 via induction of mitogen-activated protein kinase phosphatase 1. *Journal of Biological Chemistry*, 279(3), 1956-67.

Santhanam, U., Ray, A. and Sehgal, P. B. (1991) Repression of the interleukin 6 gene promoter by p53 and the retinoblastoma susceptibility gene product. *Proceedings of the National Academy of Sciences of the United States of America*, 88(17), 7605-9.

Satoh, M. and Yamazaki, M. (1992) Tumor necrosis factor stimulates DNA synthesis of mouse hepatocytes in primary culture and is suppressed by transforming growth factor beta and interleukin 6. *Journal of Cellular Physiology*, 150(1), 134-9.

Scala, G., Ruocco, M. R., Ambrosino, C., Mallardo, M., Giordano, V., Baldassarre, F., Dragonetti, E., Quinto, I. and Venuta, S. (1994) The expression of the interleukin 6 gene is induced by the human immunodeficiency virus 1 TAT protein. *Journal of Experimental Medicine*, 179(3), 961-71.

Schaper, F., Gendo, C., Eck, M., Schmitz, J., Grimm, C., Anhuf, D., Kerr, I. M. and Heinrich, P. C. (1998) Activation of the protein tyrosine phosphatase SHP2 via the interleukin-6 signal transducing receptor protein gp130 requires tyrosine kinase Jak1 and limits acute-phase protein expression. *Biochemical Journal*, 335(Pt 3), 557-65.

- Schiemann, W P , Bartoe, J L and Nathanson, N. M. (1997) Box 3-independent signaling mechanisms are involved in leukemia inhibitory factor receptor alpha- and gp130-mediated stimulation of mitogen-activated protein kinase Evidence for participation of multiple signaling pathways which converge at Ras *Journal of Biological Chemistry*, 272(26), 16631-6
- Schirmacher, P , Peters, M , Ciliberto, G , Blessing, M , Lotz, J., Meyer zum Buschenfelde, K H and Rose-John, S. (1998) Hepatocellular hyperplasia, plasmacytoma formation, and extramedullary hematopoiesis in interleukin (IL)-6/soluble IL-6 receptor double-transgenic mice. *American Journal of Pathology*, 153(2), 639-48
- Schooltink, H , Stoyan, T , Lenz, D , Schmitz, H , Hirano, T., Kishimoto, T , Heinrich, P. C. and Rose-John, S (1991) Structural and functional studies on the human hepatic interleukin-6 receptor Molecular cloning and overexpression in HepG2 cells *Biochemical Journal*, 277(Pt 3), 659-64
- Seger, R and Krebs, E. G. (1995) The MAPK signaling cascade. *FASEB Journal*, 9(9), 726-35.
- Seglen, P O (1976) Preparation of isolated rat liver cells *Methods in Cell Biology*, 1329-83
- Seidel, H. M , Milocco, L H., Lamb, P., Darnell, J E , Jr., Stein, R. B. and Rosen, J (1995) Spacing of palindromic half sites as a determinant of selective STAT (signal transducers and activators of transcription) DNA binding and transcriptional activity *Proceedings of the National Academy of Sciences of the United States of America*, 92(7), 3041-5.
- Sherr, C J and Roberts, J. M (1995) Inhibitors of mammalian G1 cyclin-dependent kinases *Genes & Development*, 9(10), 1149-63
- Sherr, C. J and Roberts, J. M (1999) CDK inhibitors positive and negative regulators of G1-phase progression *Genes & Development*, 13(12), 1501-12
- Shuai, K , Horvath, C M , Huang, L H , Qureshi, S A., Cowburn, D. and Darnell, J E , Jr (1994) Interferon activation of the transcription factor Stat91 involves dimerization through SH2-phosphotyrosyl peptide interactions. *Cell*, 76(5), 821-8
- Siebers, U , Horcher, A , Brandhorst, H., Brandhorst, D , Hering, B , Federlin, K , Bretzel, R G and Zekorn, T (1999) Analysis of the cellular reaction towards microencapsulated xenogeneic islets after intraperitoneal transplantation *Journal of Molecular Medicine*, 77(1), 215-8.
- Silvani, A., Ferrari, G , Paonessa, G , Toniatti, C , Parmiani, G and Colombo, M P (1995) Down-regulation of interleukin 6 receptor alpha chain in interleukin 6 transduced melanoma cells causes selective resistance to interleukin 6 but not to oncostatin M *Cancer Research*, 55(10), 2200-5.
- Smidsrod, O and Skjak-Braek, G (1990) Alginate as immobilization matrix for cells. *Trends in Biotechnology*, 8(3), 71-8

- Soon-Shiong, P., Feldman, E , Nelson, R , Komtebedde, J., Smidsrod, O , Skjak-Braek, G , Espevik, T , Heintz, R and Lee, M (1992) Successful reversal of spontaneous diabetes in dogs by intraperitoneal microencapsulated islets *Transplantation*, 54(5), 769-74
- Soon-Shiong, P., Heintz, R E , Merideth, N , Yao, Q X., Yao, Z., Zheng, T., Murphy, M , Moloney, M. K., Schmehl, M , Harris, M., et al (1994) Insulin independence in a type 1 diabetic patient after encapsulated islet transplantation *Lancet*, 343(8903), 950-1
- Spiotto, M. T and Chung, T. D. (2000) STAT3 mediates IL-6-induced growth inhibition in the human prostate cancer cell line LNCaP *Prostate*, 42(2), 88-98
- Squinto, S P , Block, A L and Doucet, J. P (1989) Epidermal growth factor induction of cellular proliferation and protooncogene expression in growth-arrested rat H4IIE hepatoma cells: role of cyclic adenosine monophosphate. *Molecular Endocrinology*, 3(3), 433-46
- Stahl, N., Boulton, T. G., Farruggella, T , Ip, N Y , Davis, S , Witthuhn, B A , Quelle, F W , Silvennoinen, O , Barbieri, G., Pellegrini, S , et al (1994) Association and activation of Jak-Tyk kinases by CNTF-LIF-OSM-IL-6 beta receptor components *Science*, 263(5143), 92-5.
- Stahl, N , Farruggella, T. J , Boulton, T G , Zhong, Z , Darnell, J E , Jr and Yancopoulos, G D (1995) Choice of STATs and other substrates specified by modular tyrosine-based motifs in cytokine receptors *Science*, 267(5202), 1349-53
- Starr, R , Willson, T A , Viney, E. M , Murray, L J , Rayner, J R., Jenkins, B J , Gonda, T J , Alexander, W S , Metcalf, D , Nicola, N A , et al (1997) A family of cytokine-inducible inhibitors of signalling *Nature*, 387(6636), 917-21
- Stickel, F , Schuppan, D., Hahn, E. G and Seitz, H K (2002) Cocarcinogenic effects of alcohol in hepatocarcinogenesis *Gut*, 51(1), 132-9
- Streetz, K L , Luedde, T , Manns, M. P. and Trautwein, C. (2000) Interleukin 6 and liver regeneration *Gut*, 47(2), 309-12
- Suchiro, T , Terashi, T , Shiotani, S , Soejima, Y and Sugimachi, K (2002) Liver transplantation for hepatocellular carcinoma *Surgery*, 131(1 Suppl), S190-4
- Sun, Y , Ma, X., Zhou, D , Vacek, I and Sun, A. M (1996) Normalization of diabetes in spontaneously diabetic cynomolgus monkeys by xenografts of microencapsulated porcine islets without immunosuppression *Journal of Clinical Investigation*, 98(6), 1417-22
- Sun, Z , Lu, P , Gail, M H., Pee, D , Zhang, Q , Ming, L , Wang, J , Wu, Y , Liu, G. and Zhu, Y (1999) Increased risk of hepatocellular carcinoma in male hepatitis B surface antigen carriers with chronic hepatitis who have detectable urinary aflatoxin metabolite M1 *Hepatology*, 30(2), 379-83

- Tabibzadeh, S., Kong, Q. F., Babaknia, A and May, L. T. (1995) Progressive rise in the expression of interleukin-6 in human endometrium during menstrual cycle is initiated during the implantation window. *Human Reproduction*, 10(10), 2793-9
- Taga, T., Hibi, M , Hirata, Y., Yamasaki, K , Yasukawa, K , Matsuda, T., Hirano, T and Kishimoto, T (1989) Interleukin-6 triggers the association of its receptor with a possible signal transducer, gp130 *Cell*, 58(3), 573-81
- Taga, T , Kawanishi, Y , Hardy, R R., Hirano, T and Kishimoto, T (1987) Receptors for B cell stimulatory factor 2. Quantitation, specificity, distribution, and regulation of their expression *Journal of Experimental Medicine*, 166(4), 967-81
- Takahashi, K and Suzuki, K. (1996) Density-dependent inhibition of growth involves prevention of EGF receptor activation by E-cadherin-mediated cell-cell adhesion *Experimental Cell Research*, 226(1), 214-22
- Takahashi-Tezuka, M., Yoshida, Y , Fukada, T , Ohtani, T , Yamanaka, Y , Nishida, K , Nakajima, K., Hibi, M and Hirano, T (1998) Gab1 acts as an adapter molecule linking the cytokine receptor gp130 to ERK mitogen-activated protein kinase *Molecular & Cellular Biology*, 18(7), 4109-17
- Takatsuki, F , Okano, A , Suzuki, C., Chieda, R , Takahara, Y , Hirano, T , Kishimoto, T , Hamuro, J. and Akiyama, Y. (1988) Human recombinant IL-6/B cell stimulatory factor 2 augments murine antigen-specific antibody responses in vitro and in vivo. *Journal of Immunology*, 141(9), 3072-7
- Takayama, T., Makuuchi, M , Hirohashi, S , Sakamoto, M , Okazaki, N , Takayasu, K., Kosuge, T , Motoo, Y , Yamazaki, S and Hasegawa, H (1990) Malignant transformation of adenomatous hyperplasia to hepatocellular carcinoma *Lancet*, 336(8724), 1150-3
- Takizawa, H , Ohtoshi, T , Ohta, K., Yamashita, N , Hirohata, S., Hirai, K., Hiramatsu, K and Ito, K (1993) Growth inhibition of human lung cancer cell lines by interleukin 6 in vitro a possible role in tumor growth via an autocrine mechanism *Cancer Research*, 53(18), 4175-81
- Talarmin, H., Rescan, C , Cariou, S , Glaise, D., Zanninelli, G., Bilodeau, M , Loyer, P , Guguen-Guillouzo, C. and Baffet, G. (1999) The mitogen-activated protein kinase/extracellular signal-regulated kinase cascade activation is a key signalling pathway involved in the regulation of G(1) phase progression in proliferating hepatocytes *Molecular & Cellular Biology*, 19(9), 6003-11.
- Tamemoto, H , Kadowaki, T , Tobe, K , Ueki, K., Izumi, T , Chatani, Y , Kohno, M , Kasuga, M , Yazaki, Y and Akanuma, Y (1992) Biphasic activation of two mitogen-activated protein kinases during the cell cycle in mammalian cells *Journal of Biological Chemistry*, 267(28), 20293-7
- Tamura, T , Udagawa, N , Takahashi, N , Miyaura, C , Tanaka, S., Yamada, Y , Koishihara, Y , Ohsugi, Y., Kumaki, K., Taga, T , et al (1993) Soluble interleukin-6 receptor triggers osteoclast formation by interleukin 6 *Proceedings of the National Academy of Sciences of the United States of America*, 90(24), 11924-8

- Tannapfel, A., Anhalt, K., Hausermann, P., Sommerer, F., Benicke, M., Uhlmann, D., Witzigmann, H., Hauss, J. and Wittekind, C. (2003) Identification of novel proteins associated with hepatocellular carcinomas using protein microarrays. *Journal of Pathology*, 201(2), 238-49.
- Taub, R. (2004) Liver regeneration: from myth to mechanism. *Nature Reviews Molecular Cell Biology*, 5(10), 836-47.
- Tchirkov, A., Rolhion, C., Bertrand, S., Dore, J. F., Dubost, J. J. and Verrelle, P. (2001) IL-6 gene amplification and expression in human glioblastomas. *British Journal of Cancer*, 85(4), 518-22.
- Teramoto, T., Satonaka, K., Kitazawa, S., Fujimori, T., Hayashi, K. and Maeda, S. (1994) p53 gene abnormalities are closely related to hepatoviral infections and occur at a late stage of hepatocarcinogenesis. *Cancer Research*, 54(1), 231-5.
- Thu, B., Bruheim, P., Espevik, T., Smidsrod, O., Soon-Shiong, P. and Skjak-Braek, G. (1996a) Alginate polycation microcapsules. I. Interaction between alginate and polycation. *Biomaterials*, 17(10), 1031-40.
- Thu, B., Bruheim, P., Espevik, T., Smidsrod, O., Soon-Shiong, P. and Skjak-Braek, G. (1996b) Alginate polycation microcapsules. II. Some functional properties. *Biomaterials*, 17(11), 1069-79.
- To, Y., Dohi, M., Matsumoto, K., Tanaka, R., Sato, A., Nakagome, K., Nakamura, T. and Yamamoto, K. (2002) A two-way interaction between hepatocyte growth factor and interleukin-6 in tissue invasion of lung cancer cell line. *American Journal of Respiratory Cell & Molecular Biology*, 27(2), 220-6.
- Todo, T., Adams, E. F., Rafferty, B., Fahlbusch, R., Dingermann, T. and Werner, H. (1994) Secretion of interleukin-6 by human meningioma cells: possible autocrine inhibitory regulation of neoplastic cell growth. *Journal of Neurosurgery*, 81(3), 394-401.
- Ullmann, C. D., Schlom, J. and Greiner, J. W. (1992) Interleukin-6 increases carcinoembryonic antigen and histocompatibility leukocyte antigen expression on the surface of human colorectal carcinoma cells. *Journal of Immunotherapy*, 12(4), 231-41.
- Uludag, H., De Vos, P. and Tresco, P. A. (2000) Technology of mammalian cell encapsulation. *Advanced Drug Delivery Reviews*, 42(1-2), 29-64.
- Uyttenhove, C., Coulie, P. G. and Van Snick, J. (1988) T cell growth and differentiation induced by interleukin-HP1/IL-6, the murine hybridoma/plasmacytoma growth factor. *Journal of Experimental Medicine*, 167(4), 1417-27.
- Van Snick, J., Cayphas, S., Szikora, J. P., Renauld, J. C., Van Roost, E., Boon, T. and Simpson, R. J. (1988) cDNA cloning of murine interleukin-HP1: homology with human interleukin 6. *European Journal of Immunology*, 18(2), 193-7.

- Vilcek, J (2003) In *The cytokine Handbook*, Vol. 1 (Eds, Thompson, A. and Lotze, M) Elsevier Science Ltd , London, pp 3-18
- Visted, T , Furmanek, T , Sakariassen, P , Foegler, W B , Sim, K , Westphal, H , Bjerkvig, R. and Lund-Johansen, M (2003) Prospects for delivery of recombinant angiostatin by cell-encapsulation therapy. *Human Gene Therapy*, 14(15), 1429-40
- Waage, A , Brandtzaeg, P., Halstensen, A , Kierulf, P and Espevik, T (1989) The complex pattern of cytokines in serum from patients with meningococcal septic shock Association between interleukin 6, interleukin 1, and fatal outcome *Journal of Experimental Medicine*, 169(1), 333-8.
- Wang, X J , Taga, T , Yoshida, K , Saito, M , Kishimoto, T and Kikutani, H (1998) gp130, the cytokine common signal-transducer of interleukin-6 cytokine family, is downregulated in T cells in vivo by interleukin-6. *Blood*, 91(9), 3308-14
- Ward, L. D , Hammacher, A , Howlett, G J , Matthews, J M., Fabri, L , Moritz, R L , Nice, E C , Weinstock, J and Simpson, R J (1996) Influence of interleukin-6 (IL-6) dimerization on formation of the high affinity hexameric IL-6 receptor complex. *Journal of Biological Chemistry*, 271(33), 20138-44
- Ward, L D , Howlett, G J , Discolo, G , Yasukawa, K., Hammacher, A , Moritz, R L and Simpson, R J (1994) High affinity interleukin-6 receptor is a hexameric complex consisting of two molecules each of interleukin-6, interleukin-6 receptor, and gp-130. *Journal of Biological Chemistry*, 269(37), 23286-9
- Watanabe, D , Ezoe, S., Fujimoto, M , Kimura, A., Saito, Y , Nagai, H , Tachibana, I., Matsumura, I , Tanaka, T , Kanegane, H , et al (2004) Suppressor of cytokine signalling-1 gene silencing in acute myeloid leukaemia and human haematopoietic cell lines [see comment]. *British Journal of Haematology*, 126(5), 726-35
- Weber, J D , Raben, D M., Phillips, P J and Baldassare, J J. (1997) Sustained activation of extracellular-signal-regulated kinase 1 (ERK1) is required for the continued expression of cyclin D1 in G1 phase *Biochemical Journal*, 326(Pt 1), 61-8.
- Weissenbach, J , Chernajovsky, Y., Zeevi, M , Shulman, L., Soreq, H , Nir, U , Wallach, D , Perricaudet, M., Tiollais, P and Revel, M (1980) Two interferon mRNAs in human fibroblasts: in vitro translation and Escherichia coli cloning studies *Proceedings of the National Academy of Sciences of the United States of America*, 77(12), 7152-6
- Wu, C. G , Salvay, D. M , Forgues, M., Valerie, K., Farnsworth, J., Markin, R. S and Wang, X. W. (2001) Distinctive gene expression profiles associated with Hepatitis B virus x protein *Oncogene*, 20(28), 3674-82
- Wu, S. P , Theodorescu, D., Kerbel, R S., Willson, J. K., Mulder, K. M , Humphrey, L. E and Brattain, M G (1992) TGF-beta 1 is an autocrine-negative growth regulator of human colon carcinoma FET cells in vivo as revealed by transfection of an antisense expression vector *Journal of Cell Biology*, 116(1), 187-96

- Wustefeld, T , Rakemann, T , Kubicka, S , Manns, M P. and Trautwein, C (2000) Hyperstimulation with interleukin 6 inhibits cell cycle progression after hepatectomy in mice *Hepatology*, 32(3), 514-22
- Xu, W , Liu, L and Charles, I G (2002) Microencapsulated iNOS-expressing cells cause tumor suppression in mice. *FASEB Journal*, 16(2), 213-5.
- Yamada, Y , Kirillova, I , Peschon, J J and Fausto, N. (1997) Initiation of liver growth by tumor necrosis factor deficient liver regeneration in mice lacking type I tumor necrosis factor receptor. *Proceedings of the National Academy of Sciences of the United States of America*, 94(4), 1441-6
- Yamamoto, T , Matsuda, T , Muraguchi, A., Miyazono, K and Kawabata, M (2001) Cross-talk between IL-6 and TGF-beta signaling in hepatoma cells *FEBS Letters*, 492(3), 247-53
- Yamamura, M , Yamada, Y , Momita, S , Kamihira, S and Tomonaga, M (1998) Circulating interleukin-6 levels are elevated in adult T-cell leukaemia/lymphoma patients and correlate with adverse clinical features and survival *British Journal of Haematology*, 100(1), 129-34.
- Yamanaka, Y , Nakajima, K , Fukada, T , Hibi, M and Hirano, T (1996) Differentiation and growth arrest signals are generated through the cytoplasmic region of gp130 that is essential for Stat3 activation. *EMBO Journal*, 15(7), 1557-65
- Yamasaki, K , Taga, T , Hirata, Y , Yawata, H , Kawanishi, Y , Seed, B , Taniguchi, T , Hirano, T. and Kishimoto, T (1988) Cloning and expression of the human interleukin-6 (BSF-2/IFN beta 2) receptor. *Science*, 241(4867), 825-8
- Yang, H and Wright, J R , Jr (1999) Co-encapsulation of Sertoli enriched testicular cell fractions further prolongs fish-to-mouse islet xenograft survival *Transplantation*, 67(6), 815-20
- Yasukawa, K , Hirano, T , Watanabe, Y , Muratani, K , Matsuda, T , Nakai, S and Kishimoto, T (1987) Structure and expression of human B cell stimulatory factor-2 (BSF-2/IL-6) gene *EMBO Journal*, 6(10), 2939-45.
- Yee, C., Biondi, A , Wang, X H , Iscove, N N , de Sousa, J , Aarden, L A , Wong, G G , Clark, S C , Messner, H A and Minden, M D (1989) A possible autocrine role for interleukin-6 in two lymphoma cell lines *Blood*, 74(2), 798-804
- Yin, T , Shen, R , Feng, G S and Yang, Y C (1997) Molecular characterization of specific interactions between SHP-2 phosphatase and JAK tyrosine kinases *Journal of Biological Chemistry*, 272(2), 1032-7
- Yoshikawa, H , Matsubara, K , Qian, G S , Jackson, P , Groopman, J D , Manning, J E , Harris, C C and Herman, J G (2001a) SOCS-1, a negative regulator of the JAK/STAT pathway, is silenced by methylation in human hepatocellular carcinoma and shows growth-suppression activity. *Nature Genetics*, 28(1), 29-35

Yoshikawa, H , Matsubara, K , Qian, G. S , Jackson, P , Groopman, J D , Manning, J E , Harris, C C and Herman, J. G. (2001b) SOCS-1, a negative regulator of the JAK/STAT pathway, is silenced by methylation in human hepatocellular carcinoma and shows growth-suppression activity [comment] *Nature Genetics*, 28(1), 29-35

Yu, C L , Meyer, D J , Campbell, G. S , Larner, A C., Carter-Su, C , Schwartz, J and Jove, R. (1995) Enhanced DNA-binding activity of a Stat3-related protein in cells transformed by the Src oncoprotein. *Science*, 269(5220), 81-3

Zhang, X , Blenis, J , Li, H C , Schindler, C and Chen-Kiang, S (1995) Requirement of serine phosphorylation for formation of STAT-promoter complexes. *Science*, 267(5206), 1990-4

Zhu, X F., Liu, Z C , Xie, B F , Feng, G K and Zeng, Y X (2003) Ceramide induces cell cycle arrest and upregulates p27kip in nasopharyngeal carcinoma cells. *Cancer Letters*, 193(2), 149-54.

Zimmers, T A , McKillop, I H., Pierce, R. H., Yoo, J Y and Komaris, L G (2003) Massive liver growth in mice induced by systemic interleukin 6 administration. *Hepatology*, 38(2), 326-34

Zohlhofer, D , Graeve, L , Rose-John, S , Schooltink, H , Dittrich, E and Heinrich, P C (1992) The hepatic interleukin-6 receptor Down-regulation of the interleukin-6 binding subunit (gp80) by its ligand *FEBS Letters*, 306(2-3), 219-22